UNIVERSITAT DE BARCELONA

Illuminating cAMP signalling in neurodegenerative diseases: from synaptic plasticity mechanisms to therapeutic opportunities

Laia Sitjà Roqueta

UNIVERSITAT DE BARCELONA

Illuminating cAMP signalling in neurodegenerative diseases: from synaptic plasticity mechanisms to therapeutic opportunities

---

Doctoral degree in Biomedicine by the University of Barcelona

Dissertation submitted by:

Laia Sitjà Roqueta

This work was performed at the Department of Biomedical Sciences of the Faculty of Medicine and Health Sciences of the University of Barcelona, under the supervision of Dr. Mercè Masana Nadal.

Mercè Masana Nadal	Laia Sitjà Roqueta	Jordi Alberch Vié
Director		Tutor

UNIVERSITAT DE BARCELONA

Il·luminant la senyalització d'AMPc en malalties neurodegeneratives: dels mecanismes de plasticitat sinàptica a les oportunitats terapèutiques

---

Doctorat en Biomedicina per la Universitat de Barcelona
Tesi presentada per:

Laia Sitjà Roqueta

Aquesta treball s'ha dut a terme en el Departament de Biomedicina de la Facultat de Medicina i Ciències de la Salut de la Universitat de Barcelona, sota la supervisió de la Dra. Mercè Masana Nadal.

A la gent que estimo,

ACKNOWLEDGEMENTS

ACKNOWLEDGEMENTS

No canviaria res del camí recorregut aquests últims cinc anys, des de l'inici fins la conclusió d'aquesta tesi. Cada dia ha estat una oportunitat per aprendre, i tot el que he viscut m'ha ajudat a ser qui sóc avui. N'estic profundament agraïda. El viatge d'una tesi és, però, també intens, llarg i sovint ple d'incerteses, i arribar al final és possible gràcies a tota la gent que t'acompanya i t'ajuda durant el camí. Gràcies de tot cor a tothom qui, en un moment o altre, heu estat allà per fer-me l'experiència més fàcil. Gràcies,

Mercè, per guiar-me i estar al meu costat durant tot el camí, i sobretot, per fer-me creure en mi.

Manolo, Jordi i Anna C., per ser aquell suport que no sempre es percep, però que sempre hi és i és fonamental.

A tots els PIs de l'Histolab, per a cada comentari, suggerència, i crítica constructiva que m'hàgiu pogut fer arribar, aquesta petites coses són les que realment fan millorar la ciència.

To our international collaborators, Rhein, Andreas, Mehdi, Alexander, Deniz, Igor, Edik, Neville, Evgenii, thank you for all the support and amazing ideas you have shared, which have really helped shape this work.

A tots els estudiants que, d'alguna manera o altra, han contribuït a la meva tesi; sense vosaltres, no hauria estat possible.

Maite, per ser els fonaments de l'Histolab, el més important sense el qual el laboratori no se sustentaria.

A tota aquella gent imprescindible, sovint sense el protagonisme que mereix, com tècnics, administratius, personal de laboratori i altres professionals, sense la qual res hauria tirat endavant.

A Bioquímica, per tota aquella gent que en un moment o altre ha passat pel meu camí. Esther, per ser l'alegria de Jordis. Alba, per haver sabut agafar el relleu de la millor manera. Gisela, per ser la última incorporació amb un gran potencial.

Als d'abans. Ened, per les teves rialles i suport moral que han estat essencials. Carla, per sempre aportar humor i vitalitat a totes les situacions. Anna G., per sempre transmetre'm la teva serenitat i saber estar. Laura, per transmetre la teva passió per la ciència, falta més gent com tu. Irene, per aparèixer un dia i quedar-te, sempre amb el millor dels consells.

Als que sempre heu estat allà. Isaac, per ser més que un veí d'escriptori, des del principi i fins al final. Sofía, por tu positividad, tu energía y ganas de celebrarlo todo, eres el alma del Histolab. Claudia, per representar la millor manera de fer les coses, l'esforç i la constància, mantenint sempre la teva l'energia. Ivan, qué decir, detrás de tu fachada misteriosa, siempre has estado allí, gracias amigo.

To my current colleagues, labmates, thank you. Melike, for always speaking the truth and being there to help and support me. Maryam, for all the hours spent together at the MRI, I

wish there had been even more. To the newest members of Mercè's group. Matilde, you are joy personified, and a wonderful addition to the team. Valentina, although we didn't have the opportunity to spend more time together, thank you for all your help.

Als d'ara. Marcos, por ser tú, por preocuparte siempre por los demás y querer ayudar, has sido fundamental. Sara B., per la teva energia i llum, tant de bo haver pogut compartir més moments. Alba, per transmetre un somriure i bones paraules en qualsevol situació, fent que tot millori. Xavi, per ensenyar-nos que cal fer el que es sent en cada moment, sort en el nou camí. Irene, per haver representat la tenacitat, sempre amb la millor de les actituds, i sempre allà per ajudar.

Sara, des del meu primer dia des del laboratori i fins a l'últim ja des de fora d'ell, el camí no hagués estat el mateix sense tu.

Anna, sempre allà, omnipresent, incansable i indispensable.

Carlota i Xènia, per seguir allà, any rere any i allà on siguem.

Alawis, per ser el meu suport més proper, tot i arribar més tard a la meva vida.

Als meus sogres, cunyats, i nebots, els àpats compartits han estat sempre un raig de llum en el camí.

Nenes, per ser les meves incondicionals.

Oriol, per ser allà a la teva manera.

A la Mafalda i en Houdini, per ser a mi, literalment, cada dia de l'escriptura d'aquesta tesi.

Ferran, per ser el meu company de vida, el meu suport absolut, t'estimo.

Papes, per ser els millors pares del món, us estimo.

SUMMARY

SUMMARY

With the aging population, the rising burden of neurodegenerative diseases presents a critical public health issue, potentially resulting in an unsustainable social and economic burden if current trends continue. Strikingly, most of these diseases lack a cure or even and effective treatment that improves the quality of life for affected individuals. A hallmark of neurodegenerative disorders is synaptic dysfunction, which arises despite neuronal loss and is driven by the accumulation of misfolded proteins, all leading to molecular, circuitry, and functional impairments (Palop & Mucke, 2016). Yet, the exact mechanisms driving these specific alterations are still not fully understood. This highlights the need for a deeper understanding of these diseases and, more importantly, the urgent need for novel therapeutic strategies, potentially based on modulating brain plasticity.

In the context of this thesis, we focused in two neurodegenerative diseases, Huntington's Disease (HD) and Alzheimer's Disease (AD). HD is an autosomal-dominant, genetic, neurodegenerative disorder characterised by progressive degeneration of striatal and cortical regions of the brain (Huntington, 2003; Walker, 2007). The disease manifests with motor deficits such as chorea, dystonia, and incoordination, alongside cognitive decline and psychiatric impairments. HD is caused by a mutation in the huntingtin (HTT) gene, with an expanded CAG trinucleotide repeat resulting in a mutant form of huntingtin (mHTT) that leads to neurodegeneration (The Huntington's Disease Collaborative Research Group, 1993a). HD is marked by selective neuronal loss and impaired synaptic plasticity, particularly in the cortex and striatum, with medium spiny neurons being especially vulnerable (Vonsattel & DiFiglia, 1998). Disruption of the cortico-striatal pathway, which plays a critical role in motor and cognitive functions, contributes to the disease's symptoms (Cepeda et al., 2007).AD, on the other hand, is the leading cause of dementia, characterised by progressive memory decline and impairments in language, executive function, and visuospatial skills (Scheltens et al., 2021; Stelzmann et al., 1995). AD is classified into familial, caused by mutations in genes like APP, PSEN1, and PSEN1 with earlier onset accounting for less than 0.5% of cases, and sporadic AD, present in 99,5% of cases and influenced by genetic, environmental, and lifestyle factors (Bateman et al., 2011; Bertram et al., 2010). AD is characterised by amyloid plaques, tau tangles, and neuroinflammation. Synaptic dysfunction, particularly in the hippocampus, correlates strongly with cognitive decline in AD (Querfurth & LaFerla, 2010). Therefore, synaptic plasticity is an early alteration in both diseases, underscoring the need to develop therapeutic strategies that specifically target these early changes.

Synaptic plasticity is the mechanism by which synaptic connections in the brain are strengthened or weakened in response to various stimuli. Impairments in this process are one of the main characteristics in HD and AD, contributing significantly to the functional deficits observed in these conditions (J. Y. Li et al., 2003; Selkoe, 2002). In long term synaptic plasticity, activation of receptors by neurotransmitters triggers signalling pathways that enhance synaptic strength, usually associated to calcium influx. A key component of this

strengthening is the insertion of new receptors into the postsynaptic membrane, a process that requires protein kinases and local protein synthesis. Besides calcium, another key signalling molecule sustaining plasticity is cyclic adenosine monophosphate (cAMP). cAMP is modulated by metabotropic receptor activity, and among diverse targets, activates protein kinase A (PKA), which phosphorylates transcription factors like CREB, initiating gene expression required for long-term synaptic modifications (Benito & Barco, 2010). Furthermore, the cAMP-PKA pathway is essential for establishing structural changes in synapses, and its activation has been linked to enhanced synaptic plasticity in various brain regions (C. C. Huang & Hsu, 2006; Nguyen & Kandel, 1997). Additionally, astrocytes also contribute to synaptic plasticity. However, the mechanisms underlying cAMP contribution to synaptic plasticity are not yet completely understood, neither its specific role in neurons or astrocytes.

Indeed, alterations in cAMP signalling are increasingly linked to aging and neurodegenerative diseases such as HD and AD (Kelly, 2018). Both the cortico-striatal pathway in HD and the hippocampus in AD show disruptions in the cAMP-PKA signalling pathway. In HD, decreased cAMP signalling in the cortex and striatum and increased in the hippocampus have been reported, although with controversies around it. In AD, it is more well-established that cAMP signalling is decreased in the hippocampus, playing a key role in the development of the dementia-related pathology. **Due to the still controversial knowledge of cAMP in HD, and the known importance of the cortex in the disease, our first objective is to characterise the disruptions in cortical cAMP signalling and behaviour in the R6/1 mouse model for the disease.**

Therefore, approaches aimed at enhancing synaptic plasticity through cAMP signalling modulation hold potential for mitigating or delaying network dysfunction associated with neurodegenerative disorders such as HD and AD. In this regard, optogenetic tools provide precise control of biological mechanisms through light-sensitive proteins. Particularly, photoactivated adenylyl cyclases (PACs) are enzymes that elevate cAMP levels in response to light stimulation, initiated by an AC domain coupled to a photoreceptor module (Iseki & Park, 2021). Among these, DdPAC is a recently optimised PAC that regulates cAMP in response to red light (Stüven et al., 2018). Originally developed in bacteria, DdPAC demonstrated a stronger light response compared to other red-light-sensitive PACs. However, its application in brain cells and *in vivo* remains unexplored. Considering red light's ability to penetrate tissues with minimal scattering, it is well-suited for non-invasive applications. **Given the promising potential of DdPAC as a novel optogenetic tool for modulating cAMP, our second objective is to establish its use for non-invasive modulation of synaptic plasticity *in vivo*.**

Further, considering the distinct regional vulnerabilities and pathophysiological differences between HD and AD, which may impact cAMP modulation and synaptic plasticity, **our third objective is to restore physiological function through light-driven DdPAC**

stimulation in mouse models of both diseases. Importantly, the focus will be set on the regions most affected in each condition, specifically targeting the striatum and cortex in HD, and hippocampus in AD.

In light of this information, the main aim of this thesis is to restore physiological function in neurodegenerative diseases by modulating brain plasticity through light-induced activation of DdPAC-mediated cAMP signalling in specific brain circuits.

To achieve **our first objective and characterise the disruptions in cortical cAMP signalling and behaviour in the R6/1 mouse model of Huntington's Disease**, we first assessed cortical cAMP alterations during cortico-striatal behaviours in R6/1 mice. To investigate cAMP dynamics, we performed fibre photometry recordings of the GFlamp-1 sensor, a novel cAMP sensor, in M2 cortical neurons of 14-week-old and 20-week-old WT and R6/1 male and female mice during the beetle-mania (BMT) and accelerating rotarod (ARR) tasks. First, we evaluated cAMP dynamics during the BMT and observed an increase of cAMP levels in both WT and R6/1 mice upon the introduction of the beetle. Despite R6/1 mice already exhibiting altered behaviour during the test, no genotype differences in cAMP levels were detected. These data revealed the involvement of neuronal cAMP signalling during the BMT, with minimal alterations in R6/1 mice. Then, to further understand the contribution of cAMP signalling to M2-cortex related tasks, we explored cAMP dynamics during the ARR. Our results were in line with what we observed during the BMT, as both neuronal cAMP levels from WT and R6/1 mice increased with the start of the task. In contrast of our BMT results, in this case we observed an aberrant overactivation of the M2-cortex in R6/1 mice. Lastly, to better understand if alterations in cAMP activity during M2-cortex related tasks are more prominent at later stages of disease progression, we repeated the BMT in the same cohort of mice at 20 weeks, when mice are fully symptomatic. At this age, we were still able to observe an increase in neuronal cAMP in both WT and R6/1 mice upon the introduction of the beetle. However, the increase in cAMP was significantly diminished in R6/1 mice. Altogether, these results highlight the contribution of neuronal cAMP in M2-cortex related task and display alterations in HD.

Due to the critical role of M2-cortex in HD pathophysiology, we also aimed to determine if additional symptoms associated with cortico-striatal dysfunction emerge at early disease stages of the disease in the R6/1 mouse model. To accomplish this, we selected two behavioural tests, namely the adhesive removal test and the marble-burying test, both related with the M2-cortex and the cortico-striatal pathway, and then performed them longitudinally from 4 to 16-week-old mice. In the removal adhesive test, which is related to the M2-cortex-somatosensory cortex-striatum pathway, we observed fine motor deficits as early as 8 weeks, while somatosensory deficits appeared at 16 weeks. In the marble burying test, which is related to the M2-cortex-orbitofrontal cortex-striatum pathway, we observed anhedonia-like behaviour from 8 weeks. These data indicated that cortico-striatal dysfunction emerges at very early timepoints, highlighting the potential for early therapeutic interventions.

Overall, findings from the first objective indicate that M2 cortex-related cortico-striatal dysfunction emerges at early disease stages, underscoring the potential for early therapeutic interventions. Since neuronal cAMP signalling is remains responsive in behaving mice, it it is unlikely to underlie the M2-related behavioural deficits, suggesting that alternative mechanisms may be responsible for these impairments.

To accomplish **our second objective and implement DdPAC as a novel optogenetic tool to non-invasively modulate synaptic plasticity through cAMP signalling**, we first aimed to establish a minimally or non-invasive method for the delivery of DdPAC in the brain by using AAVs constructs. Thus, we designed GFP constructs under three different promoters (CAG, CamKIIa, and FLEXon), and administered them using two different AAV serotypes (AAV9 and PHP.eB), into two different mouse strains (C57BL/6J and B6CBA), and via three delivery routes, from more to less invasive (intra-cranial, retro-orbital, and intranasal). In summary, GFP expression was detected in various brain regions and specific cell types following retro-orbital injection of PHP.eB and AAV9 constructs, with the PHP.eB serotype exhibiting broader infection. Furthermore, we were able to express PHP.eB constructs in C57BL/6J and B6CBA mouse strains, and specifically to our R6/1 mouse model. Retro-orbital injection in A2a Cre mice resulted in region-specific transduction of the virus, demonstrating its potential to target specific circuits. Nevertheless, GFP fluorescence was not observed in any of the cases after intranasal administration. These results highlight retro-orbital injection as a minimally invasive approach for efficiently targeting brain regions across various cell types and mouse strains, offering an alternative to stereotaxic surgery. However, additional research on viral capsid modifications is required to facilitate neural cell infection through intranasal administration.

To continue with our objective, we next characterised the cell-type-specific DdPAC stimulation effects in the brain. Accordingly, we first aimed to investigate if DdPAC-mediated cAMP modulation was able to enhance synaptic plasticity. Therefore, we injected DdPAC under the CamKIIa or GFAP promoters into the cortex to selectively express it in neurons and astrocytes, followed by multi-electrode array recordings. Red-light illumination enhanced neuronal potentiation in both neuronal and astrocytic-driven DdPAC activation, though the effect was more pronounced when DdPAC was activated in astrocytes. Thus, the following experiments of this objective were focused on investigating DdPAC activation in cortical astrocytes. Thereby, we further characterised the mechanism underlying this potentiation, demonstrating that DdPAC-mediated cAMP increase is PKA- and NMDAR-dependent, but calcium-independent, requires synaptic activity, and induces glutamate gliotransmission. To gain deeper insights into the *in vivo* effects of astrocytic DdPAC activation, we performed phospho-proteomics and proteomics analyses. Our omics data validated the involvement of the cAMP-PKA signalling pathway in astrocytic DdPAC-mediated effects, further supported its main role in synaptic plasticity, while also revealing a broad brain effect of astrocytic activation.

Collectively, the data from the second objective position DdPAC as a powerful tool for modulating synaptic plasticity in the brain through targeted manipulation of the cAMP-PKA pathway in astrocytes, while also establishing a robust, minimally invasive method for its *in vivo* application.

Finally, we pursued our **third objective of restoring physiological function through light-driven DdPAC stimulation in mouse models of HD and AD.** We began by investigating the functional effects of astrocytic DdPAC activation in the two most affected regions in HD, the cortex and striatum. To this end, DdPAC was injected into cortical or striatal astrocytes of the R6/1 mouse model to assess its ability to modulate brain function. First, in cortical DdPAC stimulation experiments, we examined hemodynamic changes using a light scattering imaging technique, followed by an evaluation of motor-related behaviour. Hemodynamic analysis revealed cortical overactivation following acute DdPAC activation in cortical astrocytes of R6/1 mice, a response not observed in wild-type (WT) mice. Moreover, repeated DdPAC stimulation in cortical astrocytes impaired coordination in R6/1 mice, as indicated by the vertical pole test, while enhancing motor learning in WT mice, assessed by the ARR. Notably, post-mortem analysis revealed increased GFAP expression only in WT mice after repeated stimulation and behavioural assessments. Next, we examined motor-related behaviour following DdPAC stimulation in striatal astrocytes. In this case, astrocytic DdPAC-mediated cAMP modulation impaired coordination in both WT and R6/1 mice, while sparing motor learning. Additionally, GFAP expression was elevated in both WT and R6/1 mice. Taken together, these results suggest that astrocytic DdPAC modulation varies depending on the brain region and molecular context, leading to distinct outcomes in the cortex and striatum of WT and R6/1 mice. Moreover, our data suggest that increased cAMP levels in astrocytes are detrimental in HD; therefore, strategies aimed at specifically reducing astrocytic cAMP may offer greater therapeutic potential for the disease.

In parallel, we investigated the effects of DdPAC-mediated cAMP signalling in neurons and astrocytes of the hippocampus, the most affected region in AD. For this purpose, we injected DdPAC into hippocampal neurons and astrocytes from WT and 5xFAD mice, followed by histological and proteomic analyses. Notably, histological analyses revealed a reduction in GFAP expression and amyloid-β deposits in the hippocampus where DdPAC was activated in astrocytes, but not where DdPAC was activated in neurons. Proteomic analysis of DdPAC-activated astrocytes revealed a response primarily associated with glial activation and immune processes, as well as synaptic plasticity, whereas neuronal activation predominantly influenced synaptic plasticity. In both cases, cytoskeletal regulation emerged as a key function, though the implicated proteins differed between neurons and astrocytes. Additionally, the effects of DdPAC activation in either neurons or astrocytes varied between WT and 5xFAD mice, indicating a differential effect dependent on the molecular context. These findings further support the notion that the effects of DdPAC modulation are dependent on brain region, molecular context, and cell type specificity.

In summary, this thesis provides new insights into the cAMP pathway in synaptic plasticity and neurodegenerative disorders. First, our data demonstrates the involvement of neuronal cAMP in M2 cortical behaviours and reveal altered neuronal cAMP dynamics in HD mice. Additionally, we identify early motor and psychiatric M2-cortex-related impairments, highlighting the potential for early therapeutic interventions. To facilitate in vivo application, we establish a minimally invasive method for AAV delivery that successfully achieves transgene expression in specific cell types and mouse strains. Notably, we uncover the capacity of DdPAC-mediated cAMP signalling modulation to enhance synaptic plasticity in the cortex, particularly when activated in astrocytes. In the context of neurodegeneration, DdPAC activation in HD and AD models produces differential effects: in HD, cortical astrocyte activation improves motor learning in WT but impairs coordination in HD mice, while striatal astrocyte activation disrupts coordination in both. In AD, increasing cAMP in hippocampal astrocytes reduces astrogliosis and Aβ deposits, whereas neuronal activation decreases microglial reactivity. Proteomic analysis of hippocampal samples reveals distinct DdPAC-driven proteomic changes in neurons and astrocytes, as well as between WT and AD mice, linking cAMP-PKA pathway activation to synaptic plasticity and immune responses.

In conclusion, this thesis reveals new roles for cAMP signalling and propose it as a promising therapeutic target for neurodegenerative diseases. Our results show that DdPAC-mediated modulation of cAMP in both neurons and astrocytes profoundly affects neuronal plasticity, with astrocytic cAMP-PKA modulation producing more widespread effects. Additionally, our findings highlight the importance of brain region and molecular context in shaping the outcomes of cAMP modulation, as DdPAC activation produces distinct effects in the cortex, striatum, and hippocampus, which vary depending on the disease state. Ultimately, we provide strong evidence for DdPAC as a versatile tool to modulate cAMP-PKA signalling, with potential applications in neuroscience research and therapeutic development.

Key words: cAMP, Synaptic Plasticity, Optogenetics, Huntington's Disease, Alzheimer's Disease, Mouse models

RESUM

RESUM

Amb l'envelliment de la població, les malalties neurodegeneratives representen un problema creixent de salut pública, que podria derivar en una càrrega social i econòmica insostenible si les tendències actuals persisteixen. Sorprenentment, la majoria d'aquestes malalties no tenen cura i ni tan sols un tractament efectiu que millori la qualitat de vida de les persones afectades. Una característica distintiva dels trastorns neurodegeneratius és la disfunció sinàptica, que apareix tot i l'absència de pèrdua neuronal, i està provocada per l'acumulació de proteïnes mal plegades, la qual cosa condueix a alteracions moleculars, de circuits i funcionals (Palop 2006). No obstant això, els mecanismes exactes que provoquen aquestes alteracions específiques encara no es comprenen del tot. Això posa de manifest la necessitat d'aprofundir en la comprensió d'aquestes malalties i, encara més important, la necessitat urgent de desenvolupar noves estratègies terapèutiques, potencialment basades en la modulació de la plasticitat cerebral.

En aquesta tesi, ens hem centrat en dues malalties neurodegeneratives: la malaltia de Huntington (MH) i la malaltia d'Alzheimer (MA). La MH és un trastorn neurodegeneratiu genètic autosòmic dominant, caracteritzat per una degeneració progressiva de les regions estriatals i corticals del cervell (Huntington, 2003; Walker, 2007). La malaltia es manifesta amb dèficits motors com la corea, la distonia i la descoordinació, així com amb deteriorament cognitiu i alteracions psiquiàtriques. La MH està causada per una mutació en el gen de la huntingtina (*HTT*), amb una repetició expandida del triplet CAG que dona lloc a una forma mutada de la proteïna huntingtina (mHTT), la qual condueix a la neurodegeneració (The Huntington's Disease Collaborative Research Group, 1993a). La MH es caracteritza per una pèrdua neuronal selectiva i una plasticitat sinàptica deteriorada, especialment en l'escorça cerebral i l'estriat, on les neurones espinoses mitjanes són especialment vulnerables (Vonsattel & DiFiglia, 1998). La disrupció de la via escorça-estriat, que té un paper fonamental en les funcions motores i cognitives, contribueix als símptomes de la malaltia (Cepeda et al., 2007). L'MA, per la seva banda, és la causa principal de demència i es caracteritza per un deteriorament progressiu de la memòria, així com per alteracions del llenguatge, la funció executiva i les habilitats visuoespacials (Scheltens et al., 2021; Stelzmann et al., 1995). L'MA es classifica en familiar, causada per mutacions en gens com APP, PSEN1 i PSEN2, amb un inici precoç que representa menys del 0,5% dels casos, i MA esporàdica, que representa el 99,5% dels casos i està influïda per factors genètics, ambientals i d'estil de vida (Bateman et al., 2011; Bertram et al., 2010). L'MA es caracteritza per la presència de plaques amiloides, cabdells neurofibril·lars i neuroinflamació. La disfunció sinàptica, especialment a l'hipocamp, es correlaciona de manera directe amb el deteriorament cognitiu observat en l'MA (Querfurth & LaFerla, 2010). Per tant, la plasticitat sinàptica constitueix una alteració primerenca en ambdues malalties, fet que destaca la necessitat de desenvolupar estratègies terapèutiques que específicament es focalitzin en aquests canvis inicials.

La plasticitat sinàptica és el mecanisme mitjançant el qual les connexions sinàptiques al cervell s'enforteixen o s'afebleixen en resposta a diversos estímuls. Les alteracions en aquest procés constitueixen una de les principals característiques de la MH i la MA, contribuint de manera

significativa als dèficits funcionals observats en aquestes patologies (J. Y. Li et al., 2003; Selkoe, 2002). En la plasticitat sinàptica a llarg termini, l'activació dels receptors per neurotransmissors desencadena vies de senyalització que afavoreixen l'enfortiment sinàptic, sovint associades a l'entrada de calci. Un component clau d'aquest enfortiment és la inserció de nous receptors a la membrana postsinàptica, un procés que requereix l'activitat de proteïnes quinases i la síntesi local de proteïnes. Més enllà del calci, una altra molècula de senyalització fonamental pel manteniment de la plasticitat és el monofosfat d'adenosina cíclic (AMPc). L'AMPc és modulat per l'activitat de receptors metabotròpics i, entre múltiples dianes, activa la proteïna quinasa A (PKA), la qual fosforila factors de transcripció com CREB, iniciant així l'expressió gènica necessària per a les modificacions sinàptiques a llarg termini (Benito & Barco, 2010). A més, la via de senyalització AMPc-PKA és essencial per establir canvis estructurals a les sinapsis, i la seva activació s'ha associat amb una plasticitat sinàptica enfortida en diverses regions cerebrals (C. C. Huang & Hsu, 2006; Nguyen & Kandel, 1997). Paral·lelament, els astròcits també contribueixen a la plasticitat sinàptica. No obstant això, els mecanismes pels quals l'AMPc participa en la plasticitat sinàptica encara no s'han comprès del tot, ni tampoc el seu paper específic en neurones o astròcits.

De fet, les alteracions en la senyalització de l'AMPc estan sent cada vegada més relacionades amb l'envelliment i amb malalties neurodegeneratives com MH i MH (Kelly, 2018). Tant la via escorça-estriat en MH com l'hipocamp en MH mostren disrupcions en la via de senyalització AMPc-PKA. En el cas de la MH, s'ha descrit una disminució de la senyalització de l'AMPc en l'escorça i l'estriat, i un augment a l'hipocamp, tot i que aquests resultats continuen sent controvertits. En canvi, en la MH està més ben establert que la senyalització d'AMPc disminueix a l'hipocamp, contribuint de manera clau al desenvolupament de la patologia associada a la demència. **Davant les controvèrsies sobre el paper** d'AMPc **en MH, i considerant la gran importància de l'escorça en aquesta malaltia, el nostre primer objectiu és caracteritzar les alteracions en la senyalització d'AMPc i el comportament associat amb l'escorça del model murí R6/1 per a la malaltia.**

Per tant, estratègies dirigides a potenciar la plasticitat sinàptica mitjançant la modulació de la senyalització de l'AMPc podrien tenir un gran potencial per mitigar o retardar la disfunció de xarxes neuronals associada a trastorns neurodegeneratius com la MH i la MA. En aquest sentit, les eines optogenètiques permeten un control precís de mecanismes biològics mitjançant proteïnes sensibles a la llum. Particularment, les adenilat ciclases fotoactivades (PACs) són enzims que augmenten els nivells d'AMPc en resposta a la llum, mitjançant un domini d'adenilat ciclasa acoblat a un mòdul fotorreceptor (Iseki & Park, 2021). Entre aquestes, la DdPAC és una PAC recentment optimitzada que regula els nivells d'AMPc en resposta a llum vermella (Stüven et al., 2018). Desenvolupada inicialment en bacteris, la DdPAC ha demostrat una resposta a la llum més potent en comparació amb altres PACs sensibles a la llum vermella. No obstant això, la seva aplicació en cèl·lules cerebrals i *in vivo* encara no ha estat explorada. **Considerant la capacitat de la llum vermella per penetrar en els teixits amb una dispersió mínima, DdPAC representa una eina prometedora**

per a aplicacions no invasives. Per tant, el nostre segon objectiu és establir l'ús de DdPAC com a eina optogenètica per modular la plasticitat sinàptica *in vivo*, de manera no invasiva.

D'altra banda, donada la vulnerabilitat regional i les diferències patofisiològiques observades entre MH i la AD, que poden afectar a la modulació d'AMPc i plasticitat sinàptica, **el nostre tercer objectiu és restaurar la funció fisiològica mitjançant l'estimulació lumínica de DdPAC en models murins de totes dues malalties.** En aquest cas, l'atenció se centrarà en les regions més afectades en cada patologia: l'estriat i l'escorça en el cas de la MH, i l'hipocamp en la MA.

Tenint en compte aquesta informació, l'objectiu principal d'aquesta tesi és restaurar la funció fisiològica en malalties neurodegeneratives mitjançant la modulació de la plasticitat cerebral a través de l'activació lumínica de la senyalització d'AMPc, mediada per DdPAC, en circuits cerebrals específics

Per assolir **el nostre primer objectiu i caracteritzar les alteracions en la senyalització** d'AMPc **i el comportament relacionat amb l'escorça en el model murí R6/1 de la malaltia de Huntington,** primer vam avaluar les alteracions d'AMPc en l'escorça durant tasques de comportament relacionades amb la via escorça-estriat en ratolins R6/1. Per investigar la dinàmica d'AMPc, vam realitzar enregistraments de *fibre photometry* utilitzant el sensor GFlamp-1, un nou sensor d'AMPc, en neurones de l'escorça M2 de ratolins mascles i femelles WT i R6/1 de 14 i 20 setmanes d'edat, durant les tasques de *beetle-mania* (BMT) i rotarod accelerant (ARR). Primer vam avaluar la dinàmica d'AMPc durant la BMT, observant un increment dels nivells d'AMPc tant en els ratolins WT com en els R6/1 després de la introducció de l'escarabat. Malgrat que els ratolins R6/1 ja mostraven un comportament alterat durant el test, no es van detectar diferències en els nivells d'AMPc entre els genotips. Aquestes dades revelen la implicació de la senyalització neuronal d'AMPc durant la BMT, amb alteracions mínimes en els ratolins R6/1. Posteriorment, per entendre millor la contribució d'AMPc en tasques relacionades amb l'escorça M2, vam explorar la dinàmica d'AMPc durant l'ARR. Els nostres resultats estaven en línia amb els observats durant la BMT, ja que els nivells d'AMPc neuronal tant en ratolins WT com R6/1 augmentaven amb l'inici de la tasca. A diferència dels resultats obtinguts amb la BMT, en aquest cas vam observar una sobre-activació aberrant de l'escorça M2 en els ratolins R6/1. Finalment, per esbrinar si les alteracions en l'activitat d'AMPc durant tasques relacionades amb M2 són més evidents en etapes més avançades de la malaltia, vam repetir la BMT en la mateixa cohort de ratolins a les 20 setmanes, quan els animals són plenament simptomàtics. A aquesta edat, encara vam poder observar un augment d'AMPc neuronal en WT i R6/1 després de la introducció de l'escarabat. No obstant això, aquest increment fou significativament menor en els ratolins R6/1. En conjunt, aquests resultats destaquen la implicació d'AMPc neuronal en tasques relacionades amb l'escorça M2 i mostren alteracions en el context de la MH.

Atesa la importància crítica de l'escorça M2 en la fisiopatologia de la MH, també vam voler determinar si sorgeixen símptomes addicionals associats a la disfunció escorça-estriat en les primeres etapes de la malaltia en el model R6/1. Per fer-ho, vam seleccionar dues proves conductuals, el *adhesive removal test* i el *marble-burying test*, ambdues relacionades amb l'escorça M2 i la via escorça-estriat, i les vam dur a terme longitudinalment des de les 4 fins a les 16 setmanes d'edat. En el *adhesive removal test*, relacionat amb la via escorça M2–escorça somatosensorial–estriat, vam observar dèficits motors des de les 8 setmanes, mentre que els dèficits somatosensorials van aparèixer a les 16 setmanes. En el *marble-burying test*, relacionat amb la via escorça M2–escorça orbitofrontal–estriat, vam observar un comportament similar a l'anhedònia des de les 8 setmanes. Aquestes dades indiquen que la disfunció de la via escorça-estriat sorgeix en estadis molt primerencs, remarcant el potencial de les intervencions terapèutiques precoces.

Globalment, els resultats d'aquest primer objectiu indiquen que la disfunció de la via escorça-estriat relacionada amb l'escorça M2 emergeix en estadis inicials de la malaltia, destacant el potencial de les intervencions terapèutiques en fases primerenques. Atès que la senyalització d'AMPc neuronal es manté funcional en ratolins amb comportament alterat, és poc probable que sigui la responsable directa dels dèficits conductuals relacionats amb M2, suggerint que altres mecanismes podrien estar involucrats.

Per assolir el **segon objectiu i implementar la DdPAC com a nova eina optogenètica per modular la plasticitat sinàptica de manera no invasiva a través de la senyalització d'AMPc**, primer vam voler establir un mètode mínimament invasiu per a la seva administració al cervell a través de vectors AAV. Per això, vam dissenyar constructes vírics amb GFP sota tres promotors diferents (CAG, CamKIIa i FLEXon), i les vam administrar utilitzant dos serotips d'AAV (AAV9 i PHP.eB), en dues soques de ratolins diferents (C57BL/6J i B6CBA), i mitjançant tres vies d'administració, de més a menys invasiva (intra-cranial, retro-orbital i intra-nasal). En resum, l'expressió de GFP es va detectar en diverses regions cerebrals i en tipus cel·lulars específics després de la injecció retro-orbital dels vectors PHP.eB i AAV9, mostrant el serotip PHP.eB una infecció més àmplia. A més, vam aconseguir expressar els constructes vírics de PHP.eB en dues soques murines i específicament en el nostre model R6/1. A més, la injecció retro-orbital en ratolins A2a-Cre va resultar en una transducció regional específica, demostrant el seu potencial per dirigir circuits específics. Tanmateix, no es va observar fluorescència de GFP després de l'administració intra-nasal en cap dels casos. Aquests resultats posen de manifest la injecció retro-orbital com una via mínimament invasiva per arribar a regions cerebrals de manera eficient i en diferents tipus cel·lulars i soques de ratolins, oferint una alternativa a la cirurgia estereotàxica. No obstant això, cal recerca addicional sobre la modificació de càpsides virals per facilitar la infecció de cèl·lules neurals via administració intra-nasal.

Per continuar amb aquest objectiu, vam caracteritzar els efectes de l'activació de DdPAC en tipus cel·lulars específics del cervell. En primer lloc, vam investigar si la modulació de AMPc mitjançant DdPAC era capaç d'afavorir la plasticitat sinàptica. Per això, vam injectar DdPAC

sota els promotors CamKIIa o GFAP a l'escorça per expressar-la selectivament en neurones i astròcits, respectivament, i posteriorment vam realitzar enregistraments amb matrius d'electrodes múltiples (MEAs). La il·luminació amb llum vermella va aconseguir potenciar l'activitat neuronal tant en l'activació neuronal com astroglial de la DdPAC, tot i que l'efecte va ser més pronunciat quan aquesta s'activava en astròcits. Per aquest motiu, els experiments següents d'aquest objectiu es van centrar en investigar l'activació de DdPAC en astròcits corticals. Així, vam caracteritzar el mecanisme subjacent d'aquesta potenciació, demostrant que l'augment d'AMPc induït per DdPAC és dependent de PKA i NMDAR, però independent del calci, requereix activitat sinàptica, i indueix gliotransmissió de glutamat. Per aprofundir en els efectes *in vivo* de l'activació astroglial de la DdPAC, vam realitzar anàlisis de fosfoproteòmica i proteòmica. Les dades òmiques van validar la implicació de la via AMPc-PKA en els efectes astroglials de la DdPAC, recolzant el seu paper central en la plasticitat sinàptica, alhora que revelant un efecte cerebral ampli derivat de l'activació dels astròcits.

En conjunt, les dades del segon objectiu posicionen la DdPAC com una eina potent per modular la plasticitat sinàptica al cervell mitjançant la manipulació dirigida de la via AMPc-PKA en astròcits, alhora que estableixen un mètode robust i mínimament invasiu per a la seva aplicació *in vivo*.

Finalment, vam abordar el nostre tercer objectiu: **restaurar la funció fisiològica mitjançant l'estimulació lumínica de DdPAC en models murins de la MH i la MA**. En primer lloc, vam investigar els efectes funcionals de l'activació astrocítica de DdPAC en dues de les regions més afectades en la MH: l'escorça cerebral i l'estriat. Per a això, vam injectar DdPAC en astròcits corticals o estriatals del model murí R6/1 per avaluar la seva capacitat de modular la funció cerebral. En els experiments d'estimulació cortical, es van analitzar els canvis hemodinàmics mitjançant una tècnica d'imatge basada en dispersió de llum i, posteriorment, es va avaluar el comportament motor. L'anàlisi hemodinàmica va revelar una sobre-activació de l'escorça després de l'activació aguda de DdPAC en astròcits de l'escorça dels ratolins R6/1, una resposta que no es va observar en ratolins control. A més, l'estimulació repetida de DdPAC en astròcits de l'escorça va deteriorar la coordinació en ratolins R6/1, tal com es va evidenciar en el test del pal vertical (*vertical pole*), mentre que va millorar l'aprenentatge motor en ratolins WT, avaluat mitjançant el test de rotarrod accelerat. A més, l'anàlisi post-mortem va revelar un augment en l'expressió de GFAP només en ratolins WT després de l'estimulació repetida i les proves conductuals. Tot seguit, vam examinar el comportament motor després de l'estimulació de DdPAC en astròcits estriatals. En aquest cas, la modulació d'AMPc mitjançant DdPAC en astròcits va deteriorar la coordinació tant en ratolins WT com R6/1, mentre que l'aprenentatge motor es va mantenir preservat. A més, l'expressió de GFAP va augmentar en ambdós grups. En conjunt, aquests resultats suggereixen que la modulació astrocítica de DdPAC produeix efectes diferenciats segons la regió cerebral i el context molecular, amb resultats diversos a l'escorça i a l'estriat en ratolins WT i R6/1. A més, les nostres dades suggereixen que l'augment dels nivells

d'AMPc en astròcits pot ser perjudicial en el context de la HD, de manera que estratègies dirigides a reduir específicament l'AMPc astrocític podrien tenir més potencial terapèutic.

En paral·lel, vam investigar els efectes de la senyalització d'AMPc mitjançant DdPAC en neurones i astròcits de l'hipocamp, la regió més afectada en la MA. Per a això, vam injectar DdPAC en neurones i astròcits de l'hipocamp de ratolins WT i 5xFAD, seguit d'anàlisis histològiques i proteòmiques. Notablement, les anàlisis histològiques van revelar una reducció en l'expressió de GFAP i en els dipòsits d'amiloide-β a l'hipocamp on s'havia activat DdPAC en astròcits, però no en les regions amb activació neuronal. L'anàlisi proteòmica d'astròcits activats per DdPAC va revelar una resposta principalment associada a processos d'activació glial i resposta immunitària, així com a plasticitat sinàptica, mentre que l'activació neuronal va influenciar majoritàriament la plasticitat sinàptica. En ambdós casos, la regulació del citoesquelet va emergir com una funció clau, tot i que les proteïnes implicades diferien entre neurones i astròcits. A més, els efectes de l'activació de DdPAC, tant en neurones com en astròcits, van variar entre ratolins WT i 5xFAD, indicant un efecte diferencial depenent del context molecular. Aquests resultats reforcen la idea que els efectes de la modulació mitjançant DdPAC depenen de la regió cerebral, del context molecular i de l'especificitat cel·lular.

En resum, aquesta tesi aporta nous coneixements sobre la via d'AMPc en la plasticitat sinàptica i les malalties neurodegeneratives. En primer lloc, les nostres dades demostren la participació d'AMPc neuronal en comportaments relacionats amb l'escorça M2 i revelen alteracions en la dinàmica d'AMPc neuronal en ratolins amb HD. A més, identifiquem dèficits motors i psiquiàtrics precoços associats a l'escorça M2, posant en relleu el potencial per a intervencions terapèutiques en fases inicials. Per facilitar l'aplicació de teràpies en el cervell, establim un mètode mínimament invasiu per a l'administració d'AAV que permet una expressió eficaç del transgen en tipus cel·lulars i soques murines específiques. Notablement, hem demostrat la capacitat de la modulació d'AMPc mitjançant DdPAC per potenciar la plasticitat sinàptica en escorça, especialment quan s'activa en astròcits. En el context de la neurodegeneració, l'activació de DdPAC en models de la MH i MA produeix efectes diferencials: en la MH, l'activació d'astròcits corticals millora l'aprenentatge motor en ratolins WT però deteriora la coordinació en ratolins amb MH, mentre que l'activació d'astròcits estriatals afecta negativament la coordinació en ambdós. En la MA, l'augment d'AMPc en astròcits de l'hipocamp redueix l'astrogliosi i els dipòsits d'amiloide-β, mentre que l'activació neuronal redueix la reactivitat microglial. L'anàlisi proteòmica de mostres hipocampals revela canvis diferencials induïts per DdPAC en neurones i astròcits, així com entre ratolins WT i AD, vinculant l'activació de la via AMPc-PKA a la plasticitat sinàptica i les respostes immunitàries.

En conclusió, aquesta tesi revela noves funcions de la senyalització d'AMPc i la proposa com una diana terapèutica prometedora en malalties neurodegeneratives. Els nostres resultats demostren que la modulació d'AMPc mitjançant DdPAC en neurones i astròcits té un impacte profund en la plasticitat neuronal, sent la modulació d'AMPc-PKA

en astròcits la que produeix efectes més amplis. A més, destaquem la importància de la regió cerebral i del context molecular en els resultats de la modulació d'AMPc, ja que l'activació de DdPAC produeix efectes diferenciats a l'escorça, estriat i hipocamp, i segons l'estat patològic. En última instància, aportem una evidència sòlida que posiciona DdPAC com una eina versàtil per modular la senyalització d'AMPc-PKA, amb aplicacions potencials tant en recerca en neurociència com en desenvolupament terapèutic.

Paraules clau: AMPc, Plasticitat Sinàptica, Optogenètica, Malaltia de Huntington, Malaltia d'Alzheimer, Models murins

ABBREVIATIONS

ABBREVIATIONS

AAV	Adeno-associated virus
AC	Adenylyl cyclase
AD	Alzheimer's Disease
ATP	Adenosine triphosphate
AKAP	A-kinase anchoring protein
AMPA	α-amino-3-hydroxy-5-methyl-4-isoxazole propionic acid
AMPAR	AMPA receptor
APP	Amyloid precursor protein
Aβ	Amyloid β
BBB	Blood-brain barrier
BDNF	Brain Derived Neurotrophic Factor
BLUF	Blue-light-utilizing flavin adenine dinucleotide
BPhy	Bacteriophytochrome
BTM	Beetle-mania task
CaMKII	Ca2+/calmodulin(CaM)-dependent protein kinase II
cAMP	Cyclic adenosine 3',5'-monophosphate
cAMP	cyclic adenosine monophosphate
CBF	Cerebral blood flow
CBP	CREB-binding protein
CNS	Central nervous system
CREB	cAMP response binding protein
CREM	cAMP responsive modulator
DBS	Deep brain stimulation
DG	Dentate gyrus
DREADs	Designer Receptors Exclusively Activated by Designer Drugs
EPSP	Excitatory post-synaptic potential
FAD	Flavin adenine dinucleotide
FMN	Flavin mononucleotide

ABBREVIATIONS

fMRI	functional MRI
GPCRs	G-protein-coupled receptors
HD-ISS	Huntington's Disease Integrated Staging System
HTT	Huntingtin gene
HTT	Huntingtin protein
iLID	Improved light-induced dimer
IP_3	Inositol trisphosphate
IPSP	Inhibitory post-synaptic potential
LFS	Low frequency stimulation
LTD	Long-term depression
LTP	Long-term potentiation
M2 cortex	Secondary motor cortex
MAPK	Mitogen-activated protein kinase
MCI	Mild cognitive impairment
MEA	Multi-electrode array recordings
MEK	MAPK/ERK kinase
mHTT	Mutant Huntingtin
MRI	Magnetic resonance imaging
MSN	Medium spiny neurons
NFT	Neurofibrillary tangles
NMDA	N-methyl-D-aspartate receptors
NMDAR	NMDA receptor
OF	Open field
OPCs	Oligodendrocyte progenitor cells
OPM	Output module
PAC	Photoactivatable adenylyl cyclase
PACAP	Pituitary adenylyl cyclase activating polypeptide
PCM	Photosensory core module

ABBREVIATIONS

PDE	Cyclic nucleotide phosphodiesterase
PHP.B	Peptide Hybrid AAV with Brain Delivery
PHP.eB	Peptide Hybrid AAV with Enhanced Brain Delivery
PRKAR1A	PKA catalytic unit
PKA	Protein kinase A
PKI	Protein kinase inhibitor
PLS-DA	Partial Least Squares Discriminant Analysis
PSEN1	Presenilin 1
PSEN2	Presenilin 2
sAC	Soluble Adenylyl Cyclase
TBS	Theta-burst stimulation
tmAC	Transmembrane Adenylyl Cyclase
TMS	Transcranial magnetic stimulation
TrkB	Tropomyosin receptor kinase B

TABLE OF CONTENTS

INTRODUCTION

1 Neurodegenerative diseases

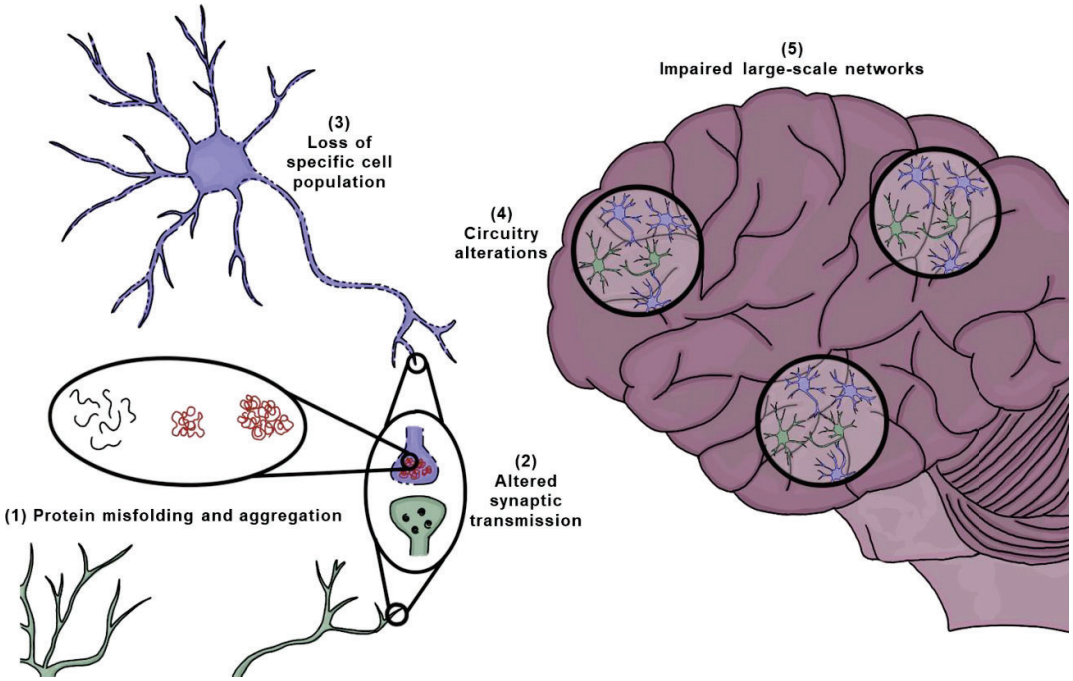

Figure 1. Neurodegenerative diseases compromise neuronal communication across multiple levels. (1) The accumulation of aberrant proteins can disrupt intracellular signalling pathways, (2) impairing synaptic communication, (3) affecting specific neuronal populations, (4) altering brain circuits within distinct regions, and (5) ultimately perturbing large-scale networks and brain functionality.

Neurodegenerative diseases represent a growing public health challenge worldwide, as life expectancy increases and the global population continues to age. These disorders form a diverse group of complex conditions that share common underlying mechanisms, ultimately leading to progressive neuronal dysfunction and cell death (Dugger & Dickson, 2017; Moujalled et al., 2021; Palop et al., 2006). They are typically characterised by the accumulation of misfolded proteins and selective anatomical vulnerability, resulting from abnormal protein processing in both hereditary cases – caused by mutations in specific protein-coding genes – and sporadic forms of the diseases (D. M. Wilson et al., 2023). However, neurodegenerative diseases also disrupt molecular pathways, synaptic function, neuronal subpopulations, and both local and high-order networks, all leading to functional impairment regardless of significant neuronal loss (Palop et al., 2006) (Figure 1). Consequently, these diseases can be considered primarily as disorders of neural circuits, in which synaptic plasticity is profoundly affected, thereby also defining them as "synaptopathies" (J. Y. Li et al., 2003; Selkoe, 2002). It is believed that a complex interplay of genetic, epigenetic, and environmental factors contributes to their development, although the precise mechanisms underlying its specific alterations is not fully understood (Dunn et al., 2019). Furthermore, despite extensive research, no effective treatments exist that significantly ameliorate the quality of life of the patients, and most proposed therapies fail in clinical trials(C. K. Kim et al., 2022; Travessa et al., 2017). This underscores the necessity for a better understanding of these diseases, and,

importantly, the urgent need for novel therapeutic strategies. Consequently, the primary aim of this thesis is to restore physiological functions in neurodegenerative diseases by modulating brain plasticity in targeted brain circuits.

1.1 Huntington's Disease

Huntington's Disease (HD) is an autosomal-dominant, genetic neurodegenerative disorder marked by the progressive degeneration of striatal and cortical brain regions (Huntington, 2003; Walker, 2007). This leads to a distinct phenotype characterised by motor deficits that present in early middle life, such as chorea, dystonia, and incoordination, alongside cognitive decline and psychiatric impairments (Walker, 2007). HD is considered a rare disease although it is also the most prevalent monogenic neurodegenerative disease and the most common genetic dementia, with an estimated incidence of 0.38 cases per 100.000 person-years and a prevalence of 2.71 per 100000 persons as of 2010 (Pringsheim et al., 2012). However, more recent estimates suggest a slightly lower incidence of 0.48 cases per 100.000 person-years and prevalence of 4.88 per 100000 persons as of 2022 (Medina et al., 2022). Moreover, a geographical analysis revealed a significantly lower incidence in Europe (6.63/100000 person-years), compared to the higher incidence in North and South America (8.87/100000 person-years; 11.42/100000) (Medina et al., 2022). Exceptions are observed in regions with populations that can be traced back to a small number of founders, such as Tasmania and the area surrounding Lake Maracaibo in Venezuela, where the incidence dramatically increases (Gusella et al., 1983; Paradisi et al., 2008).

In the 19th century, several physicians observed the hereditary nature of chorea, but it was not until 1872 that George Huntington ultimately gave the disorder its eponymous name, Huntington's Disease, along with a description of a hereditary form of chorea (Huntington, 2003). Over the following decades, the disorder was documented globally, with a major breakthrough coming in 1993, when the Huntington's Disease Collaborative Research Group discovered the gene responsible for it (The Huntington's Disease Collaborative Research Group., 1993). This event triggered a wave of research, which continues nowadays with efforts centred in understanding the disease's molecular mechanisms and exploring potential treatments, as currently there are no disease-modifying therapies for HD (McColgan & Tabrizi, 2018; Stoker et al., 2022; Walker, 2007).

1.1.1 Aetiology

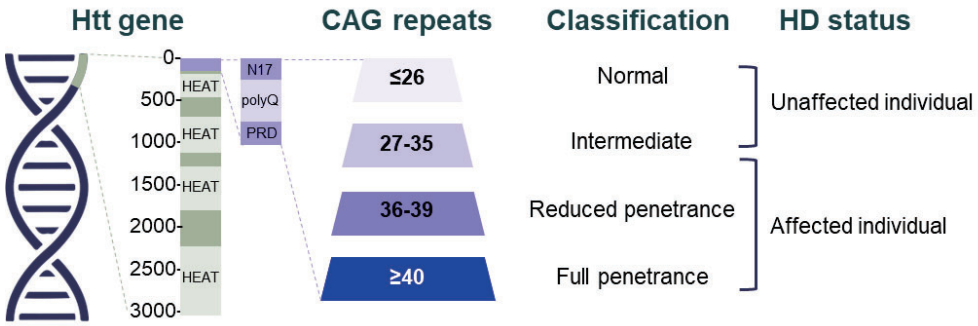

Figure 2. *HTT* gene and CAG repeat length categorisation. Schematic representation of the *HTT* gene, illustrating its amino acid sequence, including its polyglutamine stretch (PolyQ), proline-rich domain (PRD), and HEAT (Huntingtin, elongation factor 3, protein phosphatase 2A and TOR1) domains. The number of CAG repeats in the tract determines a phenotypic classification based on clinical manifestation of HD, which categorises the individual as either unaffected or affected.

HD is a monogenic neurodegenerative disease with an autosomal dominant inheritance (Walker, 2007). The causative gene named huntingtin (*HTT*), located within the first exon on the short arm of chromosome 4, encodes the Huntingtin protein (HTT). This gene harbours an expanded CAG trinucleotide repeat in the coding sequence of the protein, leading to the production of mutant HTT (mHTT), characterised by an abnormally elongated polyglutamine tract (Gusella et al., 1983; The Huntington's Disease Collaborative Research Group, 1993b). Normal alleles of the *HTT* gene contain CAG repeats, but individuals with more than 39 CAG repeats will inevitably develop HD. Alleles with 36 to 39 repeats exhibit incomplete penetrance, whereas those with 35 or fewer are not associated with the disorder (Figure 2). The length of the CAG repeats expansion accounts for approximately 60% of the variance in age of onset, with the remaining variation attributed to genetic and environmental modifiers (McColgan & Tabrizi, 2018; Snell' et al., 1993; Walker, 2007).

The age of onset of HD occurs at a younger age in successive generations, particularly when inherited paternally in cases of juvenile onset. This phenomenon is attributed to the genomic instability of CAG trinucleotide repeats exceeding 28 during replication, with larger repeat expansion showing greater instability (Kremer et al., 1995; Ranen et al., 1995). Furthermore, this instability is more pronounced during spermatogenesis compared to oogenesis, as significant expansions of CAG repeats occur almost exclusively in males (Ranen et al., 1995). Thus, alleles within the higher end of the intermediate range of CAG repeats may enlarge into the pathogenic range, especially when inherited through the paternal line (Kremer et al., 1995; Walker, 2007).

1.1.2 Clinical features

HD typically presents with a triad of clinical features, including motor, cognitive, and psychiatric symptoms, yet it has traditionally been recognised as a movement disorder due to chorea being its most characteristic feature (Huntington, 2003; McColgan & Tabrizi, 2018;

Walker, 2007). Accordingly, classical diagnostic criteria define disease onset as the moment when an individual with a CAG-expanded *HTT* allele begins to exhibit motor symptoms such as chorea, dystonia, bradykinesia, or rigidity (Kieburtz, 1996; Ross et al., 2014). Patients typically remain asymptomatic for many years before experiencing initially subtle but progressively worsening cognitive changes. This progression can be categorised into two main phases: the "premanifest" and "manifest" periods. The premanifest phase starts with a "pre-symptomatic" phase in which individuals do not exhibit clinical symptoms, typically lasting from 10 to 15 years prior the onset of symptoms, and then moves to the "prodromal" phase, characterised by subtle motor, cognitive, and behavioural changes. These subtle features are then followed by the "manifest phase", which is the onset of a movement disorder, predominantly characterised by chorea (Kieburtz, 1996; Ross et al., 2014; Stoker et al., 2022). Nevertheless, this classification is only based on clinical criteria, overlooking the comprehensive nature of the disease and omitting biomarkers related to disease progression, which can occur decades before functional decline. Thus, an evidence-based framework named the Huntington's Disease Integrated Staging System (HD-ISS) has recently been developed in order to address these limitations, stratifying the disease into four distinct stages (Figure 3) (Tabrizi et al., 2022). Stage 0 includes individuals with ≥40 CAG repeats who exhibit no signs of neurodegeneration or clinical symptoms, and consequently, have no detectable pathological biomarkers, signs, symptoms, or functional alterations associated with HD. In stage 1, neurodegeneration can be identified by a measurable indicator of underlying pathophysiology. Then, when a clinical phenotype such as motor or cognitive symptoms can be detected, stage 2 begins. Finally, stage 3 is characterised by a decline in functional capacity, including challenges in performing activities of daily living. Stage classification is determined by the pattern in which threshold criteria for key variables are met (Long et al., 2023; Tabrizi et al., 2022). Each variable has a specific cut-off value, and if any of the landmark variables exceed this threshold, the individual is assigned to the corresponding stage (Figure 3).

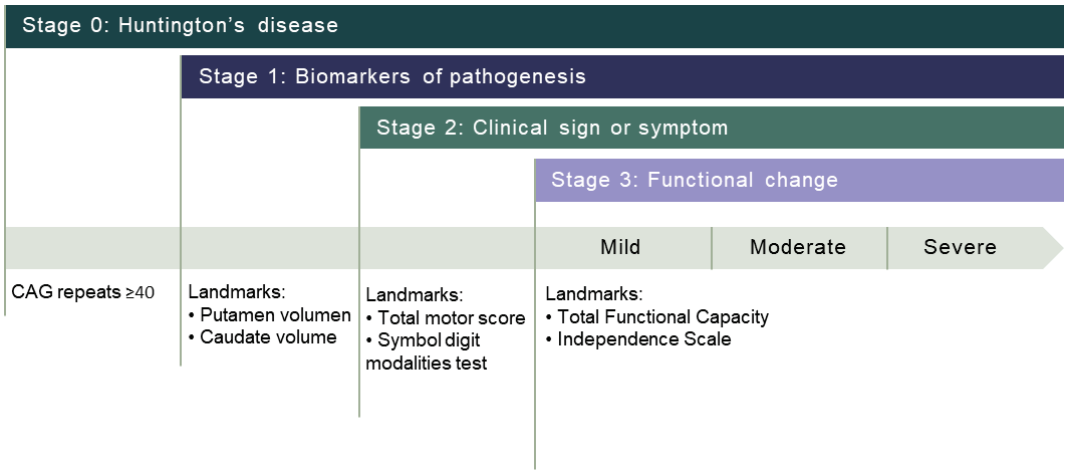

Figure 3. Comprehensive framework for the Huntington's Disease Integrated Staging System. Representation of the sequential stages of progression (from 0-4) and key landmark assessment, which define the transition into the next stage. Adapted from (Tabrizi et al., 2022).

As the disease progresses, the movement disorder evolves, moving from a hyperkinetic to a more hypokinetic state, along with a decline in cognitive function, and the emergence of mood swings. Additionally, cognitive impairments represent a significant aspect of HD, which appear during the initial stages of the disorder, and are a major factor contributing to disability, impairing executive functions and delaying the acquisition of new motor skills, worsening progressively over time (Giralt et al., 2012; Lemiere et al., 2004; Walker, 2007). Emotional disturbances and personality alterations are also frequently observed and can lead to distress, although they are not universally experienced and do not appear to progress in a linear trend (Ross et al., 2014). Psychiatric and behavioural symptoms in HD commonly emerge and can include depression, suicidal ideation, mania, and psychosis (Jauhar & Ritchie, 2010); however, they do not exhibit a consistent progression in relation to disease severity. After the onset of symptoms, patients may live around 15 to 20 years (Stoker et al., 2022; Walker, 2007).

1.1.3 Neuropathology and pathophysiology

HTT protein is expressed ubiquitously in all animals and human cells, with particularly high concentrations in the brain, and although its precise physiological function remains uncertain, there is some evidence that it may play a key role in proper brain development, transcriptional regulation, vesicle transport, and synaptic transmission (Reiner et al., 2003; Saudou & Humbert, 2016). The mutant form of huntingtin is prone to aggregation, and its pathogenicity is thought to result from both a toxic gain-of-function and a loss-of-function effect. However, the specific mechanisms underlying the resulting neurodegeneration remain poorly understood. Several processes have been implicated, including direct effects of the exon 1 *mHTT* fragment and the impact of mHTT aggregates on cellular proteostasis, axonal transport, transcription, translation, as well as mitochondrial and synaptic function (Dinamarca et al., 2022; J. H. Lee et al., 2015; W. Song et al., 2011; Wanker et al., 2019; Y. C. Wong & Holzbaur, 2014). Notably, despite widespread expression of mutant HTT across all cells, primary neuropathological alterations are observed in the cerebral cortex and striatum.

Neuronal degeneration in HD is highly selective, with prominent cell loss and bilateral atrophy in the caudate and putamen, the main input structure of the basal ganglia, representing a key histopathological feature. Specifically, medium spiny neurons (MSN), which are GABAergic neurons and comprise 95% of the striatal neuronal population, are particularly compromised in HD (Vonsattel et al., 1985; Vonsattel & DiFiglia, 1998). The loss and atrophy of this neuronal population subsequently leads to enlargement of lateral ventricles. Moreover, MSN in the striatum also exhibit pathway-specific vulnerability. Those in the indirect pathway of the basal ganglia, which express enkephalin, D2-like dopamine receptors, and project to the external globus pallidus, are particularly susceptible, whereas MSN in the direct pathway, characterised by substance P expression, D1-like dopamine receptors, and which project to the internal globus pallidus and substantia nigra pars reticulata, are relatively more resistant (Albin et al., 1992; Sapp et al., 1995). Therefore, MSNs of the indirect pathway are affected first, with subsequent degeneration of those in the direct

pathway. Interneurons, which are also primary GABAergic with some cholinergic population, remain largely intact and only die at late stages of HD (Ferrante et al., 1987).

The cortex is also profoundly affected in HD, exhibiting some of the earliest neuropathological alterations, even preceding substantial neuronal loss (Bunner & Rebec, 2016a; Estrada-Sánchez & Rebec, 2012). Notably, functional imaging studies have revealed early dysfunction in the prefrontal cortex of HD patients, even in pre-symptomatic individuals, with altered activation patterns in the dorsolateral prefrontal cortex during cognitive tasks (R. C. Wolf et al., 2007). These changes correlate with deficits in executive function, decision-making, and working memory, highlighting the prefrontal cortex, analogous to the secondary motor (M2) cortex in animal models, as a critical site of early pathology. Cortical dysfunction disrupts cortico-striatal connectivity, which is mainly glutamatergic, and impairs information processing (Miller et al., 2011). In particular, reduced functional connectivity between prefrontal regions has been observed in HD patients, further emphasising its profound impact (Thiruvady et al., 2007). Indeed, glutamate and dopamine dysregulation are known to contribute to the disrupted communication between the cortex and the striatum(Bunner & Rebec, 2016a; Dallérac et al., 2015; T.-H. Wong et al., 1982). The cerebral cortex supplies the caudate and putamen with the associative, limbic, and motor information necessary to guide suitable behavioural responses, and therefore changes in the cortico-striatal pathway in HD, particularly in premotor areas in mice (Fernández-García et al., 2020), account for the onset of motor symptoms, as well as cognitive and psychiatric disturbances (Cepeda & Tong, 2018; Tabrizi et al., 2009; Walker, 2007). Thus, chorea predominates in the early stages of the disorder due to the cortico-striatal pathway degeneration and preferential involvement of the indirect pathway within basal ganglia-thalamocortical circuitry.

Evidence of neuronal dysfunction is prevalent in early symptomatic stages, even among asymptomatic individuals (Milnerwood & Raymond, 2010). Cortical neurons display reduced staining for nerve fibres, neurofilaments, tubulin, and microtubule-associated protein 2. These alterations, which are linked to synaptic function, cytoskeletal integrity, and axonal transport, indicate a crucial role for cortical dysfunction in the pathogenesis of the disorder (DiProspero et al., 2004). Animal models have facilitated mechanistic understanding, also highlighting the fact that functional changes rather than cell death can account for a range of HD symptoms(Cepeda & Levine, 2022; Levine et al., 2004). Notably, the cortico-striatal pathway is one of the earliest and most affected pathways in the basal ganglia-thalamocortical circuitry, as disruptions in synaptic connections and miscommunication among the basal ganglia structures and cerebral cortex seem to be critical factors in the disease. This disrupted communication along the circuit supports the idea that HD is primarily a "synaptopathy" (Cepeda & Tong, 2018; J. Y. Li et al., 2003).

Multiple studies have shown that astrocyte dysfunction plays a significant role in the onset and progression of certain symptoms in HD. Astrocyte impairments are observed both in patients and mouse models with HD. Astrogliosis is observed in HD patients predominantly

in the caudate putamen (Faideau et al., 2010; Jansen et al., 2017; Vonsattel et al., 1985), and also in several animal models (Faideau et al., 2010; C.-H. Lin et al., 2001), but not in all of them, as it is the case of the widely used R6/1 and R6/2 (Mangiarini et al., 1996). Altered glutamate homeostasis is also associated to astrocyte dysfunction in HD. Specifically, loss of the cell surface glutamate transporter GLT1 and decreased glutamate synthesis has been observed in both the cortex and striatum of mice models (Khakh & Goldman, 2023; Liévens et al., 2001) and in human studies (Faideau et al., 2010; Shin et al., 2005), all leading to excitotoxicity. Furthermore, intracellular mHTT aggregates are also found in cortical and striatal astrocytes from both human tissue as well as mouse models (Jansen et al., 2017; Shin et al., 2005). K^+ homeostasis and Ca^{2+} signalling has been observed to be impaired in astrocytes from HD mouse models. Specifically, reduced Kir4.1 protein has been detected in astrocytes from the R6/2 mouse model (Tong et al., 2014), along with decreased spontaneous Ca^{2+} signals (Jiang et al., 2016a). Still, it remains unclear if astrocytes dysfunction precedes the onset of clinical symptoms or if it develops as a consequence of them.

1.1.4 Treatment

So far, no clinical trials have successfully identified disease-modifying treatments for HD, and as a result, therapeutic approaches remain mainly focused on symptom management. Current treatments address motor, cognitive, and psychiatric symptoms separately, with the goal of enhancing the quality of life for individuals affected by the disease (A. Kim et al., 2021). Choreic movements can be controlled with antipsychotic agents such as haloperidol or muscle relaxants such as benzodiazepines. Furthermore, Tetrabenzine (Xenazine) was the first treatment specifically approved against chorea, receiving authorisation in 2000 in the European Union and 2008 in the United States. Another therapeutic agent currently used to reduce muscle stiffness and rigidity is amantadine, a drug originally used for Parkinson's disease treatment, although its data on efficacy and safety is limited. Nevertheless, the exact mechanism of these treatments against choreic movements is still unknown, although it could be due to decreased uptake of monoamines into synaptic vesicles and depletion of monoamine storage. Common neuropsychiatric drugs are used to treat psychiatric symptoms, such as antidepressants or mood stabilisers (Xiang et al., 2024). Research during the past years has primarily focused on strategies to lower mutant huntingtin expression, although clinical trials for this approach have stalled (Kwon, 2021). Other approaches have also explored the use of phosphodiesterase inhibitors to modulate cyclic nucleotide signalling, which is known to be impaired in movements disorders (*See 3.3 section for more details*), although these have not yet yielded successful results either (Erro et al., 2021; Menniti et al., 2021).

1.1.5 Huntington's Disease mouse models

To date, several animal models such as zQ175, BACHD, and R6/1 and 2 have been developed for the study of HD, the majority of which are mouse models due to the relative ease of manipulating their genome and their comparatively short generation time. A large

number of this mouse models have been developed owing to the identification of the mutation responsible for HD and, consequently, the vast majority are genetically modified; although toxin-induced lesion models also exist, such as quinolinic acid injected rats (Ramaswamy et al., 2007). This section will provide a brief overview of the most commonly used genetic models. Subsequently, a more comprehensive description of the R6/1 mouse model employed in this thesis will be presented.

Genetically modified mouse models can be classified into knock-in or transgenic mouse models. Additionally, transgenic mouse models can be subdivided into truncated or full-length form, depending on the type of inserted gene.

Knock-in mouse models are based on genetic manipulations of the endogenous HTT gene, either by extending the CAG repeat sequence or by replacing the exon 1 of the gene. These models typically display early-onset symptoms and a slow progression of the disease (Menalled, 2005). The zQ175 line is among the latest and most used knock-in models, originating from a CAG expansion in the Hdh140 knock-in line (Menalled et al., 2012). The zQ175 model mimics many disease-related characteristics, effectively representing the early pathogenic changes observed in HD. The heterozygous zQ175 knock-in mice show robust phenotypes, showing hypoactivity in the open field (OF) starting at 4 months. On the other hand, homozygous zQ175 mice are more unstable, displaying motor symptoms from 4 to 8 weeks of age, coordination in the rotarod and climbing impairment at 30 weeks and cognitive deficits by 12 months (Peng et al., 2016). Neuropathological analysis reveal atrophy in both the striatum and neocortex of these mice, which appears from 3 month in homozygous and 4 months in heterozygous mice. Aggregates of mHtt are found extensively across the brain, while the number of neurons containing inclusions increases with age in both striatum and cortex (Peng et al., 2016).

In transgenic mouse models, the mutated human gene is randomly inserted into the mouse genome. The full-length models contain the entire length of the mutant human HTT gene, including all of its regulatory elements. BACHD and YAC128 are the two most popular full-length transgenic variants, which have regular lifespans and display slower progression of the disease compared to genetically modified truncated mouse lines (Gray et al., 2008; Slow et al., 2003). The YAC128 line expresses the full human HTT gene using a yeast artificial chromosome, 128 glutamines encoded by CAG and CAA repeats (Slow et al., 2003). Behavioural impairments start at 3 months of age and atrophy of the striatum and cortex is exhibited along with neuronal loss (Brooks et al., 2012; Van Raamsdonk et al., 2005). The BACHD line, on the other hand, expresses the full-length human HTT gene with 97 CAG repeats under endogenous control by use of a bacterial artificial chromosome (Gray et al., 2008). The phenotype is similar to that of the YAC128 line, with progressive motor deficits starting around 2 months of age and synaptic dysfunction in the striatal MSN population (Gray et al., 2008; Spampanato et al., 2008). These lines do not present somatic instability, which differentiates from the human condition (Gray et al., 2008; Slow et al., 2003).

The truncated lines only carry a shorter, fragmented form of the human HTT gene, usually containing only the portion of the gene with the expanded CAG repeat region. The first murine HD genetic models to be developed and the most studied are the R6 transgenic mouse lines (R6/1 and R6/2) (Mangiarini et al., 1996). The transgene used to develop these lines contains HTT promoter sequences, exon 1 of HTT, and around 200 base pairs of introns 1, which is translated to generate an exon 1 HTT protein. The R6/2 transgenic mouse model, developed in Dr. Gillian Bates's laboratory at King's College London just three years after the gene mutation was discovered, has been invaluable in advancing research on new treatments for HD and serves as the benchmark for drug testing. This model expresses 75% of the level of the endogenous gene and carries 144 CAG repeats (Mangiarini et al., 1996). This high number of repeats is translated into an early onset of symptoms and a fast progression of the disease compared to knock-in, BAC and YAC lines; the onset of symptoms starts around 4 weeks and their lifespan is limited to 10-17 weeks (Carter et al., 1999). However, it is important to note that in both R6/1 and R6/2 lines, CAG repeats are unstable during gametic transmission, tending to increase when passed through the male line and decrease through the female line, leading to variations across generations (Mangiarini et al., 1996).

The R6/1 line is the mouse model for HD used in this thesis due to its early onset of motor and cognitive impairments, which allows for the study of disease progression at premanifest and early symptomatic stages (Figure 6). It expresses 31% of the level of the endogenous gene and carries ~115 CAG repeats. Compared to the R6/2 mice, their symptoms progress slower and their lifespan is around 40 weeks (Mangiarini et al., 1996). As such, it is more suitable and sensitive model than the R6/2 mouse model for investigating early molecular and behavioural alterations, especially long-term effects of treatments. In the R6/1 mice, HTT aggregates are observed from 8 weeks, though no cell death is evident in this model (Naver et al., 2003; Turmaine et al., 2000). Dysregulation of protein synthesis contributes to striatal neuron dysfunction induced by mutant huntingtin (Creus-Muncunill et al., 2019). By 4 weeks of age, R6/1 mice exhibit initial hyperactivity, which later transitions to hypoactivity (Bolivar et al., 2004). Cognitive deficits are apparent by 8 weeks, as well as motor learning deficits, preceding coordination impairments (Brooks et al., 2012; Puigdellívol et al., 2015). Progressive weight loss and coordination deficits begin around 12 weeks, correlating with the number of striatal neurons containing intranuclear mHtt inclusions (Brooks et al., 2012; Hansson et al., 2001). A clasping phenotype emerges around 14 weeks, though not uniformly across individuals (Naver et al., 2003). Cortical dysfunction manifest before disruptions in the striatum and hippocampus (Puigdellívol et al., 2015), and cortico-striatal plasticity alterations seen by long-term depression deficits, are observed in symptomatic R6/1 (Ghiglieri et al., 2019). Sensorimotor alterations have also been observed around 16 weeks of age (Rodríguez-Urgellés, Casas-Torremocha, Sancho-Balsells, Ballasch, García-García, Miquel-Rio, Manasanch, Del Castillo, et al., 2023). Specifically, the M2 cortex connectivity is profoundly altered (Fernández-García et al., 2020). Moreover, astrocytic dysfunction is also observed in the R6/1 mouse model. Specifically, GLT1 glutamate receptor and glutamine

synthase are decreased in astrocytes from R6/1 mice (Khakh & Goldman, 2023; Liévens et al., 2001). Given the thorough characterisation of the R6/1 mouse model, it can facilitate the initial implementation of potential treatments. However, a deeper understanding of behavioural manifestations during the pre-symptomatic stages may be crucial for a more comprehensive understanding of the disease.

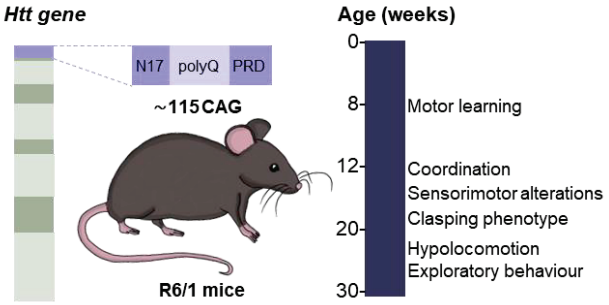

Figure 6. R6/1 mouse model for Huntington's Disease. Fragmented form of the human *HTT* gene inserted into the mouse genome. On the right, schematic representation of the timeline of behavioural characteristics of the R6/1 mouse model used in this thesis. First impairments are associated with cognitive function (motor learning) around 8 weeks, followed by motor function impairments around 12 weeks and sensorimotor alterations at 16 weeks.

1.2 Alzheimer's Disease

Alzheimer's Disease (AD), the leading cause of dementia, is a neurodegenerative disorder mainly associated with memory decline along with impairments in other cognitive domains, such as speech production, visuospatial skills, and executive function (Scheltens et al., 2021; Stelzmann et al., 1995). Currently, it is becoming one of the most expensive, fatal, and burdening diseases of this century, with the World Health Organization designating it as a major global public health concern (Dementia, 2025). AD is the most prevalent cause of dementia (Schneider et al., 2009), with an estimated incidence of 11.08 person-years and prevalence of 5.05% in Europe (Niu et al., 2017). However, several neurodegenerative or cerebrovascular pathologies can also result in dementia. Therefore, the epidemiology of AD is closely linked to that of all-cause dementia, which is expected to increase from 50 million people in 2010 to 113 million by 2050 worldwide (Brodaty et al., 2011). However, the incidence of dementia is slightly declining in some high-income countries such as the USA, UK and France(Y. T. Wu et al., 2017). This could be due to the educational, socio-economic, health-care, and lifestyle changes, and particularly the fact that superior educational levels can be a protective factor against dementia (Stern, 2012). Yet, efforts to establish cause-and-effect relationships between the different mitigating factors and the incidence of dementia have been challenging.

Dementia has been acknowledged for thousands of years although it was only in early 20th century that the main clinical disorder and the related neurodegenerative alterations were described. In 1907, Aloïs Alzheimer detailed the symptoms of a middle-aged woman named Auguste Deter, who was a patient at a state asylum in Frankfurt (Germany), and had a seriously impaired memory (Stelzmann et al., 1995). This description represents the first neuropsychological characterisation of the disease. Furthermore, after Auguste Deter's

death, Alzheimer conducted a microscopic examination of her brain, making the first observation of the Aβ-plaques and neurofibrillary tangles, that would later be recognised as key features of the disease(Scheltens et al., 2021; Stelzmann et al., 1995).

1.2.1 Aetiology

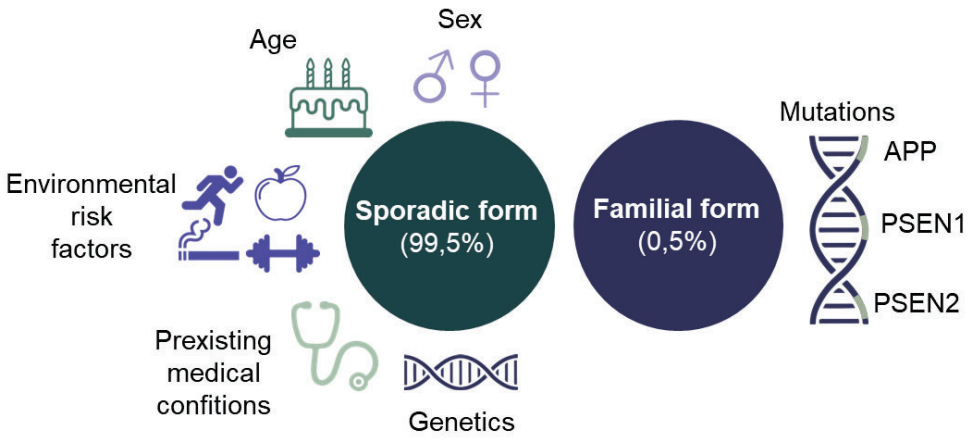

Figure 4. Aetiology of Alzheimer's Disease. Schematic representation of the genetic, environmental, and lifestyle factors contributing to the sporadic, most common form of AD, alongside the genetic mutations associated with the rare, familial form of the disease.

AD can be classified into two main types based on its origin: familial or inherited AD, which is a rare, inherited form caused by specific genetic mutations, and sporadic AD, which arises without a clear genetic link and is influenced by a combination of genetic, environmental, and lifestyle factors (Figure 4) (Lane et al., 2018). Most cases of AD, around 99,5%, appear to occur sporadically. The familial form of AD, in contrast, accounts for less than 0.5% of the cases, and presents due to mutations in three genes: amyloid precursor protein (APP), presenilin 1 (PSEN1) and presenilin 2 (PSEN2). The onset of symptoms arises earlier in the familial form of AD than in the sporadic form, typically between 30 and 50 years of age (Bateman et al., 2011; Bertram et al., 2010).

The most important risk factor for the sporadic for of AD is age. Moreover, women are more susceptible to developing AD than men, primarily due to having a higher tau load, even though their amyloid beta burden is similar (Buckley et al., 2019; Y. T. Wu et al., 2017). There are several potentially risk factors occurring in mid- and late-life that are also associated with an increased risk of later-life dementia, such as metabolic factors, hearing loss, traumatic brain injury, and alcohol abuse (Livingston et al., 2020). In later life, diabetes mellitus and hypertension are likely the most prevalent and significant risk factors, as both contribute to the development of cerebrovascular disease. Consequently, these conditions are believed to affect the clinical presentation of AD by modifying the effects of atherosclerotic and arteriolosclerotic cerebrovascular disease, rather than through a direct effect on Aβ or tau biology (Gottesman et al., 2017).

Specific genes are also significant risk factors for AD (Bertram et al., 2010), as studies of twins have showed that the risk of developing AD is 60-80% attributable to heritable factors (Gatz et al., 2006). Notably, carrying at least one APOE ε4 allele is the most important genetic risk factor for AD developing after 65 years. Carrying the APOE ε4 allele elevates the risk of dementia by 3 to 4 times in heterozygotes, and by 12 to 15 times in homozygotes, in comparison to individuals who carry the APOE ε3 allele (S. J. van der Lee et al., 2018). However, the common APOE ε4 allele accounts for a considerable part of the heritability of AD, but does not fully explain it. Extensive genome-wide association studies have identified other risk genes that contribute to a much smaller extend to the overall risk of the disease. TREM2, SORL1, and ABCA7 are some of the genes identified as susceptibility genes by next-generation sequencing techniques, and which can also help to predict incident dementia due to AD (Bellenguez et al., 2017).

1.2.2 Clinical features

The main cognitive domains affected in AD are memory, language, visuospatial and executive function, and they can be affected at different severities (Lane et al., 2018; Stelzmann et al., 1995). The most typical initial presentation of AD involves an elderly individual experiencing gradual but accelerated, progressive difficulties mainly related to episodic memory, at which stage the patient may meet the criteria for amnestic mild cognitive impairment (MCI). At this point, MCI progresses to variable degrees of impairment in language, special cognition, executive function, or working memory. As the condition advances, cognitive difficulties become more severe and widespread, disrupting daily activities, at which point the patient may be diagnosed with AD dementia (Figure 5). Moreover, increased dependence typically occurs, and as the disease progresses, behavioural changes, impaired mobility, hallucinations, and seizures may also develop (Lane et al., 2018). When the age of onset is over 70 years, amnestic presentations are most common, while non-amnestic presentation are typical in younger patients. Non-amnestic deficits can present as prominent visuospatial difficulties or progressive aphasia, among others. Both the amnestic and non-amnestic presentations of AD exhibit Aβ deposits throughout the brain, yet they display distinct, syndrome-specific patterns of tauopathy (Lehmann et al., 2013).

The assessment of the presence and severity of cognitive impairment is the first step of the diagnostic process, which is conducted by a clinician using information from someone close to the patient's daily life, along with the results of a cognitive evaluation of the patient. This information can help in assessing the severity of cognitive impairment and in making prognostic predictions (Knopman et al., 2021). Nevertheless, in order to confirm the diagnosis, biomarkers are crucial. MCI is not only caused by AD as any neurodegenerative or cerebrovascular disease could initially lead to it. Therefore, consideration of alternative disease sources should occur during the diagnosis and reliable biomarkers should be established in order to confirm AD diagnose. After the diagnose, the life expectancy of a patient is around 8 years from presentation, and currently there are no disease-modifying treatments (Jost & Grossberg, 1995).

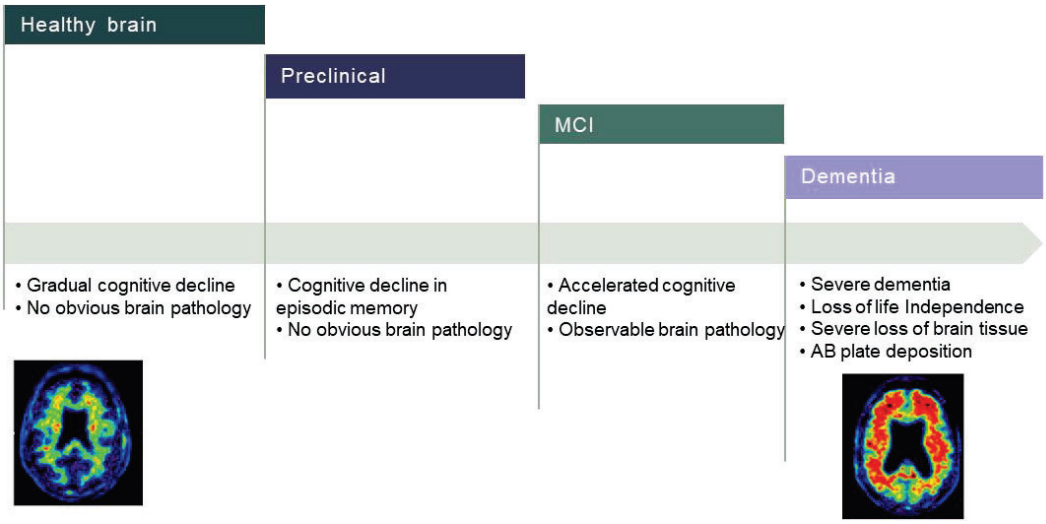

Figure 5. Clinical progression of Alzheimer's Disease. Progression of neurodegeneration from a healthy brain to dementia, illustrating the stages of preclinical, mild cognitive impairments (MCI), and dementia, alongside its main hallmarks. Florbetapir [18F] amyloid positron-emission tomography scans (Lane et al., 2018) depicting A*β* plaque depositions in a healthy brain (left) and a brain with AD dementia (right), highlighting the significant amyloid accumulation in AD patients.

1.2.3 Neuropathology and pathophysiology

AD is a disorder characterised by synaptic dysfunction, and involves failure at molecular, cellular, and macro-scale cortical circuitry levels (Querfurth & LaFerla, 2010; Selkoe, 2002). The main molecules contributing to canonical AD are Aβ-containing extracellular amyloid plaques and tau-containing neurofibrillary tangles (NFT) (Montine et al., 2012; Stelzmann et al., 1995). Additionally, neuropil threads, dystrophic neurites, associated astrogliosis and microglial activation, and subsequent inflammation are also characteristics of the disease (Fakhoury, 2017; Querfurth & LaFerla, 2010). Lastly, cortical thinning is a prominent feature, reflecting progressing neurodegeneration seen in AD (Dickerson et al., 2009).

Aβ plaques are distributed extensively across the cerebral cortex and, unlike tau-containing NFT, they also present in the entorhinal cortex and hippocampal formation (Arnold et al., 1991; Braak & Braak, 1991; Montine et al., 2012). The Aβ peptides originate from the amyloid precursor protein (APP), a transmembrane protein that is highly concentrated in neuronal synapses (Haass & Selkoe, 2007). Following synthesis, Aβ is released into the extracellular environment as a monomer. However, due to its specific amino acid sequence, it exhibits a strong tendency to aggregate in a concentration-dependent manner, and an imbalance between production and clearance ultimately causes Aβ to accumulate (Haass & Selkoe, 2007). Specifically, amyloid plaques are mainly composed of abnormally folded Aβ with 40 or 42 aminoacids. Furthermore, Aβ is produced at high levels due to synaptic activity, with both its generation and release tightly regulated by these processes, although it can be synthesised by all cell types (Querfurth & LaFerla, 2010). In its oligomeric form, Aβ is toxic, interacting with receptors such as metabotropic glutamate receptor 5 and N-methyl-D-

aspartate (NMDA) receptors (NMDAR), among others (Benarroch, 2018; Hoey et al., 2009). It also induces pathological alterations in dendritic spines and impair synaptic efficiency (Spires-Jones & Hyman, 2014). However, the accumulation of plaques in the brain does not correlate with cognitive impairments in patients (Giannakopoulos et al., 2003; Ingelsson et al., 2004).

On the other hand, tau-containing NFT first appear in pyramidal neurons from the medial temporal lobe and later extend to the isocortical regions of the temporal, parietal, and frontal lobes (Arnold et al., 1991; Ball, 1977; Braak & Braak, 1991). They are mainly composed of paired helical filaments that consist of hyperphosphorylated tau. Tau is a microtubule-associated protein which is typically located in the cytoplasm of axons but also found within both presynaptic and postsynaptic regions. It exists in six different isoforms, being the combination of 3R and 4R isoforms the ones occurring in AD. Tau's primary role is to stabilise microtubules; however, it is also vulnerable to post-translational modifications and aggregation. When these modifications occur, Tau accumulates in a hyperphosphorylated state within cell bodies and dendrites. Moreover, synaptic activity triggers the release of Tau into the extracellular space, and then it is taken by postsynaptic neurons and glia. When Tau aggregates as 3R and 4R isoforms, it appears in the tissue as neurofibrillary tangles, neuropil threads and dystrophic neurites. Importantly, the medial temporal lobe is the primary area affected by tauopathy, which is significant for cognitive function and can arise independently of Aβ pathology (Knopman et al., 2021; Lane et al., 2018). Importantly, the presence of tau correlate with cognitive decline observed in the disease (Giannakopoulos et al., 2003).

Chronic neuroinflammation, characterised by the activation of glial cells, is also observed in the cerebral cortex and hippocampus (Braak & Braak, 1991; J. A. Hardy & Higgins, 1992; Hyman et al., 2012). Specifically, microglia are highly responsible for the formation of Aβ plaques and remain in the site in an activated form, interacting with the depositions. Moreover, astrogliosis is also present in AD, both in patients and in animal models (Matsuoka et al., 2001; Nagele et al., 2003). Furthermore, the accumulation of reactive astrocytes is usually found surrounding amyloid plaques. This accumulation occurs through the phagocytosis of nearby degenerated dendrites and synapses (Fakhoury, 2017). During this process, astrocytes also release inflammatory cytokines, which further contribute to the neurodegenerative process (Fakhoury, 2017). Still, a more comprehensive understanding of the role of astrocytes and microglia in the modulation of AD pathology is essential, as it could be a target for new therapeutic approaches.

ApoE protein is encoded by APOE gene and is a key factor that integrates clinical, genetic and mechanistic aspects of AD (J. Kim et al., 2009; S. J. van der Lee et al., 2018). ApoE is synthetised in the brain mainly by astrocytes and activated microglia (J. Kim et al., 2009). Individuals carrying the APOE ε4 allele have an increased risk of developing AD in a dose-dependent manner, potentially due to ApoE's influence on modifying the clearance and seeding of Aβ in the brain (Huynh et al., 2017).

The amyloid hypothesis is still considered the most prevalent theory in AD pathogenesis (J. Hardy & Selkoe, 2002; Masters et al., 1985; Paroni et al., 2019). Based on studies of genetic forms of AD, it suggests that the accumulation of pathological Aβ, produced by the sequential cleavage of APP in the brain, is the primary pathological event. The formation of NFT and related neuronal dysfunction, along with neurodegeneration via neuroinflammation, are thought to be downstream processes (Lane et al., 2018). However, alternative hypotheses have also been proposed, such as tau being the initiating factor of pathology (Arnsten et al., 2021), or inflammation with activated microglia and astrocytes contributing to disease genesis (Mehta & Mehta, 2023), or also the cholinergic hypothesis, which posits that intracerebral acetylcholine deficiency plays a central role in the disease (P. P. Liu et al., 2019), among others.

Importantly, AD could be defined as a disorder primarily involving synaptic failure, as it is strongly correlated with cognition in patients with AD. Studies indicate that hippocampal synapses begin to deteriorate in individuals with mild cognitive impairment, evidenced by a significant reduction of approximately 25% in the presynaptic vesicle protein synaptophysin ((Koss et al., 2016; Querfurth & LaFerla, 2010). As the disease progresses, synaptic loss occurs at a higher rate compared to neuronal loss. Notably, the dentate gyrus of the hippocampus is among the regions most severely affected by this synaptic decline (Knopman et al., 2021; Querfurth & LaFerla, 2010).

1.2.4 Treatment

Although no treatments can stop or revers the progression of AD, some therapies can provide temporary relief of symptoms. The majority of current AD therapies include NMDAR agonists, such as memantine, and acetylcholinesterase inhibitors, such as donepezil. These drugs are considered traditional "symptomatic" treatments, as they aim to slow disease progression by improving cognitive and behavioural symptoms, but offer only limited and short-term efficacy and are often accompanied by significant side effects (Xiang et al., 2024). From January 2022, there are 143 therapeutic agents being investigated across 172 clinical trials for the treatment of AD, focusing on modifying the disease rather than only relieving symptoms. Notably, the U.S Food and Drug Administration approved two anti-amyloid monoclonal antibody treatments, aducanumab and lecanemab (Biogen), in June 2021 and January 2023, respectively, for the treatment of MCI associated with AD. Additionally, another anti- Aβ antibody, donanemab, is currently under review for approval in AD treatment (Xiang et al., 2024). Other strategies, such as phosphodiesterase inhibitors, are also being explored as potential treatments for AD, which is also known to involve impaired cyclic nucleotide signalling (*See 3.3 section for more details*) (Sanders & Rajagopal, 2020).

1.2.5 Alzheimer's Disease mouse models

Because the aetiology of AD is still not well understood, generating a reliable mouse model for AD presents a greater challenge compared to other neurodegenerative diseases like HD, in which the causative gene is well identified. For this reason, AD models are generally not as comprehensive in terms of mimicking all the pathological aspects of the disease, and therefore depending on the specific aim on each investigation, a specific model should be used. Because the morphological characteristics of familial AD and sporadic late-onset AD are comparable, researchers are using animal models containing familial AD mutations to study sporadic AD (Puzzo et al., 2015; Watamura et al., 2022). Affected genes in the familial AD mutations encode for APP, PSEN1 and PSEN2. Over the past 20 years, a number of AD mouse models that overexpress familial AD genes have been employed to assess the therapeutic results of *in vivo* drug screening as well as to offer a useful knowledge of the mechanism underlying Aβ pathology (Games et al., 1995; Hsiao et al., 1996; Trinchese et al., 2004; Zhang et al., 2013). Other strategies such as knock-in models or direct injection of Aβ or tau have also been applied (T. Saito et al., 2014). Therefore, the most widely used genetic models based on APP overexpression will be briefly reviewed in this section, followed by a more thorough explanation of the 5xFAD mouse model used in this thesis.

Single APP transgenic strains (PDAPP, J20, Tg2576, TgCRND8 or APP23 mouse strains) overexpress APP gene with FAD mutations such as the Swedish (K670N/M671L), which increase the total production and secretion of Aβ but does not change the Aβ42/40 ratio, or the Indiana (V717F) type, which elevates the Aβ42/40 ratio (Azhar Chishti et al., 2001; Games et al., 1995; Hsiao et al., 1996; Mucke et al., 2000; Sturchler-Pierrat et al., 1997). These mice generally display extracellular Aβ plaques in the brain, accompanied with synaptic loss, gliosis, and cognitive impairments (Watamura et al., 2022). While some of these strains demonstrate neuronal loss, none of them exhibit neurofibrillary tangles.

In order to study potential synergistic effects between familial AD mutations, transgenic mice containing multiple familial AD mutations were also developed. Double transgenic models, such as APP_{swe}/PSEN1dE9, and 5xFAD, exhibit more aggressive Aβ deposits, synaptic loss, memory deficits, and neuronal loss compared to single APP transgenic strains (Oddo et al., 2003); however, they do not exhibit NFT depositions either. A triple transgenic mouse, namely 3xTg, was also developed in order to recapitulate both the Aβ and NFT depositions (Oddo et al., 2003), overexpressing the APP Swedish, tau P301L, and PS1 M148V mutations. However, it is more challenging to understand the pathophysiological state of these animals due to the overexpression of multiple genes. This thesis employed the 5xFAD mouse model to capture the key hallmarks of AD while maintaining experimental simplicity and feasibility.

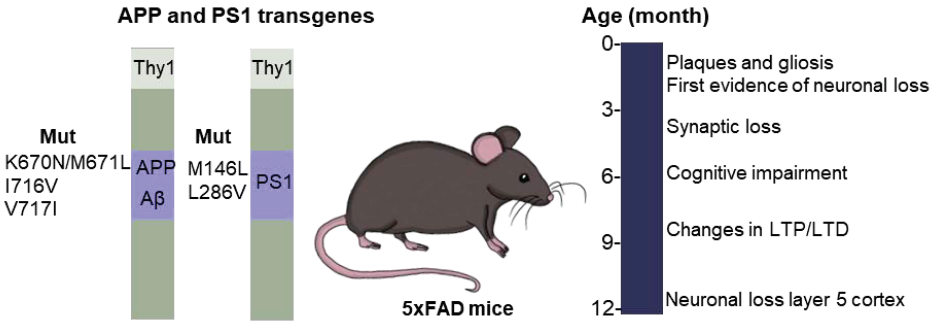

Figure 7. 5xFAD mouse model for Alzheimer's Disease. APP transgenes express the Swedish (K670N/M671L), Florida (I716V), and London (V717I) mutations together with mutant PS1 (M146L/L286V), regulated by the murine Thy1 promoter. On the right, schematic representation of the timeline of behavioural characteristics of the 5xFAD mouse model used in this thesis. Plaque deposition is one of the first observed hallmarks around 2 months followed by first evidences of neuronal loss, which are still observed at late stages of the disease. Cognitive impairment is observed around 6 months of age.

The 5xFAD mouse model is extensively used in AD research, as it replicates multiple AD-associated phenotypes, exhibiting an early onset and an aggressive, age-dependent progression (Figure 7). It was developed in 2006 and expresses human APP with the Swedish (K670N/M671L), Florida (I716V), and London (V717I) mutations together with mutant PS1 (M146L/L286V) regulated by the murine Thy1 promoter (Oakley et al., 2006). Strong neuronal loss is seen, in conjunction with elevated levels of $A\beta_{1-42}$, which quickly accumulates from 2 month of age in deep cortical layers and in the subiculum. Intraneuronal Aβ can also be observed from 1.5 month of age, just before the appearance of Aβ deposits. Aβ deposits progressively accumulate within the cerebral cortex, subiculum, and hippocampus, though they are also observed, albeit in smaller quantities, in the thalamus, brain stem, and olfactory bulb of older mice. The extend of astrogliosis and microgliosis corresponds to the level of Aβ deposition and initiates with the appearance of plaques. Closely linked to intra- and extracellular Aβ deposits, dystrophic neurites become apparent at 3 months of age. This is then followed by synaptic loss shown by decrease of synaptophysin, syntaxin, and postsynaptic density-95 markers start around 4 month of age and are significant from 9 month throughout the brain (Jawhar et al., 2012; Oakley et al., 2006; Pádua et al., 2024; Schaeffer et al., 2011). Neuronal loss is detected in the layer 5 of the cortex in 12-month-old mice. These mice exhibit an age-dependent phenotype, along with working memory deficits observed in an alternation task, as well as reduced anxiety levels demonstrated in the elevated plus maze task starting from 6 month of age (Jawhar et al., 2012).

2 Synaptic plasticity

Brain plasticity is a process that involves adaptive structural and functional changes that enable the brain to modify and reorganise itself. This process reflects the nervous system's ability to alter its activity in response to internal or external stimuli by reshaping structure, functions, or connections. Specifically, synaptic plasticity refers to changes at the synaptic level, involving adjustments at the synapse and therefore impacting communication between neurons. Understanding the molecular mechanisms governing synaptic plasticity across various brain regions and cell types is essential for uncovering the neural basis of both normal and pathological brain functions.

Santiago Ramon y Cajal introduced the concept of brain plasticity by illustrating that neurons are individual units capable of modifying their connections, describing axonal and dendritic changes that underlie learning, memory, and regeneration, and therefore establishing the foundations for modern neuroplasticity (DeFelipe, 2006). Years later, Donald Hebb expanded the concept of synaptic plasticity, suggesting that when two neurons fire simultaneously, their connection strengthens, making it more likely to fire again together in the future. With the same principle, he also said that when two neurons repeatedly fire in an uncoordinated manner, the connections between them weaken and they are more likely to act independently. This can be simplified to the principle "Cells that fire together, wire together; cells that fire apart, wire apart"(Citri & Malenka, 2008; Morris, 1999; Seung, 2000).

In 1897, Charles Sherrington introduced the term "synapse" to describe specialised structures enabling neuronal communication (Shepherd & Erulkar, 1997). Synapses are highly plastic and modulate signal transmission strength. Chemical synapses consist of a presynaptic active zone, a synaptic cleft, and a postsynaptic neuron, where neurotransmitters bind to specific receptors, initiating synaptic plasticity. Neurotransmitter receptors, including glutamatergic, dopaminergic, and GABAergic, transduce signals, leading to either excitatory (EPSP) or inhibitory (IPSP) postsynaptic responses (Feher, 2012; Hell & Ehlers, 2008).

Synaptic transmission changes occur over a range of temporal domains from milliseconds to hours, days, and probably longer (Citri & Malenka, 2008). Moreover, synaptic plasticity is categorised into short-term and long-term, depending on the time scale the plasticity is happening. Short-term synaptic plasticity refers to temporary changes in synaptic strength that last from milliseconds to a few minutes, reflecting the history of presynaptic activity (Luo et al., 2014). It is generally driven by alterations in the likelihood of neurotransmitter release, resulting from changes in the biochemical mechanisms leading synaptic vesicle exocytosis. Short-term synaptic plasticity is crucial for processing information on a rapid timescale and plays a role in filtering and modulating synaptic signals, affecting processes like sensory adaptation and short-term memory (Zucker & Regehr, 2002).

Long-term synaptic plasticity, in contrast, involves temporary changes in synaptic strength that can persist for minutes, hours, and potentially days. These long-term changes are partly

activity-dependent and modulated by experiences, which ultimately influence future behaviour. The brain represents both external and internal events as intricate spatiotemporal patterns within large groups of neurons, which can be understood as neural circuits. Experimental evidence for the presence of such long-lasting, activity-dependent changes in synaptic strength was first provided in 1973, when Bliss and colleagues reported a phenomena in which repetitive activation of excitatory synapses in the hippocampus was causing a potentiation of synaptic strength that could last for hours or even days (T. V. P. Bliss & L0mo, 1973). This was the first definition of long-term potentiation (LTP), which was then subject of extensive research due to its proposed significance in elucidating the cellular and molecular mechanisms underlying memory formation in the hippocampus (Martin et al., 2000; Whitlock et al., 2006). Nevertheless, it is now evident that hippocampal LTP represents only one of several distinct forms of long-term synaptic plasticity present in specific circuits within the mammalian brain (T. V. P. Bliss et al., 2016; Daida et al., 2024; Raymond, 2007).

2.1 NMDAR-dependent LTP

The most thoroughly investigated and exemplary form of synaptic plasticity is LTP that occurs in the CA1 region of the hippocampus (Figure 8). This process is initiated by the activation of NMDAR by glutamate. Indeed, our understanding of the molecular mechanisms underlying LTP largely originates from research on LTP at excitatory synapses on CA1 pyramidal neurons within hippocampal slices (Citri & Malenka, 2008; Malenka & Bear, 2004). Findings from these studies are frequently generalised to other regions of the brain.

NMDAR-dependent LTP is triggered by the release of presynaptic glutamate and postsynaptic depolarisation resulting from the simultaneous activation of multiple synapses (Malenka & Bear, 2004). This activation involves two major types of ionotropic glutamate receptors within the postsynaptic density: α-amino-3-hydroxy-5-methyl-4-isoxazole propionic acid (AMPA) receptors (AMPAR) and NMDAR (T. V Bliss & Collingridge, 1993; Man et al., 2000; Nicoll & Malenka, 1999). These receptors are typically co-localised on individual spines. AMPARs contain a Na+/K+ permeable channel that, upon activation, generates the majority of the inward current responsible for the excitatory synaptic response when the cell is near its resting membrane potential. In contrast, NMDAR exhibit significant voltage dependence due to the extracellular magnesium block of their channel at negative membrane potentials (Mayer et al., 1984). Consequently, during basal synaptic activity, NMDARs contribute minimally to the postsynaptic response. However, when the cell becomes depolarised, magnesium dissociates form its binding site within the NMDAR channel, allowing ion influx. Moreover, NMDARs allow Ca^{2+}, as well as sodium, to enter the postsynaptic density. Overall, LTP induction requires the activation of NMDARs during strong depolarisation, which results in an elevated concentration of postsynaptic Ca^{2+} (Malenka, 1991). Following the increase of Ca^{2+} levels within the postsynaptic density, several

signalling molecules participate in transforming this Ca^{2+} signal into a sustained enhancement of synaptic strength. Among these molecules there is Ca^{2+}/calmodulin (CaM)-dependent protein kinase II (CaMKII), which undergoes autophosphorylation upon LTP initiation (Barria et al., 1997; Citri & Malenka, 2008; Malenka & Bear, 2004).

The main mechanism underlying LTP expression at hippocampal CA1 synapses involves an increase in the number of AMPARs within the postsynaptic density, facilitated by activity-dependent modifications in AMPAR trafficking (Bredt & Nicoll, 2003). Newly expressed AMPARs in the postsynaptic density originate from recycling endosomes in the dendrites, which contain a reserve pool of AMPARs mobilised during LTP through a process dependent on the small GTP-binding protein Rab11a (M. Park et al., 2004). Upon exocytosis, AMPARs initially insert into perisynaptic sites, and then diffuse laterally to reach the postsynaptic density, aided by protein kinases like PSD-95 (Citri & Malenka, 2008).

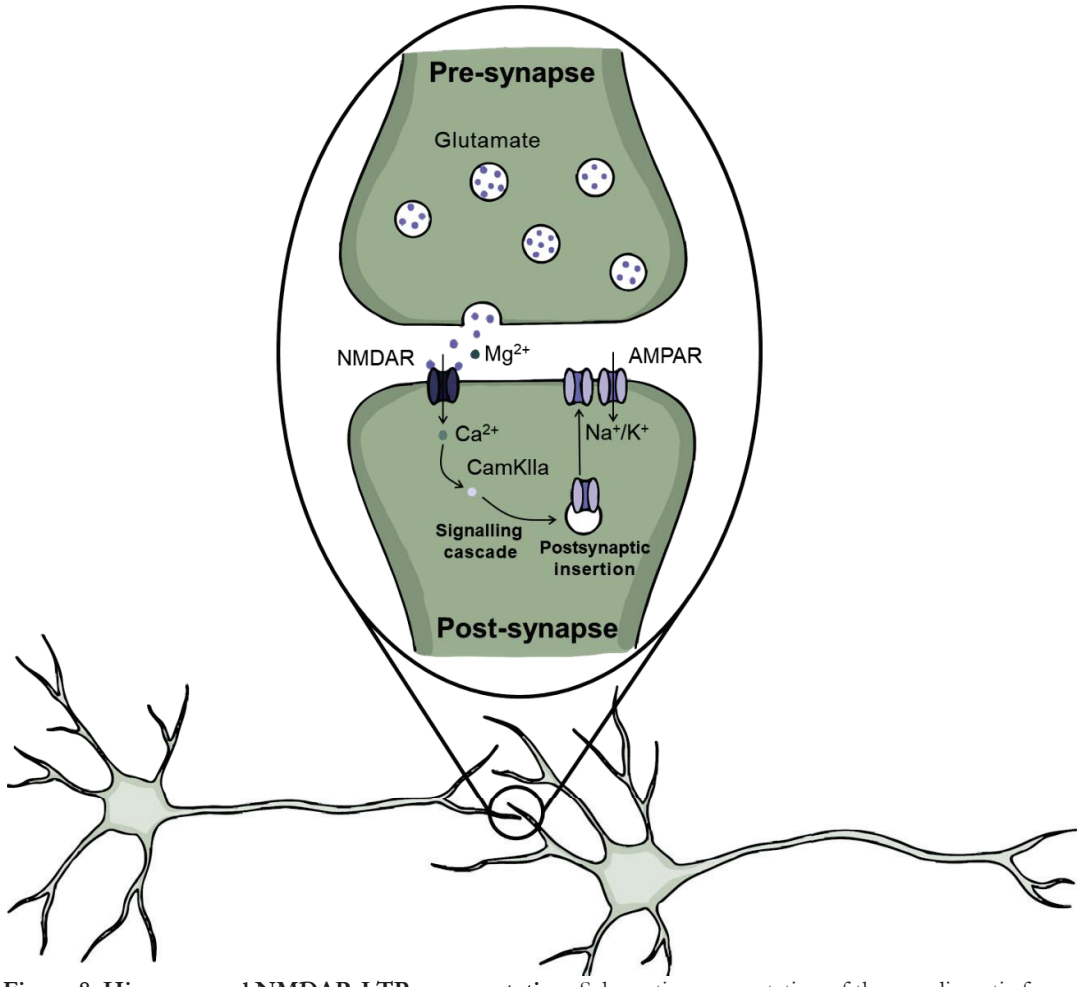

Figure 8. Hippocampal NMDAR-LTP representation. Schematic representation of the paradigmatic form of NMDAR-LTP occurring between the CA3 and CA1 neurons in the hippocampus. Presynaptic CA3 neurons release glutamate, which binds to NMDARs on post-synaptic CA1 neurons, causing the channel to open by displacing magnesium ions (Mg^{2+}) and allowing calcium ions (Ca^{2+}) to enter. This initiates a signaling cascade, starting with CamKIIa, which ultimately leads to the newly expression of AMPARs in the post-synaptic neurons, thereby maintaining synaptic activity.

LTP can persists for hours, days or even longer, and this sustained effect relies on local protein synthesis within dendrites, which provides essential components to the synapse. To achieve this, protein kinases, such as Protein Kinase A (PKA), activate transcription factors like cyclic adenosine monophosphate (cAMP) response binding protein (CREB), which stimulate the expression of effector genes necessary for sustaining synaptic enhancement (Impey et al., 1998) (*See 3.1 section for more details*). This process is followed by structural modifications, including enlargement of the postsynaptic density and dendritic spine, ultimately resulting in an expanded presynaptic active zone (J. E. Lisman & Harris, 1993).

Additionally, it has been well established that most synapses exhibiting LTP also display one or more forms of long-term depression (LTD)(Dudek & Bear, 1992), a process that, like LTP, relies on NMDAR activation but leads to a decrease in synaptic strength. While different NMDAR subtypes contribute to LTD, the expression of LTD involves the reduction and removal of both presynaptic and postsynaptic elements; however, the mechanisms underlying these changes are still not clear. LTD results in a decreased probability of glutamate release, which can be originated by alteration in either the presynaptic or postsynaptic terminal through retrograde messengers such as nitric oxide or endocannabinoids, particularly in the striatum, cortex, and cerebellum (Stanton et al., 2003; Yasuda et al., 2008). Like LTP, LTD is a postsynaptic process characterised by a decreased sensitivity to glutamate, which may result from the removal of AMPARs from the synapse or an alteration of the conductance properties of the receptors (Collingridge et al., 2010). In NMDAR-LTD, Ca^{2+} that enter through NMDARs bind to calmodulin, which activates the phosphatase calcineurin. This activation then initiates the activation of protein phosphatases that dephosphorylate AMPARs, ultimately resulting in LTD (Mulkey et al., 1993). Furthermore, the influx of Ca^{2+} induces the release of Ca^{2+} from intracellular stores, activating Ca^{2+} sensitive enzymes in the perisynaptic region that promote the endocytosis of AMPARs (Beattie et al., 2000). Protein synthesis is also required for LTD to be sustained, although the exact mechanisms are still not clear.

2.2 Astrocytes: the tripartite synapse

In 1846, Virchow was the first to identify a connective material within the brain that surrounds nervous elements, which he termed *Nervenkitt*, or "nerve glue", referring to what we now recognise as glial cells (Somjen, 1988). It is now well established that these cells serve functions far beyond merely sustaining neurons (Volterra & Meldolesi, 2005). In particular, astrocytes were traditionally thought to serve exclusively as supportive elements in brain function, relegating them to a secondary role within the central nervous system, with associated functions such as Ca^{2+} homeostasis and signalling, maintaining the blood-brain barrier (BBB), metabolic support for neurons, and clearance of extracellular ions and neurotransmitters (Alvarez et al., 2013; Bélanger et al., 2011; Duan et al., 1999; Verkhratsky & Kettenmann, 1996; Y. M. Zhang et al., 2023). Nevertheless, it is now well-known that astrocytes interact closely with neurons and actively regulate synaptic neurotransmission,

reinforcing the concept of the synapse as a tripartite structure(Araque et al., 1999; Halassa et al., 2007; Perea et al., 2009; Santello et al., 2019). In this model, astrocytes, together with pre- and postsynaptic neuronal components, are integral elements engaged in bidirectional communication, wherein astrocytes not only sense and respond to neuronal activity but also actively modulate neuronal and synaptic function (Figure 9)(Araque et al., 1999; Perea et al., 2009).

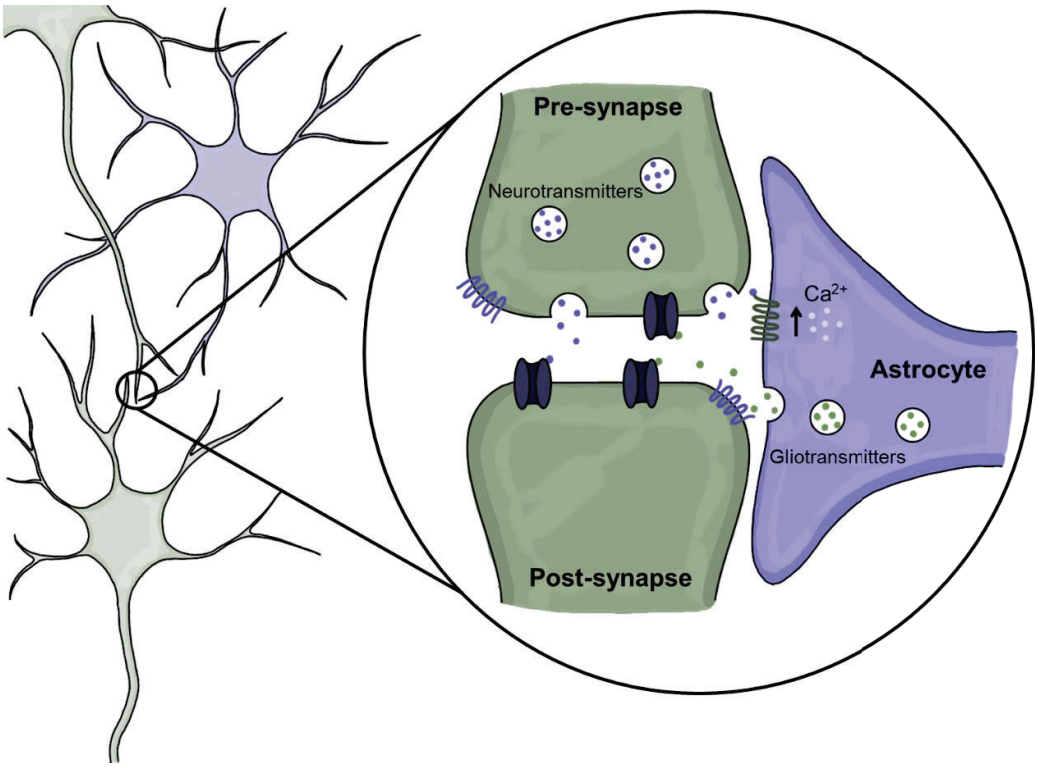

Figure 9. The tripartite synapse. Schematic representation of the bidirectional communication occurring in the tripartite synapse, involving pre- and post-synaptic neurons, and astrocytic processes. The pre-synaptic neurons release neurotransmitters which can bind to both the post-synaptic and astrocytic receptors. This binding increases calcium levels in the astrocytic process, which, in turn, triggers the release of gliotransmitters that can bind to both pre- and post-synaptic neurons.

The traditional view that neurons were the exclusive mediators of brain communications through electrical signalling was challenged with the development of calcium imaging techniques (Charles et al., 1991; Cornell-Bell et al., 1990). Thus, while neurons rely on electrical signals generated across the plasma membrane for their cellular excitability, astrocytes depend on changes in Ca^{2+} concentration within the cytoplasm (Araque et al., 2002; Perea & Araque, 2005). Therefore, while fast neurotransmission occurs within milliseconds, the effects of astrocytes on neuronal plasticity can last for seconds or even tens of seconds. Moreover, astrocyte Ca^{2+} elevations can occur spontaneously and, notably, can also be triggered by neurotransmitters released during synaptic activity or by changes in environmental signals, such as sensory or mechanical stimuli (Perea & Araque, 2005; X. Wang et al., 2006). Ca^{2+} responses in astrocytes, including amplitude, frequency, kinetics and

spatial diffusion, are shaped by the synaptic system, input patterns, and stimulation frequency, indicating that Ca^{2+} dynamics encode neuronal information (Araque et al., 2014; Perea & Araque, 2005; Todd et al., 2010; Volterra et al., 2014). Importantly, Ca^{2+} signalling can propagate to adjacent astrocytes, thereby also enabling intercellular communication among them (Araque et al., 2002).

Astrocytes express a diverse array of neurotransmitter receptors, several of which are also found in neurons (Porter & McCarthy, 1997). Therefore, these cells can bind and respond to many neurotransmitters in different forms, such as glutamate, acetylcholine, ATP, GABA, and endocannabinoids (Bowser & Khakh, 2004; N. Chen et al., 2012; Mariotti et al., 2018; Navarrete & Araque, 2010; Perea & Araque, 2005). Most of these responses occur via G protein-coupled receptors (GPCRs), which, upon stimulation by neurotransmitters released during synaptic activity, initiate various intracellular signalling pathways (Kofuji & Araque, 2021).Yet, they also express some ionotropic receptors such as NMDARs (Ahmadpour et al., 2024). GPCRs interact with G-proteins, which are heterotrimeric specialised proteins conformed by three subunits: α, β and γ. Commonly, GPCR activation in astrocytes leads to an increase of astrocytic Ca^{2+} levels when they signal through the $G\alpha_q$ subunit, being one the most well-known pathways the mobilisation of Ca^{2+} from internal reservoirs. When activated, these receptors stimulate phospholipase C through the $G\alpha_q$ subunit, which hydrolyses the membrane lipid phosphatidylinositol 4,5-bisphosphate leading to the formation of diacylglycerol and inositol trisphosphate (IP_3), which, in turn, results in IP_3 receptor activation and Ca^{2+} release from IP_3-sensitive Ca^{2+} stores (Araque et al., 2002; Kofuji & Araque, 2021). Still, astrocytic Ca^{2+} can also originate from alternative pathways, including mitochondrial release or the activation of TRPC1 channels (Agarwal et al., 2017; Malarkey et al., 2008). Some of the GPCRs that can be found in astrocytes are alpha-1 adrenergic, CB1, D1 $GABA_B$, mACh, mGlu, mGluR2, mGluR3, mGluR5 and P2Y1, among others (Kofuji & Araque, 2021).

Astrocytes not only sense and respond to neuronal activity but also actively regulate synaptic function by releasing gliotransmitters, which is a consequence of Ca^{2+} elevations (Durkee & Araque, 2019). Thus, they can influence various signalling pathways in neurons, modulating synaptic transmission and plasticity. One of the earliest pieces of evidence supporting astrocyte-induced neuromodulation is the Ca^{2+}-dependent release of glutamate from astrocytes, which activates postsynaptic NMDAR, leading to an increase in intracellular Ca^{2+} levels and potentiating excitatory transmission in hippocampal neurons from the dentate gyrus (Bezzi et al., 1998; Jourdain et al., 2007; Nedergaard, 1994). Of note, astrocytic glutamate can also activate receptors located at presynaptic terminals, thereby enhancing the frequency of both spontaneous and evoked excitatory synaptic currents. Specifically, in hippocampal CA3-CA1 synapses, astrocytic glutamate activates mGlu receptors (Navarrete & Araque, 2010). These findings illustrate that a single gliotransmitter can have multiple effects, acting on different targets in the same brain region. Furthermore, astrocytes are capable of releasing other neuroactive molecules in addition to glutamate, including D-serine,

ATP, adenosine, GABA, TNFα, prostaglandins, as well as various proteins and peptides (Perea et al., 2009). Additionally, astrocytes from the same circuit can release multiple gliotransmitters. For instance, astrocytes in the CA1 can release D-serine and ATP in addition to glutamate (J.-M. Zhang et al., 2003; Zhuang et al., 2010). Gliotransmitters can be released in a Ca^{2+}-dependent manner through vesicles and lysosomes; however, they can also be released independently of Ca^{2+} through mechanisms such as glutamate transporters or connexin hemichannels, among others (Kofuji & Araque, 2021).

It is important to note that not all synapses are functionally tripartite. Approximately 40% of recorded hippocampal synapses exhibit astrocyte-induced potentiation, which aligns with the observation that only a subset of hippocampal excitatory synapses is enveloped by astrocytic processes (Perea & Araque, 2007; Ventura & Harris, 1999). This information is relevant as it suggests that neuromodulation does not arise from widespread diffusion of gliotransmitters but indicates specific signalling between astrocytes and neurons. Further supporting this idea of specificity, astrocytes have the ability to selectively respond to various synapses that use different neurotransmitters. For instance, research have demonstrated that astrocytes in the hippocampus display different responses to acetycholine compared to glutamate, suggesting their ability to differentiate between synaptic activity from distinct axonal pathways (Perea & Araque, 2005). Furthermore, the effect of each gliotransmitter on synaptic communication depends on the specific neuronal environment. Specifically, the effects of glutamate gliotransmission vary depending on the specific receptor profile of the pre- and post-synaptic components of the tripartite synapse. For example, the release of a single gliotransmitter, such as glutamate, can exert either inhibitory or excitatory effects on synaptic plasticity, influencing both short- and long-term processes (Adamsky et al., 2018; Andersson et al., 2007; Jourdain et al., 2007; Navarrete & Araque, 2010).

Other glial cells can also contribute to synaptic plasticity, although their role is less direct and not as well characterised as that of astrocytes. Microglia, regulate neuronal activity and synaptic plasticity by continuously monitoring the microenvironment and engaging in neuron-glia communication (Cornell et al., 2022; C. J. Yu et al., 2023). They refine neural circuits through synaptic pruning, tagging weak synapses with complement proteins for removal, and thereby influencing LTP and LTD. Therefore, their balance in release of pro- and anti-inflammatory cytokines plays a crucial role in synaptic regulation (Hong et al., 2016). A recent study, nevertheless, indicates that the brain exhibits notable adaptability in executing synaptic refinement, maturation, and connectivity, even in the absence of microglia (O'Keeffe et al., 2025). On the other hand, oligodendrocytes, also have a role in plasticity(Korrell et al., 2019; Ronzano et al., 2020; Sancho et al., 2021). Their progenitor cells respond to neuronal activity via glutamatergic and GABAergic inputs, influencing myelin formation in an experience-dependent manner, modulating axonal growth and neuronal excitability(De Luca et al., 2020). However, the role of microglia and oligodendrocytes in plasticity remains less well understood than that of astrocytes, and further research is needed

to determine whether their contribution to plasticity is comparable to that of these star-shaped cells.

2.3 Synaptic plasticity impairments in neurodegenerative diseases

Synapse dysfunction is one of the main characteristics in neurodegenerative diseases, marked by loss and deterioration of synapses and neurons, along with functional decline (Dejanovic et al., 2024; D. M. Wilson et al., 2023). Moreover, synapses can be impaired in several ways in neurodegenerative diseases, including abnormal synapse elimination, impaired balance between excitation and inhibition, glutamate or calcium overflow, neuronal hyperexcitability or due to toxic protein aggregates (D. W. Choi, 1988; Fricker et al., 2018; J. Y. Li et al., 2003; Palop & Mucke, 2010; Verma et al., 2022). This section provides an overview of some of the key mechanisms related to synaptic plasticity dysfunction in neurodegenerative diseases.

The abnormal removal of synapses by glial cells, particularly microglia and astrocytes, is now acknowledged as a central mechanism underlying synapse loss (Bohlen et al., 2025). Precisely, elimination of functional synapses by microglia through the classical complement pathway has been observed in different mouse models of neurodegeneration, including AD and HD models (Dejanovic et al., 2024; Wilton et al., 2023). Therefore, the onset and progression of neurodegenerative disorders could be directly related to the immune signalling pathways, as it has been observed in AD, where most risk gens are highly expressed in microglia (Hansen et al., 2018). In connection with this, interleukin 33 is a cytokine driving microglial engulfment of the extracellular matrix and its decrease leads to deficits in synaptic plasticity and cognitive decline in 5xFAD mice (Cornell et al., 2022). In HD, increased activation and localisation of complement proteins has been related to selective loss of synaptic connections between the cortex and the striatum(Wilton et al., 2023). In addition, astrocytes in their reactive form and induced by activated microglia, have also been documented to play a role in synapse elimination (Liddelow & Barres, 2017).

Disturbance in the balance between excitation and inhibition is another mechanism that can damage synapses. This imbalance has been widely identified in neurodevelopmental disorders such as epilepsy, although it was not until recently recognised also in neurodegenerative disorders such as AD (Do-Ha et al., 2018; Palop & Mucke, 2016). Particularly, deficient synaptic inhibition due to dysfunctional inhibitory interneurons has been seen in mouse models of AD, leading to cognitive impairment (Verret et al., 2012). Additionally, glutamate can be toxic to synapses when found at elevated levels in the synaptic cleft during neurotransmission due to impaired Ca^{2+} buffering, free radical generation or mitochondrial permeability (Ankarcrona et al., 1995; X. X. Dong et al., 2009). Aβ deposits in AD or mHTT aggregate in HD can also compromise proteostasis, affecting synapses through a multitude of signalling pathways (Huffels et al., 2023; J. P. Taylor et al., 2002).

The motor cortex plays a central role in coordinating and learning motor functions, with associated motor circuits, such as the cortico-striatal pathway, which exhibits plasticity in response to motor learning and is also one of the most and earliest affected pathways in HD (Ghiglieri et al., 2019; Puigdellívol et al., 2015). It has been observed that NMDAR-dependent LTP between cortex and striatum decreases with age, which can be reverted using neuronal plasticity enhancers or with rehabilitation training (Inoue & Nishimune, 2023). Due to the central role of synaptic plasticity dysfunction in neurodegenerative disorders, there is an increasing interest in therapeutic approaches that aim to restore synaptic function and integrity by, for instance, enhancing synaptic plasticity by strengthening the synapse, protecting synapses from toxic stimuli, preventing presynaptic degeneration or rebalancing synaptic function to reduce network hyperactivity, among others (Dejanovic et al., 2024). To date, strategies targeting AMPARs and NDMARs, brain derived neurotrophic factor (BDNF) and its receptor tropomyosin receptor kinase B (TrkB) are being investigated (Dejanovic et al., 2024). Nonetheless, urgent research is required to develop precise, disorder-, region-, and cell-specific strategies that effectively enhance synaptic plasticity in neurodegenerative diseases.

3 The cAMP signalling pathway

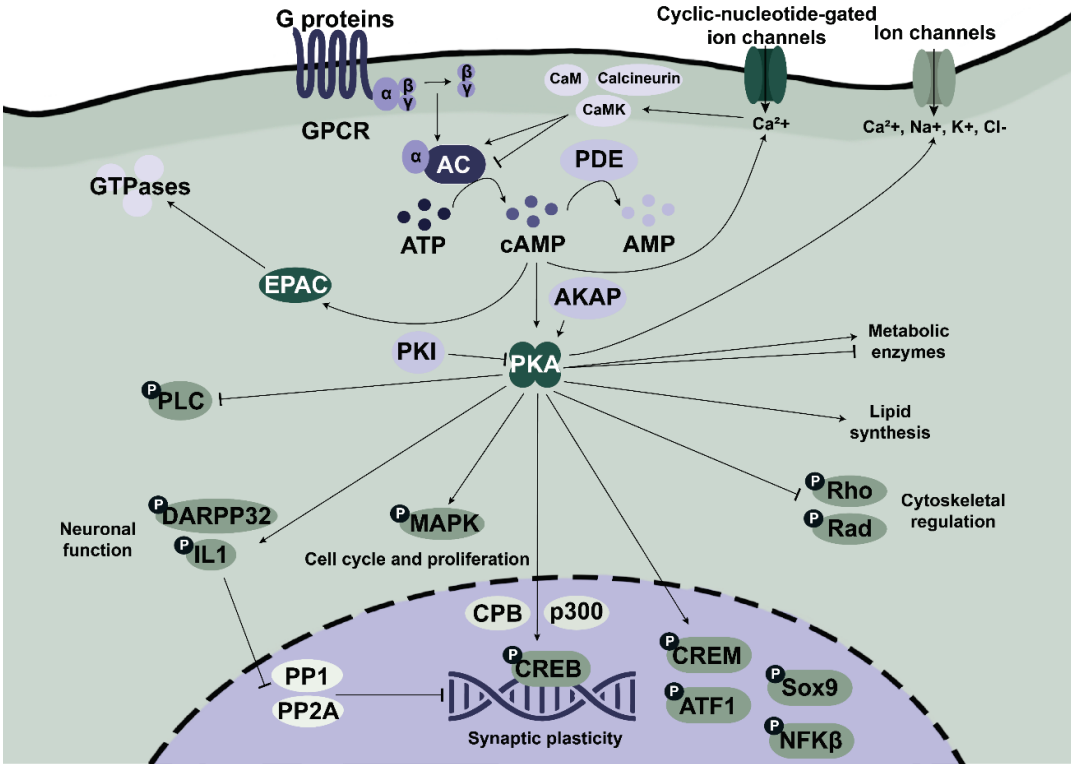

Figure 11. The cAMP pathway. Schematic representation of the key molecules involved in the cAMP signalling pathway and some of the major cellular functions it regulates.

cAMP was the first second messenger to be discovered and the classical one due to its involvement in a wide range of cellular processes, and its high sensitivity to many hormones and neurotransmitters throughout the body (Sassone-corsi, 2012; Sutherland & Rall, 1958) (Figure 11). The balance between adenylyl cyclases (AC), which synthetise cAMP, and cyclic nucleotide phosphodiesterases (PDE), which hydrolyse cAMP, precisely regulates the intracellular levels of cAMP (McKnight, 1991). Cell-type and stimulus-specific responses are induced due differential gene expression which encode for a high-variety of AC and PDE isoforms (Devasani & Yao, 2022; Erro et al., 2021; Fu et al., 2024; Kilanowska & Ziółkowska, 2020; Ostrom et al., 2022). In the brain, targeting specific isoforms expressed in distinct brain regions is being explored as a therapeutic strategy for neurodegenerative diseases (Angelopoulou et al., 2022; Erro et al., 2021; Z. Zhou et al., 2024).

GPCRs are membrane proteins that activate the majority of ACs downstream after the recognition of a wide variety of signals ranging from ions to proteins, neurotransmitters and hormones. As previously introduced, GPCR interact with the G-proteins composed of three subunits: α, β and γ (S. Liu et al., 2024). Generally, when an α subunit is dissociated from the heterotrimeric αβγ complex, it binds to the AC and either activates or inhibits or modulates its activity, depending on the subunit (α_s or α_i, respectively) (S. Liu et al., 2024). As previously

presented (see *Section 2.2*), GPCR can also express α_q subunits, which regulate Ca^{2+} signalling. Conversely, cAMP can be degraded to AMP by PDE. Besides, both ACs and PDEs can be modulated by other signalling pathways, including calcium signalling (for instance CamKIIa or calcineurin), PKC and receptor tyrosine kinases (ERK, MAP kinase, and PKB) (Cooper et al., 1995; Goraya et al., 2004; Yoshimasa et al., 1987).

cAMP is generated from ATP as a result of AC activation, which, in turn, can activate three main effectors: PKA, guanine-nucleotide-exchange factor EPAC and cyclic-nucleotide-gated ion channels (Bos, 2003; S. S. Taylor et al., 1992; Zaccolo & Pozzan, 2003). PKA is a tetrameric enzyme that consist of two regulatory and two catalytic subunits, which are able to phosphorylate a myriad of targets when they are detached from the regulatory subunits (S. S. Taylor et al., 1992). PKA is the most well-known target and characterised by its wide variety of substrates, whose specificity is enhanced by A-kinase anchoring proteins (AKAPs) that localise PKA near particular effectors and substrates (W. Wong & Scott, 2004). PKA can also be inhibited by a protein kinase inhibitor (PKI) (Walsh et al., 1971).

PKA has a diverse array of substrates that are localised both in the cytosol and in the nucleus of the cell. PKA targets participate in an extensive range of signalling pathways, including the following: glycogen synthesis and breakdown through the phosphorylation of metabolic enzymes; inhibition of lipid synthesis via acetyl CoA carboxylase; phosphorylation and subsequent inactivation of phospholipase C β2; phosphorylation and activation of MAP kinases; decreased activity of Rad and Rho; and modulation of ion channel permeability among others (Hotz et al., 1989; C. C. Huang & Hsu, 2006; U. H. Kim et al., 1989; Munday & Hemingway, 1999; Sassone-Corsi, 2012). Importantly, PKA can also directly phosphorylate transcription factors such as CREB, cAMP responsive modulator (CREM), and ATF1 alongside others. This phosphorylation permits these proteins to interact with the transcriptional coactivators CREB-binding protein (CBP) and p300. The activity of the aforementioned transcriptional factors can be counteracted with phosphatases that decrease its activity, including PP1 and PP2A, which in turn can also be inhibited by I1 and DARPP32, which are activated by PKA (Sassone-Corsi, 2012).

EPAC and cyclic-nucleotide-gated ion channels are the other two important effectors of cAMP. EPAC promotes the activation of specific GTPases while cyclic-nucleotide-gate ion channels conduct Ca^{2+}, which stimulates CaM and CaM-dependent kinases and, as a result, modulate cAMP production (Bos, 2003; Zaccolo & Pozzan, 2003).

Notably, during the past years, the focus has been put into the compartmentalisation and spatial regulation of cAMP, which is crucial for signal propagation and specificity of response (Lefkimmiatis & Zaccolo, 2014; Zaccolo et al., 2021). According to this revised paradigm, the functional outcome of a signal mediated by cAMP depends on local and temporal regulation. Moreover, cAMP signalling is also cell-specific, thereby the same stimulus can have different responses in different cells or subcellular compartments.

3.1 cAMP signalling and synaptic plasticity

cAMP is involved in diverse biological functions, including gene transcription, cell metabolism, proliferation, development, and most notably, synaptic plasticity, which is the primary focus in this thesis. In 1997, Nguyen and Kandel demonstrated for the first time the direct link between cAMP and LTP in neurons from mice. Particularly, they observed that the late phase of LTP required protein synthesis and RNA, which was inhibited in presence of PKA blockers (Nguyen & Kandel, 1997).

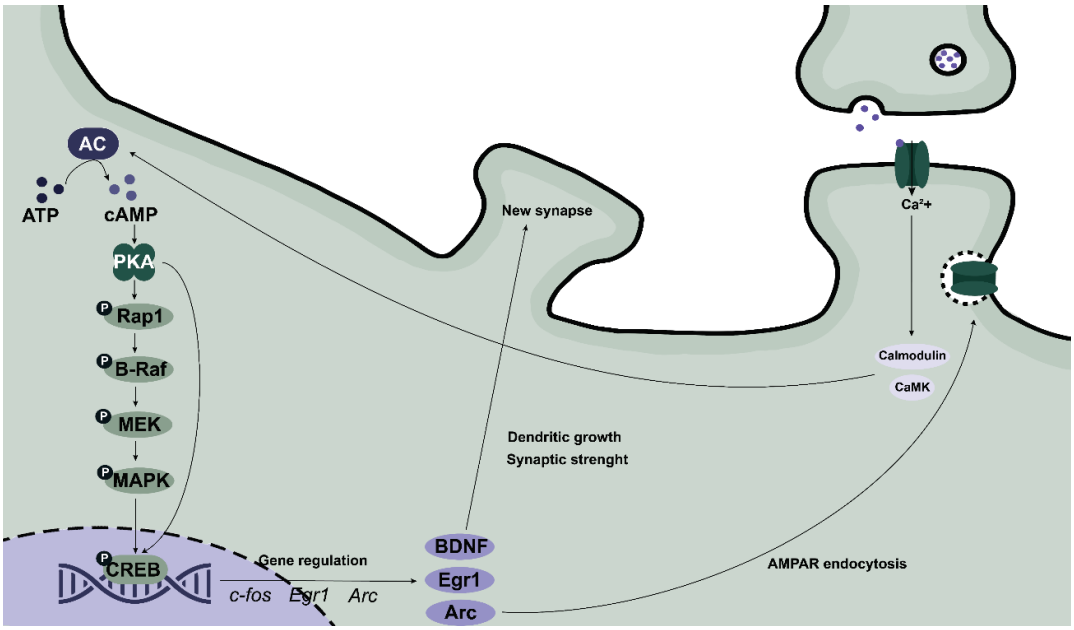

Figure 10. Late NMDAR-dependent LTP regulation involving cAMP signalling. Schematic representation of the canonical cAMP cascade signalling that sustains NMDAR-dependent LTP. Calcium influx into the post-synapse activates calcium-dependent kinases, which stimulate the production of cAMP through adenylyl cyclases (AC). This increase in cAMP activates PKA, which phosphorylates Rap1, leading to the activation of B-Raf, MEK, and MAPK, ultimately activating the transcription factor CREB. This cascade of events results in gene regulation that contributes to the formation of new synaptic connections.

As previously reviewed, NMDAR-LTP in the hippocampus is one of the first and most studied types of LTP, and experimental models for it are well established. One of the defining features of LTP is the Ca^{2+} influx into the post-synaptic neurons through NMDAR. Once LTP is induced and synaptic strength is enhanced through the insertion of new AMPARs, it needs to be maintained so it can continue for more than 1-2 hours up to days or even longer. This prolongation, known as late-phase LTP, is primarily driven by cAMP, which follows PKA activation and ultimately initiates gene transcription. Precisely, CREB phosphorylation by PKA is essential for long-term plasticity, as in mice that lacked CREB isoforms, LTP was impaired (Glazewski et al., 1999). Furthermore, phosphorylation of mitogen-activated protein kinase (MAPK) is also essential for the induction of LTP (Waltereit & Weller, 2003). The connection between CREB and MAPK phosphorylation is crucial, as this pathway has been observed to central during the induction of synaptic plasticity (C. C. Huang & Hsu, 2006; Waltereit & Weller, 2003). Overall, the most established signalling pathway for late-

phase LTP centres around cAMP, which activates PKA, then triggers Rap1 and B-Raf, leading to the phosphorylation of MAPK/ERK kinase (MEK). MEK subsequently phosphorylates MAPK, which activates CREB and other transcription factors (Waltereit & Weller, 2003) (Figure 10).

Following CREB activation, gene transcription processes that are necessary for the stabilisation of the structural and functional changes of synaptic strength are initiated, with *c-Fos* being among the first early genes linked to synaptic plasticity (Waltereit & Weller, 2003). *EgrI/Zif286* and *Arc/Arg3.1* are also early genes downstream the cAMP/PKA/CREB pathway that are related to synaptic plasticity; Arc protein regulates the endocytosis of AMPAR, while *ErgI* regulates other genes involved in synaptic growth (Didier et al., 2018). CREB also regulates BDNF expression, which has been directly associated with synaptic plasticity by increasing synaptic strength and enhancing dendritic growth and spine formation, among others (Benito & Barco, 2010; Kowiański et al., 2018; H. Park & Poo, 2012).

Based on the classical NMDAR-LTP hippocampal studies, researchers began investigating the cAMP/synaptic plasticity pathway in neurons from other brain regions. Notably, cAMP increases in granule neurons from the CA1 layer of the hippocampus enhance synaptic strength and neuronal depolarisation (Luyben et al., 2020), as well as the amplitude of EPSCs in pyramidal neurons of the medial prefrontal cortex through the PKA/MAPK pathway (C. C. Huang & Hsu, 2006). Moreover, mouse pyramidal cortical neurons can express both β-adrenergic and dopamine D1-like receptors, which are GPCRs modulated by noradrenaline and dopamine, respectively. Consequently, these neurons also signal through the cAMP/PKA pathway, enhancing synaptic plasticity (O'Donnell et al., 2012; Vincent et al., 2021). Dopamine also differently modulates D1 and D2 GPCRs receptors in the MSNs in the striatum, which also signals through the cAMP/PKA pathway and modulates its excitability (Y. Dong et al., 2006; Vincent et al., 2021). In summary, this evidence suggests that cAMP plays a pivotal role in the long-term modulation of synaptic plasticity, positioning it as a promising therapeutic target for the treatment of neurodegenerative diseases.

3.2 cAMP signalling in astrocytes

Astrocytes also express GPCRs coupled to $G\alpha_s$ and $G\alpha_i$ subunits, which can be activated by neurotransmitters, neuromodulators, neuropeptides, and hormones, thereby modulating cAMP levels. As a result, several functions of these glial cells are regulated through cAMP signalling. One of the main contributors to cAMP levels in astrocytes is the β-adrenergic receptor system, which includes three subtypes in astrocytes: β_1, β_2 and β_3, and is activated by noradrenaline (Horvat et al., 2016; Shao & Sutin, 1992). Astrocytes also express adenosine receptors, and therefore also contributing to a basal level of cAMP (Theparambil et al., 2024; Wendlandt et al., 2023). Additionally, serotonin, dopamine, and histamine can also activate GPCRs on astrocytes, further modulating cAMP signalling (Hösli & Hösli, 1984; Miyazaki et al., 2004; Zeinstra et al., 2006). Neuropeptides, such as pituitary adenylyl cyclase activating

polypeptide (PACAP), bind to VPAC1, VPAC2, and PAC1 GPCRs, which, in turn, activate AC and elevate cAMP levels (Joo et al., 2004). Furthermore, AC is present in astrocytes as membrane-associated from, known as transmembrane AC (tmAC), but also as soluble form (sAC) (H. B. Choi et al., 2012). Downstream astrocytic cAMP signalling, PKA and Epac1 appear to be the most predominantly expressed proteins. Moreover, cAMP degradation in astrocytes is specifically conducted by PDE1 and PDE4, which are cAMP-specific PDEs and can be upregulated by cytokines (Z. Zhou et al., 2019).

cAMP exhibits a complex interplay with Ca^{2+}, another crucial second messenger that has been extensively studied in astrocytes (Sobolczyk & Boczek, 2022). In this context, ACs are considered a key point of integration between these two molecules, as some tmACs expressed in astrocytes can be directly or indirectly modulated by Ca^{2+} (Willoughby et al., 2012). In this regard, sAC have been seen to be deeply influenced by intracellular Ca^{2+} dynamics (Schmid et al., 2014). Moreover, mitochondria are known to be one of the mechanisms that control Ca^{2+} levels. Interestingly, the expression of certain mitochondrial transporters may be regulated by CREB, suggesting an additional mechanism linking cAMP and Ca^{2+} (Shanmughapriya et al., 2015). Additionally, studies using hippocampal slices have demonstrated that astrocytic cAMP can influence the oscillatory activity of intracellular Ca^{2+} (Ujita et al., 2017). Yet, the precise mechanism of their relationship remains unclear.

Some of the astrocytic functions regulated by cAMP are glycogenolysis and lactate release, extracellular maintenance such as glutamate uptake, potassium buffering and water permeability, and immune response, among others (Z. Zhou et al., 2019). Notably, astrocytic glycogenolysis and lactate release have been shown to be important for neuronal activity and synaptic plasticity. This is due to the high energy demands of neuronal function, as inhibiting glycogenolysis reduces the astrocytic energy supply to neurons, leading to impairments in learning and memory (Boury-Jamot et al., 2016; Hertz et al., 2015; Suzuki et al., 2011). Moreover, it has been demonstrated that lactate is essential for the phosphorylation of CREB (Suzuki et al., 2011), which also triggers the expression of *Arc*, *c-Fos* and *EgrI* early genes in neurons (Yang et al., 2014). BDNF is a well-established neurotrophic factor that plays a key role in synaptic plasticity and which is highly expressed in neurons, although its expression has also been seen to be induced by noradrenaline, serotonin, and dopamine in cortical and cerebellar astrocytes *in vitro* (Mojca Jurič et al., 2006). All this information indicates that cAMP signalling in astrocytes may have a central role in synaptic plasticity. As a matter of fact, it has been demonstrated that an increase of astrocytic cAMP in the hippocampus is sufficient to induce synaptic plasticity and modulate memory, which reinforces the idea of cAMP expression in astrocytes is critical in synaptic plasticity and LTP (Z. Zhou et al., 2019). Nevertheless, the direct relationship between cAMP signalling and astrocytes in plasticity is still poorly understood. Manipulating cAMP in astrocytes may hold significant potential for enhancing synaptic plasticity in the brain.

3.3 cAMP-PKA signalling in neurodegenerative diseases

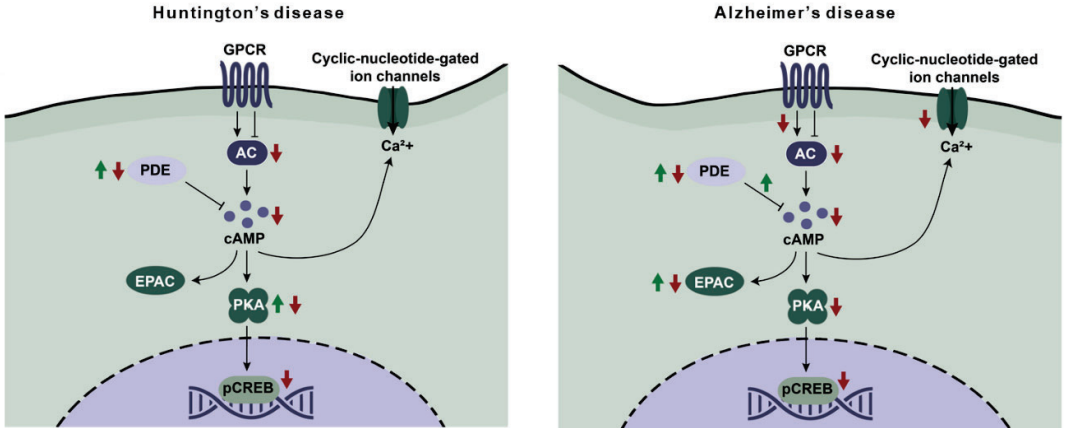

Figure 12. cAMP signalling dysfunction in Alzheimer's Disease and Huntington's Disease. Schematic representation of the key molecules involved in the cAMP signalling cascade that altered in AD and HD. Red arrows indicate a decrease in the molecule and/or activity; Green arrows indicate an increase in the molecule/and or activity. The presence of both red and green arrows indicate that the alterations are dependent on the brain region and/or isoform.

Impairments in key molecules that belong to the cAMP signalling pathway have been increasingly linked to the progression of aging and age-related neurodegenerative diseases, including HD and AD (Kelly, 2018). Furthermore, the two main regions most affected in these diseases - the cortico-striatal in HD and the hippocampus areas in AD - are highly regulated through the cAMP-PKA pathway (Heckman et al., 2018). Consequently, dysfunctions in these diseases are closely linked to disruptions in the cAMP signalling.

Data from patients with HD and corresponding mouse models indicate alterations in cAMP signalling within the striatum, hippocampus, and cortex; however, the amount of data available is significantly less than that for AD (Kelly, 2018; Xiang et al., 2024). Specifically, decreased cAMP levels have been measured in the cortex and lymphoblastoid cells of HD patients, as well as in the cortex and striatum of the Hdh^{Q111} knock-in mouse model (Gines et al., 2003). This reduction in cAMP may be linked to decreased synthesis by AC5, as its expression was found to be reduced in the striatum, or to increased degradation by PDE4 and PDE10, whose activity has been reported to be elevated in the cortex and striatum of the R6/2 mouse model (Beaumont et al., 2016; Tanaka et al., 2017). Nevertheless, PDE10A has been reported decreased in the striatum and cortex of HD patients and animal models (Ahmad et al., 2014; Hebb et al., 2004; H. Wilson et al., 2016). Furthermore, reduced PKA phosphorylation activity have been reported in the striatum of two HD mouse models, namely R6/2 and N171-82Q (J.-T. Lin et al., 2013), but increased in the R6/1 mouse model (Tyebji et al., 2015). Conversely, PKA phosphorylation levels are increased in the hippocampus of R6/1 mice (Giralt et al., 2011, 2013; Tyebji et al., 2015), but not in the Hdh^{Q111} knock-in mouse model (Tyebji et al., 2015). Notably, it has been demonstrated that PDE10A inhibitors are able to rescue behavioural and neurodegenerative deficits via the

cAMP-PKA-pCREB signalling pathway in HD animal models (Beaumont et al., 2016; Giralt et al., 2013).

Evidence from studies with patients, rodent models, and *in vitro* experiments indicate that region-specific disruption in cAMP signalling in the brain could play a role in the development of dementia-related pathology (Kelly, 2018; Xiang et al., 2024). A reduction of GPCR-related AC activity has been observed in the hippocampus (Bonkale, Fastbom, Wiehager, et al., 1996; O'Neill et al., 1994a; Schnecko et al., 1994), and temporal cortex (Cowburn, O'Neill, Ravid, Alafuzoff, et al., 1992; O'Neill et al., 1994a) of AD patients after AC stimulation, although there are controversies regarding its levels in other brain regions such as the cerebellum or other cortical regions, where some studies point to a decrease while others report no changes (Bonkale, Fastbom, Wiehager, et al., 1996; Cowburn, O'Neill, Ravid, Alafuzoff, et al., 1992; Cowburn, O'Neill, Ravid, Winblad, et al., 1992; Schnecko et al., 1994). There is also evidence for cAMP and downstream molecules reduction. Accordingly, cAMP levels have been observed to be decreased in the hippocampus of AD rodent models (J. Zhang et al., 2013). cAMP binding to PKA has also been studied as a measure of cAMP signalling activity, displaying reduced binding in the entorhinal cortex of severe AD patients (Bonkale, Fastbom, Wiehager, et al., 1996). Furthermore, diminished PKA levels and activity have been reported in AD patients, mouse models, and *in vitro* studies (Y. Chen et al., 2012b; Du et al., 2014; S. H. Kim et al., 2001; Liang et al., 2007; Shi et al., 2011; Vitolo et al., 2002). In agreement with the reduction of cAMP signalling in AD, both patient and rodent studies have also shown decreased levels of pCREB and diminished CREB-dependent transcription (Y. Chen et al., 2012b; Du et al., 2014; Shi et al., 2011; Vitolo et al., 2002). Alongside reductions in cAMP synthesis and/or activity, AD could also be associated with impairments in the degradation of cAMP by PDE, which have also been observed to be isoform and brain-region specific. Specifically, an increased expression of PDE3 has been observed in AD cerebral vessels (Maki et al., 2014), as well as increased PDE4D1 expression in the hippocampus of AD patients, while the other PDE4 isoforms were found reduced in this region (McLachlan et al., 2007; Paes et al., 2021). PDE7 and PDE8B isoforms were found altered in brains from AD patients (Pérez-Torres et al., 2003). Remarkably, stimulating AC activity (Q. wen Wang et al., 2009) or decreasing PDE expression could reverse cAMP deficits in the hippocampus of AD, cAMP-increasing drugs prevented induced hippocampal deficits (Vitolo et al., 2002), and cAMP/PKA/CREB signalling prevented and reversed AD-related deficits (Pugazhenthi et al., 2011).

Nonetheless, the reviewed research has primarily focused specifically on neurons or whole tissue, while cAMP signalling in glia remains largely unexplored. In recent years, few studies have emerged highlighting alterations in cAMP signalling specifically in glial cells in the context of neurodegenerative diseases. For instance, selective stimulation of the striatal astrocyte Gi-GPCR pathway using Designer Receptors Exclusively Activated by Designer Drugs (DREADs) in HD has been shown to correct several cellular and behavioural phenotypes associated with the disease, suggesting an altered cAMP pathway in these cells

(X. Yu et al., 2020). Therefore, more research is still needed in order to disentangle the specific alterations of cAMP in glial cells from neurodegenerative disorders.

The reviewed data indicate that specific alterations in cAMP signalling are associated with neurodegeneration, suggesting that modulating cAMP could be a logical target for treating neurodegenerative disorders. Indeed, there are several PDE inhibitors that have been or currently are being tested in clinical trials for AD and HD. PDE inhibitors are already extensively used as therapies for several human diseases, with 31 PDE inhibitors currently approved as marketable drugs (Phosphodiesterase Inhibitors | DrugBank Online, 2025.). One of the most common is PDE5 inhibitor sildenafil (Viagra, Pfizer) used for the treatment of male erectile dysfunction and pulmonary hypertension. Several PDE inhibitors entered clinical trials for AD, with their respective PDE target in brackets: Cilostazol (PDE3), MK-0952 (PDE4), BPN14770 (PDE4D), Roflumilast (PDE4), Udenafil (PDE5), PF-044447943 (PDE9), BI409306 (PDE9). For HD, several compounds entered clinical trials, with their respective PDE targets indicated in brackets: GSK356278 (PDE4), Rolipram (PDE4), OMS643762 (PDE10), PF-2545920 (PDE10), MNI-659 (PDE10), PBF-999 (PDE10 and A2A receptor antagonist), IMA107 (PDE10) (Xiang et al., 2024). Although some demonstrated promising results, most clinical trials were discontinued due to safety issues or their results remain unpublished, despite having concluded years ago. Only IMA107 for HD is currently active, finishing on 2027 (ClinicalTrials.gov identifier: NCT03434548). Therefore, alternative strategies are needed to achieve effective cAMP modulation in the context of neurodegenerative disorders. Given that the aforementioned compounds inhibit PDEs in an untargeted manner, a potential approach could involve region- and cell-specific targeting to enhance precision and therapeutic efficacy.

4 Emerging optical tools for the study and treatment of neurodegenerative diseases

During the past years, controlling brain activity has arisen as a potential therapy to treat neuropathological deficits. Approaches aimed at enhancing synaptic plasticity hold potential for mitigating or delaying network dysfunction associated with neurodegenerative disorders such as HD and AD.

Deep brain stimulation (DBS) and transcranial magnetic stimulation (TMS) are currently available to modulate neuroplasticity, although they present several limitations. DBS involves delivering electrical currents through an implanted electrode to regulate neural signalling in specific brain areas, affecting both local and network dynamics, with applications mainly in movement disorders like Parkinson's disease (Krauss et al., 2021; Okun, 2012). Although it has shown potential for neurodegenerative diseases like AD, DBS has limitations, including its lack of cell-type specificity, invasiveness, and associated risks such as infection and inflammatory reactions, and the reliability of the studies remain to be verified (Remoli et al., 2023). TMS, on the other hand, uses a magnetic field to stimulate brain regions non-invasively (Barker et al., 1985), inducing cortical plasticity and modulating neurotransmitter and glial activity (Stefan et al., 2000; Yuan et al., 2020). While TMS has applications in both healthy individuals and neuropsychiatric disorders, its effects are limited to cortical areas, and similarly to DBS, it lacks cell specificity, with no strong evidence to address the underlying causes of neurodegenerative diseases. In this context, optogenetics offer a promising alternative, providing precise control over specific cell types and brain regions, with the potential to overcome many of the current limitations of DBS and TMS.

Nevertheless, these approaches are based on the acute activation or inhibition of large brain areas or brain nuclei, which highlights the need for a method that allows for the long-term modulation and changes in gene expression of the affected brain areas or cell types. While optogenetics is still mainly used in basic research, it holds significant potential for application in clinical practice in the future, which is one of the focuses of this thesis.

4.1 Optogenetics

Optogenetics is a technology that integrates genetic and optical methods to enable precise and rapid control of specific events in biological systems (Boyden et al., 2005; Deisseroth, 2011). The need to control one type of cell in the brain while leaving others unaltered was expressed in 1979 by Francis Crick. Nevertheless, at the time, the methodology to achieve this control remained unaddressed although it was believed that light, due to its intrinsic properties, could provide a solution. Prior to this, it was already known that some microorganisms produce visible light-gated proteins that directly regulate the flow of ions across the plasma membrane (Oesterhelt & Stoeckenius, 1971). However, it was not until 2005 when Deisseroth and his team used lentiviral gene delivery to express and stimulate the

algal protein Channelrhodopsin-2, a light-sensitive cation channel, in mammalian neurons, enabling precise control of neuronal spiking (Boyden et al., 2005).

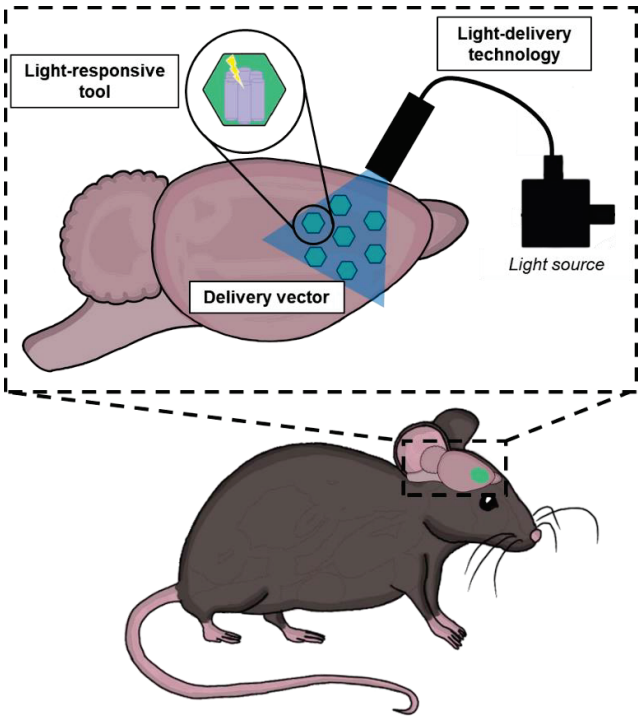

Figure 13. Optogenetic approach. Schematic representation of the key components required for an optogenetic approach. Light-responsive proteins are introduced into the target brain region and cells via delivery vectors carrying the gene of interest. Their activation is then achieved by illumination with a specific wavelength, delivered through a specialised light source and advanced technology, typically fibre-optic patch cords and cannulas implanted in the target region, enabling precise stimulation control

The optogenetic approach begins by introducing light-sensitive proteins into the cells of interest, typically delivered to a selected brain region via viral vectors (Figure 13). To start the process, light at wavelength corresponding to the activation spectrum of the light-sensitive protein is applied to the cells. To stimulate the photo-responsive protein *in vivo*, fibre-optic cannulas coupled to lasers or light-emitting diodes (LED) are inserted into the tissue, enabling precise control of intracellular signalling in selected cells during behaviour in freely moving animals. Therefore, this approach combines: 1) vectors for the delivery of the transgenes encoding for the light-responsive tool (*more details in section 4.1.1*), 2) a controllable, light-responsive tool, encoding for light-responsive proteins, capable to modulate specific cellular functions (*more details in section 4.1.2*), and 3) the technology that facilitates precise light delivery at the suitable wavelength to the targeted cells. This allows for the selective activation of the control tool within specific cells. As a result, optogenetics is a highly precise technique with both temporal and cell-type specificity that has revolutionised the field of neuroscience research (Bansal et al., 2023; Boyden et al., 2005; Deisseroth, 2011).

Currently, optogenetics is predominantly used in basic research, as it offers an exceptionally precise method for investigating a broad range of biological mechanisms, such as the neural circuits underlying disease. Still, considerable efforts are being made to make optogenetics applicable in the clinical settings. Indeed, in 2021, the first case of optogenetic therapy was published involving a patient with retinitis pigmentosa, a neurodegenerative disease that leads to vision loss. In this study, optogenetic stimulation of the eye enhanced the patient's visual

perception (Sahel et al., 2021). However, an important limitation of optogenetics in humans is the challenge of safely delivery light-responsive proteins to the brain (Bansal et al., 2023).

In the following sections, we will review the current state of optogenetic technologies, from viral construct delivery to genetically encoded light-responsive proteins, highlighting key advancements and the future improvements needed to translate this approach from the laboratory to the clinical practice.

4.1.1 Delivery of viral constructs for optogenetics

Because viral vectors can efficiently infect cells and use their transcriptional machinery to express foreign genes, they are predominantly used to deliver genes encoding light-responsive proteins in the context of optogenetics. Herein, we will review the types of viral vectors used for delivering light-responsive proteins and their associated delivery methods, with a particular emphasis on recent advancements regarding clinical applicability and non-invasiveness.

4.1.1.1 Types of adeno-associated viral vectors

Recombinant viral constructs carrying a gene of interest allow for long-term, cell-specific, and precise genetic manipulation of specific cell populations. Therefore, it is really important to choose the appropriate virus for each purpose, as it will determine several essential factors including the specificity to infect a given cell type (tropism), infectivity and toxicity, transgene expression, or packaging capacity (Nectow & Nestler, 2020). In this line, adeno-associated viruses (AAV) have become the most commonly used viral vectors for clinical gene therapy because they elicit minimal immune responses, do not integrate into the host genome, and provide long-lasting stable expression compared to other viruses like adenoviruses and lentiviruses (Cotter & Muruve, 2005; Miyake et al., 2015; Moiani et al., 2012). Notably, several AAVs have recently received approval for human use from the United States Food and Drug Administration, allowing their transition to clinical practice (Smalley, 2017).

AAVs belong to the *Parvoviridae* family and consist of non-enveloped single-stranded DNA viruses with a genome size of ~4.7 kb. Once delivered into the central nervous system, their onset of expression occurs within 1-2 weeks, and the expression can last for several months (Miyake et al., 2015). Importantly, they exhibit minimal cytotoxicity, and many serotypes can efficiently infect the brain, primarily targeting the soma of the cells (Nectow & Nestler, 2020). Recombinant AAVs, used in gene therapy, lack the viral DNA and function as protein-based nanoparticles designed to cross the cell membrane and deliver their DNA payload into the cell nucleus (Miyake et al., 2015; Naso et al., 2017).

The most commonly used serotypes in optogenetics are AAV1, AAV2, AAV5, AAV8, AAV9 and variations of these (Watakabe et al., 2015). AAV has adapted to enter cells by first interacting with carbohydrates on the surface of target cells. Consequently, slight variations in sugar-binding preferences, determined by differences in capsid proteins, can affect the cell-type transduction specificity of various AAV variants (Agbandje-McKenna &

Kleinschmidt, 2011). AAV2 was one of the first AAV serotypes to be identified and characterised starting the first generation of AAV vectors, which is why it was one of the most widely used serotypes (Beck et al., 1999; Rabinowitz et al., 2002). It is known for its strong selectivity for neurons and its limited spread following local cerebral injection (Nectow & Nestler, 2020). With AAV5 and AAV8, the second generation of AAV vectors started. These two serotypes have a more extended spread than AAV2 and they both express primarily in neurons, although astrocytic expression can also be observed (Aschauer et al., 2013; Taymans et al., 2007; Watakabe et al., 2015). AAV9 belongs to the third generation of AAV vectors and has been demonstrated to have a wide distribution in the brain and spinal cord, infecting both neurons and astrocytes, and reaching high infectivity with low doses(Cearley & Wolfe, 2006; Foust et al., 2009; Watakabe et al., 2015). AAV9 has the ability to effectively cross the BBB and infect cells of the CNS probably due to its preferential galactose binding (Bell et al., 2012; Naso et al., 2017). Besides, its tropism observed it rodents has been effectively translated to non-human primates (Watakabe et al., 2015). All these characteristics, make AAV9 the current gold standard. Nevertheless, these capsids are not suitable for systemic AAV delivery, as achieving even low transduction efficiency requires high viral load. Peptide Hybrid AAV with Brain Delivery (PHP.B) is an engineered AAV variant that demonstrates a 40-fold higher gene transfer efficiency across the central nervous system compared to AAV9, effectively transducing the majority of astrocytes and neurons across several regions of the brain (Deverman et al., 2016b) . Additionally, Peptide Hybrid AAV with Enhanced Brain Delivery (PHP.eB) is an improved variant of AAV-PHP.B that reduces the required viral load for efficient transduction of the majority of neurons in the brain (Chan et al., 2017). Overall, enhancing AAV efficacy, along with advances in delivery methods, could expand the application of gene therapy both in research and, more importantly, in clinical settings.

4.1.1.2 Viral delivery routes

To translate optogenetics into therapeutic applications, further refinement is essential to ensure efficient and safe transgene delivery. In this context, the selection of an appropriate AAV delivery method is pivotal to the success of optogenetic interventions. The current standard for optogenetic experiments in preclinical research involves the brain-targeted local injection of AAV vectors, which allows for precise and localised transgene expression, limited to the region of interest. However, it is highly invasive and requires stereotaxic surgery. Moreover, if the aim of the experiment is a widespread transduction, this strategy becomes even more aggressive, as it requires multiple intracerebral injections (Miyake et al., 2015). Undoubtedly, if the final aim is to translate optogenetics into the clinical setting with a safe approach, a minimally or even non-invasive AAV delivery method is needed.

Intracranial drug injections directly into the cerebrospinal fluid, including intracerebroventricular or intrathecal administration, are currently used for the delivery of some treatments in humans, particularly in cancer (Cohen-Pfeffer et al., 2017; Peyrl et al., 2014). Furthermore, direct injections into the cerebrospinal fluid are also performed in basic

research in the context of AAV delivery (Federici et al., 2012; G. Liu et al., 2005), although they present several limitations. First, these injections are restricted to when the main interest is to express the transgene in the peripheral nervous system, as expression is not confined to the brain, where the infection is low and preferentially to superficial structures (Federici et al., 2012; Miyake et al., 2015). Moreover, while most AAV capsids exhibit similar tropisms and distribution characteristics when directly injected into the brain, this is not observed with this procedure, where the distribution tends to be more variable (Miyake et al., 2015). Therefore, although this AAV delivery method may be suitable in certain contexts, alternative approaches are necessary to improve both efficiency and safety.

Intravenous administration of the AAV is an increasingly preferred option, as it is minimally invasive and can potentially widespread throughout the whole brain. In basic research, intravenous injection can be performed either via tail vein injection or injection into the retro-orbital sinus, providing a rapid and efficient method for administering AAV (Challis et al., 2019). In this regard, some AAV capsids can cross the BBB, such as AAV9. Nevertheless, AAV9 transduction in the adult brain after systemic delivery is low and limited to endothelial cells and astrocytes (Deverman et al., 2016a; Foust et al., 2009). Consequently, the recently engineered PHP.B and PHP.eB capsids are preferred due to their significantly higher ability to cross the blood-brain barrier and transduce both neurons and glial cells compared to AAV9 (Challis et al., 2019; Chan et al., 2017; Deverman et al., 2016a). Nevertheless, these two variants have shown limitations in certain species and mouse strains such as in BALB/cJ mice, presenting a significant constraint (Hordeaux et al., 2018). Furthermore, the risk of off-target effects in peripheral tissues could restrict the use of this approach.

Alternatively, intranasal administration of AAV might be an interesting option as non-invasive route, as the exposure of olfactory neurites into the nasal cavity directly connects the brain with the surrounding environment. Specifically, the human nose is a complex organ divided into the vestibule, respiratory, and olfactory regions, with the olfactory region playing a key role in direct drug transport to the brain. The olfactory sensory neurons in this region connect directly to the brain via the olfactory bulb, providing a unique route for drug delivery to the central nervous system, bypassing the blood-brain barrier (Gadenstaetter et al., 2022). Once the drug enters the brain through this pathway, it is thought to spread primarily via extracellular transport within the perivascular spaces surrounding cerebral blood vessels (Gadenstaetter et al., 2022). Indeed, intranasal administration of peptides has already been proven effective (Alcalá-Barraza et al., 2010; Keller et al., 2022; D. Wu et al., 2023). However, in the initial studies using intranasal administration of AAVs, transduced cells were limited to the nasal epithelium and olfactory bulb, or the behavioural effects were minimum (Ma et al., 2016; D. A. Wolf et al., 2012). More recently, some studies have demonstrated successful transgene delivery, as evidenced by increase BDNF expression in the brain (C. Chen et al., 2020; Ma et al., 2016). During the completion of this thesis, Wang et al. demonstrated widespread GFP expression in the cortex following AAV2 intranasal administration in a

model of stroke in rats, positioning this approach as a promising delivery route in determined conditions such as in cases where the BBB might be compromised (J. Wang et al., 2023).

4.1.2 Genetically encoded light-responsive proteins

When genetically encoded light-responsive proteins are expressed in the cell type of interest, they enable optical modulation of cellular functions. The first optogenetic experiments (Boyden et al., 2005; Zemelman et al., 2002) relied on light-gated ion channels and ion pumps to modulate the membrane potentials of cells, thereby activating or inhibiting neuronal populations in an acute manner (Nagel et al., 2002, 2003). By 2010, channelrhodopsins, bacteriorhodopsins, and halorhodopsin had all demonstrated the ability to rapidly and safely modulate neurons in response to various wavelength of light (Deisseroth, 2011). While this approach provides exceptional spatiotemporal precision in controlling neuronal activity, new tools are needed to control intracellular signalling cascades and gene expression for sustained long-term modulation. Consequently, during the recent years, the optogenetic toolkit has expanded to allow for the regulation of a diverse range of cellular functions (Bansal et al., 2023; Losi et al., 2018; Mahmoudi et al., 2017; Rost et al., 2017; Shcherbakova, Shemetov, et al., 2015). Moreover, to effectively translate optogenetics into clinical applications, the development of red-shifted protein variants and enhancements in light delivery methods will be necessary. Most of the existing optogenetic systems still use blue light, which has a low tissue penetration compared to red light owing to scattering and absorption by hemoglobin, water, and other cellular constituents (Lehtinen et al., 2022; Weissleder, 2001). Because red light penetrates tissues more deeply, it could eliminate the need for implanted fibre-optic cannulas in the brain, thus enabling non-invasive stimulation of the light-responsive protein. As an added benefit, due to a lower photon energy compared to blue light, red light exerts less phototoxicity (Lehtinen et al., 2022).

The use of natural photoreceptors as key components in protein engineering has facilitated significant advancements in the development of genetically encoded molecules, which are essential for optical technologies in life sciences. Photoreceptors are essential components in a wide range of organisms, including plants and bacteria, where they play a fundamental role in sensing and responding to light. For light detection, photoreceptors rely on an organic chromophore to absorb light and transduce conformational signals to the protein backbone and the effector domain (Rockwell & Lagarias, 2010; Shcherbakova, Shemetov, et al., 2015). The activated signalling pathway can operate through various mechanisms, including light-triggered dimerization, ion channel modulation, or altered enzymatic activity (Lehtinen et al., 2022). Through protein engineering, the effector domain can be modified to regulate a wide range of cellular processes.

Photoreceptors used as a template in the development of optical tools can be classified into different groups according to their chromophores and the light-sensitive protein domains: 1) Light-oxygen-voltage-sensing (LOVs) domains; 2) Blue-light-utilising flavin adenine

dinucleotide (BLUF) domains; 3) Cryptochromes; 4) Opsins; 5) Plant and cyanobacterial phytochromes; 6) Bacterial phytochromes (Shcherbakova, Shemetov, et al., 2015).

Wavelength (nm)	Natural photoreceptor	Chromophore	Examples in optogenetics
~300-500	LOV domain	FMN and FAD	iLID, LOV2
~300-500	BLUF domain	FMN and FAD	bPAC
~300-500	Cryptochromes	FMN and FAD	CRY2
~400-700	Opsins	Retinal	CHR2
~650-700	Plant and cyanobacterial phytochromes	Phycocyanobilin and phytochromobilin	PHYB
~650-750	Bacterial phytochromes	Biliverdin	IlaC, PaaC, DdPAC

Table 1. Natural photoreceptors, detected wavelengths, used chromophores, and engineered examples used as optogenetic tools.

LOV, BLUF domains and cryptochromes are UV- and blue-sensing-light (~300-500) photoreceptor proteins that integrate flavin mononucleotide (FMN) or flavin adenine dinucleotide (FAD) as chromophores (Shcherbakova, Shemetov, et al., 2015). The best-characterised and widely used LOV domain is the LOV2 domain of phototropin 1 from *Avena sativa*. Exposure to blue light triggers the reversible unfolding of terminal α-helices that can be harnessed for engineering photoreceptors(Dietler et al., 2022; Harper et al., 2003). An improved variant, denoted light-induced dimer (iLID), generates reversible interactions in response to blue light, controlling GTPase activity (Guntas et al., 2015). As an example of cryptochrome in optogenetics we find CRY2, which derives from *Arabidopsis thaliana* and can control protein homo- and hetero-oligomerization upon blue light illumination (Kennedy et al., 2010; H. Park et al., 2017).

Opsins use retinal as chromophore and can respond to diverse light bands within the near-UV to visible electromagnetic spectrum. The most commonly used one in optogenetics, channelrhodopsin-2 (ChR2), is activated by blue light (Boyden et al., 2005; Nagele et al., 2003). As previously mentioned, many opsins act as light-gated cation channels and ion pumps quickly depolarizing the cells, and are the most used photoreceptors in optogenetics. Nevertheless, certain opsins can function as light-activated GPCRs or enzymes (Dixon et al., 1986; Yoshida et al., 2017).

Phytochromes, which are widespread across plants, bacteria, cyanobacteria, and fungi, function as key photoreceptors in light-adaptive processes (Rockwell & Lagarias, 2010). These natural dimers use linear tetrapyrroles (bilins) as their chromophores for light detection and undergo modulation in response to far-red and near-infrared light, driving a photo-reversible transition between their active and inactive states. At the molecular level, phytochromes consist of a structurally and functionally conserved photosensory core module (PCM) responsible for light absorption, along with a structurally and functionally heterogenous output module (OPM). The PCM is composed of consecutive PAS, GAF, and

PHY domains, with the GAF domain housing the chromophore (Möglich et al., 2025; Shcherbakova, Baloban, et al., 2015) . The chromophore differs between plants or bacteria; plant phytochrome contain phytochromobilin, a reduced bilin, while bacterial phytochrome (or bacteriophytochromes, BPhys) contain a biliverdin. Importantly, as biliverdin occurs in mammalian cells as a heme degradation product, bacterial phytochromes are more promising for *in vivo* optogenetics (Möglich et al., 2025; Shcherbakova, Baloban, et al., 2015).

The capacity of the PCM to detect light and subsequently convert it to a biochemical signal has led to the engineering of the OPM in phytochromes, thus resulting in the development of novel optogenetic tools (Shcherbakova, Shemetov, et al., 2015). Accordingly, efforts are undertaken to modify the output type to meet a desired function. Some examples of customised output in bacterial phytochromes are diguanylate cyclases, in which the bacterial seconds messenger is cyclic dimeric GMP (Gourinchas et al., 2017.; Ryu & Gomelsky, 2014), or receptor tyrosine kinases. For instance, the tropomyosin receptor kinase, which has been found to specifically induce apoptosis in neuroblastoma and glioblastoma cells, was thus subjected to red-light control (Leopold et al., 2019).

4.1.2.1 Photoactivated adenylyl cyclases as tools for modulating cAMP signalling in the brain

Photoactivatable adenylyl cyclases (PACs) are enzymes that regulate cAMP levels in response to light (Iseki & Park, 2021). They consist of a light-sensing domain and an adenylyl cyclase domain, which, upon illumination, catalyse the conversion of ATP to cAMP. Given the central role of cAMP in various cellular processes, including synaptic plasticity, PACs have become a key focus in the field of optogenetics.

PACs were first discovered as sensors for photo-avoidance in the flagellate *Euglena Gracilis* (Iseki & Park, 2021; Schröder-Lang et al., 2007), a natural BLUF-domain flavoprotein responding to blue light. Initially, PACs were thought to be found only in Euglena species; however, a few years later, the discovery of the *Beggiatoa* PAC (bPAC) expanded their known range (Ryu & Gomelsky, 2014; Stierl et al., 2011). Since then, bPAC is becoming widely used in the field of optogenetics (Stierl et al., 2011; Z. Zhou et al., 2021). Building on this knowledge, more recent PACs have been engineered using bacterial phytochromes (BPhys) that utilise biliverdins as a chromophore, hence enabling reversibly controlled by red light (Etzl et al., 2018; Ryu & Gomelsky, 2014; Stüven et al., 2018; Xu et al., 2024). In these cases, the PCM of the BPhy is fused with an adenylyl cyclase OPM from a different biological origin. Still, the development and application of red-light-responsive PACs remain limited, and further research is needed to understand the *in vivo* effects of their activation, and ultimately their therapeutic potential.

DdPAC is a recently developed PAC regulated by red and far-red light (Stüven et al., 2018)and has been tested as an optogenetic tool in neural cells for the first time in the framework of this thesis. DdPAC derives from PaaC, another BPhy-based PAC developed by Etzl et al in 2018 (Etzl et al., 2018) and contains the DdBPhy PCM obtained from the

bacteria *Deinococcus deserti*. DdPAC is activated by light between around 650-700 nm and it is inactivated between 700-750 nm. Compared to PaaC, DdPAC shows enhanced response to light and improved photo-switching (Stüven et al., 2018). Taken together, DdPAC augurs significant potential as a tool for precisely modulating cAMP in neural cells. This precise control of cAMP may enhance synaptic plasticity, offering a promising therapeutic possibility for the treatment of neurodegenerative diseases.

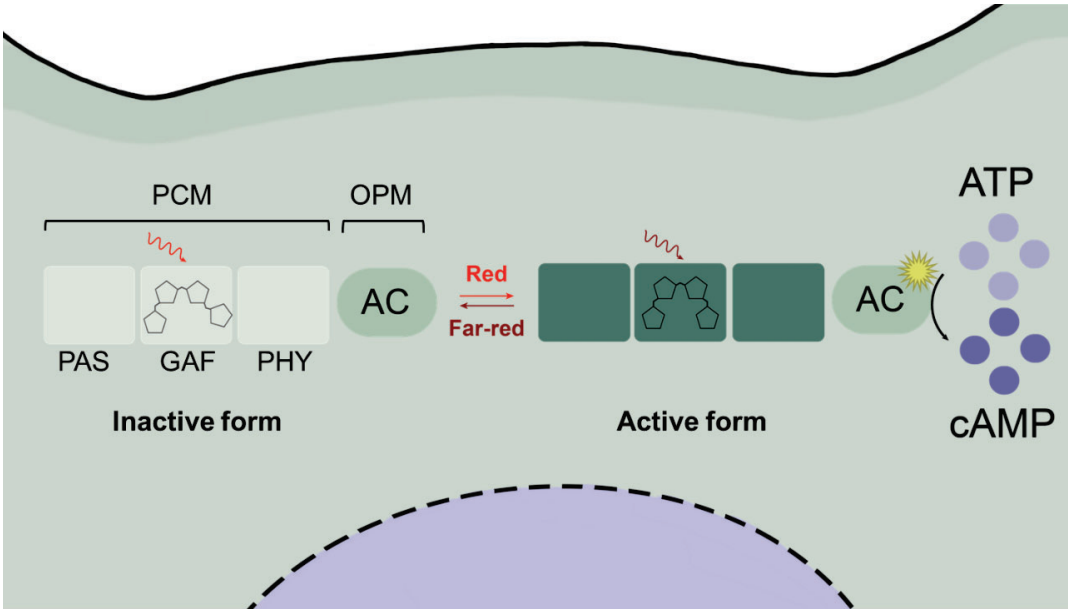

Figure 14. DdPAC structure and function. Schematic of DdPAC structure, composed of a photosensory core module (PCM) which absorbs light and an output module (OPM) that translates the signal into a biological response. The PCM consists of consecutive PAS, GAF (containing the chromophore) and PHY domains. The output module is an adenylyl cyclase (AC). Under red light, the chromophore undergoes an isomerization, thereby activating the adenylyl cyclase and increasing cAMP synthesis. Conversely, far-red illumination, inactivates DdPAC and suppresses activity.

AIMS

Therefore, the main objective of this thesis is to restore physiological functions in neurodegenerative diseases by modulating brain plasticity through the light-induced activation of DdPAC-mediated cAMP signalling in specific brain circuits.

AIM 1. To characterise disruptions in cortical cAMP signalling and behaviour in the R6/1 mouse model of Huntington's Disease

To assess cortical cAMP alterations in Huntington's Disease

To evaluate early cortico-striatal deficits in the R6/1 mouse model of Huntington's Disease

AIM 2. To implement DdPAC as a novel optogenetic tool to non-invasively modulate synaptic plasticity through cAMP signalling.

To establish a non-invasive viral delivery method

To evaluate and characterise the impact of DdPAC-mediated cAMP signalling on synaptic plasticity

AIM 3. To restore physiological function through light-driven DdPAC stimulation in mouse models of Huntington's and Alzheimer's Disease.

To evaluate the effect of increased DdPAC-mediated cAMP signalling in cortical and striatal astrocytes of a Huntington's Disease mouse model

To investigate the effects of increased DdPAC-mediated cAMP signalling in hippocampal neurons and astrocytes of an Alzheimer's Disease mouse model

METHODS

1 Animals

Wild-type (C57/Bl6), R6/1-B6CBA, R6-1-A2a-Cre and 5xFAD male and female mouse models were used in this thesis, each of them selected for a specific purpose and detailed below (Table 2). Animals were housed together in groups of mixed genotypes in a room kept at 19-22ºC and 40-60% humidity under 12:12h light/dark cycle with access to water and food ad libitum. Mice were randomly assigned to experimental groups and data were recorded for analysis by microchip mouse number. All animal procedures were performed following EU legislation and approved by local ethical review at the animal experimentation Ethics Committee of the Universitat de Barcelona (356/19, 274/18 and 10/20) and Generalitat de Catalunya (11070, 10101), in accordance to Spanish RD 53/2013. A subset of experiments (MEA recordings in C57Bl/6 and IP3R2-/2) was performed in Aston University by our collaborators Dr. H Rheinallt Parri and Neville Ngum and performed in accordance with the United Kingdom Animals Scientific procedures act of 1986. The 3Rs, replacement, refinement and reduction were considered for planning all animal procedures. Genotypes were obtained by polymerase chain reaction (PCR) from ear biopsy at the University of Barcelona. In Aston University, genotyping was conducted by Transnetyx (TN, United States).

Model	Background	Description	Origin	Sex/Age	Results section
WT	C57BL/6		Charles River	♂ ♀ 4-8wks	Multielectrode arrays *Section 2.2.1-2.2.2*
	C57BL/6		Charles River	♀ 8-12wks	Proteomics and metabolomics *Section 2.2.3-2.2.4*
	C57BL/6		Charles River	♂ 8-15wks	Non-invasive viral delivery *Section 2.1.1-2.1.2*
	C57BL/6-CBA		Jackson Laboratory	♂ 8-12wks	
	C57BL/6 A2ACre	Adenosine A2a receptor-Cre BAC transgenic mice	Dr Alban de Kerchove d'Exaerde and Pr Serge N Schiffman, Université Libre de Bruixelles	♀ 8 wks	
IP_3R2	C57BL/6	Mutant $IP_3R2^{-/-}$ do not express the R2 subtype IP_3 receptor, mediator of Ca^{2+} signalling. Amplified by crossing homozygotes.	Mice imported from Prof. Araque (Cajal Institute, Madrid). Developed by Prof. Ju Chen (San Diego)	♂ ♀ 4-8wks	Multielectrode arrays *Section 2.2.2*
R6/1	C57BL/6-CBA	Expressing the exon-1 of mutant huntingtin with ~145 CAG	Jackson Laboratory (Maintained in C57BL/6-CBA background by	♂ 4-16wks	Cortico-striatal behaviour *Section 1.2*
				♂ ♀	Fibre-photometry

		repeats at the time of experiments. WT littermates were used as the control group.	breeding transgenic male mice with C57BL/6J x CBA/J F1 females)	8-20wks	*Section 1.1*
				♀ 14-18wks	DWI imaging *Section 3.1.1*
				♂ ♀ 8-16wks	DdPAC stim. cortex *Section 3.1.2-3.1.4*
				♂ ♀ 8-16wks	DdPAC stim. striatum *Section 3.1.4*
5xFAD	C57BL/6	Overexpressing 695- amino acid isoform of the human amyloid precursor protein (APP695) carrying the Swedish, London, and Florida mutations under the control of the murine Thy-1 promoter. Besides, they express human presenilin-1 (PSEN-1) carrying the M146L/L286V mutation, also under the control of the murine Thy-1 promoter	Jackson Laboratory	♂ ♀ 7-8 mos	DdPAC stimulation hippocampus *Section 3.2*

Table 2. Mouse models. Summary of animal models used in this thesis. This table provides information on each model, including its background, a brief description (if necessary), origin, sex, and age at the time of use. Results involving each animal model are presented in the corresponding "Result section".

2 Behavioural assessment

All behavioural tests were performed by an experimented observer during the light phase and animals were habituated to the experimental room for at least 1 h before testing. All testing apparatus were carefully cleaned with water and dried between tests and animals and the light inside the experimental room was ~20 lux.

Behavioural tests	Related brain area	Function studied	Age tested	Results section
Adhesive removal	M2-SS-STR	Sensorimotor	4-16 wks	Cortico-striatal behaviour *Section 1.2.1*
Marble burying	M2-OF-STR	Compulsive-obsessive and anxiety	4-16 wks	Cortico-striatal behaviour *Section 1.2.2*

Beetle mania	M2-SC	Passive and active fear responses	14 and 20 wks	cAMP dynamics *Section 1.1.1 and 1.1.3*
Open field	M1/M2	Locomotion and spontaneous behaviour	4-12 wks 12 and 14wks 13 and 15wks	Cortico-striatal behaviour *Section 1.2.3* M2 DdPAC stim. *Section 3.1.2-3.1.3* Striatal DdPAC stim. *Section 3.1.4*
Accelerating rotarod	M2-STR	Motor learning and coordination	15wks ~15wks ~15wks	cAMP dynamics *Section 1.1.2* M2 DdPAC stim. *Section 3.1.3* Striatal DdPAC stim. *Section 3.1.4*
Balance beam	STR	Coordination	~15wks ~15wks	M2 DdPAC stim *Section 3.1.3* Striatal DdPAC stim. *Section 3.1.4*
Vertical pole	STR	Coordination	~15wks ~15wks	M2 DdPAC stim *Section 3.1.3* Striatal DdPAC stim. *Section 3.1.4*

Table 3. Behavioural tests. Summary of behavioural tests performed in this thesis. This table provides information on each behavioural test, including the main brain area involved, the function studied, and age at the time of use. Results involving each animal model are presented in the corresponding "Result section". M2: secondary motor cortex; SS: somatosensory cortex; STR: striatum; OF: orbitofrontal cortex; SC: superior colliculus; M1: primary motor cortex.

2.1 Open field

Spontaneous locomotor activity and exploratory behaviour were assessed as previously described (Fernández-García et al., 2020) in a square arena (40 x 40 x 30 cm^3). Mice were placed in the centre of the arena and allowed to freely explore. The SMART 3.0 software (Panlab) was used to track and record the behaviour of the animals. Locomotor activity and exploratory behaviour were assessed by evaluating total distance travelled, total time spend in fast movement (>12 cm/s), slow movement (2-12 cm/s) and resting (<2 cm/s). Additional parameters measured included mean speed, mean speed excluding resting periods, as well as total duration, mean duration, and frequency of rearing and grooming event, which serve as indicators of exploratory and stereotypic behaviour. The apparatus was cleaned between animals to avoid odour cues.

2.2 Accelerating rotarod

Motor learning and coordination were assessed using a rotarod apparatus (Conde-Berriozabal et al., 2025; Fernández-García et al., 2020; Puigdellívol et al., 2015). Mice were placed on a motorized horizontal rod with a diameter of 30 mm, where the rotation speed gradually increased from 4 to 40 rpm over a period of 5 minutes. This task measures the latency to fall from the rod, with each mouse undergoing four trials per day for three consecutive days, resulting in a total of 12 trials. A 1-hour interval was maintained between trials on the same day. For fibre photometry analysis, all 12 trials were conducted at 10-minute intervals during a single recording session on one day, and mice were previously trained to stay on the 4rpm moving rod before the start of the first recording session. The start time (time zero) was defined as the point when the mice were familiarized with the rod, with all four paws on the surface.

2.3 Beetle-mania task

Passive and active fear responses of mice to an unexpected moving beetle (Nano Nitro, Hexbug)(Almada et al., 2018; Bouet et al., 2009; Conde-Berriozabal et al., 2023; Heinz et al., 2017) were assessed using the beetle-mania task. The test was conducted using a white rectangular arena (15 x 40 x 30 cm) and comprised two successive phase of 5 minutes: during the habituation phase, mice freely explored the arena and distance travelled and rearing times were scored using the SMART 3.0 software (Panlab). In the testing phase, confrontations with the erratically moving robo-beetle were scored. The robo-beetle was introduced inside the arena at maximal distance to the mouse and the following behavioural responses were analysed: (1) escape, mice quickly jump (flight) with accelerated speed in the direction opposite to the beetle's movement vector ; (2) tolerance, ignorance of the robo-beetle after physical contact; (3) approach, mice follow the robo-beetle in close vicinity; (4) avoidance, mice walk in opposite direction to the robo-beetle and (5) total responses, the sum of all the events evaluated. Escape events were normalized to total responses, whereas tolerance, approach and avoidance were normalized to the sum of these three parameters, without the escape events. This test was conducted during Fibre photometry recordings of cAMP dynamics. Thus, a 120-second recording inside the home cage was performed prior to placing the mouse in the arena to stabilize the cAMP signal.

2.4 Adhesive removal test

Sensorimotor deficits were studied using the adhesive removal test (Bouet et al., 2009). This test consisted of 2 days of training (1 trial each day) and 1 day of testing (3 non-consecutive trials). Each trial included the following phases. First, the animal was placed in a standard 23 cm x 23 cm cage without bedding and was allowed to explore it for 60 seconds. Then, the animal was removed from the cage, immobilised, and two pieces of adhesive tape (0.3 x 0.4 cm) were placed on each of the forepaws. Immediately after, the animal was placed again inside the cage and 3 different timepoints were measured: a) Contact time: the time it took

for the animal to realise it had adhesive tape on its paws (indistinctively left, or right); b) Removal time 1: the time it took to remove the adhesive tape from the one of the paws; c) Removal time 2: the time it took to remove the adhesive tape from the other paw. If the animal did not realise the adhesive tapes or did not succeed in removing them, the test was finished after 120 seconds. Two observers participated in this test in order to have clear observations from different angles.

2.5 Marble burying test

Compulsive-obsessive and anxiety behaviour were analysed using the marble burying test (Angoa-Pérez et al., 2013). The test was conducted using clean rat cages (21,5 x 46,5 x 19 cm^3) with bedding material. Before the start of the test, 20 clean marbles were carefully and evenly distributed on the bedding material. Then, a mouse was carefully placed inside the cage, and left inside for 30 minutes. After this time, the animals were returned to its home-cage and the buried marbles were counted. We accepted as buried a marbled that is covered by bedding more than a 30% of its surface.

2.6 Balance Beam

Motor coordination and balance were evaluated by quantifying the ability of the mice to traverse a narrow beam without falling or slipping (Anglada-Huguet et al., 2016; Fernández-García et al., 2020). The beam consisted of a wooden square bar measuring 50 cm in length with a 1.3 cm face, divided into 5 cm sections and placed horizontally 50 cm above the bench surface, with each end mounted on a narrow support. During a training session, the mice were allowed to walk along the beam for 2 minutes to familiarize themselves with the set-up. Four hours later, during the testing session, the procedure was repeated, and the number of sections crossed and slips were recorded.

2.7 Vertical pole

Motor coordination was assessed using a vertical pole (Creus-Muncunill et al., 2019). Animals were placed at the top of a vertical bar measuring 35 cm in length and 1 cm in diameter. Mice were positioned with all four paws grasping the pole and their heads oriented upwards. Training sessions were conducted three times per day for two consecutive days. On the third day, testing was performed, and the latency for each mouse to turn downward and completely descend the pole was recorded.

3 Adeno-associated viral constructs

Different AAV serotypes and constructs were used in each experiment, each of them selected for specific purposes and detailed in the Table 4. AAV9 and PHP.eB vectors for the expression of GFlamp-1, GFP, and DdPAC were produced following the co-transfection method as described previously and purified through iodixanol gradient ultracentrifugation at Dr. Dalkara Laboratory (Sorbonne Université, INSERM, CNRS, Institute de la Vision)

(V. W. Choi et al., 2007). Concentration and buffer exchange were carried out using PBS containing 0.001% Pluronic. The titers of AAV vector stocks were subsequently determined using the real-time quantitative PCR titration method (Aurnhammer et al., 2012) with SYBR Green (Thermo Fischer Scientific). Additional AAV used were purchased from Addgene.

AAV	Reference	Titer (vg/ml)	Hemisphere
Fibre photometry			
AAV9-hSyn-G-Flamp1-WPRE	1760 G-Flamp1 plasmid was generously provided by Dr. Liang Wang and Dr. Jun Chu (Shenzhen Institute of Advanced Technology, Chinese Academy of Sciences, Shenzhen, China)	~1-3x10^{14}	Unilateral
Non-invasive delivery			
AAV9-sc-CAG-GFP	1420	~1-3x10^{14}	Bilateral
PHP.eb-sc-CAG-GFP	1421	~1-3x10^{14}	Bilateral
AAV9-CamKIIa-eGFP-WPRE	1429	~1-3x10^{14}	Bilateral
PHP.eb-CamKIIa-eGFP-WPRE	1435	~1-3x10^{14}	Bilateral
PHP.eb-FLEXon-EF1A-EGFP-3xFLAG	1639	~1-3x10^{14}	Bilateral
Multi-electrode arrays			
AAV9-CamKIIa-eGFP-WPRE	1429	~1-3x10^{14}	Unilateral
AAV9-CamKIIa-DdPAC-3xFLAG-WPRE	1544	~1-3x10^{14}	Unilateral
AAV9-GFAP-eGFP-WPRE	1749	~1-3x10^{14}	Unilateral
AAV9-GFAP-DdPAC-3xFLAG-WPRE	1750	~1-3x10^{14}	Unilateral
pAAV.hSyn.iGluSnFr.WPRE.SV40	Gift from Loren Looger; Addgene viral prep # 98929-AAV1	10^{13}	Unilateral
AAV5-GFAP-mCherry-hPMCA2w/b (CalEx)	Addgene #111568	10^{12}	Unilateral
Diffuse wave imaging			
AAV1-CaMKIIa-hChR2(H134H)-eYFP-WPRE.hGH	#26969-AAV1, Addgene	~1-3x10^{12}	Unilateral

AAV9-GFAP-DdPAC-3xFLAG-WPRE	1750	~1-3x10^{14}	Unilateral
DdPAC stimulation			
AAV9-CamKIIa-eGFP-WPRE	1429	~1-3x10^{14}	Bilateral
AAV9-CamKIIa-DdPAC-3xFLAG-WPRE	1544	~1-3x10^{14}	Bilateral
AAV9-GFAP-eGFP-WPRE	1749	~1-3x10^{14}	Bilateral
AAV9-GFAP-DdPAC-3xFLAG-WPRE	1750	~1-3x10^{14}	Bilateral

Table 4. Adeno-associated viral constructs. Summary of the adeno-associated viral constructs used in this thesis. This table provides information on each AAV, including the viral construct, reference, titre, and whether it was injected unilaterally or bilaterally. Results involving each animal model are presented in the corresponding "Result section". Most of viral constructs were supplied by Dr. Dalkara (Sorbonne Université, INSERM, CNRS, Institut de la Vision), and are referenced with their lot number. Other viral constructs are indicated in the table with their respective commercial sources.

4 Viral Delivery

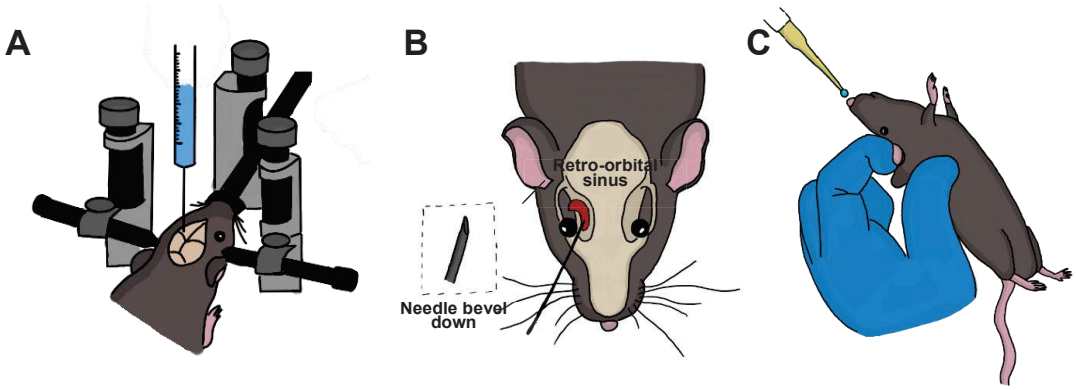

Figure 15. Viral delivery strategies. Graphic representation of the viral delivery strategies used in this thesis. A. Intra-cranial injection of AAVs, involving stereotaxic surgery for local administration in specific brain regions. B. Retro-orbital injection of AAVs, injected into the retro-orbital sinus using a needle bevel down, for systemic delivery. C. Intranasal administration of AAVs, providing a non-invasive method for delivery.

4.1 Intra-cranial injection - Stereotaxic surgery

Stereotaxic surgeries (Figure 15A) were conducted 3-4 weeks before the start of the experiment to allow mice recovery and stable expression of viral constructs (Conde-Berriozabal et al., 2023; Fernández-García et al., 2020). Surgeries were performed under isoflurane anaesthesia (5% induction, and 1.5 maintenance, Harvard Apparatus Isoflurane Vaporizer; #1371), with the mouse positioned on a heating blanket to prevent hypothermia, and fixed in a stereotaxic apparatus. Metacam (2mg/kg s.c.) was injected subcutaneously before the surgery to avoid pain and reduce inflammation. The head of the mouse was shaved and cleaned with ethanol and iodine. Then, local anaesthesia was applied (Lidocaine 2.5% and Prilocaine 2.5% EMLA®, AstraZeneca), followed by on incision in the skin on the top

of the head. Then, the skull was cleaned with deoxygenated water and holes were drilled according to the corresponding coordinates from bregma and dura matter (millimetres; mm) (Table 5). A volume of 0.5 µL of corresponding viral constructs (Table 4) was injected using a 5 µl Hamilton syringe with a 33-gauge needle at 0.1 µL/min. An additional 5 min period was left after each injection to allow diffusion and avoid refluxes.

For fibre photometry recordings and DdPAC stimulation, fibre-optic cannulas of specific lengths depending on the brain region were unilaterally or bilaterally implanted, respectively, and secured using dental cement (TAB 2000^{tm}, Kerr Dental) (Table 5).

After each experiment, mice were sacrificed by intracardial perfusion or cervical dislocation for validation of viral infection, confirmed by GFP or Flag expression, validation of location of fibre-optic cannula, assessed from histological slices (*see Immunohistochemistry*), and for biochemical analyses (*see Proteomics and Metabolomics*).

Brain area	Coordinates			Fibre-optic cannula	Results section
	AP	ML	DV		
M2 cortex	+2.46	±1	-0.6	MFC_400/430-0.66_1.0mm_MF1.25_FLT (Doric Lenses)	Fibre Photometry *Section 1.1* DdPAC cortical stimulation Proteomics and metabolomics *Section 2.2.3-2.2.4* Non-invasive delivery *Section 2.1*
SS cortex	+1.5	-3.5	-0.5	No cannula	Multi-electrode array experiments *Section 2.2.1-2.2.2*
SS cortex	-0.2	-1.8	-0.4	No cannula	DCS imaging *Section 3.1.1*
Striatum	+0.14	±2.2	-3.0	MFC_400/430-0.66_3mm_MF1.25_FLT (Doric Lenses)	DdPAC striatal stimulation *Section 3.1.4*
Hippocampus	-2	±1.25	-2 (from bone)	RWD-R-FOC-L400C-50NA Fibre length: 2mm (Biogen Cientifica SL)	DdPAC hippocampal stimulation *Section 3.2*

Table 5. Coordinates for viral infection and cannula implantation. Summary of the coordinates used for each viral local injection. This table provides information about the targeted brain region, coordinates and fibre-optic cannula. Results involving each animal model are presented in the corresponding "Result section". AP: Anterio-posterior axis; ML: medio-lateral axis; DV: Dorso-ventral axis. AP and ML coordinates are considered from bregma, and DV from dura.

4.2 Retro-orbital administration

Retro-orbital administration (Figure 15B) was performed under anaesthesia as previously described (Challis et al., 2019; Yardeni et al., 2011). The mouse was placed in a plexiglass induction chamber with ≈4-5% isoflurane. When the animal was completely anaesthetised, it was moved to a funnel-shaped nose cone connected to an apparatus with ≈1-1,5%

isoflurane (Harvard Apparatus Isoflurane Vaporizer; #1371). To decrease the possibilities of hypothermia, the mouse was placed on a heating blanket. To prepare for the injection, the skin above and below the eye was drawn back using the finger and thumb of the non-dominant hand, resulting in a slight protrusion of the eye from the socket. Then, using the dominant hand, 100µl of viral solution were injected to the retro-orbital sinus using a 27G syringe (BD Microlance 3; Ref: 302200) and by inserting the needle, bevel down, at 30/40º angle into the medial canthus and through the conjunctival membrane, positioning the needle behind the globe of the eye (figure Viral Delivery).

4.3 Intranasal administration

Intranasal administration (Figure 15C) was performed in awake mice as previously described (Hanson et al., 2013). Mice were acclimated to handling for a period of two weeks before the onset of intranasal administration in order to ensure proper body position and reduced anxiety during and after the procedure. The acclimation process included the following phases: 1) Gently handling the mouse by grasping it by the tail and placing it on the experimenter's arm to acclimate the animal to human presence; 2) Immobilizing the mouse by holding it at the scruff of the neck; 3) Performing the intranasal grip, which involved placing the mouse on the cage top, securely grasping the scruff behind the neck and shoulders, and then carefully turning the mouse onto its back once it was safely immobilized (Figure 15C). Transitioning from one phase to the next was dependent on the calmness exhibited by the animal. The intranasal administration involved delivering a 10µl of viral solution (5µl to each nostril), drawn with a micropipette, to the mouse's nostrils each day for a duration of 10 days, while the mouse was positioned in the intranasal grip, as previously described (total volume delivered 100µl). The administration was considered successful when the mouse was observed sniffing the AAV droplet.

5 Fibre photometry recording and analysis

Fibre photometry recordings were conducted to evaluate changes in cAMP dynamics in freely moving mice during the beetle mania and the accelerating rotarod tasks in WT and R6/1 mice from 14 to 20 weeks (Figure 16). We operated with a custom-made fibre photometry system from Doric Lenses Inc. and employed the G-Flamp1 fluorescent cAMP indicator (Table 4). The free Doric Neuroscience studio Software was used to control the Doric console and light-emitting diode (LED) drivers. A 465-nm LED (CLED_465) modulated at 241.58 MHz and a 405 nm LED (CLED_405) modulated at 572.21 MHz were directed and coupled into a personalized fluorescence mini cube (iFMC7_IE(400-410)_E1(460-490)_F1(500-540)_E2(555-570)_F2(590-645)_O(665-695)_S; Fluorescence MiniCube - 7 ports, F1 and F2 with Integrated Photodetector Head, Doric Lenses Inc, Quebec, Canada) through 1-meter fibre-optic patch cord (core diameter: 400 µm; numerical aperture: 0.50; M124L02 TP03030478). To allow freely moving tasks with mice, combined 465 nm and 405 nm light were launched to a fibre-optic rotary joint (RJ1 400-700nm,

Thorlabs), connected to a low autofluorescence mono fibre-optic patch cord (core diameter: 400 µm; numerical aperture: 0.57; P150799-1 FCM-ZF1.25) and mated with black covered Zicronia sleeve to the mouse-implanted fibre-optic cannula (*see Stereotaxic surgery*). Fluorescence delivered through the mini cube was detected and amplified by the Fluorescence Detector Amplifier from Doric, and data were sent to the fibre photometry console. Prior to each experiment, fibre-optic patch cords were bleached for at least 3h. To ensure stable photometric signals, mice were connected to the optic fibre 5 min before the task with the 465 and 405 LED turned on. After each recording session, mice were returned to their home cage. At the end of the experiments, mice were sacrificed by cervical dislocation for viral infection validation, confirmed by GFP expression, and location of fibre-optic cannula, assessed from histological slices (*see Immunohistochemistry*).

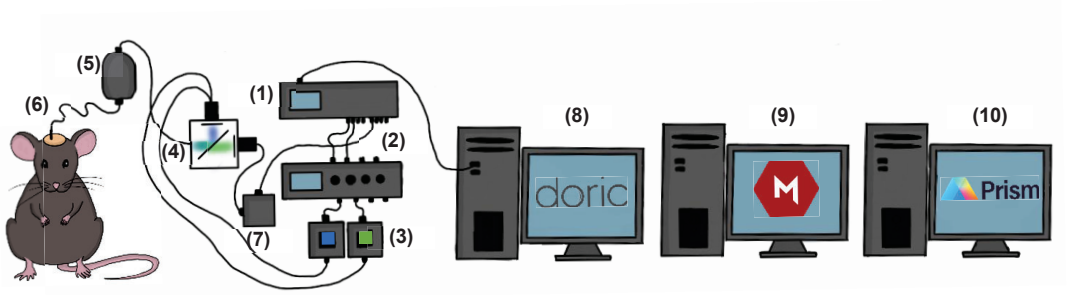

(1) Doric console (3) LEDs (5) Rotary joint (7) Amplifier (9) Signal processing
(2) LED driver (4) Fluorescence mini cube (6) Fiber-optic patchords (9) Doric Neuroscience software (10) Statistical analysis

Figure 16. Schematic representation of fibre photometry set-up *in vivo*. Intensity of raw and demodulated fluorescence was defined using Doric Neuroscience software (8) to control the Doric console (1) and LED drivers (2) 405 and 465 nm LED (3) signals were directed into a fluorescence mini cube (4) using fibre-optic patchcords (6). A fibre-optic rotary joint (5) between patchcords connecting the fluorescence mini cube and the mice was used to allow its freely movement. Recorded signals from the mini cube were amplified (7) and sent back to the Doric console. Processing of fluorescence demodulated data was done using the Metofico software (9). Further statistical analysis was performed using Graphpad Prism software (10).

Fluorescence intensity of raw and demodulated 465nm and 405nm signals was recorded at 12049 Hz in freely moving mice using the Doric Neuroscience Studio software. G-Flamp1 fluorescence (465 nm) was normalised using isosbestic fluorescent recordings (405 nm) to correct for movement and other artifacts. Data processing and analysis were performed using the Metofico Fibre Photometry Analyser (Metofico).

For fibre photometry recordings during the beetle-mania task (*see Behavioural assessment)*, data were down sampled to 1 Hz, large artefacts (>10 standard deviation) were removed using a digital filter and movement artefacts were corrected by subtracting normalized 405 nm from normalized 465 nm signal. A 2-second moving average was applied to smooth the data. The resulting ΔF/F signal was normalised using z-scoring. Average fluorescence during the 3 minuts before introducing the robo-beetle was considered as baseline. Statistical analysis was performed by comparing area under the curve, number of peaks and peak amplitude during the presence of the robo-beetle (post-baseline).

For fibre photometry recordings during the ARR task (*see Behavioural assessment*), data were down sampled to 1 Hz, artefacts were removed using a custom digital filter and movement

artefacts were corrected by subtracting normalized 405 nm from normalized 465 nm signal. Average fluorescence during the 60s in the cage prior to the placement of the mouse on the rotarod apparatus was considered as baseline. Statistical analysis was performed by comparing mean trace z-score normalised value of all animals and trials during the time on the rotarod apparatus of each group (WT vs R6/1 mice, males and females separately).

Heatmaps of activity were obtained using a custom-made MATLAB script to visualise change in activity after the corresponding stimulus.

6 Light-delivery for optogenetic stimulation

Red light (660nm or 685nm) was delivered to stimulate DdPAC, while blue (473nm) light was used to stimulate ChR2.

For slice stimulation (which were performed in Aston University by our collaborators Dr. Parri and Dr. Ngum), red light from 660nm LED (Thorlabs) was used to illuminate the slice in the MEA chamber during 10 minutes under manual control (Figure 17).

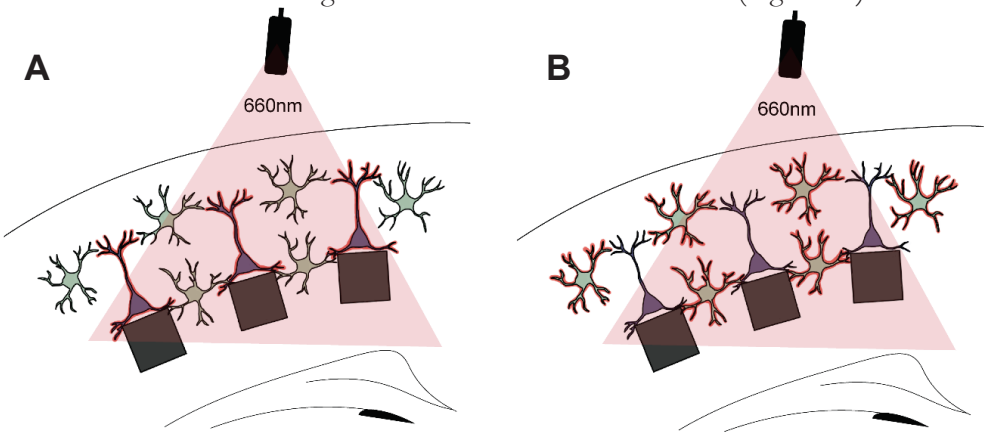

Figure 17. DdPAC stimulation in brain slices. 660nm light illumination of brain slices expressing DdPAC either in neurons (A) or astrocytes (B).

For *in vivo* DdPAC stimulations (Figure 18), red-light from a 685nm single LD Fibre Light Source (Doric Lenses) was delivered at ~6-18 mW (measured at the end of the patch cord) and was controlled by the free Doric Neuroscience studio Software. The stimulation protocol consisted of a 10-minute stimulation period, 1 second 685nm ON and 4 seconds 685nm OFF, in order to avoid heating of the tissue. Light beam was delivered from the 685 nm laser coupled to a fibre-optic patch cord (core diameter: 200μm; numerical aperture: 0.22) and split using a fibre-optic rotary joint (FRJ 1x2) to two separate fibre-optic patch cords (Core diameter: 200 μm; numerical aperture: 0.22). For omics and behavioural studies, zirconia sleeves were used to connect the patch cord to the implanted fibre-optic cannulas and stimulation was performed in freely moving animals. Specifically for behavioural studies, DdPAC stimulation was conducted 4 days (1 day every 3 days).

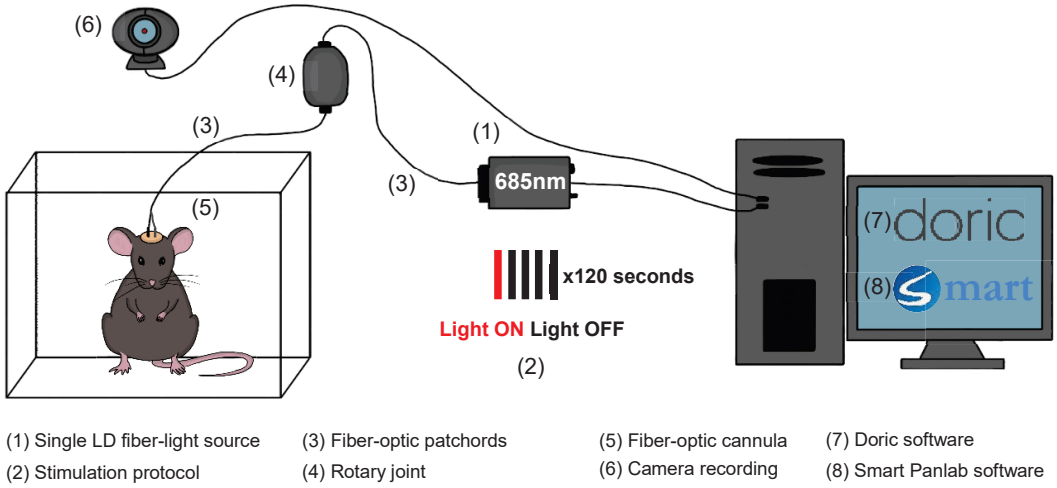

Figure 18. DdPAC stimulation *in vivo*. 685nm light was delivered from a single LD fibre-light source (1) during 10 minutes 1 seconds ON-4 seconds OFF (2) using fibre-optic patch cords (3) and a rotary joint (4) to allow the free move of the mouse. Doric Software (7) was used to control the laser parameters. A camera (4) was used to record the animal behaviour and the Smart software to analyse the behaviour during stimulation (8).

For diffuse wave spectroscopy imaging experiments, stimulation was performed in unilaterally in anesthetized head-fixed mice (*see Diffuse wave spectroscopy* for stimulation scheme). The patch cord was placed above the surface of the dura-matter, after drilling a whole on the skull the size of the tip of the cannula. In all *in vivo* cases, mice were habituated to manipulation before the experiment. For diffuse wave spectroscopy imaging experiments (*see Diffuse wave spectroscopy* for stimulation scheme), blue light was also delivered unilaterally using a 473 nm diode-pumped solid-state blue laser (Laserglow). In this case, blue light was delivered using a custom-made waveform generator (Arduino) at 10Hz, 5 ms pulses, 10mW for 1 minute.

7 Multi-electrode arrays

Multi-electrode arrays recordings (MEA) were performed by our collaborator Dr. H. Reinallt Parri and Dr. Neville Ngum from Aston University (United Kingdom).

7.1 Slice preparation

Slices of the mouse barrel cortex were prepared as previously described (Butcher et al., 2022a; Pirttimaki et al., 2017). Briefly, mice were anaesthetised with isoflurane overdose (5%) followed by cervical dislocation and the whole brain was removed and placed in an ice-cold bathing solution containing the following (in mM); NaCl 120, NaHCO3 25, KCl 1, KH2PO4 1.25, MgSO4 5, CaCl2 2, and glucose 10 and pH 7.2. Brains were glued to a metal block using cyanoacrylate adhesive and submerged in the bath of a Campden 7000 vibroslicer

(Campden Instruments) containing the same bathing solution maintained at <5° C and bubbled with 95% O2 and 5% CO2. Cortical slices (350 μm) were cut in the coronal plane and maintained in the bathing solution at room temperature oxygenated (95% O2/5% CO2) for at least 1 h recovery period before use. Recordings were performed in an artificial CSF (aCSF) solution containing the following (in mM): NaCl 120, NaHCO3 25, KCl 2, KH2PO4 1.25, MgSO4 1, CaCl2 2 and glucose 10.

7.2 Multi-electrode array recordings

The MED64 system (Alpha MED Scientific, Japan) with MEA probes consisting of 64 platinum electrodes, each 50 μm of diameter each and an inter-electrode distance of 150 μm in an 8x8 arrangement pattern, was used. Probes were pre-coated with 0.1% w/v polyethyleneimine (PEI) in a borate buffer overnight (> 12 h) at RT before first use. Cortical slices were carefully placed on the probes using an inverted microscope (10-X objective lens) such that the somatosensory barrels were on identified electrodes to enable selective stimulation of L4. fEPSPs were recorded from L2/3. Slices were held in position with mesh and slice harp. Once in position, a period of 15 min was allowed following aCSF perfusion (2 ml/min) to allow for equilibration before recordings were made. Synaptic stimulation was achieved by delivering 0.2 ms biphasic pulses to one electrode laying beneath an L4 region and fEPSPs recorded on electrodes laying beneath L2/L3 somatosentory cortex. The stimulating intensity was set 50% of a maximal fEPSP rising slope determined from the I/O curve produced using different stimulating intensities for each slice. A relatively low stimulating frequency [0.008 Hz] was used to evoke fEPSPs to avoid potential continuous stimulation-related effects on slice responses. Baseline recordings were done for 20 minutes before either stimulation with 660 nm light and/or TBS protocol, and plasticity was assessed 1 hr post-induction.

7.3 Life confocal imaging for evaluation of glutamate

Live confocal imaging was carried out by our collaborator Dr. H. Rheinallt Parri and Dr. Neville Ngum from Aston University (United Kingdom) using a Zeiss Axiovert 200M epifluorescent microscope using Leica Application Suite Advanced Fluorescence (LASAF) microscopy software (Leica Microsystems, Milton Keynes, UK). Acute cortical slices transfected with both hSyn.iGluSnFr and AAV-GFAP-DdPAC constructs were continuously perfused with aCSF and illuminated with 460 nm which is optimum for iGluSnFR stimulation in the green emission channel (Kopach et al., 2020). Experiments were done in the presence of 50 uL DL-threo-beta-benzyloxyaspartate (DL-TBOA) (Tocris) to block excitatory amino acid transporters. Images for iGluSnFR signals were collected in a time-lapse mode in 1s intervals before, during and after evoked glutamate release. For a positive control, some experiments involved bath application of glutamate (100 μM) to acute slices co-injected with both constructs. To assess DdPAC's effect on glutamate increment, experiments were done in the dark and acute slices were illuminated with 660 nm light following collection of baseline measurements. The iGluSnFR signal was expressed as the

ΔF/F0, = (F (t)- F0) / F0 where F(t) stands for intensity over time, and F0 is the baseline intensity averaged over ~ 60 s prior to the stimulus.

8 Proteomics and phospho-proteomics

Proteomics and phospho-proteomics analysis were performed at the Clinical Neuroproteomics Unit (Navarrabiomed-IdiSNA, Hospital Universitario de Navarra, Navarra, Spain).

8.1 Tissue obtention and sample preparation

Mice were euthanised by cervical dislocation immediately after the 10 minutes light stimulation (DdPAC stimulation in the cortex of HD mice) or 24 hours after stimulation (DdPAC stimulation in the hippocampus of AD mice). The tissue surrounding the cannula was obtained from the left hemisphere and immediately frozen. Tissue samples were homogenized in a lysis buffer (7 M urea, 2 M thiourea, 50 mM dithiothreitol (DTT), supplemented with protease (cOmplete Mini, Roche #11836153001) and phosphatase inhibitors (PhosSTOP, Roche #4906845001). Lysates were centrifuged at 20,000 g (1 h, 15 °C), and the resulting supernatant was quantified with the Bradford assay kit (BioRad, Barcelona, Spain). To obtain the phosphorylated peptide sample fraction, 600 μg of protein was separated for protein digestion. Proteins were reduced with DTT (final concentration of 20 mM; room temperature, 30 min), alkylated with iodoacetamide (final concentration of 30 mM; room temperature, 30 min in the dark), diluted to 0.9 M with ABC and digested with trypsin (Promega, Madison, WI, USA; 1:20 w/w enzyme protein ratio, 18 h, 37 °C). Protein digestion was interrupted by acidification (pH < 6, acetic acid), and the resulting peptides were cleaned-up using Pierce™ Peptide Desalting Spin Columns (ThermoFisher Sci., Waltham MA, USA). The following phosphorylated peptide enrichment was performed using the High-Select™ TiO2 Phosphopeptide enrichment Kit (ThermoFisher Sci., Waltham, MA, USA) according to the manufacturer's instructions. Finally, the enriched phosphopeptide sample fraction was cleaned- up as described before and dried down in a Speed-Vac system. A 10 μg aliquot of cleaned-up peptides from protein digestion was set aside for total protein analysis.

8.2 Data independent acquisition (DIA)-mass spectrometry

Dried-down peptide samples were reconstituted with 2% ACN-0.1% FA (Acetonitrile-Formic acid), spiked with internal retention time peptide standards (iRT, Biognosys), and quantified by NanoDropTM spectrophometer (ThermoFisher Sci.) prior to LC-MS/MS analysis using an EASY-1000 nanoLC system coupled to an EZ-Exploris 480 mass spectrometer (Thermo Fisher Sci.). Peptides were resolved using C18 Aurora column (75μm x 25cm, 1.6 μm particles; IonOpticks) at a flow rate of 300 nL/min using a 60-min gradient (50 ºC): 2% to 5% B in 1 min, 5% to 20% B in 48 min, 20% to 32% B in 12 min, and 32% to 95% B in 1 min (A = FA, 0.1%; B = 100% ACN:0.1% FA). Peptides were ionized using

1.6 kV spray voltage at a capillary temperature of 275 °C. Sample data were acquired in data-independent acquisition (DIA) mode with full MS scans (scan range: 400 to 900 m/z; resolution: 60,000; maximum injection time: 22 ms; normalized AGC target: 300%) and 24 periodical MS/MS segments applying 20 Th isolation windows (0.5 Th overlap: Resolution: 15000; maximum injection time: 22 ms; normalized AGC target: 100%). Peptides were fragmented using a normalized HCD collision energy of 30%.

8.3 Bioinformatics and statistical analysis

Mass spectrometry data files were analyzed using Spectronaut (Biognosys) by direct DIA analysis (dDIA). MS/MS spectra were searched against the Uniprot proteome reference from mouse database using standard settings. Enzyme was set to trypsin in a specific mode. On the one hand, Carbamidomethyl (C) was set as a fixed modification, and oxidation (M), acetyl (protein N-term), deamidation (N), and Gln-> pyro-Glu as variable modifications for total protein analysis. On the other hand, Carbamidomethyl (C) was set as a fixed modification, and oxidation (M), acetyl (protein N-term), and Phospho (STY) as variable modifications for phospho-proteome analysis. Identifications were filtered by a 1% Q-value.

The obtained quantitative data for total protein were exported to Perseus software (version 1.6.15.0) (Tyanova et al., 2016) for statistical analysis and data visualization. For total protein analysis, unpaired Student's t test was used for direct comparisons. Statistical significance was set at p-value lower than 0.05 in all cases and 1% peptide FDR threshold was considered. Differentially expressed proteins were considered significant when their absolute fold change was below 0.77 (downregulated proteins) and above 1.3 (up-regulated proteins) in linear scale. Quantitative data obtained from the phosphoproteome were collapsed using a custom coded plugin Peptide Collapse (v.1.4.4) in Perseus (v.1.6.15.0) that convert a normal Spectronaut report into a site-level report (Martinez-Val et al., 2021). Plugin settings were set as default grouping posttranslational modifications (PTMs) by sample (FileName), collapsing matrix by site-level and setting the PTM localization probabilities filter at more than 0.75. Statistical analysis were conducted following the same protocol as the total protein study.

The functionality associated to the differential (phospho)proteomes was assessed using Metascape (Y. Zhou et al., 2019) using default settings (min. overlap: 3, min. enrichment: |1.5|, $P<0.05$). Synaptic ontologies were obtained from SYNGO tool (Koopmans et al., 2019). Protein interactomes and activation predictions were analyzed using QIAGEN's Ingenuity Pathway Analysis (IPA; QIAGEN Redwood City) (Krämer et al., 2014).

Mass-spectrometry data and search results files were deposited in the Proteome Xchange Consortium/PRIDE with the identifiers PXD054633 (Proteomics data; for reviewers: Username: reviewer_pxd054633@ebi.ac.uk; Password: 078LQM64Kunm) and PXD054635 (phosphoproteomics data: Username: reviewer_pxd054635@ebi.ac.uk; Password: HyU81N9RTXR0

Partial least squares differential analysis (PLS-DA)

In the context of proteomics data from AD. Variable distribution was scaled by calculating Z-scores for proteomics raw data. Then, we performed a partial least squares differential analysis (PLS-DA) with repeated cross-validation to analyze the effect of DdPAC activation in WT and 5xFAD samples in the cerebral protein profile. To evaluate the performance of the PLS-DA classification, we calculated the optimal number of components, the balanced error rate (BER), and the area under the curve (AUC) scores, which estimate the specificity and sensitivity of the model from training cross-validation with 50 repetitions. The accuracy of the whole PLS-DA model was validated through a permutation system with 1,000 iterations. Finally, we calculated the variable importance in projection (VIP) scores to estimate the significance of each variable in the projection used in the PLS-DA model and to select those proteins that contribute most to the underlying differences. VIP scores ≥ 1.4 were considered significant. Unsupervised principal component analysis (PCA) and Pearson's distance clustering were also performed. All analyses were performed with R. The PLS-DA model was generated and validated with the MixOmics R package (Rohart et al., 2017). R packages were executed in RStudio 2022.12.0-353 for Windows (Posit.co) and R 4.2.2 for Windows (The Comprehensive R Archive Network -CRAN-).

PKA network analysis

In the context of proteomics data from AD. The interaction network map of PKA-related proteins was generated using Cytospace 3.10.3 (U.S.A. National Human Genome Research Institute (NHGRI) based in the STRING functional protein association network database. Also using the STRING database, we performed a Gene ontology (GO) enrichment analysis to find GO terms over-represented, using annotations for the PKA-related protein set. We considered enriched GO terms with FDR-corrected $P < 0.05$ statistically significant.

9 Metabolomics

Targeted metabolomics was performed in the VIB Metabolomics core facility (Leuven, Belgium).

9.1 LC–MS/MS analysis of metabolites

Mice were euthanised by cervical dislocation immediately after the 10 minutes light stimulation. The tissue surrounding the cannula including the frontal cortex was obtained from the right hemisphere and immediately frozen. 10 µl of each sample was loaded into a Dionex UltiMate 3000 LC System (Thermo Scientific Bremen, Germany) equipped with a C-18 column (Acquity UPLC -HSS T3 1. 8 µm; 2.1 x 150 mm, Waters) coupled to a Q Exactive Orbitrap mass spectrometer (Thermo Scientific) operating in negative ion mode. A step gradient was carried out using solvent A (10 mM TBA and 15 mM acetic acid) and solvent B (100% methanol). The gradient started with 5% of solvent B and 95% solvent A and remained at 5% B until 2 min post injection. A linear gradient to 37% B was carried out

until 7 min and increased to 41% until 14 min. Between 14 and 26 minutes the gradient increased to 95% of B and remained at 95% B for 4 minutes. At 30 min the gradient returned to 5% B. The chromatography was stopped at 40 min. The flow was kept constant at 0.25 mL/min and the column was placed at 40°C throughout the analysis. The MS operated in full scan mode (m/z range: [70.0000-1050.0000]) using a spray voltage of 4.80 kV, capillary temperature of 300 °C,sheath gas at 40.0, auxiliary gas at 10.0. The AGC target was set at 3.0E+006 using a resolution of 140000, with a maximum IT fill time of 512 ms. Data collection was performed using the Xcalibur software (Thermo Scientific). The data analysis was performed by integrating the peak areas (El-Maven – Polly - Elucidata).

9.2 Multivariant analysis of metabolites

Raw abundance was calculated as the integrated area of the peak of the metabolite and corrected by tissue weight. Then, we performed multivariate statistical analysis for differential concentration assessment. The pipeline includes fold-change and multiple T-test analysis, correlation heatmaps, principal component analysis (PCA), and hierarchical clustering to identify differential metabolite concentrations. LC–MS/MS data was log-transformed and scaled. The correlation between differential metabolites was analyzed using the Pearson correlation method. The set of metabolites was also subjected to enrichment pathway analysis using RaMP-data base (integrating KEGG via HMDB, Reactome, and WikiPathways) as the reference database. Adjusted-p values < 0.05 were considered as significant. All the analysis were performed using the MetaboAnalyst 6.0 platform (Pang et al., 2024).

10 DCS-based brain hemodynamics imaging system

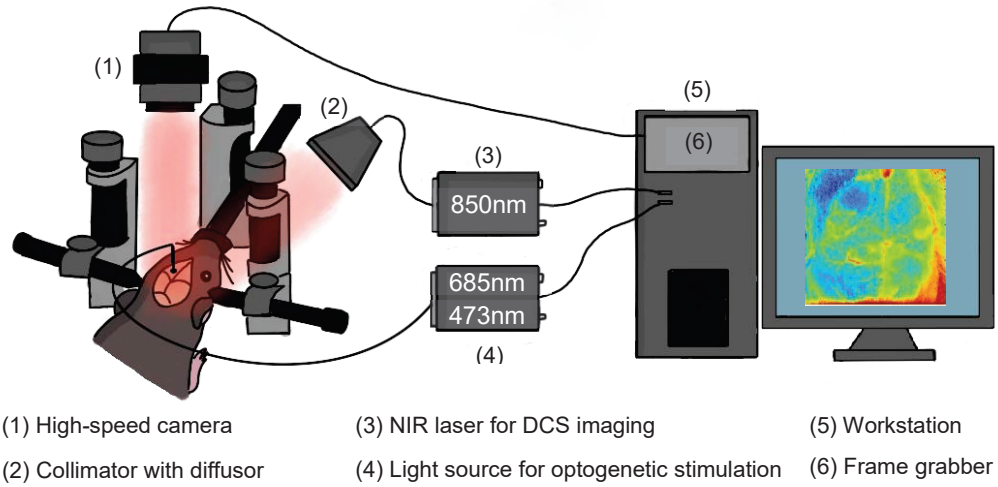

Figure 19. DCS-based brain hemodynamics imaging system setup. Imaging setup for mapping light dependent cortical blood flow changes obtained with DCS-based imaging setup in a head-fixed anesthetized mouse. Images were obtained with (1) a high-speed camera coupled with the (3) 850 nm NIR laser illumination attached to (2) a collimator with diffusor. (4) Light sources for optogenetic stimulation, 685 nm to stimulate DdPAC or 473 to stimulate ChR2, were used.

Diffusion Correlation Spectroscopy (DCS) (Sdobnov et al., 2024) is a technique used to measure blood flow in biological tissues, including the brain. In DCS, a coherent laser light illuminates the tissue, and the diffusely reflected light scattered within the tissue is analysed. The motion of red blood cells within the tissue causes fluctuations in the intensity of the scattered light. These temporal intensity fluctuations are captured by a high-speed camera. The basic principle of DCS is that the faster the red blood cells move, the shorter the correlation time will be. The time correlation, derived from the auto-correlation function of the temporal intensity fluctuations, can be used to assess cerebral blood flow in brain tissues.

R6/1 and WT mice were injected unilaterally (*see Local injection - Stereotaxic surgery*) with DdPAC or ChR2 (*see Adeno-associated viral constructs*) one month before the acquisition of the images. Diffuse wave spectroscopy images were acquired under isoflurane anaesthesia (5% induction, and 1.5 maintenance, Harvard Apparatus Isoflurane Vaporizer; #1371) while the mouse was positioned on a heating blanket to prevent hypothermia, and fixed in a stereotaxic apparatus to avoid movement. Metacam (2mg/kg s.c.) was injected subcutaneously before the procedure to avoid pain and reduce inflammation. The head of the mouse was shaved and cleaned with ethanol and iodine. Local anaesthesia was then applied (Lidocaine 2.5% and Prilocaine 2.5% EMLA®, AstraZeneca), followed by an incision in the skin on the top of the head. Subsequently, a hole was drilled at the location corresponding to the mark from the previous viral injection surgery, ensuring the dura mater remained intact. A cannula was positioned over the drilled hole, without contacting the brain, during the stimulation phase.

Our setup for the transcranial blood flow imaging (Figure 19) comprised a high-speed camera (EoSens 3CL, Germany), a frame grabber card (Silicon Software, Germany), an 850 nm distributed Bragg reflector single-frequency NIR laser (Thorlabs Inc, USA), and a collimator with a diffuser. At the surface of the studied object, the laser intensity was maintained at 20 mW/cm^2. Crossed polarizers were employed on the collimator and camera objective to eliminate surface reflections. This configuration enabled the reconstruction of blood flow images with a resolution of 240 x 240 pixels and facilitated the calculation of the temporal intensity autocorrelation function of light at each of the measured pixels within a range of 10^{-4} to 1 second. Specifically, in our study, we recorded 50,000 frames per measurement at a frame rate of 8,000 fps for subsequent processing.

The protocol for image acquisition was the following. First, 3 baseline images (10s recording each) were acquired, followed by the placement of the cannula and a 10-minute stimulation (*see Optogenetic stimulation*). Then, 5 post-stimulus images (10s each) were acquired.

Blood flow index (BFI) maps were calculated as an average value of the power spectrum obtained through the Fourie transform of the measured autocorrelation function in each pixel according to the equation (Leahy et al., 1999):

$$BFI_{i,j} = \left(\int \omega S\left[g_2^{i,j}(t) - 1\right] d\omega\right) / \langle I_{i,j} \rangle.$$

Here $S[g_2(t) - 1]$ is the power spectrum obtained through the Fourier transform of the temporal autocorrelation function, $\langle I \rangle$ is the average DC signal from the pixel, *i* and *j* are correspondingly the row and column number of the image map identifying the pixel. All data were processed on Matlab (version 9.4.0.813654 (R2018a), and final images were opened with Image J software (Schindelin et al., 2012), mounted as stack images and intensity of the whole hemisphere was measured using the measure tool plugin in all images obtained from each mouse.

11 Immunohistochemistry and image acquisition

Antigen	Host species	Dilution	Target	Reference and source
GFP	Chicken	1:500	G-Flamp1 AAV9/PHP.eb-CAG-GFP AAV9/PHP.eb-CamKIIa-GFP	132 006, Synaptic Systems
GFP	Rabbit	1:500	AAV9/PHP.eb-CamKIIa-GFP AAV9/PHP.eb-GFAP-GFP	
Flag	Mouse	1:200	AAV9/PHP.eb-CamKIIa-DdPAC-Flag AAV9/PHP.eb-GFAP-DdPAC-Flag	F1804, Sigma Aldrich
GFAP	Rabbit	1:500	GFAP positive astrocytes	Z0334, DAKO
AQP4	Rabbit	1:500	Aquaporin 4 channel	AB3594, Merck
p21	Rat	1:200	Proliferative astrocytes	ab107099, Abcam
APP	Rabbit	1:800	Aβ precursor protein	NBP2-62566, Novus Biologicals
Iba1	Goat	1:500	Iba1 positive microglia	Ab5076-1001, Abcam

Table 6. Primary antibodies. Summary of the primary antibodies used in this thesis. This table provides information about the antigen, host species, dilution, specific target, and reference and source.

For immunohistochemical analysis, mice were sacrificed by cervical dislocation and brains were post-fixed with 4% PFA and dehydrated in a PBS/sucrose gradient [from 15% (48h postmortem) to 30% (32 h postmortem)] with 0.02% sodium azide and finally stored at 4ºC. Sections (30µm) were cut on a vibratome (Leica VT1000S) and preserved in cryopreservation solution (30ml Ethylene glycol; 30ml Glycerol; 25ml TB (1M Tris HCl pH 7,5); 15ml H2O miliQ for 1 litre of solution) at -20ºC. Free-floating sections were first washed in PBS 0.01M, then treated with 50mM NH4Cl, permeabilized with 0.01M PBS containing 0.5% Triton X-100 and blocked for 2hrs with a solution of 0.01M PBS with azide 0.02%, 0.3% Triton X-100, BSA 0.2% and 5% normal goat serum (Pierce Biotechnology). Sections were then incubated overnight at 4ºC with the primary antibodies (Table 6), which were diluted in a solution of 0.01M PBS with azide 0.02%, 0.5% Triton X-100, BSA 0.2% and 5% normal goat serum. After washing with 0.01M PBS, brain sections were incubated for 1:30hrs with the secondary antibodies (Table 7), diluted in 0.01PBS. After secondary antibody incubation, sections were washed in 0.01M PBS and mounted on microscope slides using DAPI Fluoromount-G (Southern Biotechnology) and kept in the dark. All washes and incubations were completed on a shaker and at RT, except for the primary antibody incubation, which was conducted at 4 ºC.

Secondary antibody	Wavelenght	Dilution	Reference and source
Anti-chicken	Alexa Fluor 488	1:200	A11039, Invitrogen
Anti-mouse	AlexaFluorTM 647	1:200	A21236, Invitrogen
Anti-rabbit	Cy3 555	1:200	JAC 111-165-003
Anti-rat	Cy3 555	1:200	712-165-150, Jackson ImmunoResearch

Table 7. Secondary antibodies. Summary of the secondary antibodies used in this thesis. This table provides information about the antigen, detected wavelength, dilution, and reference and source.

Fluorescence images were acquired by an epifluorescence microscope (DMI6000 Widefield Leica) or a confocal microscope (Carl Zeiss LSM880). ImageJ/Fiji software was used to analyse the images (Schindelin et al., 2012)(Table 8).

12 Statistical analysis

All results are expressed as mean ± SEM, with individual mouse data represented by single points when possible. Statistical significance was set at $P < 0.05$ (*), $P < 0.01$ (**), and $P < 0.001$ (***). Statistical analysis was performed using GraphPad Prism version 10.0.0, except for diffuse wave imaging experiments, which were analysed in MATLAB (version 9.4.0.813654 (R2018a) (*see 10 DCS-based brain hemodynamics imaging system section for detailed analyses*) and omics results (*see 8 Proteomics and 9 Metabolomics sections for detailed analyses*). Comparisons between two groups were conducted using either the two-tailed unpaired Student's t-test or the Mann-Whitney U test. For comparisons between LTP and baseline in MEA recordings, the Wilcoxon test was used. Multiple comparisons to the same control were analysed using one-way ANOVA with the non-parametric Kruskal–Wallis test, followed by Dunn's post hoc test. Hemodynamic and behavioural experiments were analysed using the one-sample t-test, two-tailed unpaired Student's t-test, or two-way/three-way ANOVA, followed by Bonferroni post hoc test when appropriate. The specific statistical tests used are indicated in the Results section and/or figure legends.

RESULTS

1 To characterise disruptions in cortical cAMP signalling and behaviour in the R6/1 mouse model of Huntington's Disease

cAMP is a second messenger involved in a diverse range of processes, including synaptic plasticity, and its signalling pathway has been observed to be disrupted in HD (Gines et al., 2003; Giralt et al., 2011; Kelly, 2018; Tyebji et al., 2015). Notably, the degree of impairment varies across brain regions and cell types, and controversies are observed between research findings (Kelly, 2018). Thus, further investigation is necessary to fully understand the contribution of cAMP signalling to HD, which could open new possibilities for novel therapeutic strategies.

In this context, we aimed to investigate whether cAMP dynamics are altered during M2-cortex-dependent behaviours, given that the M2 cortex is a brain region profoundly affected in HD (Fernández-García et al., 2020; Hintiryan et al., 2016; Thiruvady et al., 2007). These behaviours include motor learning tasks such as the accelerating rotarod (ARR) and stimuli-induced defensive responses like the beetle mania task (BMT), both of which are known to exhibit altered performance in HD models and are M2-cortex dependent (Conde-Berriozabal et al., 2023; Fernández-García et al., 2020; Puigdellívol et al., 2015). In this regard, modulation of M2-dorsolateral striatum circuitry using optogenetics ameliorates motor learning deficits in the ARR in R6/1 mice (Fernández-García et al., 2020). Additionally, in another study from the group, we demonstrated that exposure to a moving robo-beetle induced Ca^{2+} increase in the M2 cortex of WT mice, which was absent in R6/1 mice (Conde-Berriozabal et al., 2023). Building on this knowledge, we sought to uncover if cAMP dynamics contribute to the alterations in cortico-striatal-related behaviours in HD, including the ARR and the BMT. Additionally, we aimed to explore if other M2-cortex behaviours are affected in HD, as well as to determine their onset to further comprehend the progression of M2-associated behaviours. Identifying early markers could enable the initiation of therapeutic interventions at prodromal stages, potentially improving their efficacy and offering a strategy to assess treatment outcomes.

1.1 Assessment of cAMP signalling pathway alterations in the R6/1 mouse model of Huntington's Disease

1.1.1 cAMP levels increase in the M2 cortex of 14-week-old mice in response to an expected stimulus during the beetle-mania test

Despite the numerous cAMP fluorescent sensors developed, until recently it was difficult to study cAMP dynamics in vivo. In the context of this thesis, we successfully utilised the novel cAMP sensor G-Flamp1(L. Wang et al., 2022a). G-flamp1 plasmid was generously provided by Dr. Liang Wang and Dr. Jun Chu (Shenzhen Institute of Advanced Technology, Chinese Academy of Sciences, Shenzhen, China) and encapsulated into an AAV9 construct by Dr

Dalkara. By using this cAMP sensor under a neuronal promoter, we first assessed real-time cAMP fluctuations during the BMT task in 14-week-old male and female mice, a stage at which R6/1 mice already exhibit behavioural phenotype (Conde-Berriozabal et al., 2023).

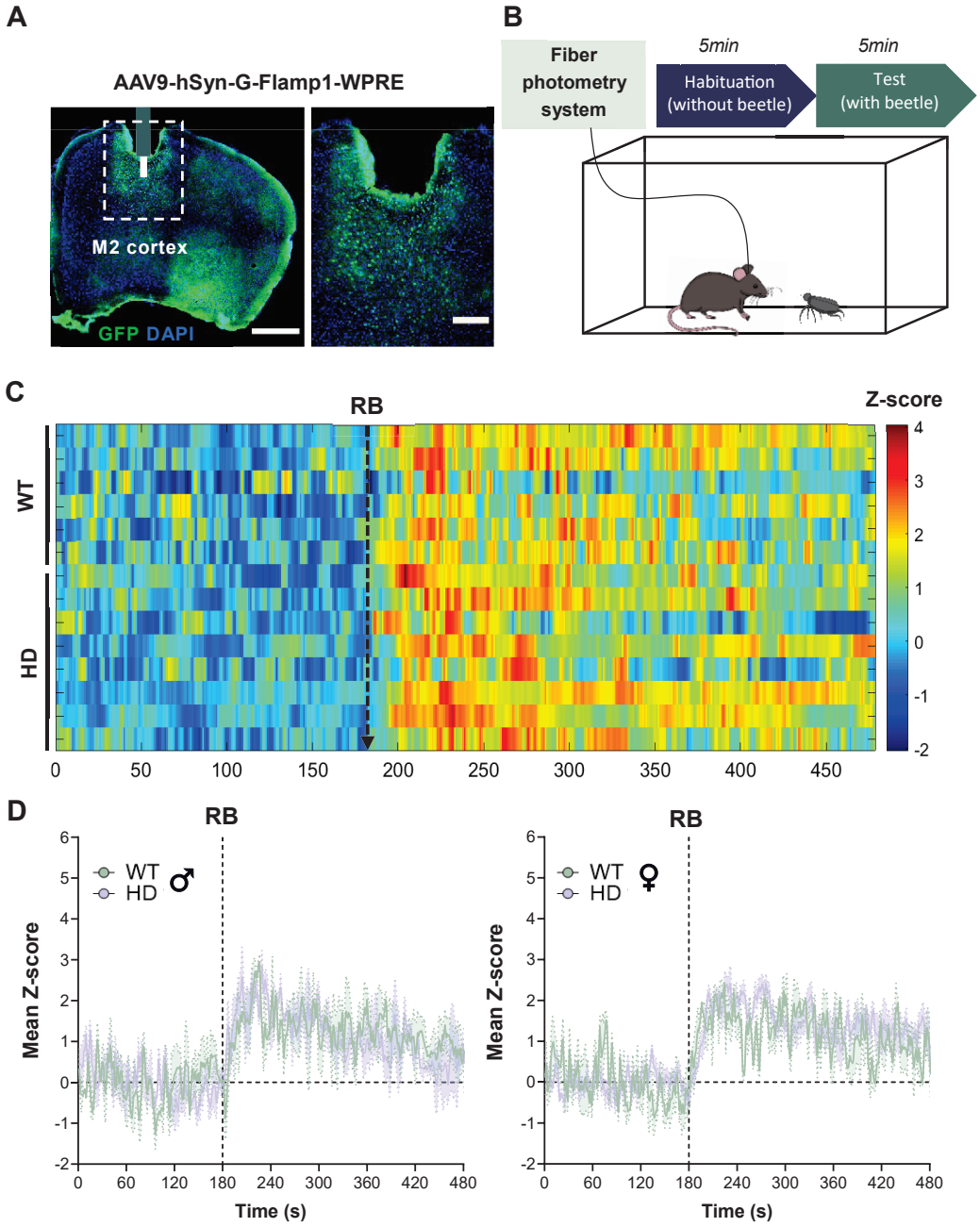

Figure 20. Neuronal GFlamp-1 fluorescence increases in response to an unexpected sensory stimulus in the M2 cortex of 14-week-old WT and R6/1 mice. (A) Representative histological images showing GFlamp-1 expression in neurons (green) from the M2 cortex, indicating the position of the fibre-optic cannula (scale bars: 600 µm (left) and 200µm (right)) (B) Schematic representation of the beetle mania task during fibre-photometry recordings. After 5 minutes of habituation in the arena, the moving beetle (RB, dashed arrow) is added for an additional 5 minutes (C) Heatmap of activity showing changes in GFlamp-1 fluorescent signal (ΔF/F0 normalised to z-score) in WT and R6/1 mice (Y axis, each line represents an individual mouse) at 14 weeks of age. X axis represents the duration of the recording (in seconds). Only the last 180s of habituation are considered and represented as baseline for the analysis. ΔF/F0 changes are transformed to z-score normalised

to baseline, colour-coded and represented from >-2 (blue) to <4(red). (D) Mean GFlamp-1fluorescent traces (Y axis: ΔF/F0 normalised to z-score) from male (left) and female (right) WT and R6/1 mice during the performance of the test. The placement of the robo-beetle (RB) is represented at the second 180 of the X axis. $N_{WT♂}=3$; $N_{WT♀}=3$; $N_{R6/1♂}=3$; $N_{R6/1♀}=5$

Hence, we expressed the cAMP sensor in M2 cortical neurons by injecting an AAV9-hSyn-G-Flamp1-WPRE construct (Figure 20A) and recorded cAMP fluorescence throughout the 10-minute BMT. The stimulus, an erratically moving robo-beetle, was introduced at the 5-minute mark to asses stimulus-dependent cAMP dynamics (Figure 20B). Both genotypes showed stable and similar fluorescent signal during the habituation phase (3 last minutes of the baseline, shown in the graph), which notably increased after placing the robo-beetle in the arena in both genotypes (Figure 20C). In order to evaluate possible sex differences in cAMP signalling, we decided to examine the cAMP traces of male and female separately (Figure 20D). Our data showed similar qualitative increases upon the introduction of the beetle in both genotypes, as well as between male and female traces.

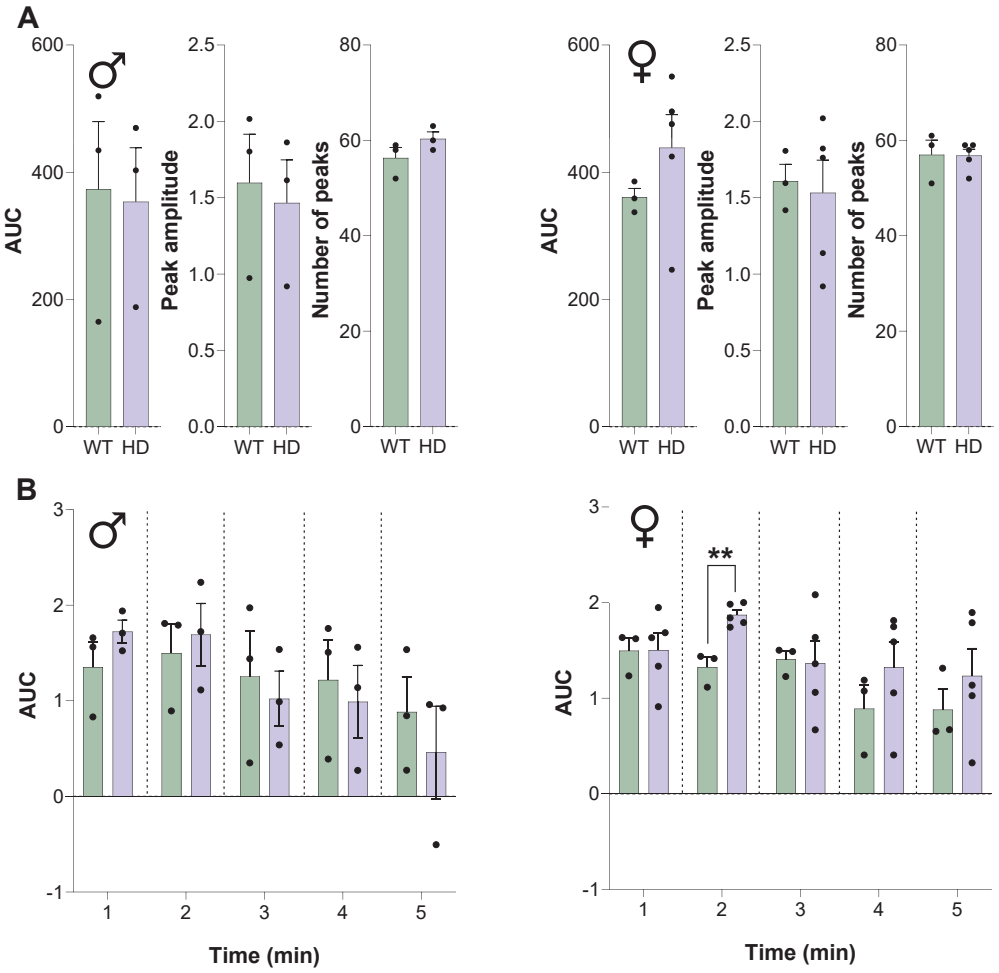

Figure 21. GFlamp-1 fluorescence changes are similar between WT and R6/1 mice. (A) Histogram representing the 5-min post-baseline area under the curve (AUC), peak amplitude and number of peaks of the GFlamp-1 z-score normalised fluorescent signal between WT and R6/1 male (left) and female (right) mice. (B) Histogram representing the comparison of area under the curve (AUC) of the GFlamp-1 z-score normalised signal between male (left) and female (right) WT and R6/1 mice. X axis represents each minute with the

presence of the robo-beetle. Each point represents data from an individual mouse. Unpaired T-test was performed. $N_{WT♂}=3$; $N_{WT♀}=3$; $N_{R6/1♂}=3$; $N_{R6/1♀}=5$. *p<0.05, **p<0.01, ***<0.001.

To further quantify these results, we calculated the area under the curve (AUC), the peak amplitude, and the total number of peaks, and assessed genotype differences in each sex separately (Figure 21A). We confirmed that there were no differences between genotypes in neither of the metrics analysed during the 5 minutes. In males, unpaired t-test displayed a p=0.90, p=0.77, and p=0.20 for the AUC, peak amplitude and total number of peaks, respectively. In females, unpaired t-test showed a p=0.31, p=0.81, and p=0.95 for the AUC, peak amplitude, and total number of peaks, respectively. To further investigate if cAMP dynamics were changing along time, we analysed the G-Flamp1 signal each minute the beetle was present in the arena (Figure 21B). Again, we did not observe any genotype differences in any of the time slots analysed in males. Nevertheless, female R6/1 mice displayed an increase in the G-Flamp1 signal during the second minute with the presence of the beetle (Unpaired t-test, p=0.002). Overall, these results reveal the involvement of cAMP signalling in neurons from the M2 cortex during the BMT, although they suggest that cAMP dynamics are minimally altered in R6/1 mice. Along with our previous findings indicating calcium changes during the BMT (Conde-Berriozabal et al., 2023), these results demonstrate that both second messengers contribute to M2-cortex dependent task modulation in neurons.

To ensure that the lack of genotype effects is not due to lack of phenotype, we analysed locomotion and spontaneous behaviour during habituation, along with the behavioural responses to the beetle during the test phase. Our prior findings (Conde-Berriozabal et al., 2023) exhibited changes in time spent rearing, but not locomotion, during habituation phase, and altered reactions to the robo-beetle from 12-week-old male and female mice. Our data presented here at 14-week-old mice also show altered responses in R6/1 mice, similar to our previous results. During the first 5 minutes of the test, when no threatening stimulus was present and the mice were acclimating to the arena, we analysed the distance travelled and the time spent rearing (Figure 22A and 22B). These parameters allow us to study if these mice already show altered spontaneous activity, such as rearing and locomotor deficits. Indeed, this was not the case, as locomotion was similar between genotypes (Genotype: $F_{(1,16)}=0.01$, P=0.92; Sex: $F_{(1,16)}=1.09$, P=0.31; Interaction: $F_{(1,16)}=1.06$, P=0.32). Moreover, it is known that symptomatic R6/1 mice usually show decreased rearing time. In this case, there are no significant differences between groups (Genotype: $F_{(1,16)}=1.31$, P=0.27; Sex: $F_{(1,16)}=0.028$, P=0.87; Interaction: $F_{(1,16)}=3.91$, P=0.06) (Figure 22B). Then, during the testing phase, we measured escape, avoidance, approach, and tolerance responses to the randomly moving robo-beetle. Consistent with our previous publication, R6/1 mice reduced defensive behaviours such as escape and avoidance, while increased tolerance to the beetle. Moreover, sex differences were not observed. In detail, Two-way ANOVA with sex and genotype as factors showed genotype effect but not sex or interaction for the number of total responses (Genotype: $F_{(1,16)}=4.32$, P=0.05; Sex: $F_{(1,16)}=0.30$, P=0.59; Interaction: $F_{(1,16)}=5.27$, P=0.03); escape responses (Genotype: $F_{(1,16)}=6.36$, P=0.02; Sex: $F_{(1,16)}=0.59$, P=0.45; Interaction: $F_{(1,16)}=0.54$, P=0.47); avoidance (Genotype: $F_{(1,16)}=6.45$, P=0.02; Sex: $F_{(1,16)}=0.01$, P=0.93;

Interaction: $F_{(1,16)}$=0.16, P=0.69) and tolerance (Genotype: $F_{(1,16)}$=17.98, P=0.0006; Sex: $F_{(1,16)}$=0.27, P=0.61; Interaction: $F_{(1,16)}$=0.18, P=0.68) behaviours (Figure 22F and 22H). However, Two-way ANOVA did not display differences in the percentage of approach responses (Genotype: $F_{(1,16)}$=1.66, P=0.22; Sex: $F_{(1,16)}$=0.24, P=0.62; Interaction: $F_{(1,16)}$=0.008, P=0.92) (Figure 22D and 22G). Moreover, Bonferroni post hoc analysis of the total number of responses showed that female R6/1 mice exhibited a decreased number compared to female WT mice (P = 0.04), whereas no genotype differences were observed in male mice (Figure 22C). Also, for tolerance behaviour, Bonferroni post-hoc showed significant differences between male WT and male R6/1 (P=0.03) and female WT and male R6/1 mice (P=0.02) (Figure 22F).

Overall, in 14-week-old mice, we found reduced defensive behaviours, while increased tolerance responses in R6/1 mice compared to WT, similar to previous data and with no sex effects. This suggests that other mechanisms or signalling pathways, rather than neuronal cAMP dynamic changes, contribute to the observed behavioural alterations.

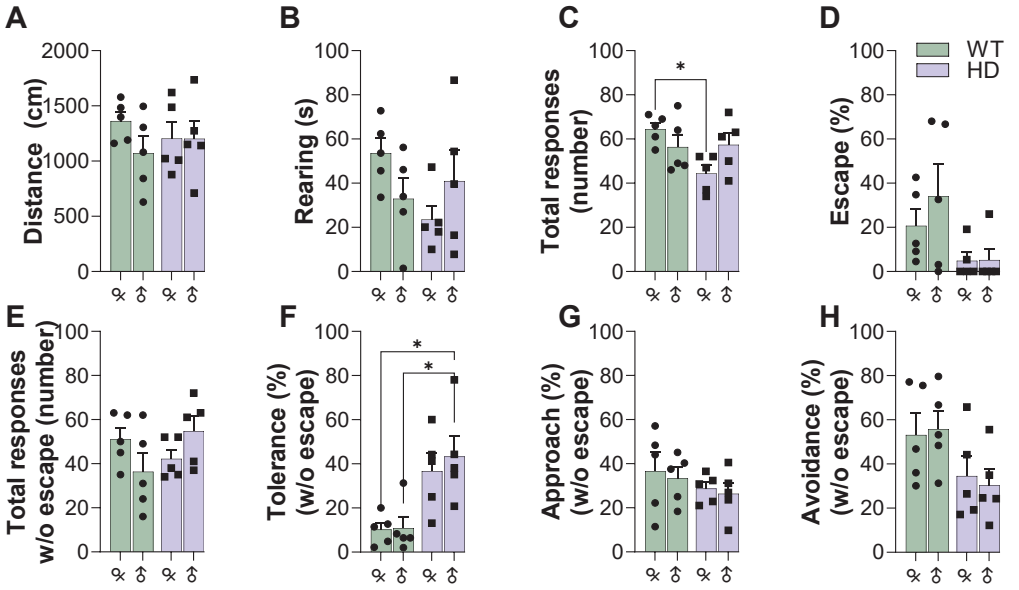

Figure 22. Behavioural responses to a randomly moving robo-beetle are altered in both male and female R6/1 mice compared to WT mice at 14 weeks of age. (A-B) During the habituation phase (A) distance travelled and (B) time mice spent rearing were measured. (C-H) During the test phase, with the presence of the robo-beetle, (C) total induced responses to the beetle are represented. Percentage of (D) escape responses, (E) total responses without escape and percentage of (F) tolerance, (G) approach and (H) avoidance responses when excluding escape response were analysed. Each point represents data from an individual mouse. Two-way ANOVA with genotype and sex as factors was performed. Data are represented as mean ± SEM. $N_{WT♂}$=3; $N_{WT♀}$=3; $N_{R6/1♂}$=3; $N_{R6/1♀}$=5. *p<0.05, **p<0.01, ***<0.001.

1.1.2 cAMP dynamics in the M2 cortex are increased in 15-week-old R6/1 female mice during the ARR task

To further understand the contribution of cAMP signalling to M2-cortex-related tasks, we decided to explore cAMP dynamic changes during the ARR. The ARR is a test used to evaluate motor learning and coordination in mice, functions known to rely on M2 cortex function and to be altered in Huntington's Disease mice (Fernández-García et al., 2020; Puigdellívol et al., 2015). In R6/1 mice, impairments in motor learning shown by the ARR start to be present from 8 weeks, while coordination deficits are observed around 12 weeks (V. Y. Cao et al., 2015; Puigdellívol et al., 2015). Hence, we used the same batch of G-Flamp1-expressing mice and conducted the ARR task during fibre photometry recordings in 15-week-old male and female mice. To this end, the 12 trials of the ARR were performed during the same recording session, with 10 minutes inter-trial time (Figure 23A).

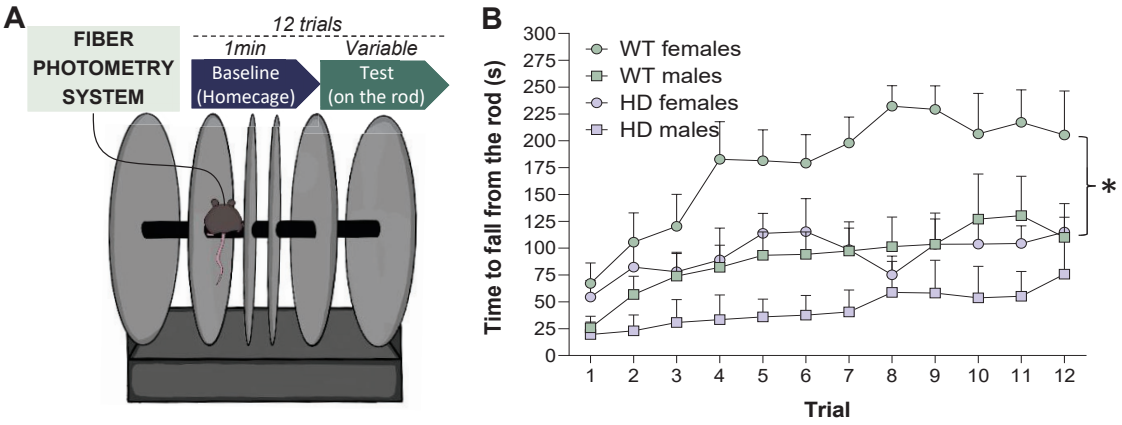

Figure 23. Motor learning procedure during fiber photometry recordings. (A) Schematic representation of the ARR protocol during fibre-photometry recordings. 12 trials were performed every 10 min while GFlamp1 signal was simultaneously recorded. Before each trial, 1 min was recorded in the homecage as baseline (B) Latency to fall from the rod during the ARR task. Two-way ANOVA with genotype and sex as factors was performed. Data are represented as mean ± SEM. $N_{WT♂}$=3; $N_{WT♀}$=3; $N_{R6/1♂}$=3; $N_{R6/1♀}$=5. *p<0.05, **p<0.01, ***<0.001.

We first analysed the animals' performance during the test (Figure 23B). In this test, male mice exhibited worse performance than female mice, while reduced performance was observed in R6/1 for both genotypes. However, only R6/1 females compared to their respective female controls, showed genotype differences, as shown by two-way ANOVA with genotype and trial as factors (Genotype: $F_{(1,8)}$=9.6, P=0.04; Trial: $F_{(3.344,25\text{-}23)}$=9.6, P=0.0001; Interaction: $F_{(11,83)}$=3.31, P=0.0008). Male mice two-way ANOVA failed to show significant effects (Genotype: $F_{(1,8)}$=2.21, P=0.17; Trial: $F_{(11,88)}$=7.05, P<0.0001; Interaction: $F_{(11,88)}$=1.28, P=0.25). These data suggest that impairments in females may be more pronounced than in males in this group of animals, and that increasing the sample size might reveal more robust effects.

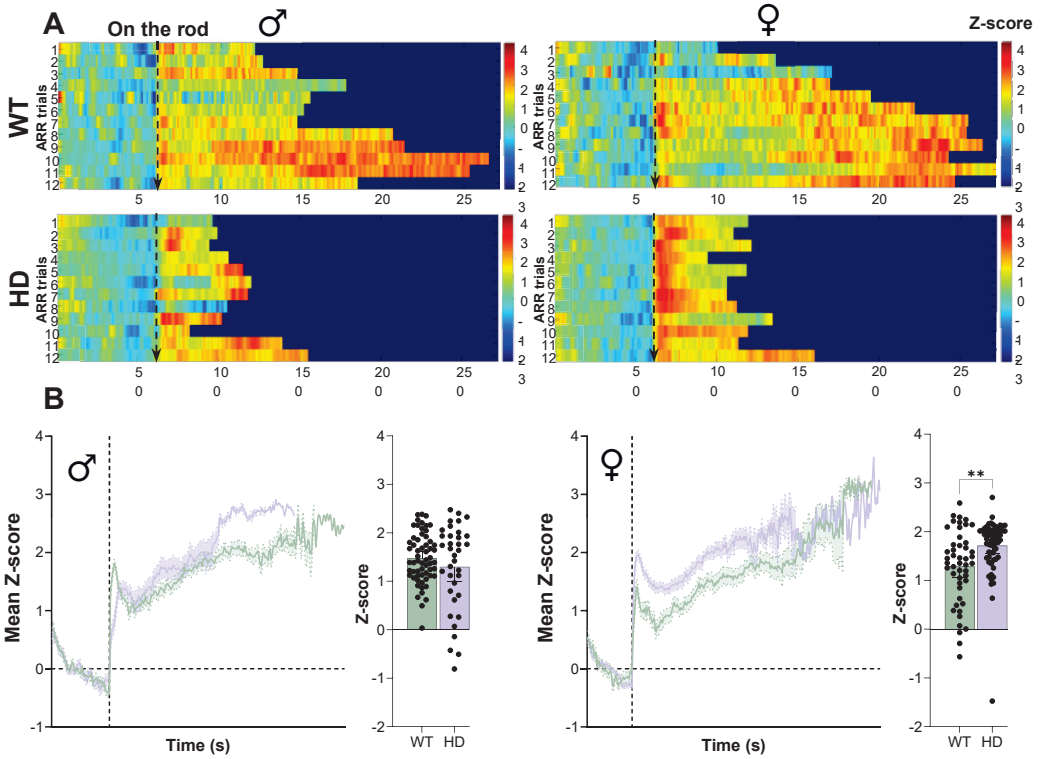

Figure 24. GFlamp-1 fluorescence increases during motor learning in neurons from the M2 cortex of 14-week-old WT and R6/1 mice. (A) Representative heatmaps of activity showing fluorescent changes in GFlamp-1 fluorescent signal (ΔF/F0 normalised to z-score) in male (left) and female (right) WT (top) and R6/1 (bottom) mice. X axis: each row represents 1 of each of the 12 trials; X axis represents the duration of the recording. The dashed arrows represent the moment the mouse was placed on the rotarod. Each trial consists in 60s baseline period and a period when mice stayed in the rotarod (up to 300s, variable time for each trial/mouse). Changes in normalised GFlamp-1 signal (z-score,) are colour-coded and represented from >-3 (blue) to <4(red) ΔF/F0 normalised to z-score. Data recorded during the placement of the mice from the cage to the rod by the experimenter was excluded from the analysis and representations. (B) Mean GFlamp-1 traces (X axis: ΔF/F0 normalised to z-score) from male (left) and female (right) WT and R6/1 mice during the performance of the test. Histograms compare WT vs HD performance on the rod, each dot representing the mean value of each of the trials. Unpaired T-test was performed. Data are represented as mean ± SEM. $N_{WT♂}$=3; $N_{WT♀}$=3; $N_{R6/1♂}$=3; $N_{R6/1♀}$=5. *p<0.05, **p<0.01, ***<0.001.

Next, we investigated the changes in cAMP during each of the ARR' trials. Considering the sex differences observed in the test, we assessed the cAMP dynamics separately. Prior to placing the animals to the rod apparatus, we recorded 1 minutes of G-Flamp1 fluorescence, when the mouse was freely moving in a home-cage with bedding material, which was considered the baseline measurement. On the whole, we observed that in both male and female WT and R6/1 mice, there was an increase in G-Flamp1 fluorescence when the mouse was placed on the rod apparatus in all the trials (Figure 24A). The profile of fluorescent traces was similar in all trials, with an initial peak after the animal is placed on the rod, followed by a more stable and increasing cAMP signal during the performance of the task (Figure 24B left). Nevertheless, while no striking differences can be discerned in cAMP dynamics between WT and HD male mice, female HD mice tended to exhibit an increased cAMP response to the stimulus compared to female WT mice in most of the trials. This effect was

also qualitatively observed in all fluorescent changes over time for each trial and each animal (data not shown). In order to quantify it, and considering that no major differences could be observed between trials, we determined the mean z-score from the time on the rotarod apparatus (Figure 24B right). Thus, we were able to confirm that while male mice do not display significant genotype differences in this cohort (Unpaired T-test, p=0.22), female HD mice respond with an over-increased cAMP response compared to female WT mice (Unpaired T-test, p=0.001) (Figure 24B). Altogether, these data highlight that female R6/1 mice show an aberrant overactivation of cAMP levels in front of a M2-cortex-related task at ~ 15 weeks of age. Moreover, while cAMP dynamics in male mice remain unaltered, caution need to be taken here, as male mice did not perform well in the ARR task. Further analysis, including increasing the number of animals, will help to better describe the role of cAMP in this task and its alterations in HD.

1.1.3 cAMP activity in neurons from the M2 cortex is decreased in 20-week-old male mice during the beetle-mania task

To further understand if alterations in cAMP activity during an M2-cortex related task are more prominent at later stages of disease progression, we repeated the BMT in the same cohort of animals at 20 weeks, when mice are fully symptomatic (Conde-Berriozabal et al., 2023; Fernández-García et al., 2020).

We first analysed cAMP activity in these animals, and we again observed and increase in cAMP levels upon the presence of the robo-beetle regardless of the genotype (Figure 25A). Moreover, we observed a smaller increase in fluorescence levels in R6/1 mice compared to WT mice. When analysing sexes separately, the responses were further reduced in R6/1 male mice, while female mice showed a milder decrease. We then analysed both responses quantitatively, as performed in our previous BMT results (*1.2.3 section*), by quantifying AUC, peak amplitude, and peak number (Figure 25B). Male R6/1 mice showed decreased AUC (Unpaired T-test, p=0.0002) and peak amplitude (Unpaired T-test, p=0.0006) compared to WT, although no differences in the number of peaks was observed (Unpaired T-test, p=0.92). In female mice, fluorescence z-score profile looked smaller, but quantification did not show genotype differences neither in the AUC (Unpaired T-test, p=0.49), peak amplitude (Unpaired T-test, p=0.20), nor number of peaks (Unpaired T-test, p=0.38).

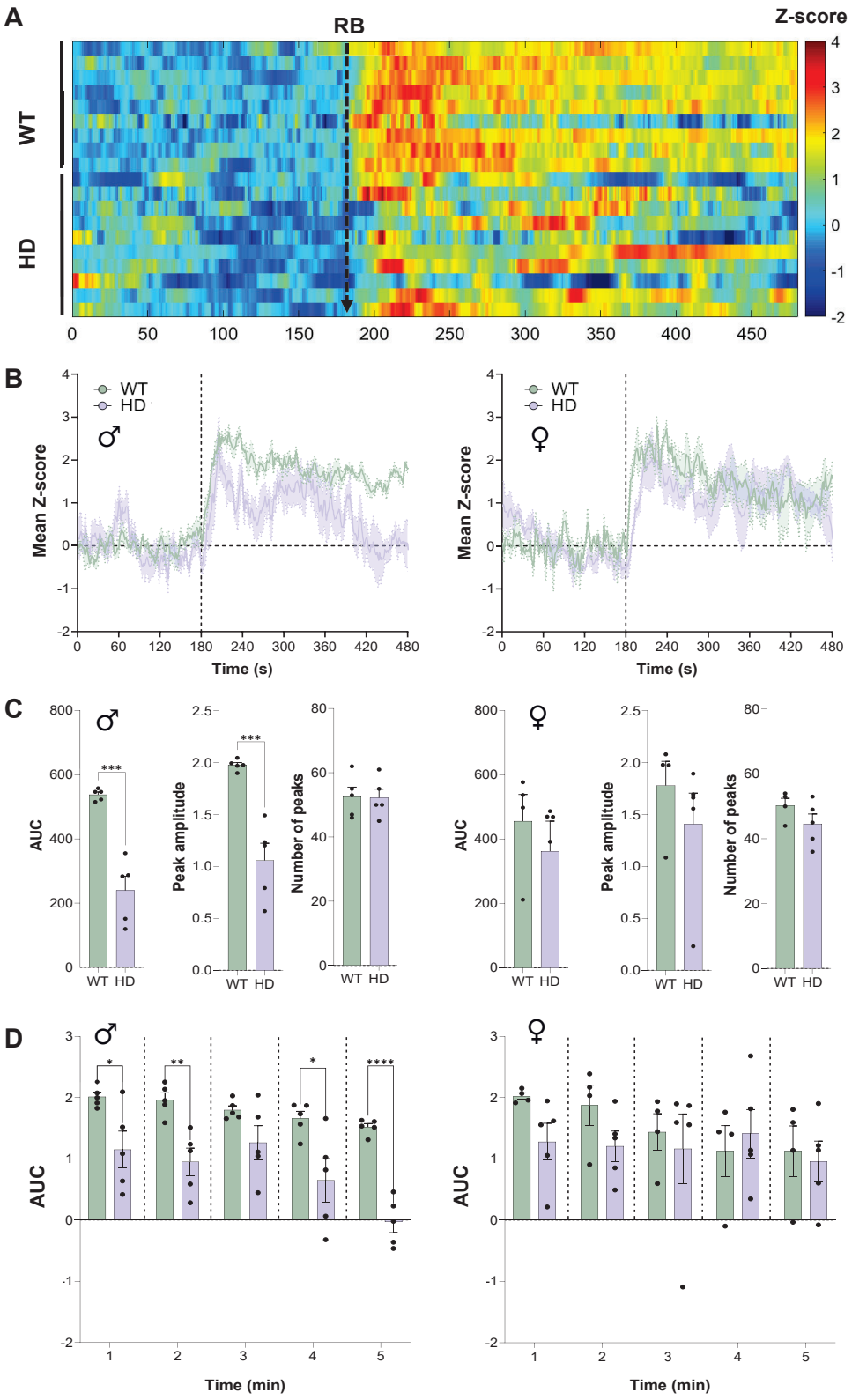

Figure 25. cAMP dynamics are decreased in R6/1 mice compared to WT mice in response to a threatening stimulus at 20 weeks of age. (A) Heatmap of activity showing changes in GFlamp-1 fluorescent signal (ΔF/F0 normalised to z-score) in WT and R6/1 mice (Y axis, each line represents an individual mouse)

at 14 weeks of age. X axis represents the duration of the recording (in seconds). Only the last 180s of habituation are considered and represented as baseline for the analysis. ΔF/F0 changes are transformed to z-score normalised to baseline, colour-coded and represented from >-2 (blue) to <4(red). (B) Mean GFlamp-1 fluorescent traces (Y axis: ΔF/F0 normalised to z-score) from male (left) and female (right) WT and R6/1 mice during the performance of the test. The placement of the robo-beetle (RB) is represented at the second 180 of the X axis. (C) Histogram representing the 5-min post-baseline area under the curve (AUC), peak amplitude and number of peaks of the GFlamp-1 z-score normalised fluorescent signal between WT and R6/1 male (left) and female (right) mice. (D) Histogram representing the comparison of area under the curve (AUC) of the GFlamp-1 z-score normalised signal between male (left) and female (right) WT and R6/1 mice. X axis represents each minute with the presence of the robo-beetle. Each point represents data from an individual mouse. Unpaired T-test was performed. $N_{WT♂}$=3; $N_{WT♀}$=3; $N_{R6/1♂}$=3; $N_{R6/1♀}$=5. *p<0.05, **p<0.01, ***<0.001.

As in previous analyses, we also investigated cAMP dynamics along time by analysing the G-Flamp1 signal each minute with the presence of the beetle in the arena (Figure 25C). An unpaired t-test revealed significant differences between genotypes for all time points, except for the third minute, in male mice (Unpaired T-test, minute 1 p=0.02, minute 2 p=0.004, minute 3 p=0.1, minute 4 p=0.03, minute 5 p<0.0001). Female mice failed to show significant differences between genotypes at any of the time points (Unpaired T-test, minute 1 p=0.07, minute 2 p=0.14, minute 3 p=0.71, minute 4 p=0.64, minute 5 p=0.76). As previously, increasing the number of animals might help to decipher how cAMP dynamics contribute to the BMT, especially between male and female mice. This preliminary data indicate that neuronal cAMP responses are present but diminished in symptomatic R6/1 mice. Considering our previous findings where Ca^{2+} increases in response to the robo-beetle were undetectable at this symptomatic stage (Conde-Berriozabal et al., 2023), along with the absence of cAMP alterations at 14 weeks despite the presence of the phenotype, we hypothesise that changes in cAMP dynamics are not an early event contributing to the HD phenotype.

In addition, we confirmed the phenotype alterations in the BMT from the animals that underwent cAMP fiber photometry recordings. Interestingly, when we analysed the spontaneous behaviour during the habituation phase, two-way ANOVA showed that there were no genotype differences, while showed sex differences in both locomotion (Genotype: F(1,15)=0.002, P=0.96; Sex: F(1,15)=5.53, P=0.03; Interaction: F(1,15)= 1.75, P=0.20) and rearings (Genotype: F(1,14)=0.26, P=0.61; Sex: F(1,14)=8.78, P=0.01; Interaction: F(1,14)= 0.58, P=0.45) (Figure 26A and 26B), suggesting that repetitive testing can affect these behaviours in HD. When analysing the testing phase at 20 weeks, phenotype-dependent alterations in response to the robo-beetle were more pronounced than at 14 weeks in both male and female mice. Still, in the escape response, WT mice no longer exhibited this behaviour (Genotype: $F_{(1,15)}$=0.017, P=0.89; Sex: $F_{(1,15)}$=1.35, P=0.26; Interaction: $F_{(1,15)}$=0.07, P=0.78) (Figure 26D), possibly due to repeated handling or the photometry procedure, as previously observed in Conde-Berriozabal et al 2023. Nevertheless, the phenotype remains robust in the other behavioural responses, with sex differences also observed in some of the responses. Two-way ANOVA showed decreased number of total

responses (Genotype: $F_{(1,15)}$=5.66, P=0.03; Sex: $F_{(1,15)}$=1.73, P=0.20; Interaction: $F_{(1,15)}$=2.21, P=0.15), increased tolerance (Genotype: $F_{(1,15)}$=50.10, P<0.0001; Sex: $F_{(1,15)}$=1.45, P=0.51; Interaction: $F_{(1,15)}$= 0.12, P=0.73), and decreased avoidance towards the robo-beetle (Genotype: $F_{(1,15)}$=15.91, P=0.0012; Sex: $F_{(1,15)}$=1.56, P=0.22; Interaction: $F_{(1,15)}$= 0.80, P=0.38) (Figure 26C, 26F and 26H). Herein, we observed sex differences in the total responses without escape (Genotype: $F_{(1,15)}$=6.13, P=0.02; Sex: $F_{(1,15)}$=6.01, P=0.02; Interaction: $F_{(1,15)}$= 2.92, P=0.10) (Figure 26E). Moreover, this decrease was observed only in females, while male's number of responses remained similar between genotypes. Similarly, the percentage of approach responses was decreased, displaying sex differences (Genotype: F(1,15)=7.37, P=0.01; Sex: F(1,15)=6.55, P=0.02; Interaction: F(1,15)= 2.92, P=0.11) (Figure 26G). Overall, our results indicate that at 20 weeks, R6/1 mice have robust phenotype alterations in the BMT, although increasing number of animals per group would help to better decipher sex differences at this disease stage.

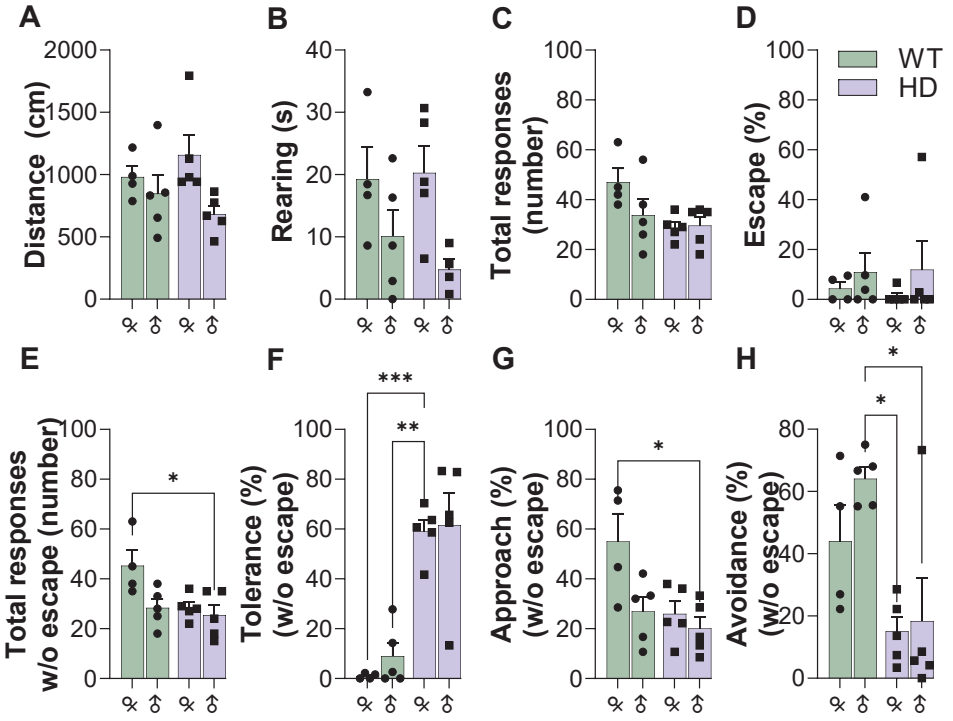

Figure 26. Behavioural responses to a randomly moving robo-beetle are altered in both male and female R6/1 mice compared to WT mice at 14 weeks of age. (A-B) During the habituation phase (A) distance travelled and (B) time mice spent rearing were measured. (C-H) During the test phase, with the presence of the robo-beetle, (C) total induced responses to the beetle are represented. Percentage of (D) escape responses, (E) total responses without escape and percentage of (F) tolerance, (G) approach and (H) avoidance responses when excluding escape response were analysed. Each point represents data from an individual mouse. Two-way ANOVA with genotype and sex as factors was performed. Data are represented as mean ± SEM. $N_{WT♂}$=3; $N_{WT♀}$=3; $N_{R6/1♂}$=3; $N_{R6/1♀}$=5. *p<0.05, **p<0.01, ***<0.001.

1.2 Characterisation of early cortico-striatal related deficits in the R6/1 mouse model of HD

Given the critical role of M2 cortex in HD pathophysiology, this study aimed to determine whether additional symptoms associated with cortico-striatal dysfunction emerge at early disease stages in the R6/1 mouse model. Identifying early markers could enable the initiation of therapeutic interventions at prodromal stages, potentially improving their efficacy and offering a strategy to assess treatment outcomes.

To do so, we selected two behavioural tests which assess different functions of the cortico-striatal pathway: the adhesive removal and the marble burying test. The adhesive removal test is linked to the SS/M2 cortex - striatal pathway and evaluates fine motor and somatosensory deficits (Bouet et al., 2009), while the marble burying test is associated to the orbitofrontal cortex - striatal pathway and allows to study obsessive-compulsive and anxiety-like behaviour (Angoa-Pérez et al., 2013). Of note, these cortical regions are known to show reduced functional connectivity with the striatum in the symptomatic R6/1 mice (Fernández-García et al., 2020). In order to investigate each of the cortico-striatal functions longitudinally, we performed the aforementioned tests once per week in three different batches of mice that went 1) from 4 to 7 weeks old, 2) from 8 to 12 weeks old, and 3) from 13 to 16 weeks old. We also performed open field tests in the earlier timepoints in order to control for major motor deficits that could confound our results (Figure 27).

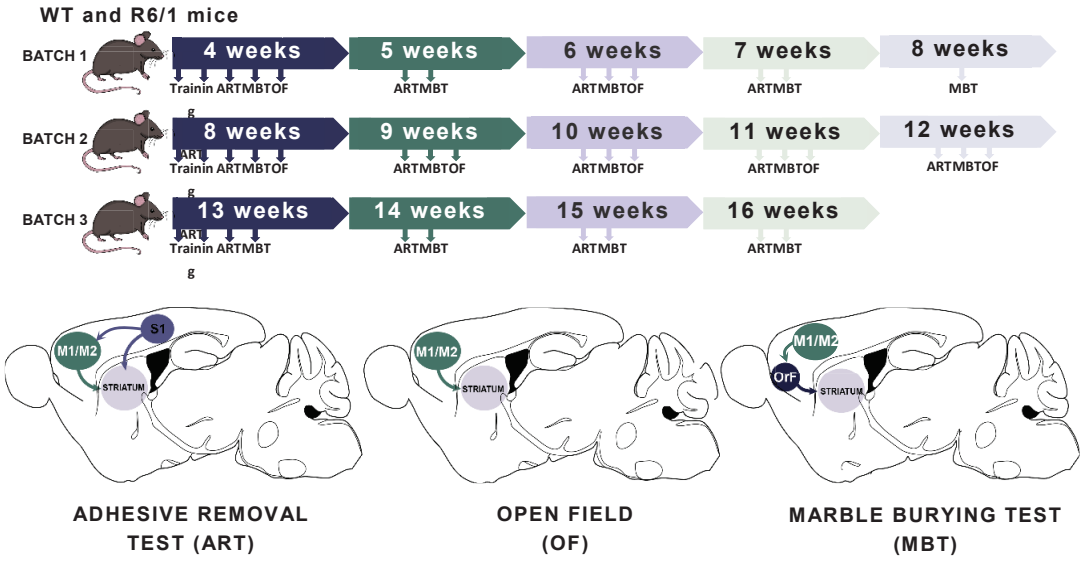

Figure 27. Schematic representation of the experimental timeline indicating the time points at which M2-related cortico-striatal tests were conducted. 3 different batches of mice were used to investigate the behavioural alterations in the adhesive removal test (ART), associated to motor (M2) and sensory (S1) corticostriatal circuitry; the open field (OF), linked to motor cortex, and marble burying test (MBT), linked to orbitofrontal circuitry. Animals from batch 1 performed weekly the ART and MBT from 4 to 8 weeks of age. Animals from batch 2 performed weekly the ART and MBT from 8 to 12 weeks of age. Animals from batch 3 performed the ART and MBT from 13 to 16 weeks of age. The first two days of the first week constituted the ART training phase. The OF was performed at 4, 6, 8, 9, 10, 11 and 12 weeks.

1.2.1 Fine motor deficits emerge at 8 weeks, while somatosensory deficits appear at 16 weeks in R6/1 mice, as assessed using the adhesive removal test

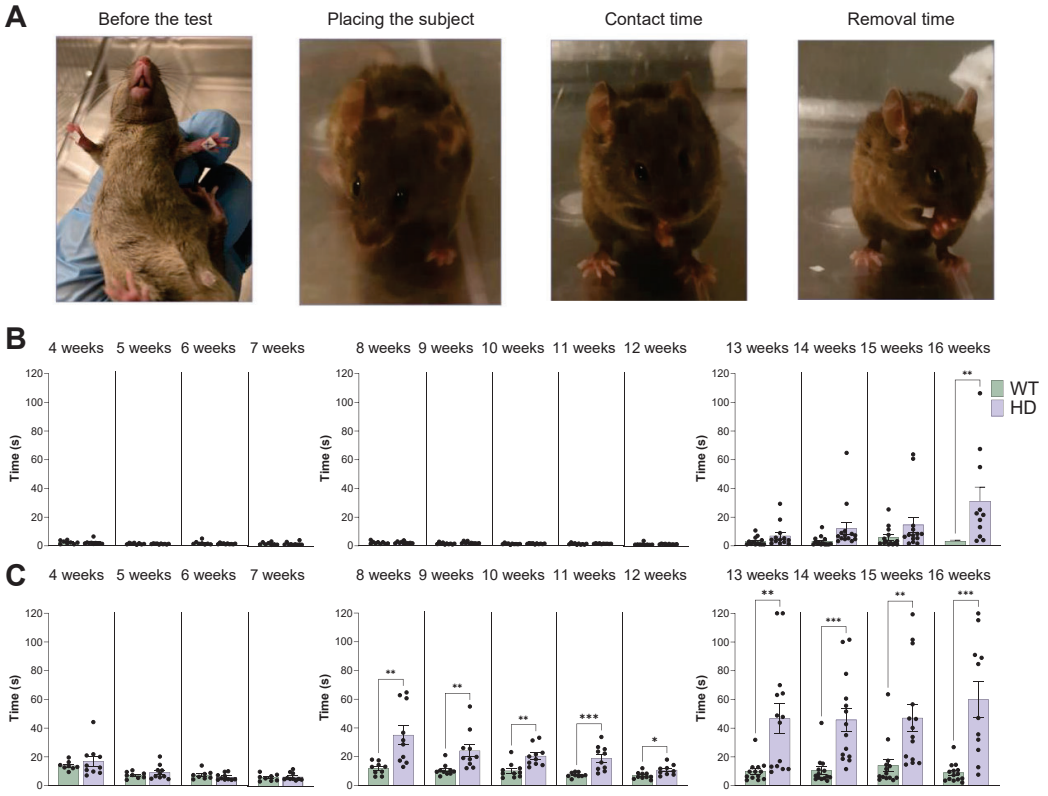

Figure 28. Fine-motor deficits emerge at 8 weeks of age, whereas somatosensory impairments become evident at 16 weeks of age in R6/1 male mice. WT and R6/1 mice were tested from 4 to 16 weeks, grouped into three different batches of mice (4-7, 8-12, and 13-16 weeks). (A) Representative images of the main phases of the test, starting with the (i) placing of the adhesive tapes on both right and left forepaws, (ii) placing the subject in the arena, and quantifying (iii) time to first contact and (iv) time to remove the tape. (B) Histograms showing the average contact time from 4 to 16-week-old WT and R6/1 mice, grouped according to the three different batches of mice. (C) Histograms showing the average removal time from 4 to 16-week-old WT and R6/1 mice, grouped into the three different batches. Each dot represents data from an individual mouse. Unpaired T-test was performed. Data are represented as mean ± SEM. N_{WT}=8-14; $N_{R6/1}$=10-14. *p<0.05, **p<0.01, ***<0.001.

We first performed the adhesive removal test and, to assess somatosensory deficits, we quantified the time the animal took to realise the adhesive tape was attached on the paw (contact time). In turn, to evaluate fine motor performance, we analysed the time the animal took to remove the adhesive tape (removal time) (Figure 28A). The mean contact and removal time between left and right paw is represented in each of the graphs. We did not observe differences between WT and R6/1 mice in any of the timepoints from 4 to 7 weeks, neither in the contact or the removal time, shown by unpaired t-test analysis (P_{4WEEKS}=0.44; P_{5WEEKS}=0.31; P_{6WEEKS}=0.27; P_{7WEEKS}=0.66) (Figure 28B and 28C). Significant differences between genotypes were observed for the removal time from 8 weeks (P_{8WEEKS}=0.004), where R6/1 displayed longer time to remove the tape, indicating that fine motor deficits start at

this age (Figure 28C). No contact time differences were observed in any of the timepoints from this batch of mice (P_{8WEEKS}=0.82; P_{9WEEKS}=0.08; $P_{10WEEKS}$=0.45; $P_{11WEEKS}$=0.40; $P_{12WEEKS}$=0.91). Somatosensory deficits shown by the contact time measure were observed at 16 weeks ($P_{13WEEKS}$=0.12; $P_{14WEEKS}$=0.05; $P_{15WEEKS}$=0.13; $P_{16WEEKS}$=0.003) (Figure 28B). Broadly, this test demonstrated that fine motor symptoms start at very early stages of the disease (8 weeks), whereas somatosensory deficits would appear later on (16 weeks), aligning with the progression of core motor symptoms in HD (Brooks et al., 2012; Puigdellívol et al., 2015; Rodríguez-Urgellés, Casas-Torremocha, Sancho-Balsells, Ballasch, García-García, Miquel-Rio, Manasanch, del Castillo, et al., 2023).

1.2.2 Anhedonia-like behaviour is detected from 8 weeks of age in R6/1 mice, as assessed using the marble burying test

As compulsive-like and anxiety behaviour has been observed in Huntington's Disease patients (De Marchi et al., 1998; Zadegan et al., 2024), we then conducted the marble burying test to study these behaviours at different timepoints of the disease in the R6/1 mouse model. Usually, when compulsive-like behaviour is present, mice bury more marbles (Angoa-Pérez et al., 2013). Our results show differences in the number of buried marbles from 8 weeks old.

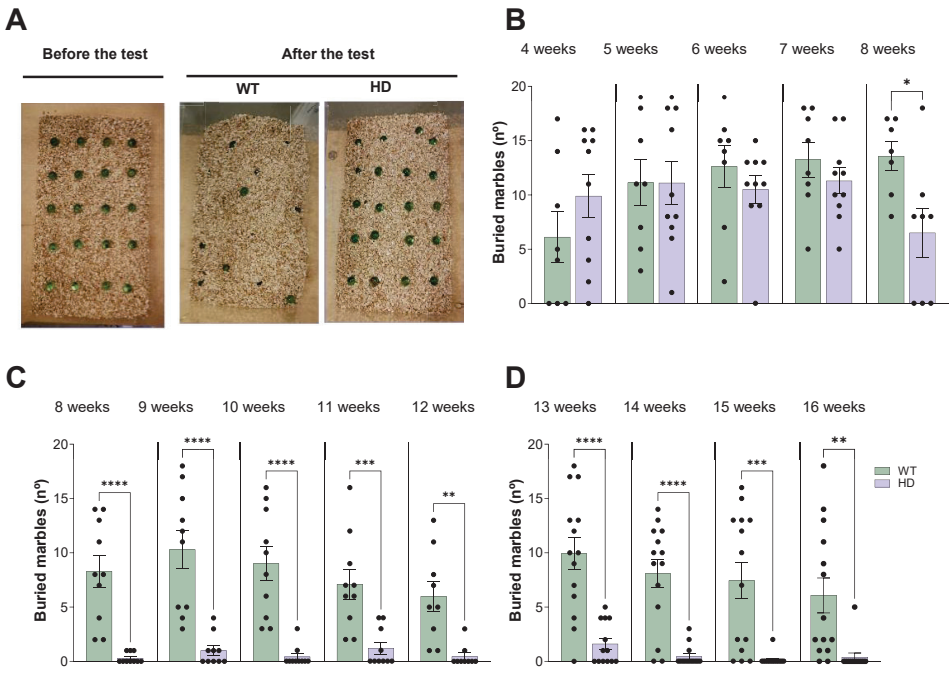

Figure 29. Anhedonia-like behaviour emerge at 8 weeks of age in R6/1 mice. WT and R6/1 mice were tested from 4 to 16-week-old, grouped into three different mice batches (4-7, 8-12 and 13-16 weeks). (A) Representative images of the 20 marbles placed over the sawdust in the cage before and after the 30-minute test in WT and R6/1 mice. (B-D) Histogram representing the number of buried marbles from 4 to 16-week-old WT and R6/ mice, grouped into different batches. Each dot represents data from an individual mouse. Unpaired T-test was performed. Data are represented as mean ± SEM.. NWT=8-14; NR6/1=10-14. *p<0.05, **p<0.01, ***<0.001.

However, in our case, R6/1 mice significant- and prominently buried less marbles than WT mice in all timepoints from the week 8 ($P_{8WEEKS}<0.0001$, $P_{9WEEKS}<0.0001$, $P_{10WEEKS}<0.0001$, $P_{11WEEKS}$ 0.0009, $P_{12WEEKS}$ 0.0014, $P_{13WEEKS}<0.0001$, $P_{14WEEKS}<0.0001$, $P_{15WEEKS}=0.0002$, $P_{16WEEKS}=0.0002$) which could be indicating a lack of motivation in these mice (Figure 29). In order to make sure that this effect was not batch dependent, we prolonged the behavioural study at week 8 in the batch of mice that was analysed from 4 to 7 weeks, confirming that mice from 8 weeks of age start showing this clear phenotype of burying less marbles (First batch: $P_{8WEEKS}=0.02$). In fact, anhedonia has also been observed in patients with HD at early stage of the disease (J. Brandt, 2018; Mclauchlan et al., 2022), and hence we named R6/1 aberrant performance as anhedonia-like behaviour.

1.2.3 Locomotor alterations are not present at early stages of the disease

To ensure that the observed deficits were not due to prominent motor dysfunction, we analysed locomotor activity at early stages (Figure 30). No differences were observed between groups at any of the timepoints ($P_{4WEEKS}=0.28$; $P_{6WEEKS}=0.46$; $P_{8WEEKS}=0.60$; $P_{9WEEKS}=0.95$; $P_{10WEEKS}=0.89$; $P_{11WEEKS}=0.79$; $P_{12WEEKS}=0.95$). Thus, cortico-striatal deficits observed during the adhesive removal and marble burying tests are not due to major motor deficits.

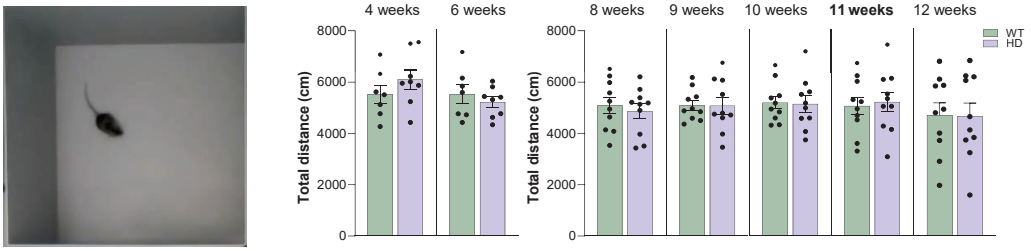

Figure 30. Locomotion is spared at early timepoints of the disease. WT and R6/1 mice were tested from 4 to 16-week-old, grouped into three different mice batches (4-7, 8-12 and 13-16 weeks). (A) Representative images of a mouse walking in the open field (B) Histograms representing the total distance walked by WT and R6/1 mice throughout the test duration, grouped into different batches. Each dot represents data from an individual mouse. Unpaired T-test was performed. Data are represented as mean ± SEM. NWT=8-14; NR6/1=10-14. *p<0.05, **p<0.01, ***<0.001.

Collectively, data from the first objective highlight two key findings. First, M2-cortex-related cortico-striatal dysfunction emerges at very early timepoints, starting at 8 weeks, highlighting the potential of these timepoint for early therapeutic interventions. Second, cAMP dynamics in neurons can be detected and respond to a stimulus in behaving mice, confirming its involvement in M2-cortex-related tasks, at least in the ARR and BMT. Nevertheless, although slight behavioural differences can be observed at 15-week-old mice, genotype differences only become pronounced at 20-week-old mice. Given that M2-related behavioural deficits are evident as early as 8 weeks, neuronal cAMP signalling changes do not appear to drive these impairments. Thus, while neuronal cAMP signalling is implicated in these responses, its deficits in neurons are unlikely to be the primary cause of the observed behavioural alterations.

2 To implement DdPAC as a novel tool to non-invasively modulate cAMP signalling *in vivo*

To establish DdPAC as a non-invasive tool for modulating cAMP signalling in vivo, it is first necessary to evaluate different viral administration routes to identify a minimally or non-invasive method for its delivery into the brain. Subsequently, the efficacy of DdPAC must be validated by assessing its expression, activation through red-light illumination, and the resulting molecular and functional consequences *in vivo*.

2.1 Implementation of a non-invasive approach for viral delivery

Local brain injection for viral delivery is a common practice in neuroscience laboratories to achieve cell- and region-specific viral infection. While intravenous injections are increasingly used in basic research, stereotaxic surgeries remain the predominant approach (Deverman et al., 2016b; Haery et al., 2019; K. Zhou et al., 2022). However, for the successful clinical translation of therapies, the development of non-invasive methods is critical. Intravenous injections are minimally invasive although not entirely non-invasive, so further research is required to refine viral delivery strategies that minimise potential harm. In this study, we evaluated three viral delivery approaches to achieve region-, cell-, and mouse strain-specificity (Figure 31).

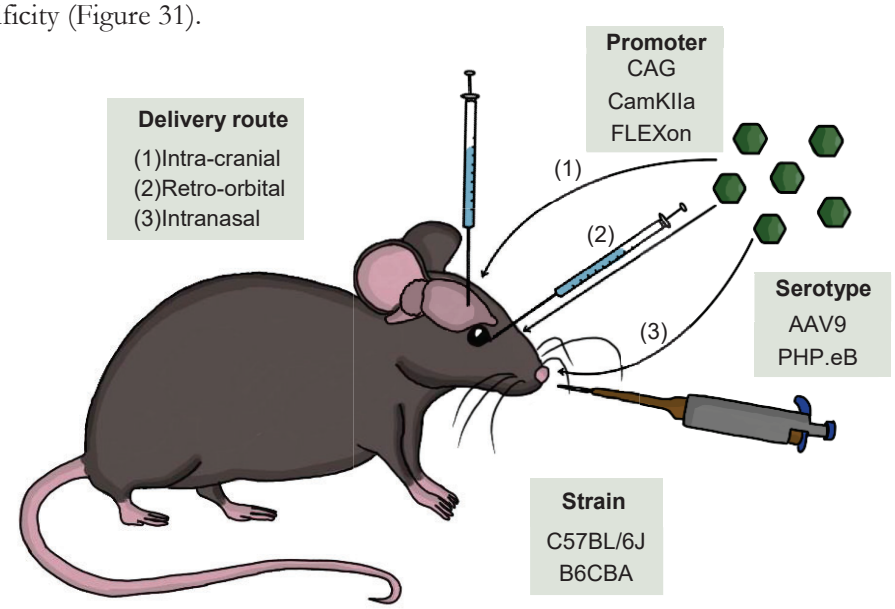

Figure 31. Schematic representation of the viral delivery approaches, AVV serotypes and constructs, promoters, and mouse strains used in this section. Two distinct AAV serotypes (AAV9 and PHP.eB) were administered via intracranial injection, retro-orbital injection, and intranasal delivery to drive GFP expression under three different promoters (CAG, CamKIIa and FlexON) in two mouse strains (C57BL/6J and B6CBA).

2.1.1 Both AAV9 and PHP.eB constructs carrying GFP under the CAG promoter are expressed in brain cells following intra-cranial and retro-orbital injections, but not after intranasal administration

First, we compared the infection potential of two different viral serotypes, namely AAV9 and PHP.eB. AAV9 is a commonly used serotype for central nervous system delivery due to its natural affinity for infecting neuronal and glial cells, its ability to cross the BBB, and its capacity for long-term expression (Cearley & Wolfe, 2006; Foust et al., 2009)On the other hand, the PHP.EB serotype is a modified AAV designed to improve gene delivery to the central nervous system by enhancing its ability to penetrate the blood-brain barrier (BBB) and increase its tropism for brain tissues. It has also been shown to exhibit remarkable transduction efficiency in the central nervous system (CNS) following intravenous injection (Deverman et al., 2016b; Hordeaux et al., 2018).

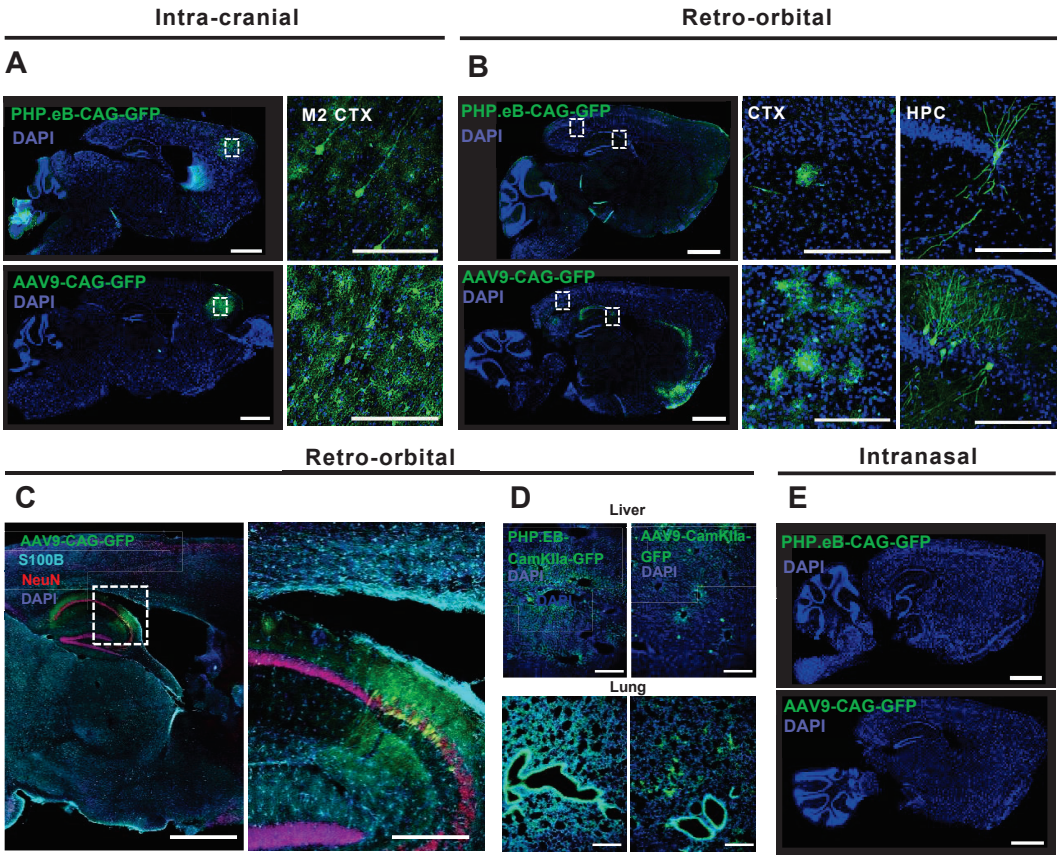

Figure 32. Expression of GFP after intra-cranial, retro-orbital and intranasal administration of AAV9-CAG-GFP and PHP.eB-CAG-GFP viral constructs. (A) Representative histological sagittal images (left) of GFP expression (green) and DAPI (blue) after intra-cranial injection of GFP constructs using PHP.eB (top) and AAV9 (bottom) serotypes in the M2-cortex of C57BL/6J mice (scale bar: 1500µm). Amplified images (right) show GFP expressed in both neurons and astrocytes, assessed by the morphology of the cells (scale bar: 200 µm). (B) Representative histological sagittal images (left) of GFP expression (green) and DAPI (blue) after retro-orbital injection of GFP constructs using PHP.eB (top) and AAV9 (bottom) serotypes (scale bar: 1500µm). Amplified images (right) show GFP expression in both neurons and astrocytes in the cortex (CTX) and hippocampus (HPC) of C57BL/6J mice (scale bar: 200 µm). (C) Representative histological sagittal image (left) of GFP (green), S100B (Cyan), red (NeuN) and DAPI (blue) staining after GFP expression by retro-orbital injection of AAV9-CAG.GFP construct (scale bar: 1500µm). Amplified image (right) show co-

expression of GFP and S100B, as well as GFP and NeuN, specifically marking astrocytes and neurons, respectively (scale bar: 300 μm). (D) Representative histological images showing GFP expression (green) and DAPI (blue) after retro-orbital injection of PHP.eB (left) or AAV9 (right) serotypes in the liver (top) and lung (bottom) (scale bar: 250 μm). (E) Representative histological sagittal images of GFP expression (green) and DAPI (blue) after intranasal administration of GFP constructs with PHP.eB (top) and AAV9 (bottom) serotypes (scale bar: 1500 μm).

Our collaborator, Dr. Deniz Dalkara (Sorbonne Université), provided constructs designed to express GFP under the CAG promoter, enabling expression in all murine cells, and encapsulated them in AAV9 and PHP.eB serotypes, resulting in the AAV9-sc-CAG-GFP and PHP.eB-sc-CAG-GFP viral constructs. We then administered the two constructs to C57BL/6J mice using the following viral delivery approaches: intra-cranial injection, retro-orbital injection, and intranasal administration (Figure 31). Intra-cranial injection was performed in the M2-cortex using stereotaxic surgery, after which GFP expression was observed with both the AAV9 and PHP.eB serotypes. Furthermore, both neurons and astrocytes can be identified through visual examination of the GFP images (Figure 32A). Retro-orbital injection of both AAV9 and PHP.eB viral constructs resulted in GFP expression in the brain, although expression was not detected in the same extend nor in all regions (Figure 32B). Qualitative examination of GFP fluorescence revealed a higher number of transfected cells with AAV9 compared to the PHP.eB construct. Furthermore, in both cases, GFP expression was more pronounced in the cortex and hippocampus, particularly in the CA2 layer (Figure 32B). Due to the higher GFP expression using the AAV9 serotype, we aimed to further characterise its target cells. Thus, we performed immunofluorescence staining using S100β to label astrocytes and NeuN antibody to label neurons, confirming that both cell types were expressing GFP, as previously observed (Figure 32C). Lastly, because retro-orbital injection directly enters the bloodstream, we sought to determine whether AAV constructs reached organs beyond the brain (Figure 32D). We evaluated the liver and lungs, detecting GFP expression for both AAV9 and PHP.eB serotypes, as previously described (Chan et al., 2017). Unfortunately, no GFP fluorescence was detected after intranasal administration.

2.1.2 Cell-type specificity of PHP.eB is achieved using gene regulatory elements in different mouse strains

Then, we aimed to enhance the specificity of GFP construct expression in neurons. To achieve this, we designed AAV constructs to express GFP under the CamKIIa promoter. Our collaborator, Dr. Dalkara, encapsidated these constructs in both AAV9 or PHP.eB serotypes: AAV9-CamKIIa-eGFP-WPRE and PHP.eb-CamKIIa-eGFP-WPRE. Thereafter, we administered them again via intra-cranial injection, retro-orbital injection, and intranasal administration to C57BL/6J mice. As previously observed, we detected GFP fluorescence following retro-orbital injections of AAV9 and PHP.eB serotypes. In this case, the expression of PHP.eB was significantly higher than that of the AAV9 construct, with GFP-positive cells observed across all brain regions, whereas AAV9 construct expression was minimal (Figure 33A). Intra-cranial injection confirmed neuronal expression of both

constructs (Figure 33B). Moreover, and as noted earlier, we could not observe GFP expression in neurons after intranasal administration, which may indicate that these capsids are unable to cross the blood-brain barrier in this context (Figure 33C).

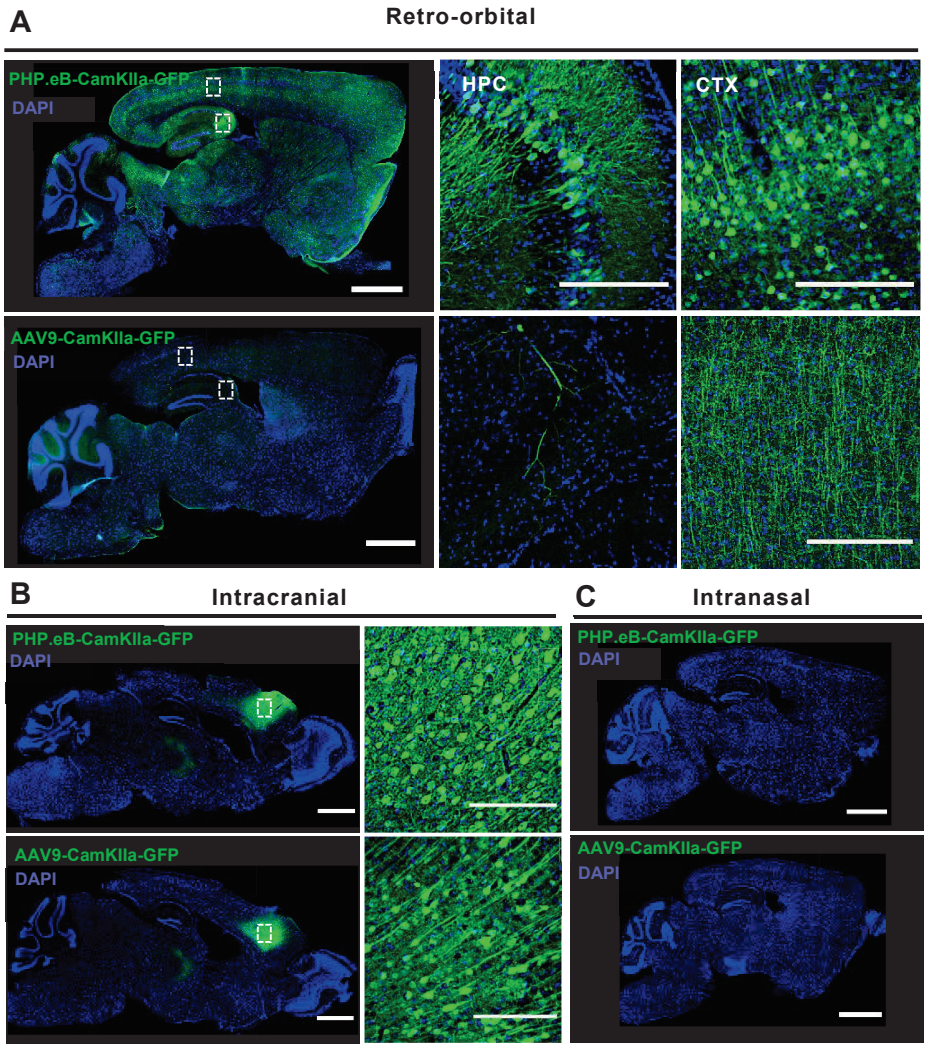

Figure 33. Expression of GFP after intra-cranial, retro-orbital and intranasal administration of AAV9-CamKII-GFP and PHP.eB-CamKII-GFP viral constructs in C57BL/6J mice. (A) Representative histological sagittal images (left) of GFP expression (green) and DAPI (blue) after retro-orbital injection of GFP constructs using PHP.eB (top) and AAV9 (bottom) serotypes (scale bar: 1500µm). Amplified images (right) show GFP expression neurons from the hippocampus (HPC) and cortex (CTX) of C57BL/6J mice (scale bar: 200 µm). (B) Representative histological sagittal images (left) of GFP expression (green) and DAPI (blue) after intra-cranial injection of GFP constructs using PHP.eB (top) and AAV9 (bottom) serotypes (scale bar: 1500µm) in the M2-cortex of C57BL/6J mice. Amplified images (right) show GFP expression in neurons (scale bar: 200 µm). (C) Representative histological sagittal images of GFP expression (green) and blue (DAPI) after intranasal administration of GFP construct using PHP.eB (top) and AAV9 (bottom) serotypes (scale bar: 1500 µm).

PHP.eB serotype has been reported to be strain specific, being limited to the C57BL/6J (Hordeaux et al., 2018). Therefore, previous experiments of this section were performed in this specific strain. The R6/1 mouse model for Huntington's Disease has B6CBA background, thus we aimed to determine if retro-orbital injection of PHP.eB-CamKIIa-eGFP-WPRE was also able to widely transduce to the CNS in WT and R6/1 mice (Figure

34A). We also intended to investigate if this expression could be cell-specific by retro-orbitally injecting a PHP.eB viral construct that expresses GFP only in Cre-expressing cells (PHP.eB-FLEXon-EF1A-EGFP-3xFLAG) in an A2a receptor-Cre BAC transgenic mice (Figure 34B). First, we were able to detect GFP-positive cells broadly in the brain in both WT and R6/1 mice (Figure 34A). Moreover, retro-orbital injection in A2a Cre mice resulted in a region-specific transduction of the virus, where neurons express A2a receptor (Figure 34B), such as the one of the indirect pathway from the striatum. Here, we demonstrate that the PHP.eB serotype is not restricted to the C57BL/6J background but can also achieve widespread expression in the CNS of B6CBA background mice, making it a suitable candidate for use in the R6/1 mouse model of Huntington's disease. Furthermore, its expression can be targeted to specific brain cell types through the use of different promoters.

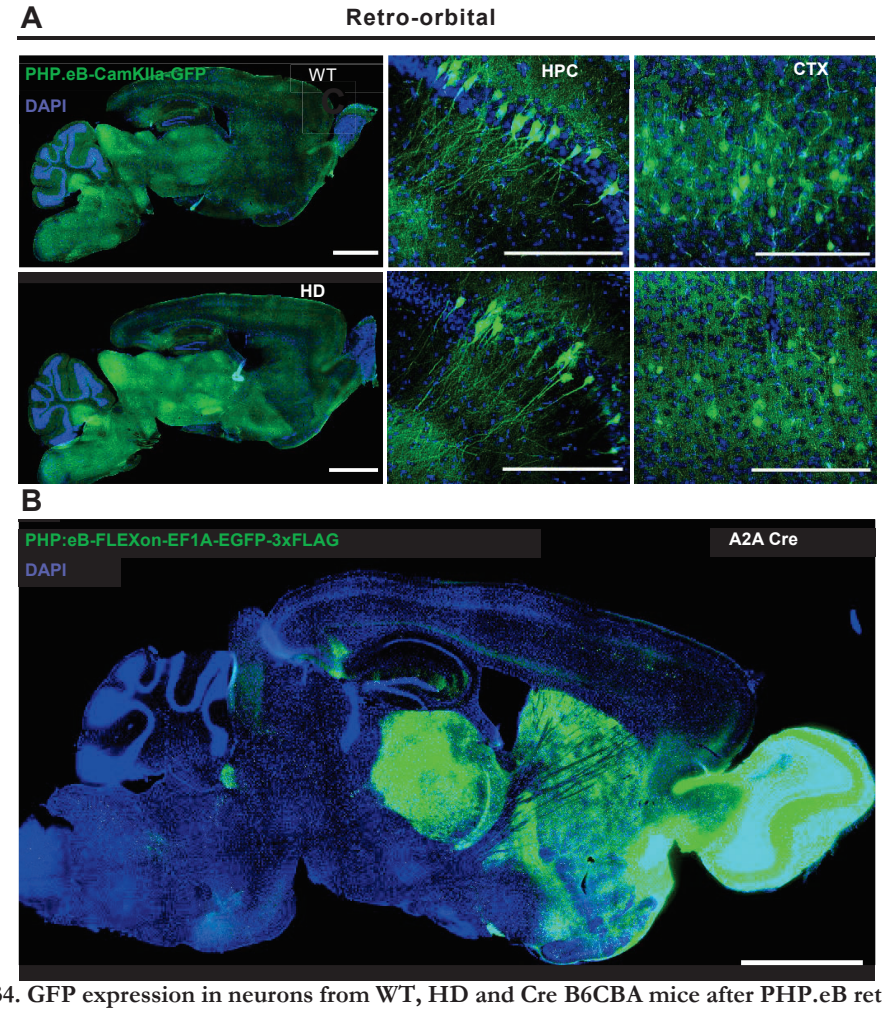

Figure 34. GFP expression in neurons from WT, HD and Cre B6CBA mice after PHP.eB retro-orbital injections. Expression of GFP after intra-cranial administration of PHP.eB-CamKII-GFP and PHP.eB-FLEXon-EF1A-EGFP-3xFlag viral constructs in C57BL/6J mice. (A) Representative histological sagittal images (left) of GFP expression (green) and blue (DAPI) after retro-orbital injection of GFP construct using PHP.eB serotypes in WT (top) and HD (bottom) B6CBA mice (scale bar: 1500μm). Amplified images (right) show GFP expression in neurons from the hippocampus (HPC) and cortex (CTX) (scale bar: 200 μm). (B) Representative histological sagittal image of GFP expression in A2A neurons after retro-orbital injection of PHP.eB serotype (scale bar: 1500μm) in A2A Cre BCBA mice.

These results demonstrate the potential of retro-orbital injection as a minimally invasive method for effectively infecting brain cells across different cell types and mouse strains, providing an alternative to stereotaxic surgery. Nevertheless, the volume used for retro-orbital injection (100 µl) is 200 times higher than that used in stereotaxic surgery (0.5 µl), which should be considered when designing future experiments. Moreover, further research on viral capsid modifications is necessary to enable neural cell infection via intranasal administration—an ongoing investigation led by our collaborator, Dr. Dalkara (Sorbonne Université).

2.2 Characterisation of cell-type-specific DdPAC stimulation effects in the brain

One of the main objectives of this work was to establish DdPAC as a novel optogenetic tool for modulating cAMP in vivo. cAMP plays a crucial role in synaptic plasticity, which is highly relevant for neurodegenerative diseases. DdPAC is a red-light-activated bacteriophytochrome that catalyses cAMP synthesis and can be inactivated by far-red light, providing precise temporal control (Stüven et al., 2018). However, it had never been tested in neural cells or *in vivo* before. To address this, DdPAC plasmids were obtained from Dr. Andreas Möglich and packaged into AAV9 constructs with neuronal and astrocytic promoters by Dr. Deniz Dalkara's group. Here, we tested and validated its ability to modulate synaptic plasticity in the mouse cortex, demonstrating its potential as a powerful optogenetic tool for neuroscience research.

2.2.1 Selective light-induced cAMP signaling in neurons and astrocytes via DdPAC activation induces synaptic potentiation, which is particularly enhanced when expressed in astrocytes

To this end, we first sought to characterise the potential of DdPAC stimulation to enhance neuronal responses when selectively expressed either in neurons or astrocytes. Accordingly, we used AAV9 constructs expressing DdPAC under CamkIIa or GFAP promoters to selectively express them in excitatory neurons or astrocytes. A 3xFlag Tag was also included in the construct (AAV9-CamKIIa-DdPAC-3xFlag-WPRE, AAV-CamKIIa-DdPAC; AAV9-GFAP-DdPAC-3xFlag-WPRE, AAV-GFAP-DdPAC) to enable post-experiment cellular expression localization (Figure 35A).

As a first step to establish whether light activation of DdPAC in neurons and astrocytes could induce a measurable and physiologically relevant effect in neuronal plasticity, recordings of field excitatory post-synaptic potentials (fEPSPs) were conducted in acute slices in collaboration with Dr. Parri and Dr. Ngum from Aston University. Since DdPAC construct is non-fluorescent, it was co-injected along with AAV9-CamKIIa-eGFP-WPRE or AAV9-GFAP-eGFP-WPRE (AAV-CamKIIa-GFP; AAV-GFAP-GFP), and the expression of eGFP was used as a guide to locate potential areas of DdPAC co-expression. Slices were placed on MEA chips and positioned with layer 4 and layer 2/3 overlying

identified electrodes within the grid (Figure 35B-C). The selective expression of DdPAC in neurons and astrocytes was confirmed by immunohistochemical staining for GFP (Figure 35D).

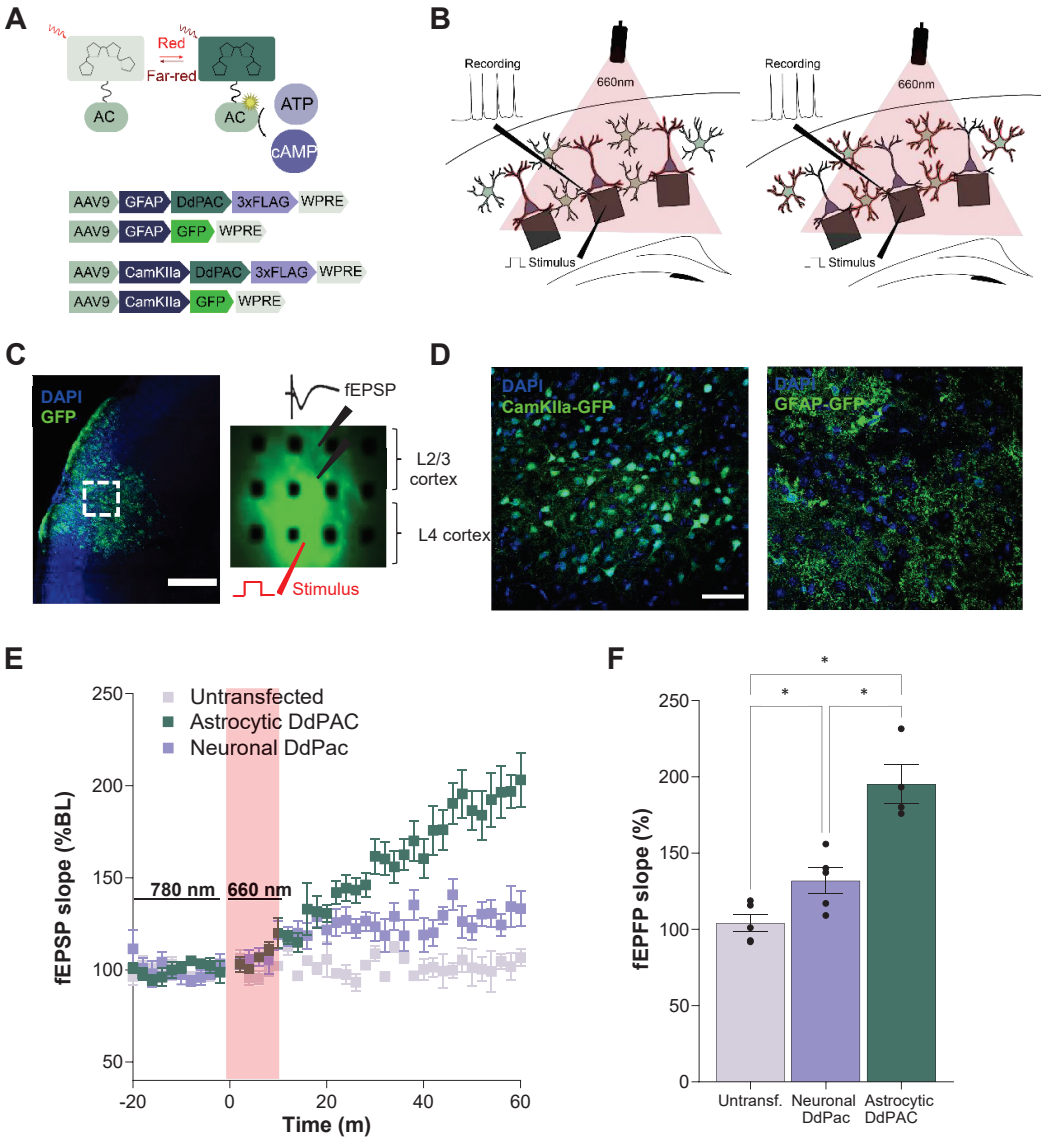

Figure 35. Selective light activation of DdPAC in cortical neurons and astrocytes induces synaptic plasticity. (A) Schematic representation of DdPAC and its selective activation by red and inactivation by far-red light. A conformation change in the photoreceptor domain induces the activation of AC in the catalytic domain leading to cAMP increase. Bottom panel show AAV9 construct under GFAP or CamKIIa for selective DdPAC and GFP expression. (B) Experimental set-up representation. DdPAC and GFP AAV constructs were coinjected in either neurons (left) or astrocytes (right) from layers 2/3 barrel cortex of WT mice to facilitate visualisation and correct placement on MEA probes for recording (scale bar: 500 µm). (C) Immunostaining of GFP (green) showing the placement of the MEA (left) and an example of the fluorescent slice image on MEA (right). (D) Representative histological image expressing GFP in neurons (left) or astrocytes (right). (E) Relative fEPSP slope (normalised to baseline values) versus time in 660nm light activated DdPAC neurons (n=5), astrocytes (n=4), and non-transfected (n=4) slices. (F) Average fEPSP slope from the 60 minutes after the stimulation. Mann-Whitney test was performed. Data are represented as mean ± SEM. *p<0.05, **p<0.01, ***<0.001

Electrical stimulation of cortical L4 resulted in fEPSP response in cortical L2/3 that, when stimulated every 120s, displayed a consistent amplitude and slope for 80 minutes. In recordings from areas expressing DdPAC, illumination with 660nm resulted in an increase in fEPSP slope indicative of synaptic potentiation. These effects were observed when DdPAC was expressed in both neurons and in astrocytes (Mann-Whitney: Unstransfected vs Neuronal DdPAC: P=0.05; Unstransfected vs Astrocytic DdPAC: P=0.01; Neuronal vs Astrocytic: 0.01). The potentiation was sustained for at least 60 minutes and so we termed it DdPAC long-term potentiation (DdPAC-LTP). Surprisingly, astrocytic DdPAC-LTP fEPFP slope was significantly higher than neuronal DdPAC-LTP, highlighting that modulation of cAMP in astrocytes results in stronger neuronal potentiation than modulation of cAMP in neurons (T-test Neuronal DdPAC vs Astrocytic DdPAC: P=0.003). In light of these results, the following experiments focused on the use of DdPAC under astrocytic promoter to modulate cAMP signalling selectively in astrocytes.

2.2.2 Astrocytic DdPAC-LTP induces glutamate gliotransmission, shares properties of theta burst potentiation, is PKA dependent, Ca^{2+} independent, and requires synaptic activity

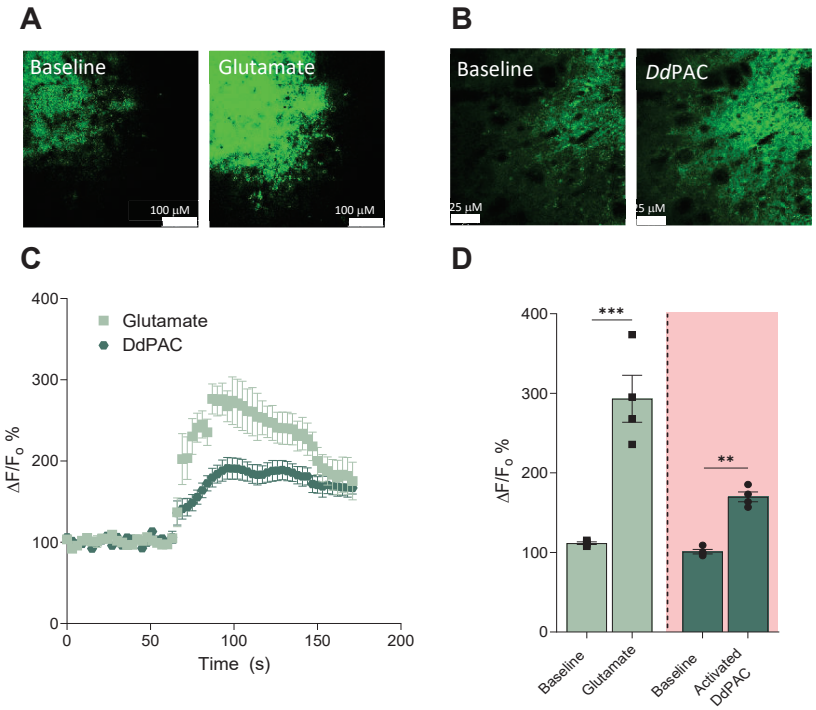

Figure 36. Selective light activation of DdPAC in cortical astrocytes induces glutamate release. (A) Representative images showing expression of iGluSnFR in neuronal cell membranes and increase in iGluSnFR signals following application of 100 mM glutamate. (B) Representative images showing expression of iGluSnFR in neuronal cell membranes and increase in iGluSnFR signals following stimulation of DdPAC expressed in astrocytes with 660 nm light. (C). Averaged iGluSnFR ΔF/F0 signal traces for 100 mM glutamate square (light green) and DdPAC hexagon (dark green) ± SEM, n = 4 each normalized to their [ΔF/F0] values during baselines. (D) Histogram detailing the change in iGluSnFR [ΔF/F0] values after application of 100 mM Glutamate ($p < 0.001$) or 660 nm stimulation of DdPAC ($p < 0.01$) from baseline. Mann-Whitney test was performed. Data are represented as mean ± SEM. *p<0.05, **p<0.01, ***<0.001

To further understand how light activation of DdPAC in astrocytes could mediate the observed synaptic potentiation (Parri et al., 2001), we examined whether astrocytic DdPAC activation resulted in gliotransmitter glutamate release. The genetically encoded glutamate sensor iGluSnFr under a neuronal promoter (AAV-hSyn.iGluSnFr) was co-injected with AAV-GFAP-DdPAC. After 3 weeks, acute slices were prepared and iGluSnFR fluorescence was imaged using confocal microscopy (460nm excitation, 530-565 nm emission). Bath application of glutamate (100uM) resulted in a 309.1 ± 32.7 % (n = 4) increase in fluorescence confirming the glutamate sensitivity of expressed iGluSnFR (Figure 36A, C and D). DdPAC activation with a 660nm LED also resulted in iGluSnFR fluorescence increase of 167.70 ± 4.99% (n = 4) (Figure 36B, C and D). These results establish that astrocyte DdPAC activation has a signalling effect following light activation and leads to glutamate release which is able to activate receptors on neighbouring neurons.

To determine the mechanism of astrocyte DdPAC-LTP, we compared it to conventional electrical synaptic stimulation-induced LTP (Figure 37A). Theta burst stimulation (TBS) was used as an established protocol for inducing LTP in cortical L4-L2/3 synapses (Butcher et al., 2022b) TBS-induced LTP (TBS-LTP) lasted for over 60 minutes (Figure 37A), with a magnitude similar to DdPAC-LTP (Figure 37B) (TBS: 214.80 ± 5.56%, n = 4, DdPAC: 187.90 ± 6.92%, n = 4, p = 0.05), although both forms had their own distinctive kinetic profiles (Figure 37A-B). TBS-LTP and DdPAC-LTP induction were blocked by the presence of the NMDAR inhibitor AP5, indicating a requirement for NMDAR activation (Figure 37A-B). Furthermore, DdPAC-LTP and TBS-LTP induction were also blocked in the presence of MK801, an open channel blocker, and 5,7 DCK, an antagonist of the NMDAR Glycine/Serine site (DdPAC MK801: 104.90 ± 1.36, p = 0.049, TBS MK801: 119.95 ± 6.32, p = 0.029, and DdPAC 5,7 DCK: 102.30 ± 3.15, p = 0.029, TBS 5,7 DCK: 108.32 ± 3.84, p = 0.028). (Figure 37A-B). These results indicate that both DdPAC-LTP and TBS-LTP require NMDAR ionotropic signalling and co-agonist activation of the Glycine/D-serine site. Since DdPAC activation catalyses the formation of cAMP, we then tested the role of protein kinase A (PKA) as one of the main targets of cAMP. DdPAC-LTP induction was abrogated in the presence of PKA inhibitor KT5270 (96.67 ± 4.09%, n = 4, p = 0.002), but TBS-LTP induction was unaffected (198.90 ± 7.24%, n = 5, p = 0.52) (Figure 37A-B).

Recognition of the role of astrocytes in LTP in the cortex, hippocampus and other brain areas is increasing (Butcher et al., 2022b; Henneberger et al., 2010; Perea & Araque, 2007). This role often depends on increases in intracellular Ca^{2+} levels within astrocytes (Henneberger et al., 2010; Min & Nevian, 2012; Shigetomi et al., 2008). We therefore sought to address this in the case of DdPAC-LTP. Therefore, DdPAC was expressed in the cortex of the $IP_3R2^{-/-}$ mice (Figure 37C). The R2 subtype of the IP_3 receptor is the most expressed in astrocytes and an important mediator of Ca^{2+} signalling (Holtzclaw et al., 2002; Sherwood et al., 2017). In the mutant $IP_3R2^{-/-}$ mouse, spontaneous and evoked astrocyte calcium signalling is greatly reduced (Agulhon et al., 2008; Butcher et al., 2022b). 660nm stimulation resulted in LTP in both $IP_3R2^{+/+}$ and $IP_3R2^{-/-}$ (176.33 ± 12.29 %, n=4, p > 0.99), indicating

a lack of a role for IP_3R2 signalling. To further address the role of calcium, we expressed the plasma membrane Ca^{2+} extrusion pump isoform PMCA2w/b in astrocytes, developed by Khakh and colleagues (X. Yu et al., 2021) and named CalEx. Co-expression of CalEx and DdPAC still resulted in DdPAC-LTP in response to 660nm stimulation (195.98 ± 9.50%, n=4, p > 0.99) (Figure 37C). Hence, these findings indicate that DdPAC-LTP is not dependent on Ca^{2+} signalling.

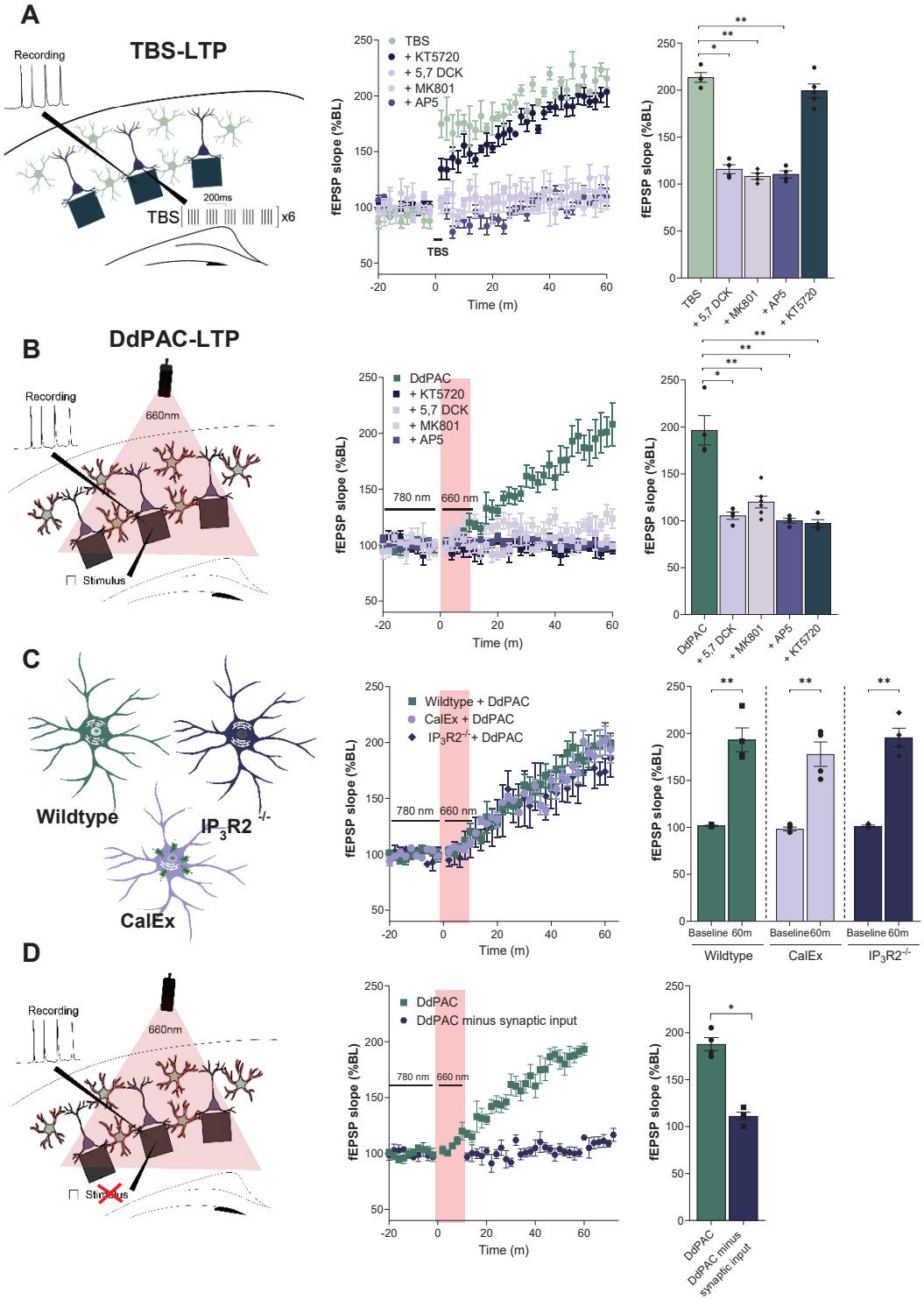

Figure 37. Light activated DdPAC-induced synaptic potentiation (DdPAC-LTP) shares properties of theta burst-induced potentiation (TBS-LTP). (A) Theta-burst stimulation induced LTP in cortical slices. Left panel shows schematic representation of the experimental setup detailing TBS in layer 4 barrel cortex and recording of evoked field potentials in layer 3/4. Middle panel shows the induction of TBS-LTP in the presence of PKA inhibitor (KT5720), NMDA receptor blockers (5,7 DCK, MK801 and AP5). Right panel summarises fEPSP slope effects at 60 minutes in the different conditions. N_{TBS}=4; N_{KT5720}=5; $N_{5,7DCK}$=4; N_{MK801}=4; N_{AP5}=4. (B) DdPAC stimulation by 660 nm light increases slope of evoked fEPSPs. Left panel shows schematic representation of the experimental setup detailing 660 nm illumination, input stimulation (1 Hz) in layer 4 barrel cortex and recording of evoked fEPSPs in layer 3/4. Middle panel shows the induction of fEPSP potentiation by 660 nm light and in the presence of PKA inhibitor (KT5720), NMDA receptor blockers (5,7 DCK, MK801 and AP5). Right panel shows summary of effects on fEPSP slope. N_{DdPAC}=4; N_{KT5720}=4; $N_{5,7DCK}$=4; N_{MK801}=6; N_{AP5}=4 (C) 660 nm light evoked fEPSP in cortical slices expressing DdPAC in WT, IP3R2-/- and CalEX mice. Left panel shows schematic representation of the astrocytic characteristics of the mouse lines used for MEA recording. Middle panel shows the induction of fEPSP slope potentiation by 660nm light in the different mouse lines. Right panel shows summary of fEPSP slope potentiation effects. N=4/group (D) 660nm light evoked field potentials in cortical slices expressing DdPAC in WT in the presence or absence of 1 Hz input during MEA recordings. Middle panel show the induction of fEPSP slope potentiation by light. Right panel shows summary of fEPSP slope potentiation effects. N_{DdPAC}=4; $N_{DdPACminusinput}$=3. Differences were analysed either by Kruskall Wallis with Dunn's post-hoc or Mann-Whitney test. Data are represented as mean ± SEM. *p<0.05, **p<0.01, ***<0.001

We finally examined whether 660 nm stimulation alone could induce synaptic change that resulted in LTP. Following a period of baseline synaptic stimulation at 0.008Hz, this stimulation was paused, and DdPAC was activated by 660nm light for 10 minutes. After 660nm light stimulation cessation, baseline stimulation was resumed. Against expectations, there was no potentiation of the subsequent synaptic responses (111.23 ± 4.12%, n=4, p = 0.014) (Figure 37D).

These results indicate two things: that astrocyte PKA-dependent LTP induction requires co-activation of astrocyte pathways and likely postsynaptic depolarization, and that the effect of DdPAC and PKA does not last beyond the 660 nm light stimulus. DdPAC light activation enhanced synaptic activity at 1 Hz and 0.008 Hz, but not at 0 Hz. This indicates that while DdPAC-induced LTP requires synaptic activity, unlike TBS-LTP, it is synaptic frequency-independent.

The finding that the DdPAC-LTP induction mechanism shares pathways with electrically induced activity-dependent TBS, led us to further characterise the properties of DdPAC-LTP (Figure 38). When TBS was applied in DdPAC expressing slices in conjunction with 660nm light stimulation, there was no increase in the degree of LTP (TBS-LTP: 214.80 ± 5.56%, n = 3, DdPAC-LTP: 187.90 ± 6.92%, n=4, and 201.5 ± 9.36% for TBS + DdPAC-LTP n=5, P= 0.58) (Figure 38). TBS stimulation applied following the 660 nm induction of DdPAC-LTP also did not further increase potentiation (Figure 38B). Therefore, TBS-LTP and DdPAC-LTP are not additive, which is consistent with the respective LTP induction being through common mechanisms.

LTP and LTD are considered opposing mechanisms in the brain that act to modify and balance synaptic strength (Artola & Singer, 1993). In L4-L3 synapses low frequency stimulation (LFS) of 900 stimuli at 1Hz induces synaptic depression (Figure 38C-D). If DdPAC-LTP shares a mechanism with electrically induced TBS-LTP, then electrically

induced LFS should be able to reverse it. Indeed, this was the case (Figure 38C). This means that electrical synaptic activity can reverse the effect of DdPAC cAMP-mediated light activation.

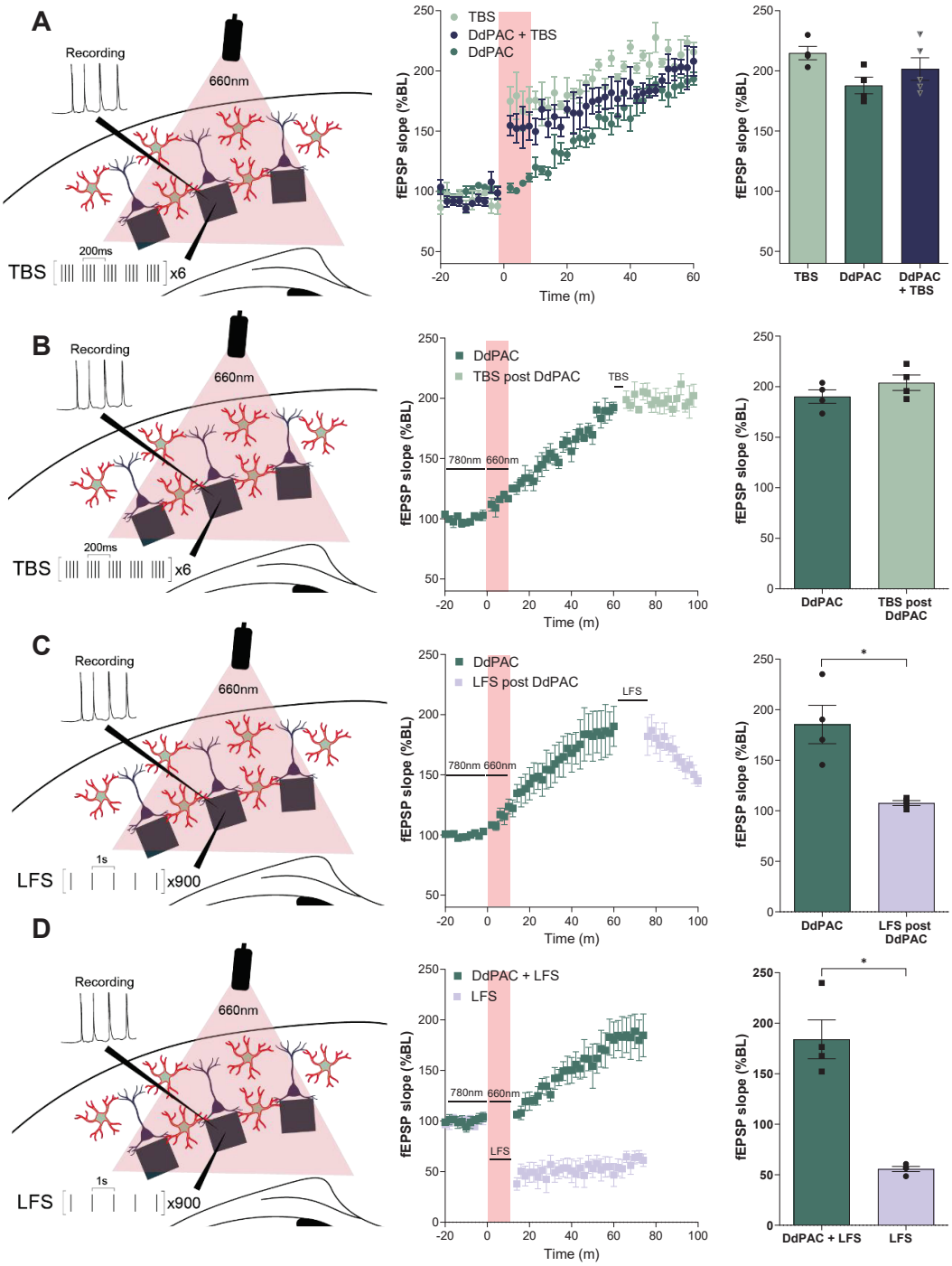

Figure 38. DdPAC activation instigates an activity dependent but frequency independent potentiation. (A) Combination of TBS with DdPAC stimulation with 660 nm light. Left panel show the schematic representation of the experimental setup detailing TBS in layer 4 barrel cortex during 660nm illumination and recording evoked field potentials in layer 3/4. Middle panel show the induction of fEPSP slope only with TBS, with both the presence of TBS and DdPAC stimulation, or only DdPAC stimulation. Right panel summarises fEPSP slope effects at 60 minutes in the three different conditions. N_{TBS}=4; N_{DdPAC}=4; $N_{DdPAC+TBS}$=5 (B).

Effects of TBS stimulation after DdPAC stimulation with 660 nm light. Left panel show schematic representation of the experimental setup detailing TBS in layer 4 barrel cortex after 660nm illumination and recording evoked field potentials in layer 3/4. Middle panel show induction of fEPSP slope with TBS applied after 60 minutes of 660nm illumination in DdPAC expressing slices. Right panel symmarises fEPSP slope effect during DdPAC stimulation or TBS after DdPAC stimulation. N_{DdPAC}=4; $N_{TBSpostDdPAC}$=4. (C) Effects of LFS stimulation after DdPAC stimulation with 660 nm light. Left panel show the schematic representation of the experimental setup detailing LFS in layer 4 barrel cortex after 660nm illumination and recording evoked field potentials in layer 3/4. Middle panel show induction of fEPSP slope with LFS applied after 60 minutes of 660nm illumination in DdPAC expressing slices. Right panel symmarises fEPSP slope effect during DdPAC stimulation or LFS after DdPAC stimulation. N_{DdPAC}=4; $N_{LFSpostDdPAC}$=4. (D) Combination of LFS with DdPAC stimulation with 660 nm light. Left panel show the schematic representation of the experimental setup detailing LFS in layer 4 barrel cortex during 660nm illumination and recording evoked field potentials in layer 3/4. Middle panel show the induction of fEPSP slope only with LFS, or with both the presence of TBS and DdPAC stimulation. Right panel summarises fEPSP slope effects at 60 minutes in the two different conditions. N_{DdPAC}=4; $N_{LFS+DdPAC}$=3. Differences were analysed either by Kruskall Wallis with Dunn's post-hoc or Mann-Whitney test. Data are represented as mean ± SEM. *p<0.05, **p<0.01, ***<0.001

Finally, it is known that TBS-LTP and LFS-induced LTD (LFS-LTD) utilize some of the same cellular mechanisms including NMDAR and astrocyte Ca^{2+}. We therefore tested whether 660 nm DdPAC activation would enhance or abrogate LFS-induced LTD. In fact, when they were co-applied, 660nm DdPAC activation counteracted the effect of LFS and instead induced DdPAC-LTP (LFS-LTD: 55.65 ± 2.53 %, n = 4, versus induced DdPAC-LTP: 184.02 ± 19.26%, n=4, p = 0.029) (Figure 38D).

Overall, these results demonstrate that DdPAC-mediated cAMP increase in cortical astrocytes triggers glutamate release, operates through the cAMP-PKA pathway, is independent of Ca2+ signaling, and requires synaptic activity. These findings further suggest that DdPAC activation could serve as a powerful tool for inducing potentiation in active neural networks through red-light exposure.

.

2.2.3 *In vivo* astrocyte DdPAC stimulation mainly impacts synaptic signalling pathways

To elucidate the molecular targets underlying DdPAC potentiating response, we conducted phosphoproteomics and proteomics analysis. Frontal cortex tissue was obtained immediately after *in vivo* light stimulation of DdPAC or GFP expressed in cortical astrocytes (Figure 39A). Both phosphoproteome and proteome heatmaps (Figure 39B-C) reveal a clear separation between GFP-injected and DdPAC-injected, red-light stimulated mice. Moreover, volcano plots (Figure 39 B-C) displayed and confirmed differential phosphoprotein and protein expression between groups. Indeed, the changes induced by DdPAC stimulation are stronger in the phospho-proteome than proteome dataset (Figure 39D-E).

In detail, ontology analysis of the phospho-proteome confirmed that DdPAC stimulation in astrocytes leads to the phosphorylation of synaptic plasticity associated proteins (Figure 40A). Interestingly, the top-modulated ontology includes the modulation of chemical synapses, followed by signalling by Rho GTPases which has been reported to modulate actin dynamics, (Tolias et al., 2011) a finding that also appears in the analysis. Moreover, the most

abundant phosphoprotein changes were localised at the pre- and post-synapse, including the synaptic cleft (Figure 40B), consistent with its involvement in synaptic plasticity mechanisms. In turn, the proteome dataset (Figure 40C) included ontologies related to synaptic transmission, neuron projection development, BDNF signalling, transynaptic signalling, postsynaptic neurotransmitter receptor activity, as well as to cytoskeletal remodelation. All these changes are indicative of abundant synaptic changes within minutes, as expected from the observed DdPAC-induced synaptic plasticity from slice experiments.

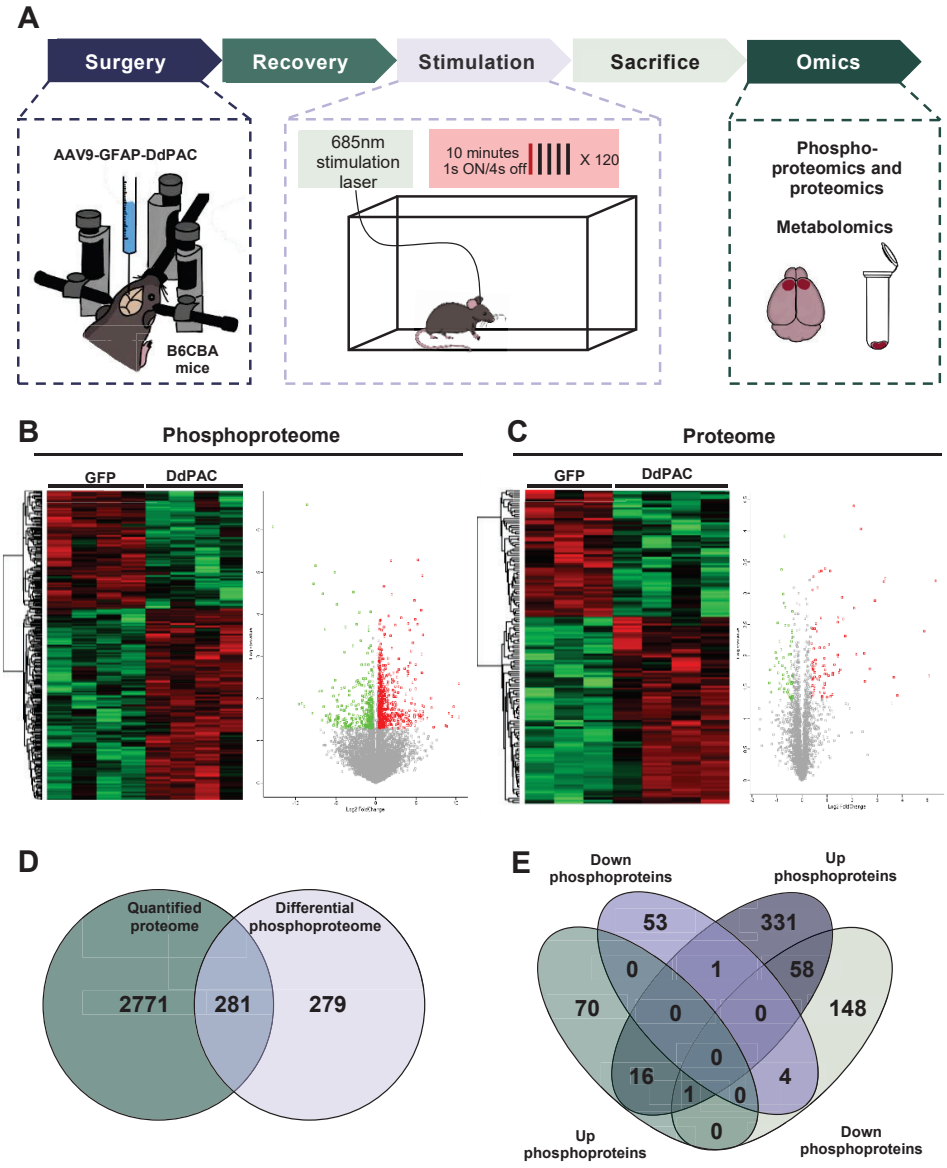

Figure 39. Astrocytic DdPAC activation affects both the phosphoproteome and proteome profiles (A) Schematic representation of the experimental design. Injection of AAV-GFAP-DdPAC or AAV-GFAP-GFP as control was performed in the M2 cortex of WT mice (n=4 each). DdPAC stimulation was performed in freely moving mice using 685nm light source for 10 minutes (1 second light ON and 4 seconds light OFF cycle). Frontal cortex brain tissue was dissected immediately after *in vivo* light delivery (B) Differential

phosphoproteome heatmap and volcano plot (C) Differential proteome heatmap and volcano plot (D) Number of quantified proteins and phosphoproteins (E) Representation of the increased (up) or decreased (down) phosphoproteins.

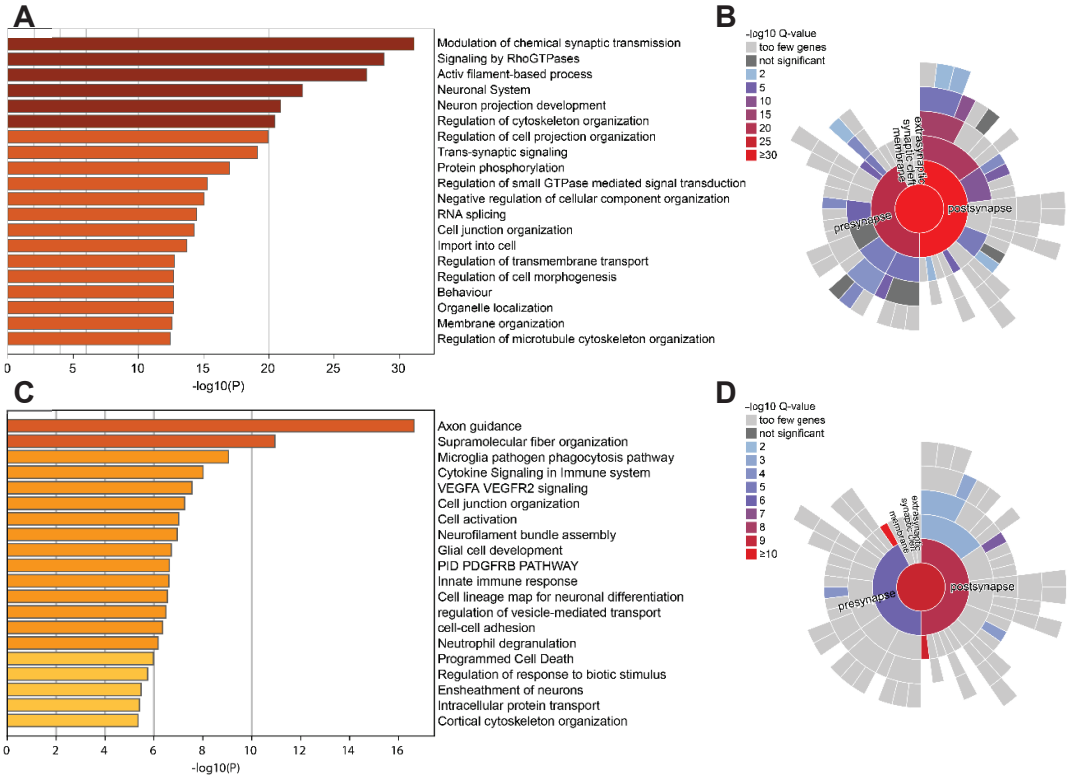

Figure 40. Astrocytic DdPAC activated phosphoproteome and proteome reveals synaptic plasticity modulation (A) Top 20 main phospho-proteome ontologies from differential expressed phospho-proteins between DdPAC and GFP stimulation. (B) Main synaptic localisation of the phospho-proteome. (C) Top 20 main proteome ontologies. (D) Main synaptic localisation of the proteome.

Moreover, PKA network analysis (Figure 41) confirmed that *in vivo* DdPAC activation in astrocytes operates through PKA signalling. First, cAMP-dependent protein kinase type I-alpha regulatory subunit (PRKAR1A) and A-kinase anchor protein 8 (AKAP8) were found higher phosphorylated in DdPAC stimulated cortical samples compared to control. Additionally, many PKA downstream effector proteins were also phosphorylated, such as the actin-binding protein Adducin, the focal adhesion kinase-associated protein Paxillin (PXN) and Vasodilator-stimulated phosphoprotein (VASP), all involved in actin and cytoskeletal modulation (Bachmann et al., 1999; Matsuoka* et al., 2000; Turner, 2000).

Finally, while phospho-proteomic and proteomic differential proteins include proteins associated with astrocyte development, which are indicative of cell-autonomous effects, the impact of DdPAC stimulation was observed beyond the astrocyte cell type. Analysis of cell-type markers (Sharma et al., 2015) shows phosphoprotein changes in proteins enriched not only in astrocytes, but also in neurons, microglia and oligodendrocytes. This indicates that DdPAC activation in astrocytes has a broad impact involving wide variety of responses in diverse brain cells in just a few minutes.

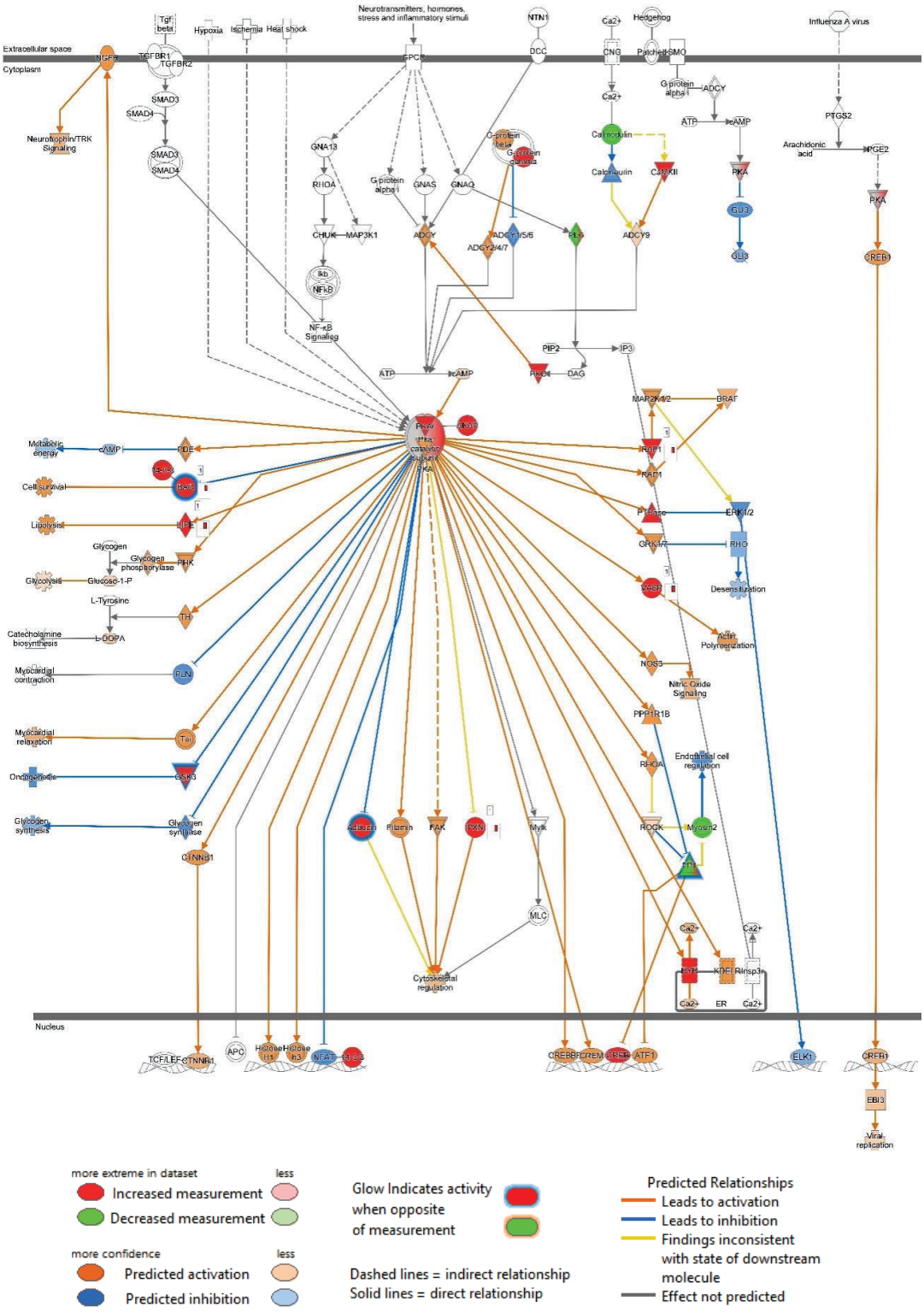

Figure 41. Astrocytic DdPAC activated phosphoproteome confirms activation of PKA-dependent pathways. PKA network analysis obtained from the phospho-proteome dataset. Legend indicating the meaning of protein colours, protein glow colours and lines, showing red and green increase/decrease measurement, orange/blue predicted, and yellow as inconsistent finding.

2.2.4 *In vivo* DdPAC stimulation in cortical astrocytes modulate metabolomic profile

cAMP is a purine derivative of adenosine triphosphate (ATP), and along pyrimidines are one of the more abundant metabolite classes in cells involved in the generation of DNA and RNA, cellular energy and intracellular signalling (Chandel, 2021). Because their complex metabolism and the relevance in cell homeostasis, we sought to study the effects of cAMP induction by astrocytic DdPAC stimulation on the profiles of 28 metabolites, including mainly nucleotides and related metabolites (Figure 42). PCA analysis evidenced a clear segregation of DdPAC samples from controls in the graph of the first two principal components (Figure 42A). Heatmap representation shows that DdPAC stimulation induce overall changes in the metabolite profile compared to control group (Figure 42B). The differential concentration analysis showed an effect of light activation of DdPAC in the concentration of 12 of the 28 metabolites analyzed (Figure 42C). While cAMP levels are spared, significant reductions of glutamate and nucleotides TTP, UTP, CDP, ATP, and UDP, where observed, among others. DdPAC activation only increased the concentration of oxidized glutathione, indicative of an increased energetic demand. Therefore, these results suggest that the effects of DdPAC stimulation might also be a consequence of the quick changes in at least the related metabolites analysed, which can contribute to further explain the broad effect observed in the phosphoproteomic and proteomic assays.

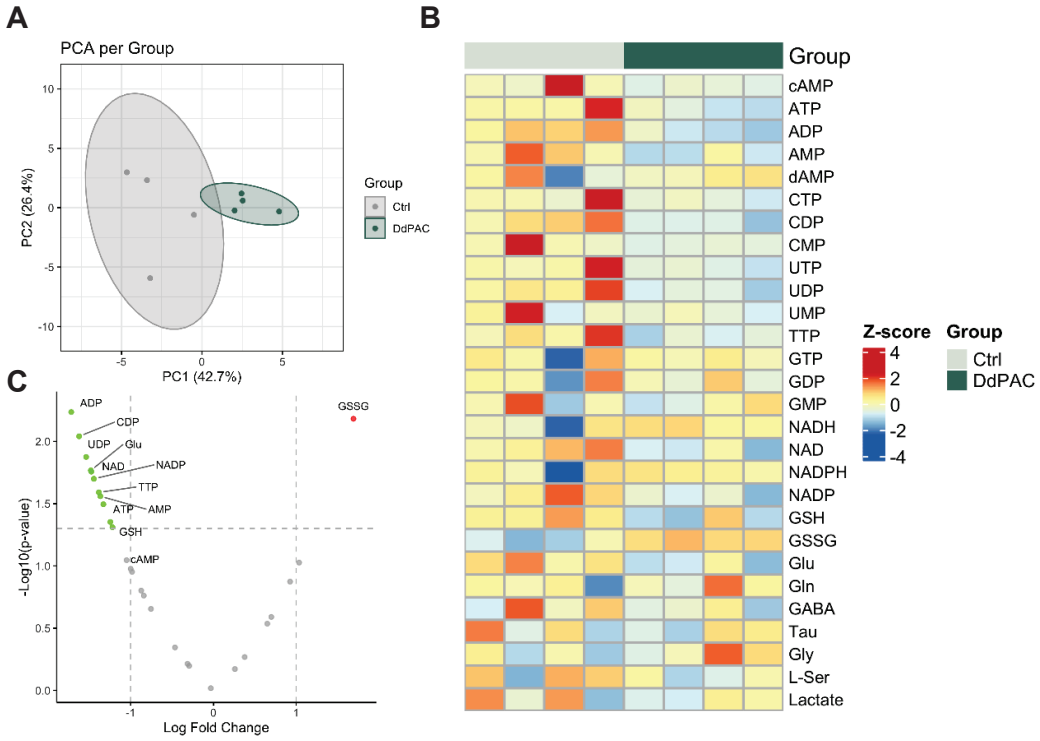

Figure 42. Astrocytic DdPAC activation affects the metabolome profile. (A) Unsupervised clustering analysis representing two separate groups, control (Ctrl) and DdPAC stimulated mice (DdPAC) (B) Distance heatmap indicating each of the selected metabolites and its z-score. (C) Volcano plot indicating the overexpressed (green) and underexpressed (red) metabolites.

3 To restore physiological function through light-driven DdPAC stimulation in mouse models of Huntington's and Alzheimer's Disease

HD and AD are devastating neurodegenerative disorders for which no cure or effective treatment currently exist to significantly improve patient's quality of life. Synaptic plasticity deficits and dysregulated cAMP signalling are hallmark features of these diseases (Cepeda & Levine, 2022; Griffiths & Grant, 2023; Kelly, 2018; S. H. Kim et al., 2001; H. Wilson et al., 2016), contributing to the observed functional impairment. Based on our previous findings demonstrating that DdPAC can modulate cAMP *in vivo* and enhance synaptic plasticity, we aimed to investigate whether this approach could restore physiological function in mouse models of HD and AD. Moreover, given our prior evidence highlighting the role of astrocytic cAMP modulation, we placed a particular emphasis on its contribution to disease pathology and potential therapeutic relevance.

Hence, we first investigated the impact of DdPAC-mediated cAMP modulation in astrocytes from the cortex and striatum – the two brain regions most affected in HD – on brain functionality and behaviour in the R6/1 mouse model of the disease (Figure 43A). Subsequently, we employed the 5xFAD mouse model of AD to examine the effects of cAMP modulation in both neurons and astrocytes of the hippocampus, the region most relevant in the disease (Figure 43B).

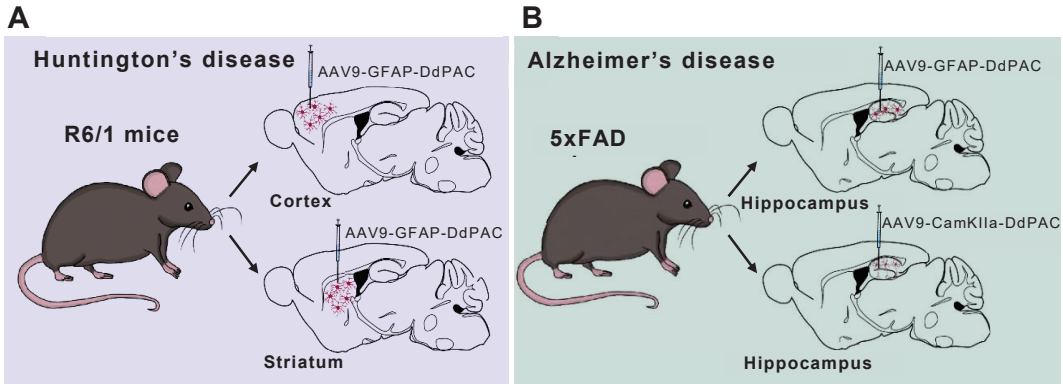

Figure 43. Schematic representation of the experimental design outlining DdPAC injections in mouse models of Huntington's Disease and Alzheimer's Disease. (A) DdPAC injection in astrocytes from the M2-cortex (top) or striatum (bottom) of R6/1 mice. (B) DdPAC injection in astrocytes (top) or neurons (bottom) from the hippocampus of 5xFAD mice. Specific analysis were conducted following viral expression.

3.1 Evaluation of the effects of enhanced DdPAC-mediated cAMP signalling in cortical and striatal astrocytes in a Huntington's Disease mouse model

3.1.1 DdPAC activation in cortical astrocytes induces hemodynamic responses in WT and R6/1 mice

In the previous section, we have demonstrated a clear association between DdPAC activation and synaptic plasticity. Furthermore, astrocytes are known to regulate cerebral blood flow (CBF) in response to neuronal activity (Diaz-Castro et al., 2019; Jiang et al., 2016b; Sdobnov et al., 2024). Therefore, here we investigated whether DdPAC activation exerts a broader cortical effect by assessing cortical blood flow in both WT and HD mice. For this purpose, we took advantage of the Dynamic Light Scattering imaging technique, known as Diffusion Correlation Spectroscopy (DCS) (Sdobnov et al., 2024) which allows the direct visualization of blood flow trans-cranially at mesoscale level, enabling acquisition of label free wide-field images from the dorsal surface of the adult mouse cortex (Figure 44). This bespoke application was developed by our collaborators, Dr. Bykov from Oulu University and Dr. Meglinski from Aston University (Sdobnov et al., 2024).

Mice were anaesthetised, head-fixed, and a small hole was performed in the skull to ensure that delivered red light reached the cortex during DCS imaging (Figure 44A). After five baseline image collection, we stimulated with red light for ten minutes and obtained additional five images right after (Figure 44C). Our data showed that red light induced an increase in CBF throughout the cortex in mice expressing DdPAC in astrocytes (Figure 44C). Specifically, red light-mediated DdPAC stimulation in the left hemisphere induced a 1.5% increase in blood flow in WT mice (one sample t-test, $p=0.07$). In contrast, in R6/1 mice, activation of DdPAC induced a 3.5% increase in blood flow, (one sample t-test, $p=0.02$). As a control for neuronal activity, we also expressed blue-dependent ChR2 in cortical neurons with AAV-CamKIIa-ChR2 in WT mice (Figure 44E-F).

Activation of opsins with 685 nm red-light induced a ~1.6 % change (one sample t-test, $p=0.03$), while 473 nm blue light-induced ~5.8 % change in blood flow (one sample t-test, $p=0.01$) (Figure 44G). No effects were induced by red 685 nm light stimulation in control (naïve) mice (one sample t-test, $p=0.7$), indicating specificity of the light-induced effects by opsins. This set of data demonstrates that astrocytic cAMP activity induced by DdPAC can modulate cortical CBF and provides further evidence on aberrant astrocytic function in R6/1 mice.

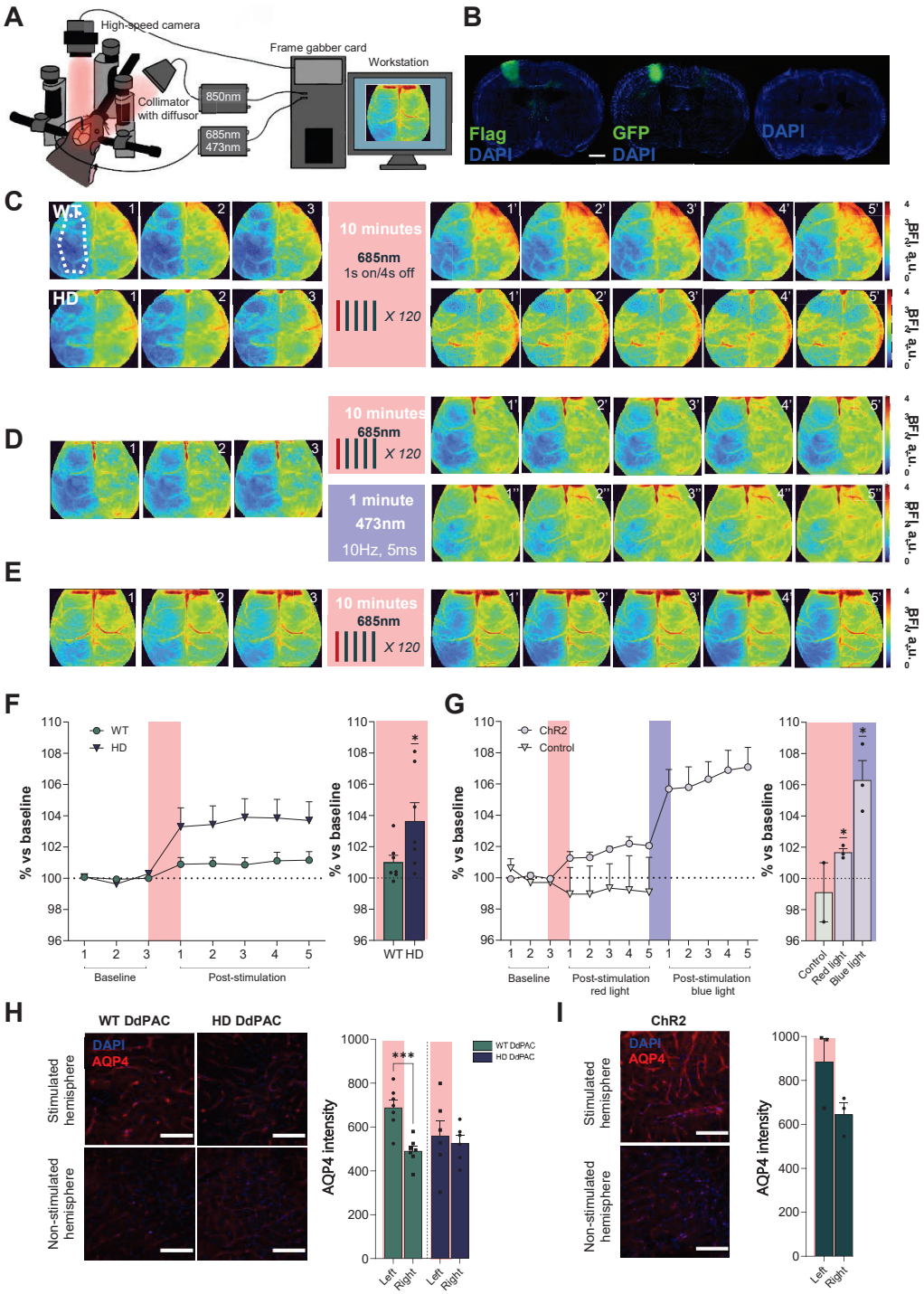

Figure 44. Astrocytic DdPAC stimulation induces distinct cortical hemodynamic changes in WT and R6/1 mice. (A) Imaging setup for mapping light dependent cortical blood flow changes obtained with DWS in a head-fixed anesthetized mouse. (B) Validation of expression of DdPAC and opsins (ChR2) in astrocytes and neurons respectively in the cortex from the left hemisphere. Naïve mice were used as control. Representative immunofluorescence shows virus constructs (green) and DAPI (blue) staining (Scale bar 1 mm). (C) Color-coded brain images indicating cortical blood flow before (1, 2, 3) and after red light (1', 2', 3', 4', 5') stimulation in DdPAC-expressing WT (top images) and the R6/1 mouse model of HD (bottom images). (D) Color-coded brain images indicating cortical blood flow before (1, 2, 3) and after (1', 2', 3', 4', 5') red (top) and

blue (1", 2", 3", 4", 5", bottom) light stimulation in WT mice expressing opsins (ChR2) in neurons. (E) Color-coded brain images indicating cortical blood flow before (1, 2, 3) and after (1', 2', 3', 4', 5') red light stimulation on control (naïve) WT mice. (F) Quantification of the percentage of hemodynamic change induced by DdPAC in the left hemispheres in WT and the R6/1 mouse model of HD (left) and mean percentage change (right). (G) Quantification of the percentage of hemodynamic change induced by red and blue light in mice expressing CHR2 and control (left) and mean percentage change (right). WT DdPAC n=7; HD DdPAC n=7; WT ChR2 n=3; Controls n=2. Values are expressed as mean ± SEM. Hemodynamic effects were analyzed by one sample T-test (*p<0.05). (H) Representative immunofluorescent images of Aquaporin4 expression (red) in light stimulated (top panels) or control hemisphere (bottom panels), from WT (left) and HD (right) expressing DdPAC (Scale bar=100μM). Histograms show the quantification of the AQP4 intensity in both hemispheres. (I) Representative immunofluorescent images of Aquaporin4 expression (red) in light stimulated (top panels). or control hemisphere (bottom panels) of WT expressing ChR2 (Scale bar = 100μM). Histograms show the quantification of the AQP4 intensity in both hemispheres. Each point represents data from an individual mouse (WT DdPAC n=7; R6/1 DdPAC n=7; WT ChR2 n=3; Controls n=2. Differences were analyzed by T-test (*** p<0.001).

To further investigate the hemodynamic changes observed by DdPAC stimulation in astrocytes, we evaluated Aquaporin 4 (AQP4) expression in the cortex of stimulated animals. AQP4 is a water channel highly expressed in the end-feet of astrocytes which facilitate water movement at the blood-brain interface (Amiry-Moghaddam & Ottersen, 2003; Bocci et al., 2016). At the synapse, AQP4 also regulates water and potassium fluxes in astrocytes through cAMP (Iliff et al., 2012) and synaptic activity through the mobility of the astrocytic processes (Y. Song & Gunnarson, 2012). Thus, we explored the levels of AQ4 expression in the DdPAC-stimulated hemisphere vs the non-stimulated hemisphere (Figure 44H-I). Immunofluorescence results showed an increase in APQ4 expression in the DdPAC expressing hemisphere (left) in WT mice stimulated with red light (Paired t-test, two-tailed, p=0.0002). In contrast, no differences were observed between hemispheres in DdPAC-stimulated R6/1 mice (Paired t-test, two-tailed, p=0.7). WT mice stimulated with neuronal ChR2 also did not show a change in AQP4 expression (Paired t-test, two-tailed, p=0.2). These results indicate that astrocyte activity induced by DdPAC triggers local changes in AQP4 expression which are absent in R6/1 mice.

3.1.2 Acute DdPAC-mediated cAMP increase in cortical astrocytes modulate spontaneous behaviour in R6/1 mice

To determine whether DdPAC-stimulation could impact network function and behaviour, we conducted *in vivo* behavioural studies in WT and in the R6/1 mouse model. To do so, we bilaterally injected DdPAC in cortical astrocytes of WT and R6/1 mice and performed DdPAC repetitive stimulation for 4 days, with 2 days in between stimulations (Figure 45A). To assess if DdPAC activation in M2 cortex was having an acute impact on behaviour, we tested paradigms of locomotion, exploration, and stereotypic behaviour (Figure 45A-C). During a 10 minute-stimulation period, total distance walked by the animals remained unaltered (genotype: $F_{(1,29)} = 3.78$ p = 0.06; stimulation: $F_{(1,29)} = 0.48$ p = 0.5); genotype/stimulation: $F_{(1,29)} = 0.32$ p = 0.6). Similarly, exploratory behaviour, measured by the time spent rearing, was unchanged (genotype: $F_{(1,29)} = 0.43$ p = 0.5; stimulation: $F_{(1,29)} =$

0.1.94 p = 0.2); genotype/stimulation: $F_{(1,29)}$ = 0.013 p = 0.9). Whilst, stereotypic behaviour, measured by the time spent grooming, was increased specifically in HD DdPAC mice. Two-way ANOVA revealed a significant genotype ($F_{(1,29)}$ = 9.03 p = 0.005) and genotype-treatment interaction effect ($F_{(1,29)}$ = 7.38 p = 0.01), although no treatment effect ($F_{(1,29)}$ = 9.03 p = 0.1). Bonferroni *post hoc* showed significant differences between HD DdPAC with all other groups (vs WT GFP p = 0.02; vs WT DdPAC p = 0.003 and vs HD GFP p = 0.04). Our data demonstrate that modulation of cortical astrocytes has minor impact on spontaneous behaviour in WT but can generate associated behavioural responses such as self-grooming (Ozawa et al., 2023) after only a brief period of DdPAC activation in R6/1 mice.

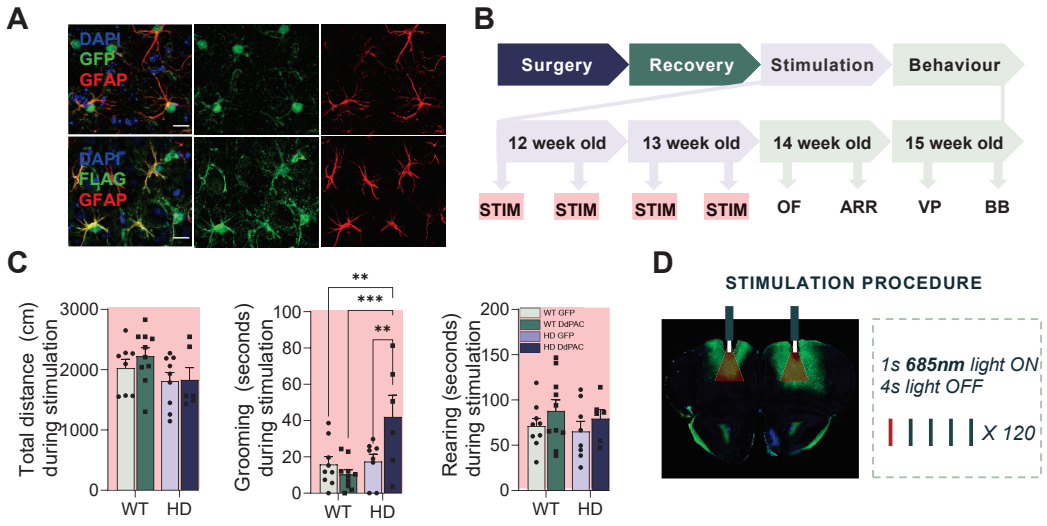

Figure 45. Acute DdPAC activation in M2 cortical astrocytes increases stereotypic behaviour in R6/1 mice. (A) Representative immunostaining of DdPAC (flag) or GFP with GFAP and DAPI in mouse cortical slices revealing the co-localisation of DdPAC/GFP in astrocytes (scale bar: 15µm) (B) Experimental timeline. Injection of AAV-GFAP-DdPAC or AAV-GFAP-GFP as control was performed bilaterally in the M2 cortex of WT and R6/1 mice at 8 weeks. DdPAC stimulation started at 12 weeks and was repeated 4 times every 3 days. Behavioural tests started the day after the last stimulation with 14 weeks old mice and included open field (OF), accelerating rotarod (ARR), vertical pole (VP) and balance beam (BB). (C) . Short-term behavioural effects during the first stimulation on: locomotion, as total distance travelled; time spent grooming, as a measure of stereotypic behaviour; and time spent doing rearing, as a measure of exploration time. (D) DdPAC stimulation consisted of 1 second of 685nm light ON followed by 4 seconds light OFF, 5-min per hemisphere. Differences were analysed by Two-way ANOVA followed by Bonferroni post-hoc test. *p <0.05. WT GFP n=12, WT DdPAC n=13, HD GFP n=10, HD DdPAC n=10.

3.1.3 Repetitive DdPAC-mediated cAMP increase in cortical astrocytes modifies motor behaviour by improving motor learning in WT mice and compromising coordination in R6/1 mice

We then investigated the long-term effects of repetitive DdPAC stimulation *in vivo* using well-characterised motor-related behavioural tests which are associated with HD cortico-striatal pathology (Fernández-García et al., 2020; Kalueff et al., 2016) (Figure 46). Starting the day after the last stimulation, we again assessed locomotion, stereotypies, and exploratory behaviour during an open field test (Figure 46A). Similar to the short-term effects observed by DdPAC stimulation, after four sessions of light stimulation, HD DdPAC increased grooming while locomotion and exploratory behaviour remained unaltered. Two-way ANOVA showed no differences in genotype ($F_{(1,34)} = 2.06$ $p = 0.2$) nor stimulation ($F_{(1,34)} = 2.43$ $p = 0.1$), nor genotype/stimulation interaction effects ($F_{(1,34)} = 1.206$ $p = 0.3$) in locomotion. Exploratory behaviour showed genotype ($F_{(1,34)} = 6.94$ $p = 0.01$) but not stimulation ($F_{(1,34)} = 0.25$ $p = 0.6$) or genotype/stimulation interaction effects ($F_{(1,34)} = 0.15$ $p = 0.7$). Regarding the time the animals spent grooming, we observed genotype effects ($F_{(1,34)} = 20.82$ $p < 0.0001$) and a tendency for the stimulation effect ($F_{(1,34)} = 3.02$ $p = 0.09$), but not genotype/stimulation interaction effect ($F_{(1,34)} = 2.34$ $p = 0.1$). Bonferroni post-hoc showed significant differences between HD DdPAC and both WT GFP ($p = 0.002$) and WT DdPAC ($p = 0.002$).

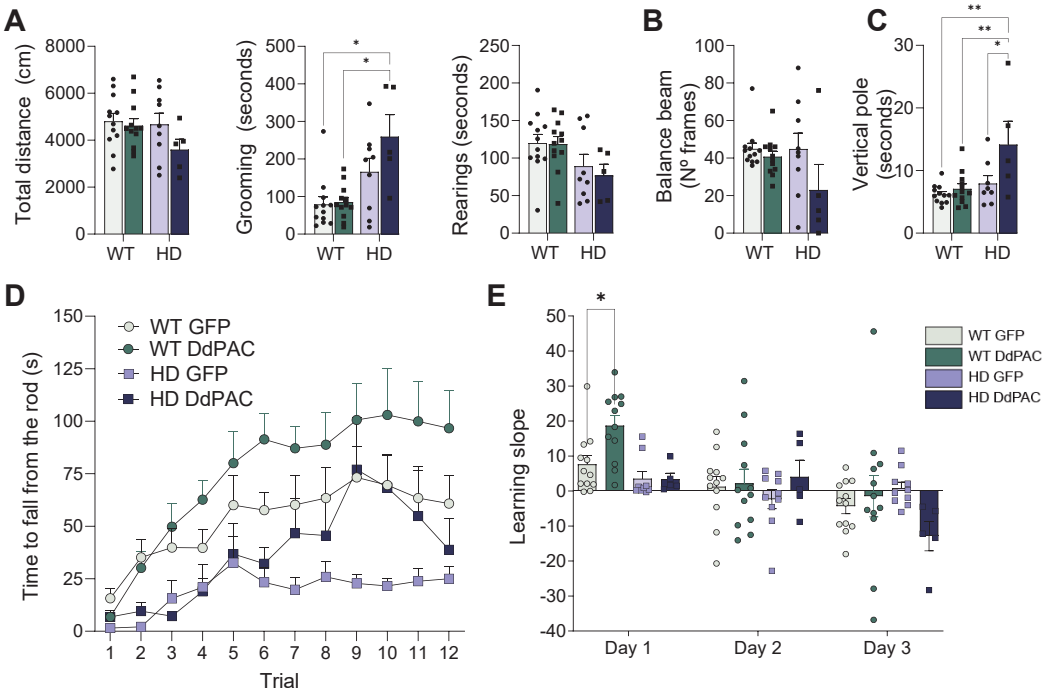

Figure 46. Repetitive DdPAC activation in M2 cortical astrocytes differentially impacts motor behaviour in WT and R6/1 mice. (A) Long-term behavioural effects of DdPAC stimulation on locomotion, grooming and rearing in the open field. (B) Effects of DdPAC stimulation on motor coordination evaluated as number of frames traveled in the balance beam. (C) Effects of DdPAC stimulation on motor coordination evaluated in the vertical pole, quantified with the seconds used to flip and descend the pole (D) Effects of DdPAC stimulation on motor learning evaluated by an accelerated rotarod, as the latency to fall from the

rotarod (left) and the learning slope per each day and group (right). Differences were analysed by Two or Three-way ANOVA followed by Bonferroni post-hoc test. *p <0.05. WT GFP n=12, WT DdPAC n=13, HD GFP n=10, HD DdPAC n=10.

Next, we evaluated motor learning using the cortico-striatal dependent accelerating rotarod test (Creus-Muncunill et al., 2019; Kupferschmidt et al., 2017) (Figure 46D-E). We observed that R6/1 mice display impaired motor learning compared to WT control, shown by reduced latency to fall from the rotarod, as expected in 14-week-old-mice (A. hua Cao et al., 2012) DdPAC stimulation improved the performance in the rotarod in both genotypes, although the effects were more prominent in WT mice. Three-way ANOVA showed trial ($F_{(11,385)}$ = 17.47 $p < 0.0001$), genotype ($F_{(1,35)}$ = 12.07 $p = 0.001$) and trial/stimulation interaction effect ($F_{(11, 385)}$ = 2.66 $p = 0.003$); but not stimulation ($F_{(1,35)}$ = 3.56 $p = 0.07$), trial/genotype ($F_{(11,385)}$ = 1.404 $p = 0.2$), nor genotype/stimulation ($F_{(1,35)}$ = 0.04 $p = 0.8$), trial/genotype/stimulation ($F_{(11,385)}$ = 0.92 $p = 0.5$). When the learning slope was investigated, we observed an improvement in learning on the first day in WT mice, as indicated by a two-way ANOVA analysis with group ($F_{(3,104)}$ = 2.72 $p = 0.05$) and day effect ($F_{(1483,77.11)}$ = 11.66 $p = 0.0002$), although not day/group effect ($F_{(6,104)}$ = 2.04 $p = 0.06$). Bonferroni post hoc test revealed significant differences during the first day of stimulation between the WT DdPAC and WT GFP ($p = 0.04$), HD GFP ($p = 0.002$) and HD DdPAC groups ($p = 0.002$). This demonstrates an enhanced motor learning on the first day of stimulation in WT mice.

Finally, we assessed coordination changes with the balance beam and vertical pole test, which are associated with basal ganglia function and are strongly affected at late symptomatic stages of R6/1 mice (>16-week-old R6/1 mice). These coordination changes have been previously shown to be modulated by cortico-striatal optogenetic stimulation in R6/1 mice (Ciappelloni et al., 2019a) (Figure 46B-C). In 15-week-old AAV-GFAP-GFP expressing mice, no coordination deficits were observed neither in the vertical pole test nor balance beam in HD compared to WT, as expected at this stage of HD. In both tests, detrimental effects of DdPAC stimulation on coordination were observed, particularly in R6/1 mice. The balance beam test showed stimulation effects ($F_{(1,34)}$ = 4.23 $p = 0.04$) but no genotype ($F_{(1,34)}$ = 1.97 $p = 0.2$), nor genotype/stimulation interaction ($F_{(1,34)}$ = 1.96 $p = 0.2$). Bonferroni *post hoc* did not show significant differences between groups. In the vertical pole test, which also evaluates coordination, stimulation ($F_{(1,33)}$ = 7.2 $p = 0.01$) and genotype ($F_{(1,33)}$ = 11.05 $p = 0.002$) and genotype/stimulation interaction effects ($F_{(1,33)}$ = 4.08 $p = 0.05$) were observed by a two-way ANOVA. Bonferroni *post-hoc* showed a significant increase in the total time to perform the test between HD DdPAC and the WT GFP ($p=0.002$), HD GFP ($p=0.04$), and WT DdPAC ($p=0.007$) groups.

Moreover, during the confirmation of the expression of the virus constructs in the brains of mice in all groups (Figure 47A), we observed changes in GFAP expression levels in the tissue of stimulated mice compared to their respective controls. Thus, we decided to analyse the intensity of GFAP by immunofluorescence (Figure 47B). We observed significantly increased GFAP expression levels in both WT and HD DdPAC stimulated mice compared to GFP controls. This aligns with our proteomic data, which indicated that short-term

DdPAC stimulation elevated GFAP levels in WT mice and indicates astrocytic activation by DdPAC. Two-way ANOVA showed the effects of the simulation ($F_{(1,33)}$=29.67 p<0.0001), but not genotype ($F_{(1,33)}$=1.617 p = 0.2) or genotype/stimulation interaction ($F_{(1,33)}$=3.02 p = 0.09). Using a Bonferroni *post-hoc* analysis we detected a significant increase in between WT GFP and WT DdPAC (p<0.0001) and HD DdPAC (p>0.03), and between WT DdPAC and HD GFP (p<0.0002).

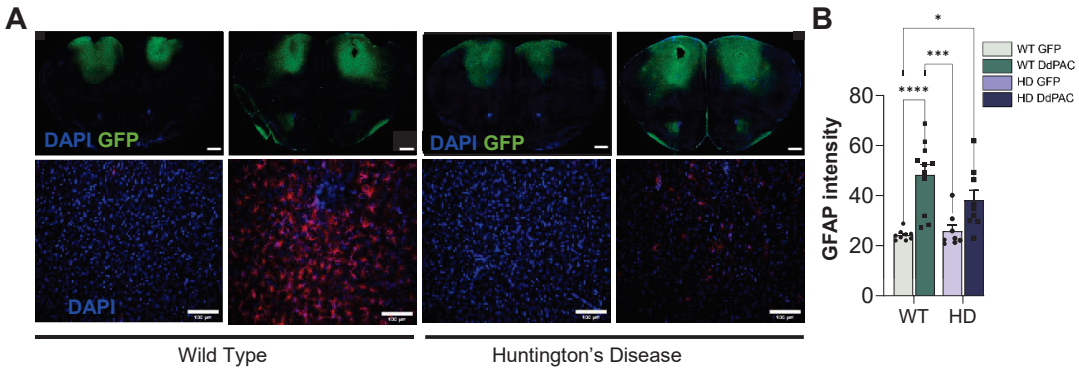

Figure 47. Repetitive DdPAC activation increase GFAP expression in M2-cortical astrocytes from WT mice. (A) Top row: representative fluorescent images showing in green the AAV-infected brain regions (GFP for AAV-GFAP-GFP; FLAG, for AAV-GFAP-DdPAC) and in blue DAPI staining (scale bar 100µm) in WT (left) and R6/1 mice (right). Bottom row: representative fluorescent images showing GFAP positive astrocytes on the infected region (scale bar 100µm). (B) Quantification of GFAP intensity. Differences were analyzed by Two-way ANOVA followed by Bonferroni post-hoc test. *p <0.05. WT GFP n=12, WT DdPAC n=13, HD GFP n=10, HD DdPAC n=10.

Overall, these findings indicate that an increase in cAMP in cortical astrocytes triggers cortico-striatal-associated behavioural responses in mice, particularly by enhancing motor learning. Notably, DdPAC stimulation produces different behavioural outcomes in WT and R6/1 mice, improving motor learning while impairing coordination in R6/1 mice. This suggests that alterations in astrocytic cAMP signalling in the cortex may contribute to motor symptoms in HD. Further research is needed to fully understand the role of astrocytic cAMP signalling in HD pathology.

3.1.4 Acute DdPAC-mediated cAMP signalling increase in striatal astrocytes induce anxiety-like behaviour in R6/1 mice, while repetitive DdPAC stimulation impairs locomotion, spontaneous behaviour, and coordination in both WT and R6/1 mice

Striatal degeneration is a key hallmark of HD, with the cortico-striatal pathway being among the earliest and most severely affected connections (Cepeda et al., 2007; Miller et al., 2011). Following our investigation of the impact of increased cAMP signalling on behaviour of R6/1 mice, we sought to explore the effects of DdPAC stimulation on striatal astrocytes. To this end, we injected DdPAC under the GFAP promoter into the striatum of both WT and R6/1 mice (Figure 48A), and then we followed the same stimulation protocol used in the

cortex: 4 days of 10-minute stimulation, with two days between each session. Following the stimulation, we performed a series of tests to assess motor behaviour (Figure 48B).

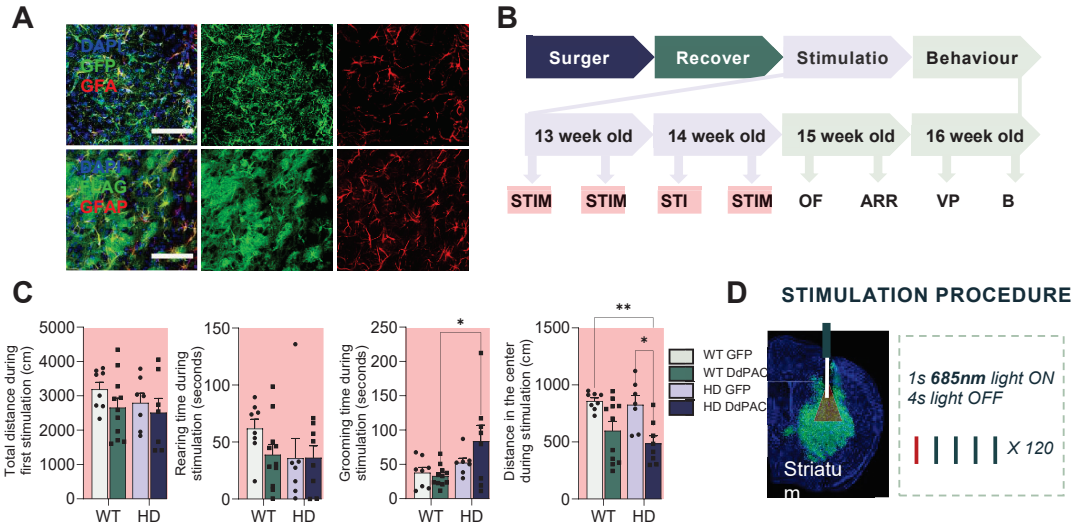

Figure 48. Acute DdPAC activation in striatal cortical astrocytes increases anxiety-like behaviour in R6/1 mice. (A) Representative immunostaining of DdPAC (flag) or GFP with GFAP and DAPI in mouse cortical slices revealing the co-localisation of DdPAC/GFP in astrocytes (scale bar: 15µm) (B) Experimental timeline. Injection of AAV-GFAP-DdPAC or AAV-GFAP-GFP as control was performed bilaterally in the striatum of WT and R6/1 mice at 8-9 weeks. DdPAC stimulation started at 12-13 weeks and was repeated 4 times every 3 days. Behavioural tests started the day after the last stimulation with 14-15 weeks old mice and included open field (OF), accelerating rotarod (ARR), vertical pole (VP) and balance beam (BB). (C) Short-term behavioural effects during the first stimulation on: locomotion, as total distance travelled; time spent grooming, as a measure of stereotypic behaviour; and time spent doing rearing, as a measure of exploration time. (D) DdPAC stimulation consisted of 1 second of 685nm light ON followed by 4 seconds light OFF, 5-min per hemisphere. Differences were analysed by Two-way ANOVA followed by Bonferroni post-hoc test. *p <0.05. WT GFP n=8, WT DdPAC n=11, HD GFP n=7, HD DdPAC n=7.

First, we aimed to investigate if acute DdPAC stimulation on striatal astrocytes had an impact in spontaneous behaviour, by analysing locomotion, rearings, and groomings during the first stimulation session in WT and R6/1 mice (Figure 48C). Contrary to what was observed with cortical astrocytes, an acute increase in cAMP did not affect locomotion (Two-way ANOVA: Genotype: $F_{(1,29)}$=0.80, P=0.38; Stimulation: $F_{(1,29)}$=1.8, P=0.19; Interaction: $F_{(1,29)}$=0.18, P=0.68) nor rearing (Two-way ANOVA: Genotype: $F_{(1,30)}$=1.62, P=0.21; Stimulation: $F_{(1,30)}$=1, P=0.32; Interaction: $F_{(1,30)}$=1.1, P=0.3) or grooming time (Two-way ANOVA: Genotype: $F_{(1,30)}$=6.9, P=0.01; Stimulation: $F_{(1,30)}$=1.14, P=0.29; Interaction: $F_{(1,30)}$=2.11, P=0.15), although a tendency to increased grooming in R6/1 mice was observed. Specifically, Bonferroni Post-hoc showed significant differences between WT stimulated vs HD stimulated mice (p=0.03). Moreover, we measured the distance spent in the centre of the open field as a measure of anxiety (Figure 48C). Two-way ANOVA with genotype and stimulation as factors, showed a stimulation effect for the distance travelled in the centre of the arena (Genotype: $F_{(1,30)}$=1.01, P=0.3227; Stimulation: $F_{(1,30)}$=17.44, P=0.0002; Interaction: $F_{(1,30)}$= 0.30, P=0.58). Particularly, we observed a decrease in the distance that the animals walked in the centre of the arena, especially for R6/1 mice, in which Bonferroni post-hoc test showed significantly reduced travelled distance during the 10 minutes of

stimulation (P=0.02), indicating increased anxiety-like behaviour. Significant differences between WT GFP and HD DdPAC mice were also observed (P=0.007).

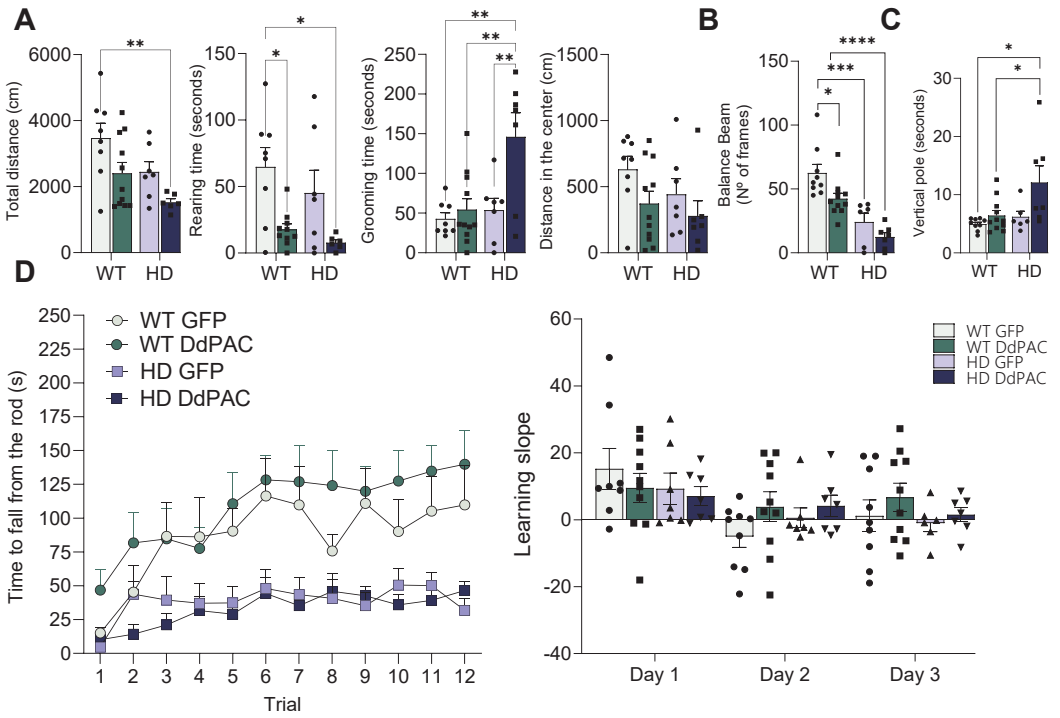

Figure 49. Repetitive DdPAC activation in striatal astrocytes differentially alters spontaneous behaviour and worsens coordination in WT and R6/1 mice. (A) Long-term behavioural effects of DdPAC stimulation on locomotion, grooming and rearing in the open field. (B) Effects of DdPAC stimulation on motor coordination evaluated as number of frames traveled in the balance beam. (C) Effects of DdPAC stimulation on motor coordination evaluated in the vertical pole, quantified with the seconds used to flip and descend the pole (D) Effects of DdPAC stimulation on motor learning evaluated by an accelerated rotarod, as the latency to fall from the rotarod (left) and the learning slope per each day and group (right). Differences were analysed by Two or Three-way ANOVA followed by Bonferroni post-hoc test. *p <0.05. WT GFP n=8, WT DdPAC n=11, HD GFP n=7, HD DdPAC n=7

To determine which were the consequences of repetitive DdPAC-mediated cAMP increase in striatal astrocytes on motor phenotype, we conducted the same battery of motor-related behavioural tests as was performed previously for cortical astrocyte stimulation (Figure 48B). Generally, we observed that DdPAC stimulation had an effect both in WT and R6/1 mice, impairing their behaviour. Specifically, the time WT mice spent rearing was decreased while the time R6/1 mice spent grooming was increase, both indicative of aberrant function. Precisely, two-way ANOVA with genotype and stimulation as factors, showed stimulation effect on the total distance travelled during the last stimulation, although no genotype nor interaction effects were observed (Genotype: $F_{(1,28)}$=7.09, P=0.012; Stimulation: $F_{(1,28)}$=7.67, P=0.009; Interaction: $F_{(1,28)}$= 0.04, P=0.83). Rearing time also showed stimulation effect, with not genotype nor interaction effects (Genotype: $F_{(1,27)}$=1.71, P=0.2; Stimulation: $F_{(1,27)}$=13.9, P=0.009; Interaction: $F_{(1,27)}$= 0.18, P=0.67). However, grooming time displayed interaction, genotype and stimulation effects (Genotype: $F_{(1,29)}$=8.57, P=0.006; Stimulation: $F_{(1,29)}$=8.76, P=0.006; Interaction: $F_{(1,29)}$= 5.26, P=0.02). Bonferroni post-hoc showed significant decrease

in total distance between WT GFP and HD DdPAC mice (P=0.007), as well as significant decreased in the time spent rearing between WT GFP mice vs WT DdPAC mice (P=0.03) and WT GFP mice vs HD DdPAC mice (P=0.01). For the time spent grooming, Bonferroni post hoc displayed significant differences between WT GFP and HD DdPAC (P=0.002), WT DdPAC and HD DdPAC (P=0.004), and HD GFP and HD DdPAC (P=0.01). These results suggest that spontaneous, stereotypic behaviour is affected in both WT and R6/1 mice after increase in cAMP in astrocytes from the striatum.

Next, we evaluated coordination in these mice by conducting the balance beam and vertical pole tests. Again, we observed that DdPAC stimulation impaired coordination in both WT and R6/1 mice. Two-way ANOVA exhibited both genotype and stimulation effects the in number of frames walked during the balance beam test (Genotype: $F_{(1,29)}$=8.01, P=0.008; Stimulation: $F_{(1,29)}$=36.98, P<0.0001; Interaction: $F_{(1,29)}$= 0.55, P=0.46) and the total time needed to conduct the vertical pole test (Genotype: $F_{(1,29)}$=5.97, P=0.02; Stimulation: $F_{(1,29)}$=0.67, P=0.01; Interaction: $F_{(1,29)}$= 2.43, P=0.12). No interaction effect was shown in neither of these tests. Bonferroni post-hoc displayed a decrease in the number of frames walked by WT DdPAC (P=0.04), HD GFP (P=0.0004) and HD DdPAC (P<0.0001) compared to WT GFP mice, as well as a significant decrease between WT DdPAC and HD DdPAC (P=0.002). Regarding the vertical pole test, Bonferroni Post-hoc displayed increased total time in HD DdPAC mice compared to WT GFP (P=0.007) and WT DdPAC (P=0.03). These results indicate that an increase of cAMP signalling in striatal astrocytes from both WT and R6/1 mice is compromising the ability to coordinate in these animals.

Lastly, motor learning was assessed using the ARR test. Contrary to what we observed in the cortex, motor learning was not affected by DdPAC-mediated cAMP increase in striatal astrocytes. In this context, Three-way ANOVA with genotype, stimulation and time as factors showed genotype, time and genotype x time but no stimulation effect (Genotype: $F_{(1,29)}$=14.32, P=0.0007 ; Stimulation: $F_{(1,29)}$=0.28, P=0.59; Time: $F_{(11,315)}$=11.29, P<0.0001; Interaction genotype x time: $F_{(11,315)}$= 3.09, P=0.0006; Interaction stimulation x time: $F_{(11,315)}$=1.01, P=0.43; Interaction stimulation x genotype: $F_{(1,29)}$=0.60, P=0.44; Interaction stimulation x genotype x time: $F_{(11,315)}$=0.82, P=0.61) in the time to fall from the rod. We also analysed the learning slope, where Two-way ANOVA with time and group as factors only showed time effect (Group: $F_{(3.29)}$=0.48, P=0.69; Time: $F_{(1.949,\ 54.58)}$=5.88, P=0.005; Interaction: $F_{(6,56)}$= 0.98, P=0.44), suggesting that motor learning is not affected by modulated cAMP signalling in striatal astrocytes.

After sacrificing the animals, we removed, post-fixed, and sliced the brain to confirm the expression of either GFP or DdPAC in the striatum as well as correct cannula placement. Considering our previous results where we detected an increase in GFAP expression in DdPACs stimulated astrocytes, we aimed to further investigate if this effect was also present in the striatum or if it was region-dependent (Figure 49A). Therefore, we immunolabeled GFAP in these mice striatal slices. We detected an increase of GFAP expression in both WT and HD DdPAC stimulated mice. Two-way ANOVA revealed stimulation and genotype but

not interaction effects (Genotype: $F_{(1,25)}$=5.13, P=0.03; Stimulation: $F_{(1,25)}$=62.75, P<0.0001; Interaction: $F_{(1,25)}$= 1.56, P=0.22) (Figure 49B). Moreover, Bonferroni post-hoc confirmed significant differences between WT GFP and WT DdPAC group (P<0.0001), and HD GFP and HD DdPAC group (P=0.002). Post-hoc differences were also observed between WT GFP and WT DdPAC (P<0.0001), and WT GFP and HD DdPAC (P=0.003). These results indicate that, similar to our observation in the cortex, DdPAC stimulation activates astrocytes in the striatum. Furthermore, in this brain region, repeated activation appears to negatively influence both spontaneous behaviour and coordination in both groups.

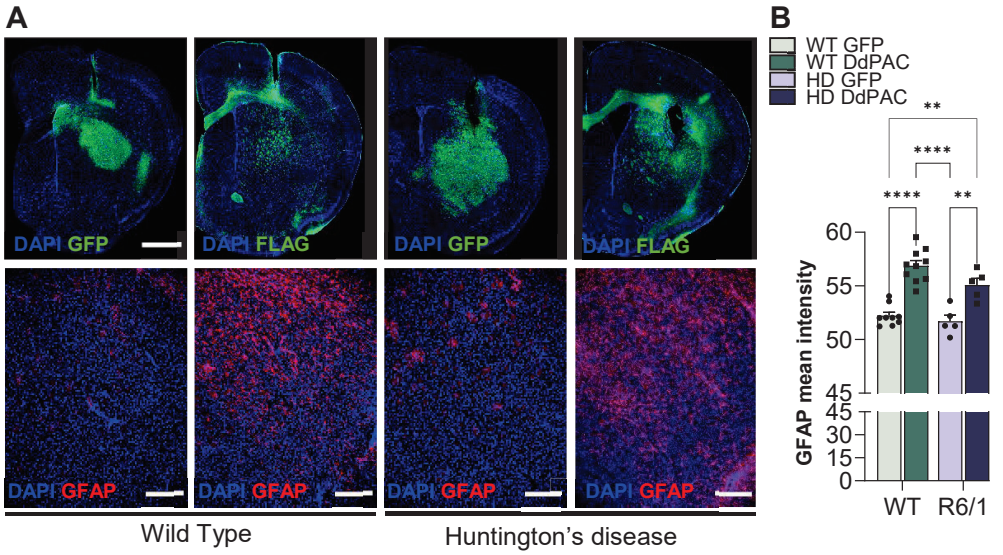

Figure 49. Repetitive DdPAC activation increase GFAP expression in striatal astrocytes from WT and R6/1 mice. (A) Top row: representative fluorescent images showing in green the AAV-infected brain regions (GFP for AAV-GFAP-GFP; FLAG, for AAV-GFAP-DdPAC) and in blue DAPI staining (scale bar 100μm) in WT (left) and R6/1 mice (right). Bottom row: representative fluorescent images showing GFAP positive astrocytes on the infected region (scale bar 100μm). (B) Quantification of GFAP intensity. Differences were analyzed by Two-way ANOVA followed by Bonferroni post-hoc test. *p <0.05. WT GFP n=8, WT DdPAC n=10, HD GFP n=5, HD DdPAC n=5.

3.2 Evaluation of DdPAC-mediated cAMP signalling effect in hippocampal neurons and astrocytes of an Alzheimer's Disease mouse model

Given the impact of DdPAC stimulation on neuronal plasticity in WT mice (*see section 2.2*) and the differential hemodynamic and behavioural responses observed in HD, here we sought to further investigate the potential of DdPAC to restore physiological function in AD. Moreover, as our previous findings demonstrated that DdPAC activation in neurons differentially affects neuronal plasticity (*see section 2.2.1*), we aimed to extend our investigation by exploring the impact of increased cAMP signalling selectively in neurons or in astrocytes within the hippocampus, as well as its effects in the context of AD. We chose to examine DdPAC effects using the 5xFAD model of the disease, which is well-characterised and

presents with an aggressive AD-like pathology, which includes early-onset Aβ deposits, synaptic loss, and neuronal degeneration (Oakley et al., 2006). We injected AAV9-CamkIIa-DdPAC and AAV9-GFAP-DdPAC in the dentate gyrus (DG) of WT and 5xFAD male and female mice, as well as AAV9-CamkIIa-GFP and AAV9-GFAP-DdPAC as controls (Figure 50). Similar to our previous experiments, we stimulated for 10 minutes (1s ON + 4s OFF) using a 685 nm laser and sacrificed the mice 24h later for tissue analysis.

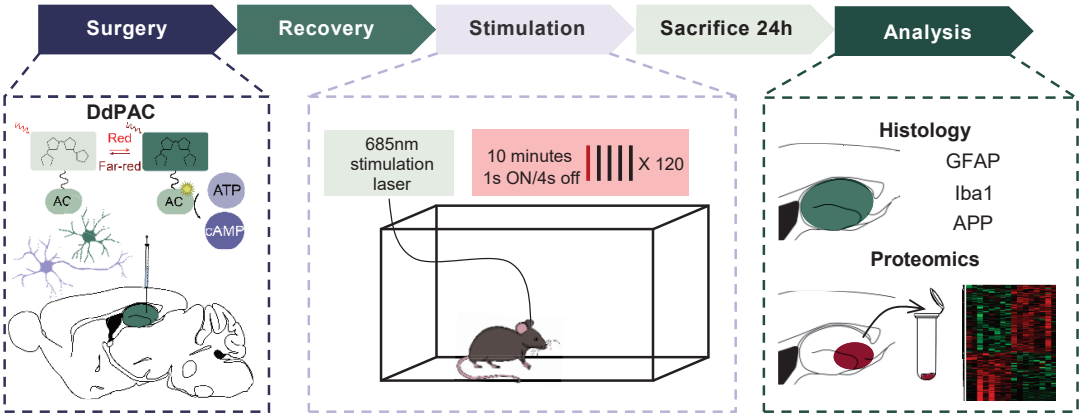

Figure 50. DdPAC activation in neurons and astrocytes from the hippocampus of Alzheimer's Disease mouse model. Schematic representation of the experimental design. Injection of AAV-GFAP-DdPAC or AAV-CamKIIa-GFP as control was performed in the CA1 region of the hippocampus in WT and 5xFAD mice (n=8 each). DdPAC stimulation was performed in freely moving mice using 685nm light source for 10 minutes (1 second light ON and 4 seconds light OFF cycle). Mice were sacrificed 24 hours after red-light stimulation. One hemisphere was post-fixed for immunolabeling and CA1 brain tissue from the other hemisphere was dissected and frozen for proteomics analysis.

3.2.1 DdPAC-mediated cAMP increase in astrocytes, but not in neurons, specifically reduces GFAP-positive astrocytes in the hippocampus of 5xFAD mice

We first validated the expression of the AAV construct in the hippocampus and observed that most mice predominantly expressed either GFP or Flag not only in the dentate gyrus but also in other hippocampal regions, including CA1 (Figure 51A and Figure 52A).

The presence of Aβ deposits and inflammation in the hippocampus are two key hallmarks of AD. Thus, we first decided to analyse GFAP expression intensity in the hippocampus of WT and 5xFAD mice (Figure 51-52). One day after a 10-minute red-light stimulation, we analysed GFAP intensity in the hippocampus from mice expressing DdPAC in astrocytes. Notably, we observed an overall hippocampal GFAP increase in 5xFAD control mice, while DdPAC stimulation in astrocytes from 5xFAD mice induced a decrease in GFAP expression. Both genotype and interaction effects were observed after a two-way ANOVA analysis (Genotype: $F(1,40)=9.10$, $p=0.004$; Stimulation: $F(1,40)=3.43$, $p=0.07$; Interaction:

F(1,40)=1.97, p=0.04). Bonferroni Post-hoc showed differences specifically between 5xFAD GFP and 5xFAD DdPAC mice (p=0.03) displaying specific stimulation effects in 5xFAD mice (Figure 51B).

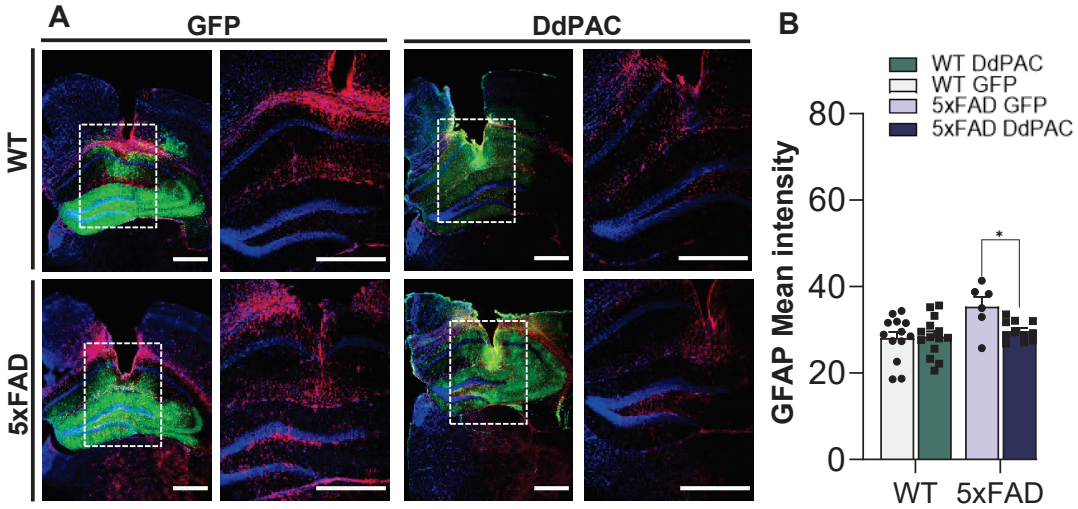

Figure 51. DdPAC activation in astrocytes decrease GFAP expression in hippocampal astrocytes from Alzheimer's Disease mice. (A) Representative fluorescent images (left) showing in green the AAV-infected brain regions (GFP for AAV-GFAP-GFP; FLAG, for AAV-GFAP-DdPAC) and in blue DAPI staining (scale bar 500μm) in WT (top row) and 5xFAD mice (bottom row). Amplified images (right) show GFAP positive astrocytes on the infected region (scale bar 500μm). (B) Quantification of GFAP intensity. Differences were analysed by Two-way ANOVA followed by LSD Fisher test. *p <0.05. WT GFP n=13, WT DdPAC n=14, AD GFP n=6, AD DdPAC n=11.

Then, we analysed GFAP expression in mice expressing DdPAC or GFP in neurons. In this scenario, we observed again overall GFAP increase in 5xFAD mice (Figure 52A), as expected. Two-way ANOVA displayed genotype differences but not stimulation or interaction in animals where DdPAC was expressed in neurons (Genotype: F(1,36)=8.2, p=0.01; Interaction: F(1,36)=0.3, p=0.59; Stimulation: F(1,36)=2.18, p=0.15) (Figure 52B). Therefore, in this case, DdPAC stimulation did not impact GFAP expression. Overall, GFAP expression results indicate that DdPAC-mediated effects have major impact when cAMP modulation happens in astrocytes, but not in neurons. Surprisingly, cAMP modulation in astrocytes reduced overall hippocampal astrogliosis in 5xFAD mice, while no effects were detected in WT mice, suggesting altered cAMP signalling responses in AD.

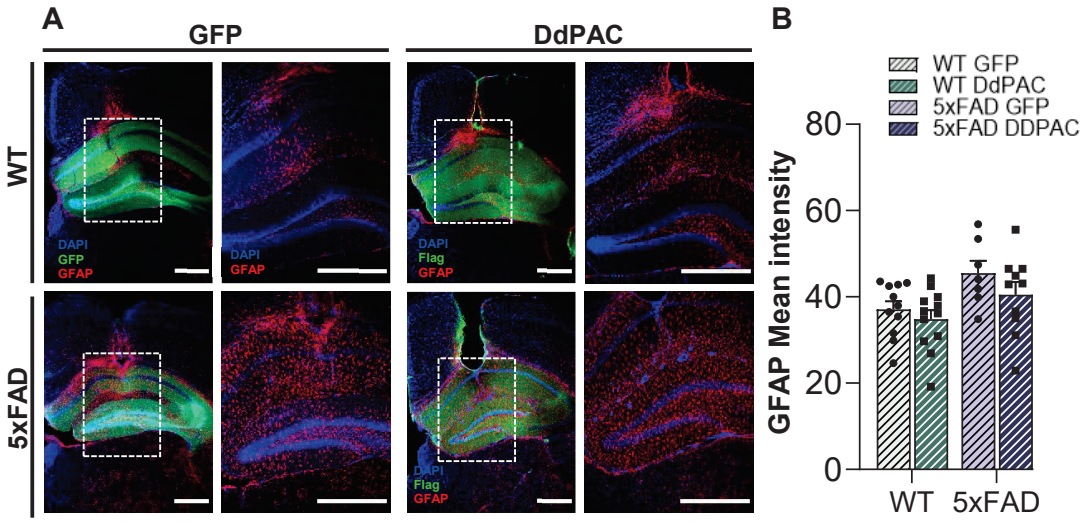

Figure 52. DdPAC activation in neurons do not changes GFAP expression in hippocampal astrocytes from Alzheimer's Disease mice. (A) Representative fluorescent images (left) showing in green the AAV-infected brain regions (GFP for AAV-GFAP-GFP; FLAG, for AAV-GFAP-DdPAC) and in blue DAPI staining (scale bar 500µm) in WT (top row) and 5xFAD mice (bottom row). Amplified images (right) show GFAP positive astrocytes on the infected region (scale bar 500µm). (B) Quantification of GFAP intensity. Differences were analysed by Two-way ANOVA followed by LSD Fisher test. *p <0.05. WT GFP n=15, WT DdPAC n=15, AD GFP n=6, AD DdPAC n=11.

3.2.2 DdPAC-mediated cAMP increase in astrocytes, but not in neurons, specifically reduces Aβ deposits in the hippocampus of 5xFAD mice

Aβ deposits represent another key histopathological hallmark of AD. To evaluate the effects of DdPAC stimulation on Aβ deposits, we analysed the percentage of Aβ plaques and the number of plaques per mm^2 (Cummings & Cotman, 1995; Garcia-Alloza et al., 2006). Significantly, we observed both reduced percentage of Aβ plaques and number of plaques per mm^2 in 5xFAD mice expressing DdPAC in astrocytes, but not in neurons (Figure 55A-B). Unpaired t-test did not show significant differences between 5xFAD GFP and DdPAC mice neither in the immunoreactive area (p=0.98) nor the number of plaques (p=0.47) in the animals where both were expressed in neurons (Figure 55C). Nevertheless, DdPAC expressed in astrocytes from 5xFAD mice was able to reduce both the immunoreactive area (p=0.007) and the number of plaques (p=0.03) (Figure 55D). Overall, these results suggest that cAMP modulation in hippocampal astrocytes using DdPAC could be a novel therapeutic opportunity for AD.

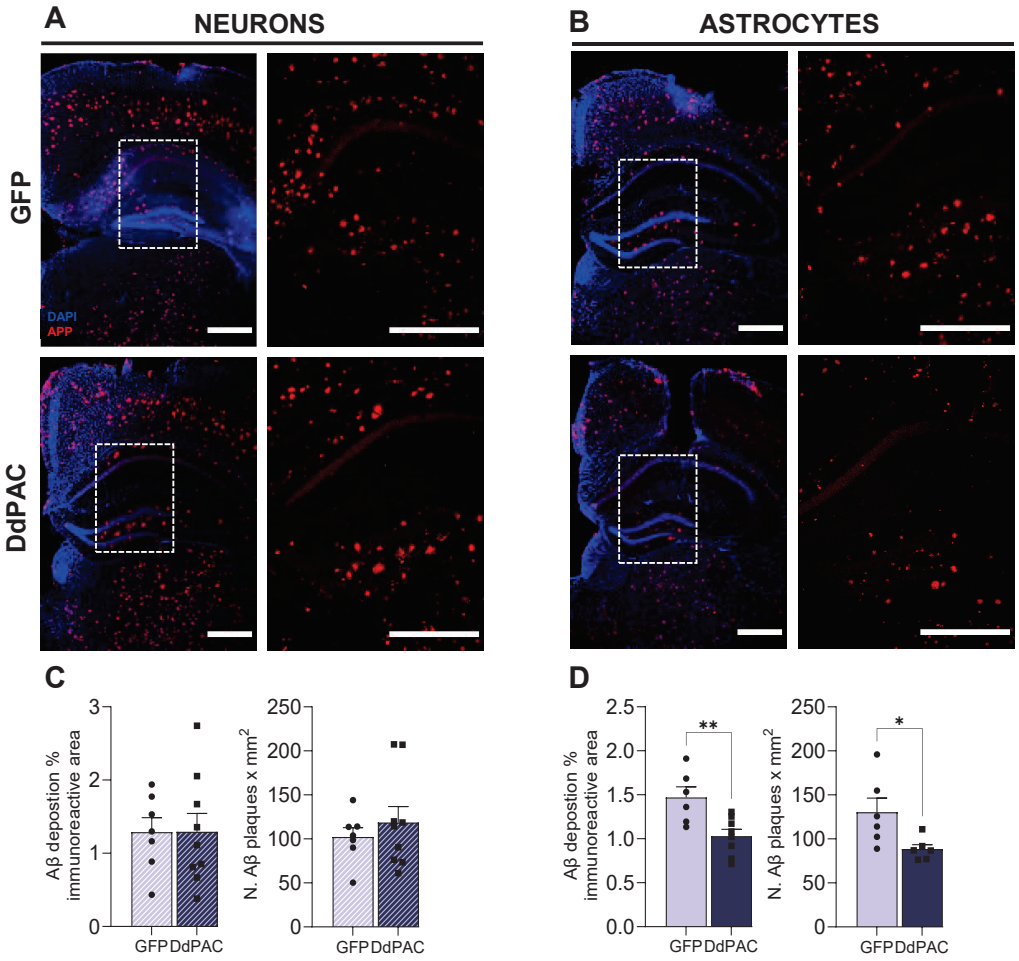

Figure 55. DdPAC activation specifically in astrocytes decrease APP deposits in the hippocampus of Alzheimer's Disease mice. (A) Representative fluorescent images (left) showing in red the Aβ deposits and in blue DAPI staining (scale bar 500μm) in 5xFAD mice expressing GFP (top row) and DdPAC (bottom row) in neurons. Amplified images (right) show Aβ deposits and were used for the quantifications (scale bar 500μm). (B) Representative fluorescent images (left) showing in red the Aβ deposits and in blue DAPI staining (scale bar 500μm) in 5xFAD mice expressing GFP (top row) and DdPAC (bottom row) in astrocytes. Amplified images (right) show Aβ deposits and were used for the quantifications (scale bar 500μm). (C) Quantification of Aβ deposits in 5xFAD mice expressing DdPAC in neurons. (D) Quantification of Aβ deposits in 5xFAD mice expressing DdPAC in neurons. Differences were analysed by Unpaired T-test. *p <0.05. WT GFP n=15, WT DdPAC n=15, AD GFP n=6, AD DdPAC n=11.

3.2.3 DdPAC-mediated cAMP increase in neurons, but not in astrocytes, specifically reduces Iba1-positive microglia in the hippocampus of 5xFAD mice

Considering our findings on Aβ deposits, we investigated the state of microglia, given their crucial role in plaque clearance. Therefore, to further investigate inflammation in the hippocampus, we quantified Iba1 intensity in the CA1 and DG regions, both of which are known to be affected in AD (Nairuz et al., 2024). We first analysed Iba1 intensity in the

hippocampus of DdPAC-activated astrocytes from 5xFAD and WT mice (Figure 53). Broadly, we observed that while no main changes were detected in the CA1, a slight increase was noted in the DG of DdPAC stimulated animals. Indeed, Two-way ANOVA with genotype and stimulation as factors revealed stimulation effects in the DG (Genotype: $F(1,40)=3.64$, $p=0.06$; Interaction: $F(1,40)=0.60$, $p=0.44$; Stimulation: $F(1,40)=4.35$, $p=0.04$), but no effects in the CA1 region (Genotype: $F(1,40)=2.8$, $p=0.10$; Interaction: $F(1,40)=2.35$, $p=0.13$; Stimulation: $F(1,40)=2.8$, $p=0.35$). Furthermore, Bonferroni Post-hoc reported significant changes between WT GFP and 5xFAD DdPAC mice in the DG but not with any of the other groups. Further analysis in the morphology of the microglia might help to further confirm how microglia is modulated by DdPAC.

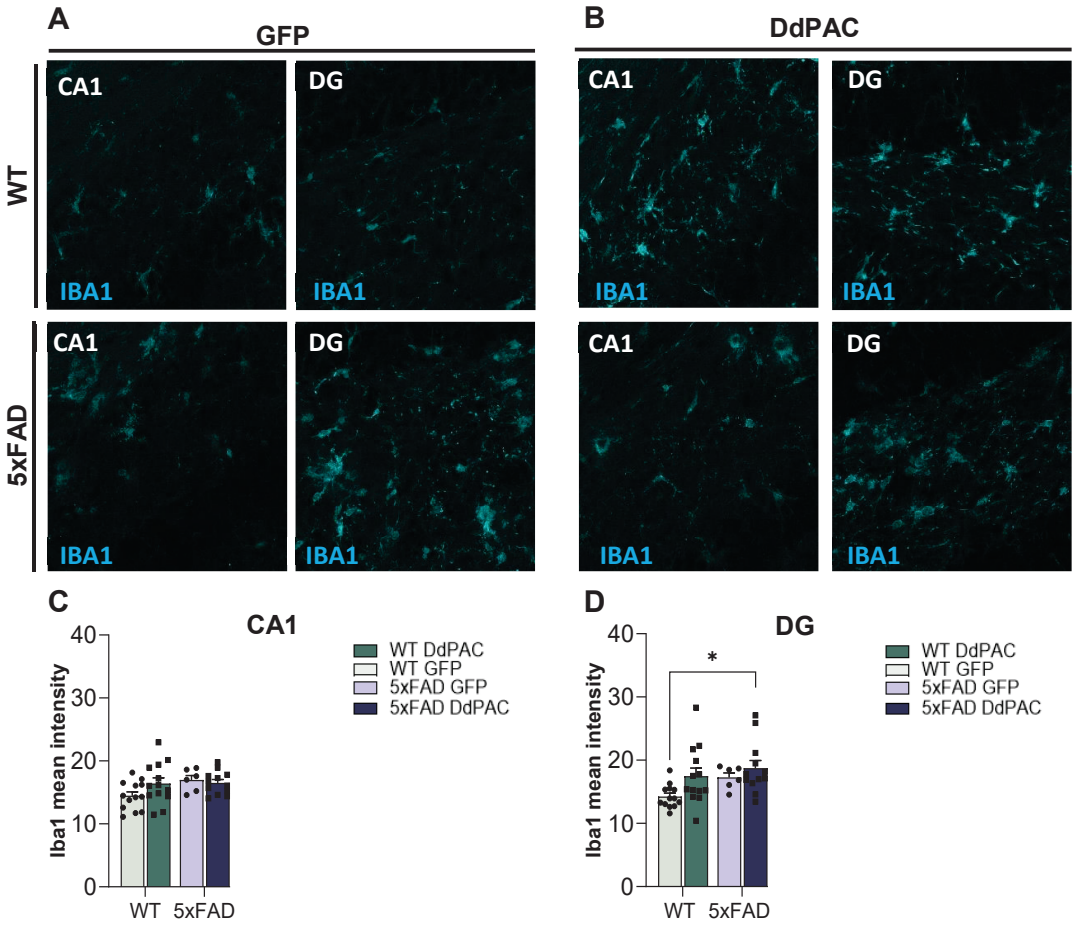

Figure 53. DdPAC activation in astrocytes modulates microglia in the DG. (A) Representative fluorescent images (left) showing Iba1 expression (light blue) in the CA1 (left) and DG (right) regions from WT (top) and 5xFAD (bottom) mice expressing GFP. (B) Representative fluorescent images (left) showing Iba1 expression (light blue) in the CA1 (left) and DG (right) regions from WT (top) and 5xFAD (bottom) mice expressing DdPAC. (C) Quantification of Iba1 intensity in the CA1 region. (D) Quantification of Iba1 intensity in the DG region. Differences were analysed by Two-way ANOVA followed by Bonferroni Post-hoc test. *p <0.05. WT GFP n=13, WT DdPAC n=13, AD GFP n=6, AD DdPAC n=11.

Subsequently, we analysed Iba1 intensity in the hippocampus of DdPAC-activated neurons from 5xFAD and WT mice. Conversely to our results in DdPAC-activated astrocytes, we observed a general decrease in Iba1 intensity, especially in the CA1 of 5xFAD mice. Two-

way ANOVA reported both genotype and stimulation effects in the CA1 region (Genotype: F(1,36)=13.86, p=0.0005; Interaction: F(1, 36)=2.08, p=0.16; Stimulation: F(1, 36)=1.36, p=0.0005), whereas no main effects were observed in the DG (Genotype: F(1,38)=1.28, p=0.26; Interaction: F(1, 38)=0.11, p=0.75; Stimulation: F(1, 38)=2.73, p=0.10). Specifically in the CA1, Bonferroni Post-hoc displayed significant changes between WT GFP and 5xFAD GFP (p=0.007), 5xFAD GFP and WT DdPAC (p=<0.0001), and 5xFAD GFP and 5xFAD DdPAC (p=0.01). This data indicates that while DdPAC activation in astrocytes seems to activate microglia, its stimulation in neurons drives the contrary effect, suggesting that the modulated cell type should be carefully considered when choosing a therapeutic approach.

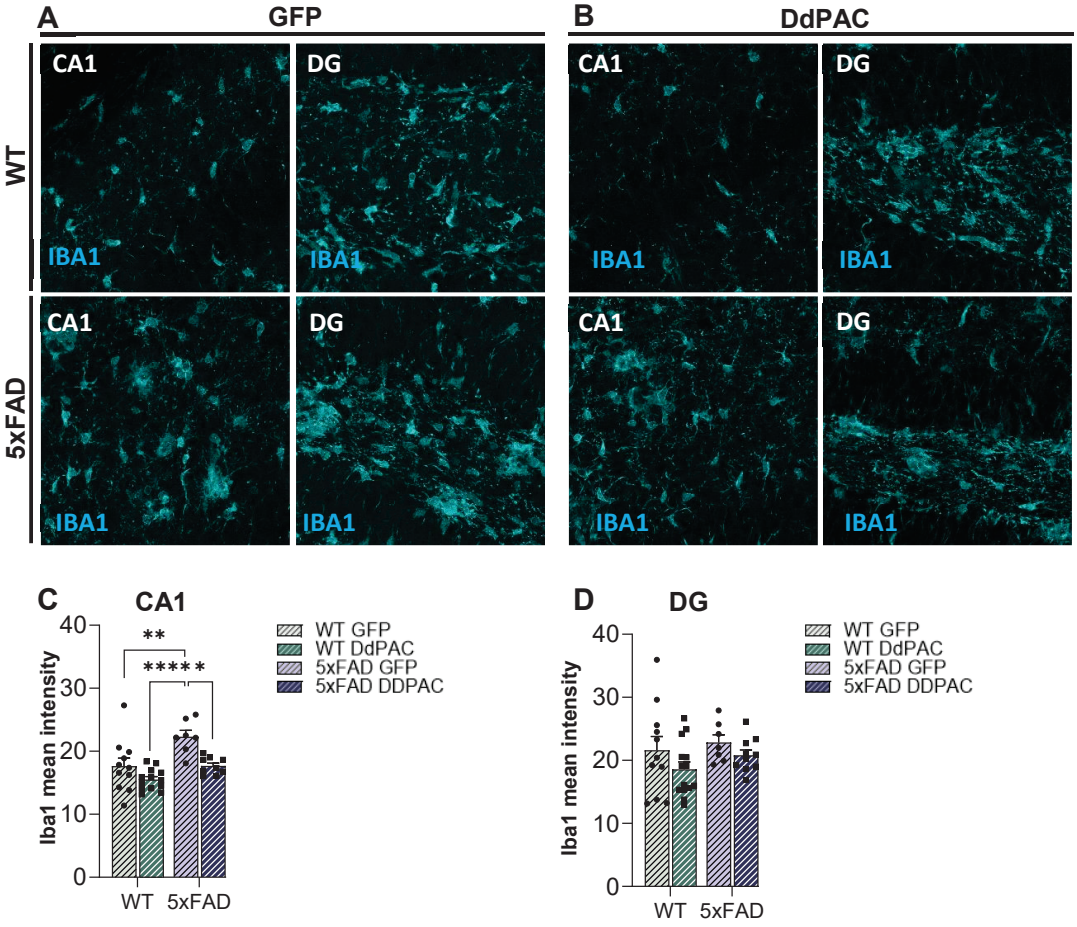

Figure 54. DdPAC activation in neurons decrease microglial activation in the CA1 region from Alzheimer's Disease mice. (A) Representative fluorescent images (left) showing Iba1 expression (light blue) in the CA1 (left) and DG (right) regions from WT (top) and 5xFAD (bottom) mice expressing GFP. (B) Representative fluorescent images (left) showing Iba1 expression (light blue) in the CA1 (left) and DG (right) regions from WT (top) and 5xFAD (bottom) mice expressing DdPAC. (C) Quantification of Iba1 intensity in the CA1 region. (D) Quantification of Iba1 intensity in the DG region. Differences were analysed by Two-way ANOVA followed by Bonferroni Post-hoc test. *p <0.05. WT GFP n=13, WT DdPAC n=13, AD GFP n=6, AD DdPAC n=11.

3.2.4 Proteomic analysis uncovers cell-type and AD-specific DdPAC activation effects

Proteomic analysis of DdPAC-induced changes in hippocampal neurons and astrocytes in WT and 5xFAD mice may provide insight into the molecular mechanisms underlying glial and Aβ deposits changes that we observed in the histological analyses. DG tissue from the hippocampus of WT and 5xFAD mice injected with either DdPAC or GFP as control was collected 24 hours after stimulation to assess changes in the proteome. In samples from mice expressing GFP or DdPAC in astrocytes, 5651 proteins were detected, compared to 4494 in samples from mice expressing GFP or DdPAC in neurons.

In samples where DdPAC was expressed in astrocytes, the Partial Least Squares Discriminant Analysis (PLS-DA) model generated provided 4 as the optimal number of clusters, highlighting clear differences between the 4 proteomic profiles, corresponding to our experimental groups: WT GFP, WT DdPAC, 5xFAD DdPAC and 5xFAD GFP, and as evidenced in the sample plots that include 95% confidence elipses (Figure 56A). To estimate the risk of overfitting and evaluate the performance of the generated model, we calculated the optimal number of PLS-DA components, the BER, and the AUC scores, which estimate the specificity and sensitivity of the model. The analysis reached 4 as the optimal number of components, with a BER of 11.16% and an AUC of 96.65%. The accuracy of the whole model was validated through a permutation system with 1,000 iterations, which provided a $p < 0.001$ as the probability that the model occurs by chance. In detail, 5xFAD GFP and 5xFAD DdPAC groups are clustered closely but separate from the WT groups, indicating a distinct proteomic profile in 5xFAD mice. Moreover, DdPAC shift the proteomic profile in both WT and 5xFAD mice, but the extent of the shift depends on the component analysed (Figure 56A). We then estimated the contribution of every protein to the differences found in our PLS-DA model by calculating their VIP scores. We found 363 proteins with VIP scores ≥ 1.4 that were considered significant. A final unsupervised clustering analysis with the standardised values of these 363 proteins split WT and 5xFAD samples. It also segregated DdPAC and GFP samples from the 5xFAD group but not from WT. The column dendogram (Figure 56B) further confirms the separation between groups. Moreover, the dendrogram indicate that WT DdPAC resembles more to 5xFAD GFP than to WT GFP, as they do not fully segregate, suggesting that activating DdPAC is triggering molecular pathways that are affected in 5xFAD pathology.

In samples where DdPAC was expressed in neurons, the PLS-DA highlighted clear differences between 2 proteomic profiles, WT vs 5xFAD, but not between treatment, GFP vs DdPAC, as evidenced in the sample plots that include 95% confidence elipses (Figure 56C). The model performance analysis reached 7 as the optimal number of components, with a BER of 19.05% and an AUC of 94.83%. The accuracy of the whole model was validated through a permutation system with 1,000 iterations, which provided a $p < 0.001$ as the probability that the model occurs by chance. Thus, the model denotes significant differences in the protein concentration between all four experimental groups. In detail,

5xFAD groups are clustered closely but separate from the WT groups, indicating a clear distinct proteomic profile in 5xFAD mice. However, DdPAC do not shift significantly the proteomic profile in WT and 5xFAD mice, especially for component 2 (Figure 56C). We then estimated the contribution of every protein to the differences found in our PLS-DA model by calculating their VIP scores. We found 171 proteins with VIP scores ≥ 1.4 that were significant. A final unsupervised clustering analysis with the standarised values of these 171 proteins split WT and 5xFAD samples. It also segregated DdPAC and GFP samples in the 5xFAD group, but not from WT. Therefore, the column dendrogram (Figure 56D) further confirms the separation between genotypes but not stimulation.

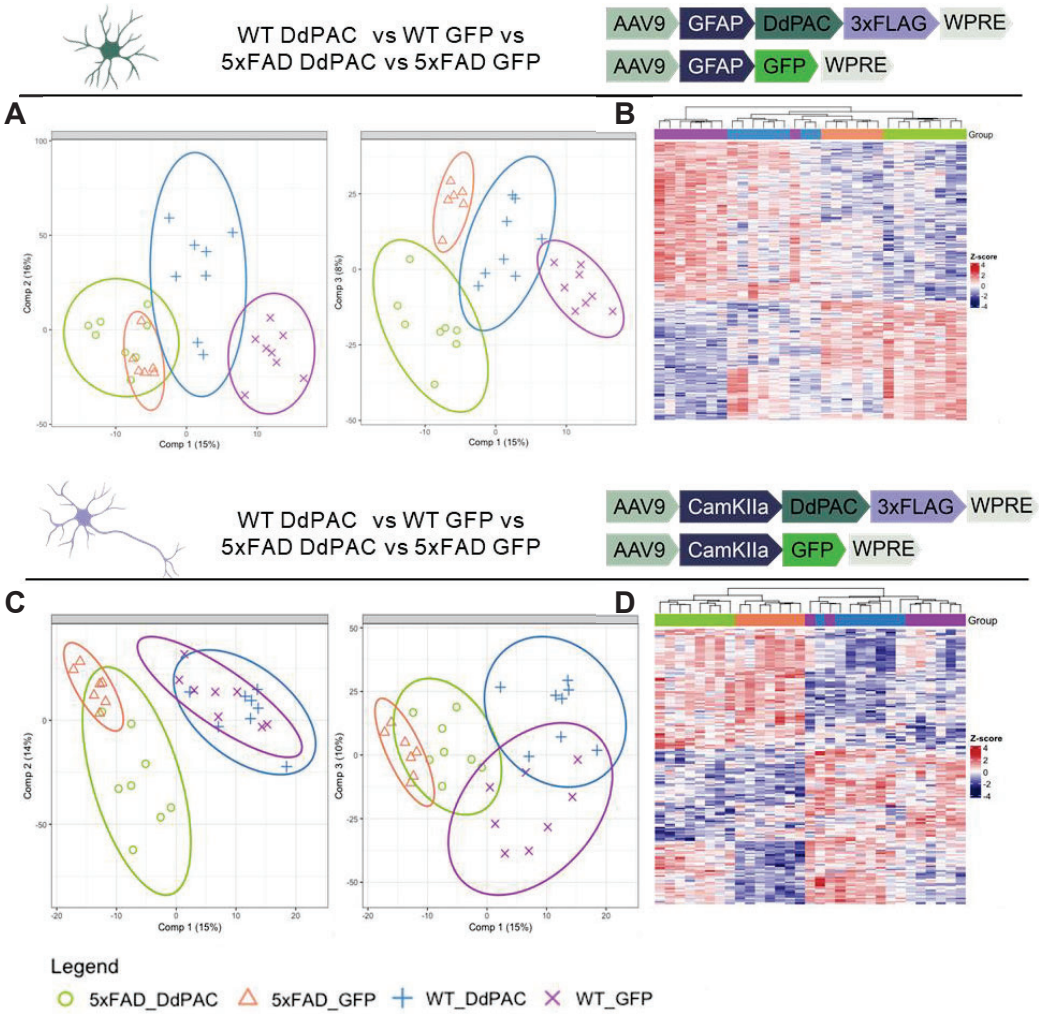

Figure 56. DdPAC activation in neurons or astrocytes triggers differential effects in WT and 5xFAD mice at proteome level. Proteome dataset in astrocytes: (A) PLS-DA model with components 1 (15%) and 2 (16%) on the left, and components 1 (15%) and 3 (8%), on the right. (B) Column dendrogram representing the proteins with VIP scores ≥ 1.4. Proteome dataset in neurons: (C) PLS-DA model with components 1 (15%) and 2 (14%) on the left, and components 1 (15%) and 3 (10%), on the right. (D) Column dendrogram representing the proteins with VIP scores ≥ 1.4.

3.2.4.1 DdPAC activation in astrocytes expands the proteome towards cytoskeletal regulation and immune response, while neuronal activation primarily influences synaptic plasticity in WT mice

In order to know how DdPAC-mediated cAMP increase impacts on neurons or astrocytes in physiological conditions, we first analysed the impact of DdPAC activation in WT mice (WT DdPAC vs WT GFP comparison). We observed that the number of differential proteins is considerably higher when DdPAC is activated in astrocytes compared to when it is activated in neurons in WT mice (Differential $proteins_{DdPACastrocytes}$=488; Differential $proteins_{DdPACneurons}$=168).

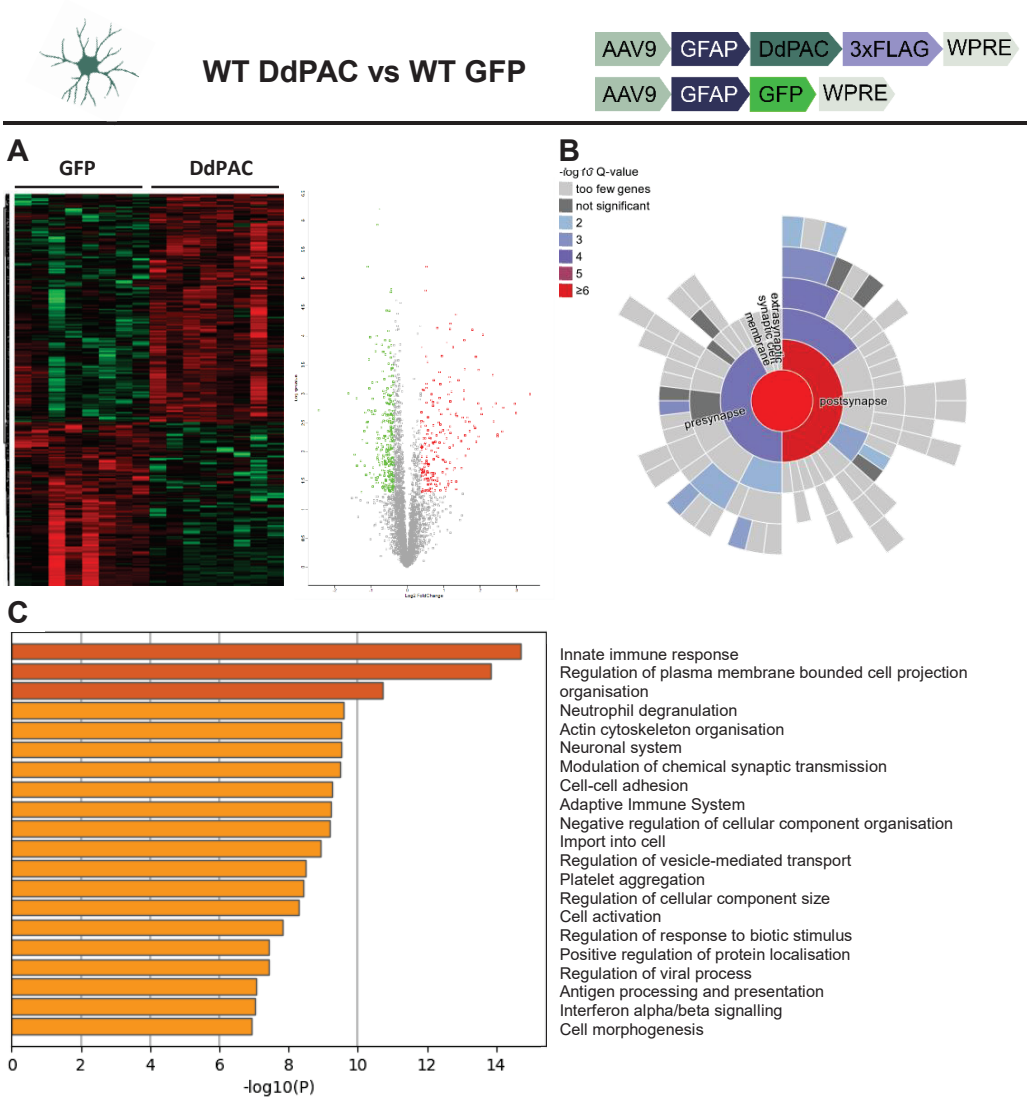

Figure 57. DdPAC activation in astrocytes from WT mice primarily impacts on plasticity and immune response. (A) Differential proteome heatmap and volcano plot. (B) Main subcellular localisation of the proteins related to the synapse (C) Top 20 main proteome gene ontologies

To further investigate the consequences of cAMP modulation in each cell type, we first specifically compared the proteomes of WT DdPAC and WT GFP in astrocytes (Figure 57). Astrocytic proteome heatmap revealed a clear separation between hippocampal GFP-injected and DdPAC-injected, red-light stimulated mice. Furthermore, the volcano plot displayed and confirmed differential protein expression between groups (Figure 57A). Based on the plasticity modulation observed through DdPAC activation in our previous results, we specifically analysed synaptic ontologies (Figure 57B). Synaptic ontology analysis revealed a strong enrichment of proteins localised in the synaptic cleft and post-synapse, with additional representation in the pre-synapse. This suggests that astrocytic cAMP signalling may broadly influence synaptic architecture and function. Lastly, we aimed to study the characterised ontologies based on our proteome dataset (Figure 57C). Gene ontology analysis of the proteomic profile identified the top 20 enriched biological processes, including immune regulation, cytoskeletal organization, and synaptic function. These involved processes related to the innate and adaptive immune response (neutrophil degranulation, antigen processing and presentation, interferon alpha/beta signalling), cellular structure and transport (actin cytoskeleton organization, regulation of vesicle-mediated transport, regulation of cellular component size), and synaptic modulation (modulation of chemical synaptic transmission, neuronal system, cell-cell adhesion). These results imply that DdPAC-mediated cAMP modulation in astrocytes from the hippocampus has a main impact in immune and synaptic function, strongly influencing the whole tissue protein profile.

We then aimed to study the effects of DdPAC-mediated cAMP modulation in neurons from the hippocampus of WT mice (Figure 58). Once again, a clear distinction was observed between the hippocampal GFP-injected and DdPAC-injected groups in the neuronal proteome heatmap. Moreover, the volcano plot revealed and validated differential protein expression between the groups (Figure 58A). Synaptic ontology analysis following neuronal DdPAC stimulation revealed that the main identified proteins were localised in the synaptic cleft and post-synapse compartments, with undetectable representation in the presynaptic compartment (Figure 58B). This indicates that neuronal cAMP modulation via DdPAC primarily influences postsynaptic and extracellular synaptic processes rather than presynaptic mechanisms. Finally, the top 20 gene ontology analyses highlighted significant enrichment in pathways related to synaptic function, intracellular signalling, and cellular organization (Figure 58C). Notably, we observed enrichment in processes associated with synaptic transmission (modulation of chemical synaptic transmission, regulation of postsynaptic neurotransmitter receptor internalization, and neuroinflammation and glutamatergic signalling) and neuronal structure and development (neuron projection development, axon guidance, and telencephalon development). Additionally, enrichment in intracellular regulatory processes (endomembrane system organization, vesicle-mediated transport, and intracellular chemical homeostasis) suggests broader modulation of cellular dynamics. These results suggest that DdPAC-mediated cAMP modulation in neurons from the hippocampus have a key role in synaptic plasticity.

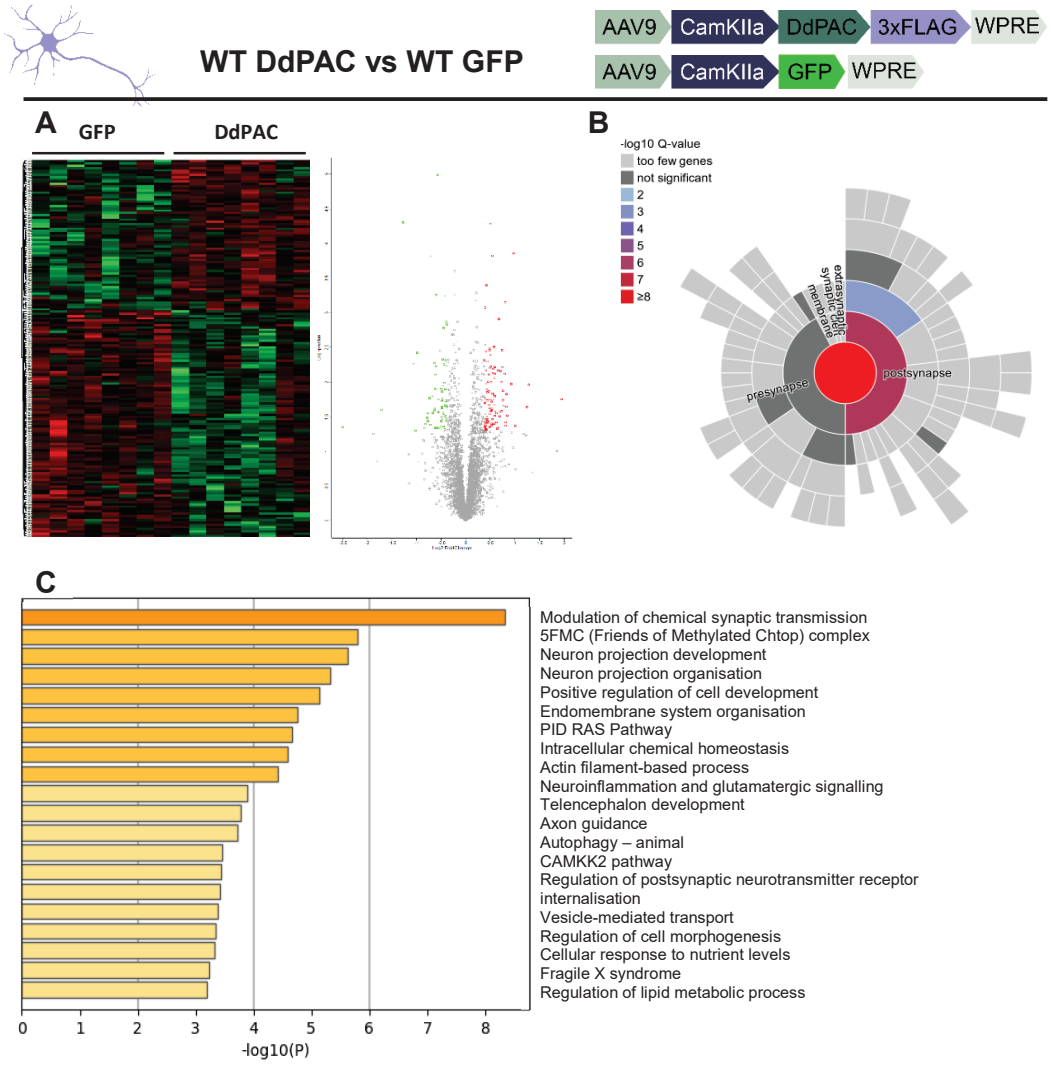

Figure 58. DdPAC activation in neurons from WT mice has a main impact on synaptic plasticity. (A) Differential proteome heatmap and volcano plot. (B) Main subcellular localisation of the proteins related to the synapse (C) Top 20 main proteome gene ontologies

3.2.4.2 Proteomic analysis reveals strong immune response regulation by DdPAC activated astrocytes in 5xFAD mice

In order to investigate how DdPAC-mediated cAMP increase was impacting neurons and astrocytes from AD, we checked the number of differential proteins for neuronal or astrocytic proteome when comparing 5xFAD DdPAC and 5xFAD GFP mice. In contrast to our previous observations in WT mice, a higher number of differential proteins was detected in neuronal DdPAC-activated samples compared to the astrocytic ones (Differential $proteins_{DdPACastrocytes}$=268; Differential $proteins_{DdPACneurons}$=532).

To further investigate the effects of DdPAC in AD, we first compared the proteomes of astrocytes from 5xFAD DdPAC and 5xFAD GFP mice (Figure 59). The heatmap of the astrocytic proteome clearly distinguished between the hippocampi of GFP-injected and DdPAC-injected, red-light stimulated 5xFAD mice. Additionally, the volcano plot

highlighted and validated the differential protein expression between the groups (Figure 59A). We then analysed the synaptic ontologies (Figure 59B). Consistent with our findings in wild-type mice, the synaptic ontology analysis of astrocytic DdPAC activation showed a significant enrichment of proteins localised in the synaptic cleft and post-synapse, along with some presence in the pre-synapse. The top 20 gene ontology analyses revealed significant enrichment in pathways associated with immune response, cellular signalling, and cytoskeletal organization (Figure 59C). Notably, we observed enrichment in processes related to immune activation and response (innate immune response, cytokine signalling, and antigen processing and presentation). Furthermore, pathways associated with cell adhesion (leukocyte cell-cell adhesion) and inflammation (inflammatory response, immune effector process) were prominently enriched, confirming the strong immune-related response. In addition, the enrichment of processes related to actin cytoskeleton organization and proteasome degradation suggests extensive cellular reorganization and protein regulation.

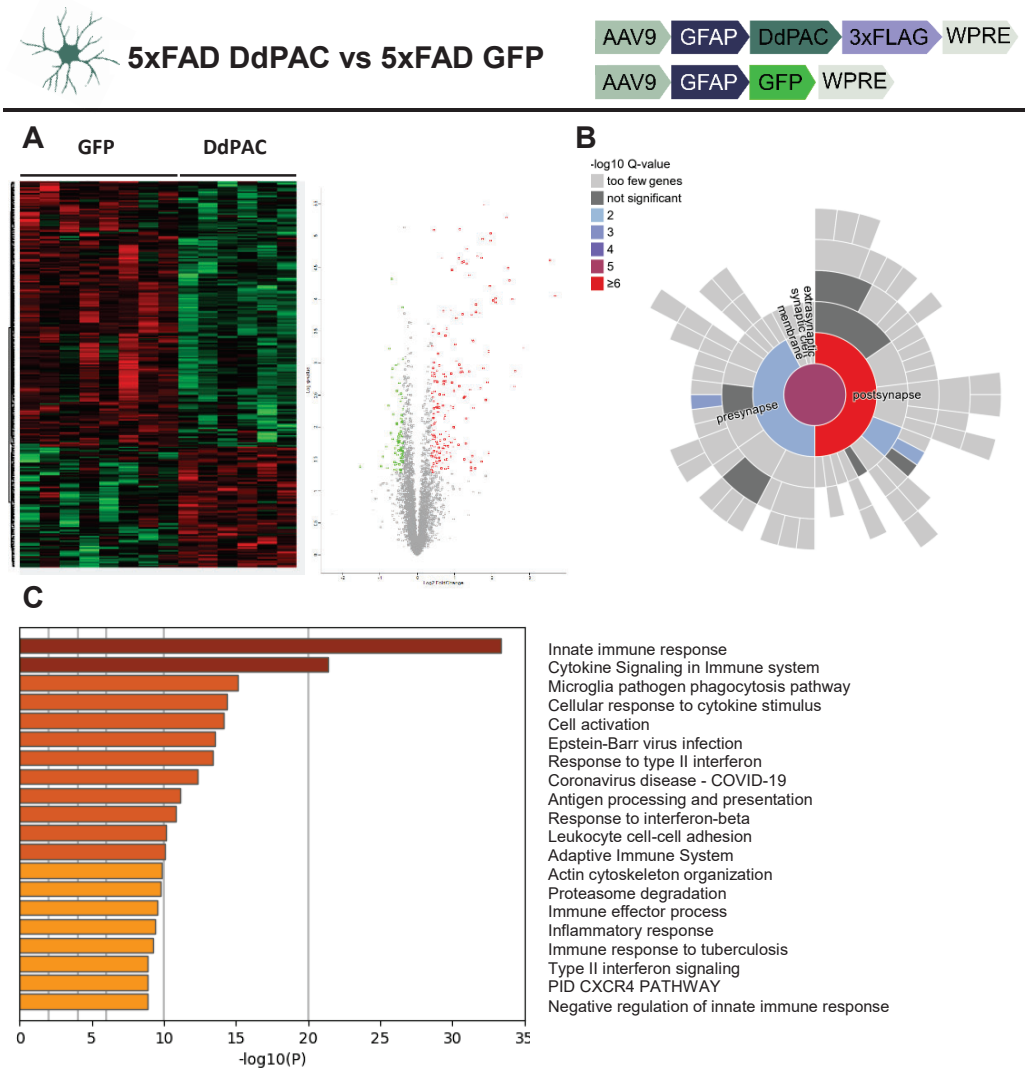

Figure 59. DdPAC activation in astrocytes from 5xFAD mice mainly modulates immune response (A) Differential proteome heatmap and volcano plot. (B) Main subcellular localisation of the proteins related to the synapse (C) Top 20 main proteome gene ontologies.

These findings suggest that DdPAC-mediated cAMP modulation in astrocytes plays a critical role in regulating both immune and structural responses, potentially contributing to the modulation of neuroinflammation and cellular dynamics in neurodegenerative disease contexts.

We next sought to investigate the impact of DdPAC-mediated cAMP modulation in hippocampal neurons of 5xFAD mice by comparing the proteome dataset of 5xFAD DdPAC vs 5xFAD GFP mice (Figure 60). Again, the heatmap of the astrocytic proteome clearly distinguished between the hippocampi of GFP-injected and DdPAC-injected, red-light stimulated 5xFAD mice. Additionally, the volcano plot highlighted and validated the differential protein expression between the groups (Figure 60A).

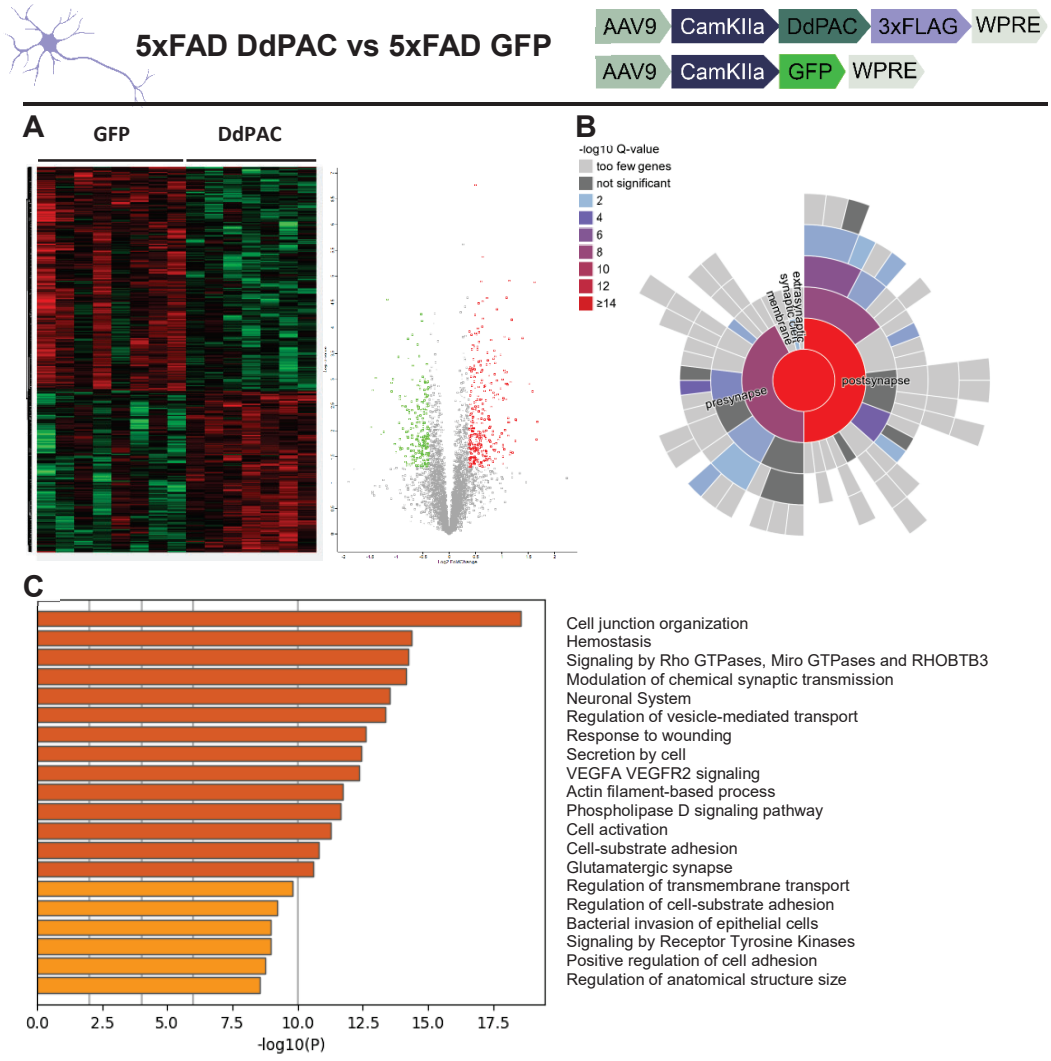

Figure 60. DdPAC activation in neurons from 5xFAD mice mainly modulates cellular organisation and synaptic function. (A) Differential proteome heatmap and volcano plot. (B) Main subcellular localisation of the proteins related to the synapse (C) Top 20 main proteome gene ontologies.

Unlike WT DdPAC-stimulated mice, synaptic ontologies in 5xFAD DdPAC mice exhibited a pronounced enrichment of proteins localised not only in the synaptic cleft and post-synapse, but also in the pre-synapse (Figure 60B). Finally, the top 20 gene ontology analyses revealed significant enrichment in pathways associated with cellular organization, signalling, and synaptic function (Figure 60C). Notably, we observed a strong enrichment in processes related to cell junction organization, cell-substrate adhesion, and hemostasis, highlighting the importance of cellular structure and adhesion in response to DdPAC-mediated cAMP modulation. Additionally, pathways associated with neuronal signalling (modulation of chemical synaptic transmission and glutamatergic synapse regulation) were enriched, suggesting enhanced synaptic activity. Enrichment in vesicle-mediated transport and phospholipase D signaling pathway indicates dynamic intracellular processes involved in secretion and signalling. Furthermore, pathways related to cell activation (Rho and Miro GTPases, as well as receptor tyrosine kinase signaling), suggest that DdPAC activation modulates cellular responses to external stimuli. These findings point to a complex interplay between cell adhesion, intracellular signalling, and synaptic modulation, with potential implications for neuronal plasticity in neurodegenerative disease contexts.

3.2.4.3 PKA interactome mainly reveals cytoskeleton regulation

Since DdPAC modulates cAMP, we also aimed to explore the cAMP pathway in the whole tissue. Thus, we analysed the PKA interactome from neurons and astrocytes in WT and 5xFAD mice. We observed that when there was a DdPAC-mediated cAMP increase in astrocytes, the PKA interactome involved 17 proteins (PRKACA=12; PRKACB=4; PRKACG=1), whereas when the increase was in neurons, the interactome reduced to 5 proteins (PRKACA=4; PRKACB=1). Therefore, it seems that DdPAC activation in astrocytes has a greater impact on the cAMP pathway, although the specific cell types expressing these proteins are unknown. Still, this aligns with the fact that astrocytic modulation has a greater impact on the whole tissue proteome than neuronal modulation, and suggests that astrocytes may play a major role in regulating cAMP-PKA signalling at the whole-tissue level. PRKACA (PKA catalytic subunit α) is the most abundant subunit in the brain (Cadd & McKnight, 1989; London et al., 2019), supporting the idea that more proteins belong to its interactome in both neurons and astrocytes. Specifically, the proteins associated with the PRKACA interactome in neurons are: MAVS, CAMKK2, VTN and XPO5. In astrocytes, PRKACA interactome is: CDK17, FYN, PKIA, CALR, CAPZB, DOCK1, GSTM2, NXF1, OCIAD1, TRIM21, UGDH and VIM. In neurons, CAMKK2, which is a kinase that participates in calcium-mediated signalling, and VTN, involved in extracellular matrix interactions (Furutani et al., 2012; J. Lisman et al., 2002; Oishi et al., 2021; Ruzha et al., 2022; Tokumitsu & Sakagami, 2022), may reflect a role for PRKACA in synaptic plasticity and neuronal network stability. The presence of XPO5, a protein implicated in RNA export,

hints at a contribution of PRKACA to the regulation of gene expression and post-transcriptional control in the brain(Bohnsack et al., 2004; J. Wang et al., 2020). In astrocytes, the PRKACA interactome is more complex and diverse, with proteins such as CDK17, FYN, and PKIA, which are involved in cell cycle regulation, intracellular signalling, and phosphorylation events related to plasticity(de Lecea et al., 1998; Hirose et al., 1997; Y. D. Saito et al., 2010). The presence of CALR and CAPZB, which are proteins related to calcium homeostasis and actin filament dynamics (Mukherjee et al., 2016; Venkatesan et al., 2021), suggests that PRKACA signalling in astrocytes may influence both structural and functional plasticity within the glial network. Proteins like DOCK1 and NXF1, which are involved in cytoskeletal remodelling and nucleocytoplasmic transport (Koubek & Santy, 2022; Y. Li et al., 2016), further indicate that PRKACA may modulate astrocytic responses to cellular stress and environmental changes. The presence of VIM in astrocytes highlights the potential role of PRKACA in regulating glial activation and cytoskeletal dynamics (K.-Z. Chen et al., 2023), which are crucial for supporting neuronal function and maintaining the blood-brain barrier integrity. Therefore, these results suggest that neuronal PKA interactors are specialised, focusing on calcium signalling, RNA transport, and plasticity, whereas astrocytic PKA interactors affect metabolism, cytoskeleton, immune function, and oxidative stress.

Then, we explored the PKA interactome in 5xFAD DdPAC vs 5xFAD GFP, red-light stimulated mice. Conversely to what we observed in WT mice, the PKA interactome from neuronal stimulated 5xFAD mice involved 28 proteins (PRKACA=16; PRKACB=8; PRKACG=4), whereas the astrocytic stimulated 5xFAD mice interactome was reduced to 12 proteins (PRKACA=9; PRKACB=3; PRKACG=0). Consequently, it seems that DdPAC activation in neurons has a greater impact on cAMP pathway in AD. Due to the higher abundance of PRKACA in the brain, we specifically focused on its interactome. Specifically, the proteins belonging to the PRKACA interactome in neurons are: AKAP7, AKAP9, RYR2, FGG, SNAP23, AKAP12, CAPZB, CREB1, FERMT2, FOXO1, HSPD1, IMMT, IQGAP1, MARCKSL1, PDZD8 and PIK3R2. In astrocytes, PRKACA interactome is: MAVS, SNAP23, EMD, GNA13, RAC1, RHOA, TOR1AIP1, TRIM21 and VIM. In neurons, the PRKACA interactome is enriched with proteins involved in critical cellular processes such as synaptic plasticity, cellular signalling, and mitochondrial function. For example, proteins like AKAP7 and AKAP9 are known to scaffold PKA signalling complexes, facilitating the spatial and temporal regulation of cAMP-dependent processes (Wild & Dell'Acqua, 2018). RYR2 and CREB1 are associated with calcium signalling and gene expression regulation, respectively, both of which are pivotal in neuronal function and plasticity (Glazewski et al., 1999; Hiess et al., 2022). Furthermore, proteins like FOXO1 and IQGAP1, which are involved in cellular stress response and cytoskeletal organization (D. Cao et al., 2015; Wątroba et al., 2012), may highlight an adaptive or maladaptive response in neurons under pathological conditions. In contrast, the PRKACA interactome in astrocytes presents a more restricted set of interactions, with proteins such as MAVS, which are linked to immune and inflammatory pathways (Sun et al., 2006). The presence of RHOA and RAC1, both key regulators of the actin cytoskeleton (Corbetta et al., 2009; Dupraz et al., 2019),

suggests that PRKACA signalling in astrocytes could play a role in glial cell morphology and neuroinflammation. The involvement of VIM, a protein typically associated with glial activation, further supports the hypothesis that astrocytic PRKACA signalling may be modulating glial responses to neurodegenerative stress in AD (K.-Z. Chen et al., 2023). These findings underscore the cell-type-specific nature of cAMP signalling and suggest that DdPAC activation may differentially affect neuronal and astrocytic functions, potentially offering insights into targeted therapeutic strategies for AD.

In our proteomics analysis, we identified 22 differentially expressed proteins related to the PKA interacting network in the different conditions of the DdPAC-stimulated astrocyte experimental set (WT-DdPAC, 5xFAD-DdPAC and their controls) (Figure 61). The most enriched biological processes and KEEG pathways were predicted using the fold enrichment tool of the STRING database and visualized as an interaction network using Cytospace. These pathways were functionally related to neural cell morphogenesis processes, such as cytoskeleton arrangement and axon guidance. Eight of the proteins in the network showed a DdPAC-induced concentration increase in 5xFAD samples compared to controls, according to the differential expression analysis. In contrast, in WT samples, the treatment either had no significant effect or led to a decreased concentration of most proteins in the network.

In the DdPAC-stimulated neuron experimental set, we identified 24 differentially expressed proteins related to the PKA interacting network. In this case, the KEGG pathways were functionally related to the actin cytoskeleton and processes regulation and the AMPK signaling pathway. In 5xFAD samples, eleven proteins in the network showed a DdPAC-induced concentration decrease, while eight proteins exhibited a DdPAC-induced decrease compared to controls. In contrast, in WT samples, the treatment had no significant effect on the expression of most proteins in the network.

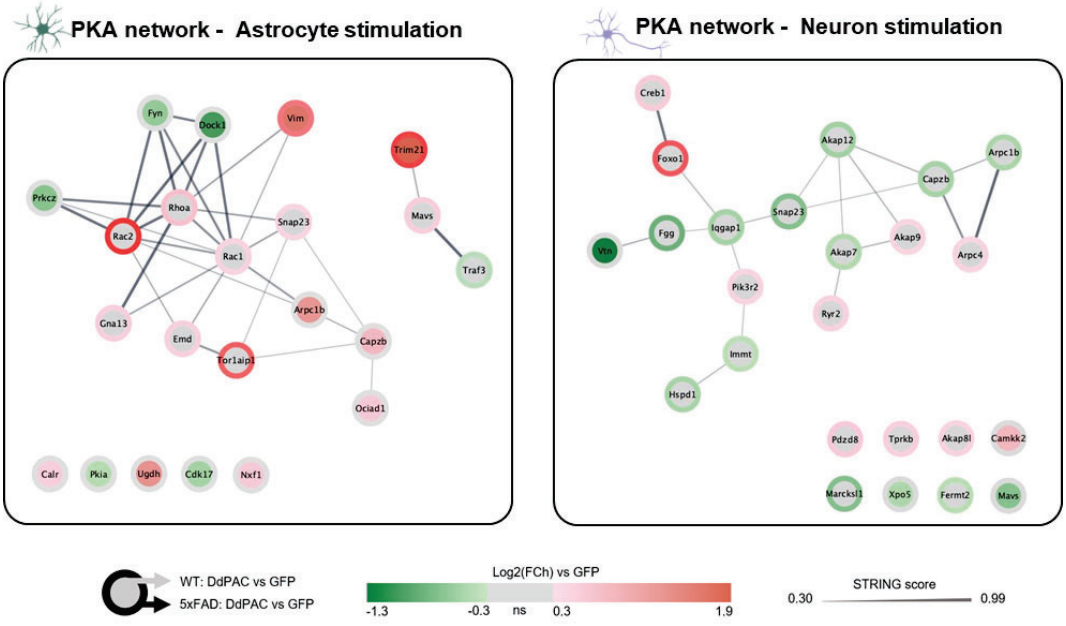

Figure 61. Network analysis of the PKA-related proteins modulated by the DdPAC stimulation. Cytospace network models showing protein-protein interactions of the 22 and 24 proteins in the PKA network in the different conditions (WT-DdPAC, 5xFAD-DdPAC and their controls) of the DdPAC-stimulated astrocytes or neurons, respectively. The color bar represents the log2 fold change protein ratios from the differential expression analysis. Node color represents an increase (red), decrease (green), or non-significant change (gray) in DdPAC-stimulated vs GFP-stimulated samples. Edges show interactions from the STRING database.

Notably, the main related function of the proteins involved in the astrocytic and neuronal PKA networks (Figure 61), is cytoskeleton regulation. However, most of the proteins involved in each network are different, highlighting the differential effect DdPAC-mediated cAMP modulation in neurons and astrocytes.

Overall, our proteomic analyses reveal that cAMP signalling exerts distinct functions in neurons and astrocytes, which may further diverge under pathological conditions such as Alzheimer's Disease. These findings highlight the need to investigate cAMP-mediated responses in disease contexts to guide the design of more effective therapeutic interventions.

DISCUSSION

Neurodegenerative disorders represent a growing challenge in modern society. With the aged population increasing, the incidence of these diseases is expected to rise significantly, creating a growing social and economic burden that may become unsustainable if the current trend persists. For instance, the number of people living with Alzheimer's Disease is expected to nearly triple by 2050 (Brodaty et al., 2011), a striking number considering that this disease, like most other neurodegenerative disorders, currently has no cure or effective treatment.

Huntington's and Alzheimer's Disease are the two neurodegenerative disorders central to this study. Both are primarily characterised by the accumulation of aberrant proteins – huntingtin in HD and amyloid plaques and neurofibrillary tangles in AD – which ultimately lead to cell death (Glenner & Wong, 1984; Huntington, 2003). Crucially, a key feature and a consequence of the protein accumulation is the impairment or dysfunction of synapses (Cepeda & Levine, 2022; Selkoe, 2002). Additionally, synapse dysfunction can impair specific neuronal populations, molecular pathways, and both local and large-scale networks, all of which contribute to functional deficits prior to cell death or even in the absence of it (Palop et al., 2006). Hence, therapies aimed at enhancing synaptic plasticity could offer a ground-breaking solution for these devastating diseases, addressing both the underlying molecular disruptions and the resulting functional impairments. Furthermore, a better understanding of the early-stage impairments associated with these diseases could help identifying the optimal timepoint for initiating potential therapies.

In this regard, cAMP is a second messenger involved in numerous cellular processes throughout the body but plays a particularly significant role within the brain (C. C. Huang & Hsu, 2006). The cAMP-PKA pathway is well-established as a key mechanism initiating gene transcription during NMDAR-dependent long-term potentiation in neurons (Nguyen & Kandel, 1997). Building on this evidence, along with the documented disruptions in cAMP signalling in neurodegenerative disorders (Kelly, 2018; Xiang et al., 2024), we focused on modulating cAMP as a potential strategy to enhance synaptic plasticity and mitigate the pathological hallmarks of these diseases.

Along these lines, photoactivated adenylyl cyclases (PAC) are enzymes capable of increasing cAMP levels in response to light stimulation, achieved through the activation of an AC domain coupled to a photoreceptor module (Iseki & Park, 2021). In particular, DdPAC is a recently developed and optimised PAC that modulates cAMP levels in response to red light stimulation. Originally engineered in bacteria, DdPAC exhibits an enhanced light response compared to other red-light-sensitive PACs (Stüven et al., 2018). However, until now, it had not been applied to brain cells, nor to the brain *in vivo*. Furthermore, red light is known for its ability to penetrate tissues due to its longer wavelength, which allows it to pass through biological material with less scattering compared to shorter wavelengths (Lehtinen et al., 2022). Accordingly, we propose that DdPAC holds significant potential as a tool for modulating cAMP *in vivo*, with the added advantage of red-light activation, making it a promising candidate for non-invasive applications.

In essence, this thesis aimed to restore molecular and behavioural functions in neurodegenerative diseases by modulating cAMP signalling through DdPAC. In parallel, we sought to characterise previously unknown disruptions in cortical cAMP signalling and behaviour in HD. First, we tested a cAMP fluorescent sensor that allows to measure cAMP dynamic changes using fibre photometry in behaving mice. By using this sensor, named G-Flamp1, we demonstrated the involvement of cAMP signalling in M2-cortex-related behavioural tests, while also revealing altered neuronal cAMP dynamics at 16 and 20 weeks in HD mice. Furthermore, HD's early impairments are less understood compared to other neurodegenerative disorders, making it a valuable focus for investigation and helping in the identification of an earlier timepoint for initiating treatments. Consequently, we have characterised early alterations in HD, as its mouse models are well-established and faithfully replicate the symptoms observed in humans. From these findings, we have demonstrated that subtle fine motor and anhedonia-like alterations can be observed as early as 8 weeks, similar to cognitive and motor learning symptoms onset, and before described major coordination alterations occur. In parallel, we aimed to implement DdPAC as a novel optogenetic tool to non-invasively modulate synaptic plasticity through cAMP signalling. As first step, we aimed to develop a non-invasive method for AAV delivery and to characterise the expression and functionality of DdPAC for *in vivo* applications. Using retro-orbital injection of the PHP.eB capsid, we successfully delivered GFP transgene across various brain regions and mouse strains, opening the possibility for future minimally-invasive optogenetic treatments. In parallel, we evaluated and characterised the impact of DdPAC-mediated cAMP signalling on synaptic plasticity. Notably, DdPAC-mediated increases in cAMP levels significantly enhanced synaptic plasticity, with a more pronounced effect when activated in astrocytes. Finally, we aimed to restore physiological functions in neurodegenerative disorder —specifically addressing molecular and behavioural deficits in HD and AD— by enhancing cAMP signalling through DdPAC activation within affected brain circuits. In the context of HD, elevating cAMP levels in cortical astrocytes generated cortical hemodynamic responses and improved motor learning in WT mice but impaired coordination in HD mice. Additionally, DdPAC-mediated cAMP increase in striatal astrocytes impaired coordination in both WT and HD mice. In AD, cAMP elevation in hippocampal astrocytes reduced astrogliosis and Aβ deposits in AD mouse model, whereas an increase in cAMP in neurons led to a reduction in microglial activation. Finally, proteomics analyses in DdPAC-activated neurons and astrocytes from AD mice revealed changes in the proteome associated with activated cAMP-PKA pathway. Specifically, in hippocampal tissue where DdPAC was activated in neurons, the proteomic response was confined to synaptic plasticity. In contrast, activation of DdPAC in astrocytes led to proteomic changes involving both synaptic plasticity and immune response pathways.

Overall, these findings highlight the capacity of both neuronal and astrocytic DdPAC-mediated cAMP modulation to influence neuronal plasticity, while also emphasising the differential effects of cAMP modulation across various cell types and in the context of neuropathology. Furthermore, our results underscore the importance of the specific brain

region and molecular context in targeting cAMP modulation, as the outcomes of DdPAC stimulation vary between the cortex, striatum, and hippocampus, as well as depending on the pathological condition. Finally, we provide compelling evidence for the potential of DdPAC, an approach that could be extended to other PACs, to modulate cAMP signalling pathways. This offers not only a powerful tool for investigating brain function but also a promising therapeutic strategy.

1. Cortical cAMP impairments in Huntington's Disease

Alterations in cAMP signalling have been identified in the context of aging and various neurodegenerative disorders, including AD, PD, and HD. Notably, these impairments exhibit disease-specific patterns and are localised to distinct brain regions (Bonkale et al., 1996; Chen et al., 2012; Gines et al., 2003; Giralt et al., 2013; J.-T. Lin et al., 2013; O'Neill et al., 1994; Tyebji et al., 2015; Zhang et al., 2013). For instance, while AD is associated with decreased cAMP signalling in the hippocampus and temporal cortex, HD is attributed to decreased cAMP signalling in the striatum and cortex but increased cAMP signalling in the hippocampus, although there are some controversies between groups and animal models (Gines et al., 2003; Giralt et al., 2013; J.-T. Lin et al., 2013; O'Neill et al., 1994; Tyebji et al., 2015; Zhang et al., 2013). However, this remains a subject of debate among research groups. Moreover, cAMP is a small, highly dynamic molecule, making its direct quantification challenging. Consequently, insights into cAMP signalling are often inferred by measuring components of the pathway, such as AC, pPKA/PKA, pCREB/CREB, or PDEs. Therefore, in this study, we aimed to elucidate the alterations in cAMP signalling in our HD mouse model, the R6/1. In this model, data regarding cAMP signalling is still limited. To date, increased pPKA levels in the striatum and hippocampus have been reported in R6/1 mice (Giralt et al., 2011, 2013; Tyebji et al., 2015). Notably, a recent study shows that cAMP signalling in astrocytes from the striatum of R6/2 mice is increased due to decreased GPCRi signalling(X. Yu et al., 2020). Therefore, to draw definitive conclusions, cell-specific studies are essential. In this work, we provided an initial overview of cAMP signalling in cortical neurons from R6/1 mice, offering a preliminary insight of its status in this model. However, further research is needed, with a comprehensive analysis of additional components of the cAMP signalling pathway, to achieve a more complete understanding of the mechanisms at play in this model.

cAMP sensors offer a powerful tool for investigating cAMP dynamics with high specificity in distinct cell types. Over the past few years, significant efforts have been made to develop a cAMP sensor suitable for fibre photometry (Harada et al., 2017; Odaka et al., 2014; Ohta et al., 2018). However, most available sensors use Förster resonance energy transfer requiring two different wavelengths (requiring more complex optical systems), are indirect as they rely on PKA activity, or exhibit fluorescence changes that are not optimised for fibre photometry applications (Massengill et al., 2021). For instance, Pink Flamindo is a single-fluorescence protein sensor that has demonstrated the ability to track cAMP dynamics *in vivo* using two-photon imaging (Harada et al., 2017), but exhibited limited performance when applied to

fibre photometry. In fact, when tested in our laboratory, Pink Flamindo did not yield successful results, as cAMP dynamics were not detected (data not shown). Recently, (L. Wang et al., 2022b) developed GFlamp-1, which showed promising results compared to other cAMP sensors. Herein and for the first time, we have successfully characterised neuronal cAMP dynamics using GFlamp-1 during two M2-dependent behavioural tasks – the beetle mania and accelerating rotarod tests – using fibre photometry.

Notably, by using GFlamp-1 sensor, we have demonstrated that excitatory CamKIIa neurons signal through cAMP during two M2-cortex-dependent tests. In the cortex, many neurotransmitters, including dopamine, norepinephrine or serotonin, signal through the cAMP pathway by binding G_s-coupled GPCRs, such as D1, β-adrenergic or 5-HT4 receptors(Gurevich, 2022; Jones-Tabah et al., 2022; Sgambato, 2024). In a recent paper from the group, we showed an increase in calcium during the BMT in WT mice (Conde-Berriozabal et al., 2023). Therefore, it seems that both calcium and cAMP signalling would be involved in regulating these behaviours. Furthermore, we have investigated cAMP dynamics not only in WT but also in R6/1 mice. In both cases, WT and R6/1 exhibit an increase in cAMP in response to the presented stimulus; however, we also display that 15-week-old R6/1 mice show an abnormal cAMP rise during the ARR task. These results align with functional studies in HD patients, which have shown that the cerebral cortex becomes hyperexcitable during the disease, as well as with *in vivo* electrophysiological studies that observed decreased inhibition of cortical pyramidal neurons in 6-month-old R6/2 mice (Cepeda et al., 2019). Nonetheless, this hyperactivation of cortical neurons mediated by cAMP exhibits sex differences, as it is observed exclusively in female mice in the present cohort. Sex-related differences in cAMP signalling have already been observed in different regions of the mouse brain (Basu et al., 2021; Jain et al., 2019; Nazarian et al., 2009). Yet, in this specific case wild type male mice did not perform as expected during the accelerating rotarod test, so these experiments should be repeated in order to obtain conclusive results regarding sex differences. To further investigate the temporal dynamics of cAMP, we repeated the beetle mania task at 20 weeks. Although engagement in the response was still present, it was reduced compared to that of WT mice. This is consistent with the findings of (Gines et al., 2003), who reported reduced cAMP levels in the striatum of HdhQ111 knock-in mice. However, it contrasts with the increased striatal cAMP levels observed in R6/1 mice by (Tyebji et al., 2015), although the latter was estimated indirectly through the analysis of phospho-PKA substrates.

Taken together, these findings suggest that cAMP plays a central signalling role in the M2-cortex, with its alterations varying across different disease stages and exhibiting sex-dependent differences. Further investigation of cAMP dynamics in additional brain regions is essential to elucidate the region- and cell-type-specific dysregulation in the R6/1 mouse model of HD. In this regard, the use of genetically encoded cAMP sensors offers a significant advantage by enabling the study of cell-type-specific alterations, which is crucial to understand the molecular mechanisms underlying behavioural impairments. Recent evidence

has demonstrated impaired G_i-coupled GPCR signalling in striatal astrocytes of the R6/2 mouse model, leading to increased cAMP levels in this cell type and brain region (X. Yu et al., 2020). This highlights a key limitation of the present study, as our findings are restricted to cortical neurons, without insights into astrocytic cAMP dynamics. Addressing this gap, future studies should aim to express GFlamp-1 in astrocytes to investigate cAMP signalling during M2-dependent behavioural tasks. Furthermore, previous work from our group reported an inability of cortical neurons to activate through calcium signalling during the beetle mania task in R6/1 mice (Conde-Berriozabal et al., 2023). Despite the observed genotype differences, our current results show that R6/1 mice still exhibit an increase in cAMP in response to a threatening stimulus. This suggests that calcium and cAMP may contribute differently to the behavioural alterations observed in HD. Given the known interplay between these two second messengers (Sobolczyk & Boczek, 2022), further studies are needed to explore the relationship between calcium and cAMP during M2-cortex dependent tasks in HD, thereby providing insight into the potential mechanisms underlying M2-cortex-related behavioural impairments.

2. Disrupted cortico-striatal circuitry as key pathological alteration in Huntington's Disease

The striatum, as the main input nucleus of the basal ganglia, integrates excitatory projections from the entire cortical mantle and the thalamus. This extensive network, in which the striatum directly receives input from nearly all cortical regions, plays a critical role in regulating movement and cognitive processes (Bunner & Rebec, 2016b; Rebec, 2018). Notably, the cortex plays a crucial role in providing the striatum with associative, limbic, and motor information, essential for selecting and guiding appropriate behavioural responses (Kreitzer & Malenka, 2008).

In HD, the striatum is among the most severely affected brain regions, playing a key role in the motor deficits, cognitive disorganization, and emotional dysregulation characteristic of the condition. Nevertheless, significant cortical atrophy also occurs in HD, with its severity varying across different cortical regions (Rebec, 2018). The pronounced atrophy of the striatum in HD primarily results from the loss of GABAergic medium spiny neurons, coupled with the degeneration of cortical pyramidal glutamatergic neurons (Miller et al., 2011; Vonsattel et al., 1985; Vonsattel & DiFiglia, 1998). HD disrupts the cortico-striatal system by impairing the mechanisms underlying communication between cortical and striatal neurons (Dallérac et al., 2015; T.-H. Wong et al., 1982). However, alterations in neuronal function emerge well before visible cell death, suggesting that circuit dysfunction contributes to the early symptoms of the disease (Blumenstock & Dudanova, 2020). Given this information, the cortico-striatal pathway is recognised as one of the earliest and most significantly affected pathways in the disease.

Our findings in this study provide further evidence of disruptions in the cortico-striatal circuitry in HD, particularly involving the M2-cortex. In previous work from our group, we

demonstrated that the M2 cortex is functionally disconnected from the striatum in the R6/1 mouse model of HD (Fernández-García et al., 2020). This disconnection aligns with the behavioural alterations observed during the beetle-mania task, a test closely related to M2-cortex functionality (Conde-Berriozabal et al., 2023). Specifically, we observed significant impairments in task performance in 14- and 20-week-old R6/1 mice. This aligns with our previous findings (Conde-Berriozabal et al., 2023), in which we demonstrated that behavioural deficits in the beetle mania task are present at 12 and 20-week-old R6/1 mice. Importantly, as previously discussed, we have revealed that cAMP signalling plays a role in M2-cortex-related tasks, although it seems that alterations in cAMP may not be directly related to the observed behavioural impairments.

Notably, most studies concentrate on the motor cortex's projections to the striatum, due to their role in the initiation and control of voluntary movements (Blumenstock & Dudanova, 2020; Bunner & Rebec, 2016b). Herein, we demonstrate that cortico-striatal projections beyond the M2 cortex-striatum pathway are also impaired in the R6/1 mouse model of HD. Specifically, the connection between M2-cortex, SS-cortex, and striatum appear to be disrupted, as shown by the early revealed alterations in the removal adhesive and marble burying tests. Altered sensory processing through the basal ganglia was reported in HD symptomatic patients (Boecker et al., 1999; Mirallave et al., 2017), as well as decreased connectivity in the somatosensory cortices in zQ175DN mice at 12-month of age and R6/1 symptomatic mice (Conde-Berriozabal et al., 2023; Fernández-García et al., 2020; Vasilkovska et al., 2024). These results are in line with our data, which reveal impairments in behaviours associated to the somatosensory cortex (Bouet et al., 2009) at 16 weeks of age, when mice fail to detect a stimulus on their forepaws during the removal adhesive test. Indeed, our experiments involving astrocytic DdPAC stimulation in the SS during in vivo hemodynamic imaging reveal impaired SS activity in 16-week-old R6/1 mice. Specifically, we observe cortical hyperactivation following the modulation of cAMP signalling, which may reflect a compensatory mechanism. Furthermore, this test enabled us to uncover fine motor deficits in 8-week-old R6/1 mice, a very early stage of the disease. As a matter of fact, only motor learning and other cognitive impairments had previously been reported at this timepoint (Puigdellívol et al., 2015), with main motor abnormalities typically observed starting at 14 weeks (Naver et al., 2003).

The orbitofrontal cortex-striatum connection represents another cortico-striatal pathway identified as impaired in this study, which leads to anhedonic behaviour in R6/1 mice. Psychiatric symptoms are common yet a variable feature of HD, differing both in severity and onset among patients. These symptoms, which may include depression, anxiety, irritability, and apathy, often precede motor impairments (Jauhar & Ritchie, 2010). Increased anhedonia has been observed in our animals, measured by a decreased number of buried marbles in the marble burying test, a task associated to the orbitofrontal cortex (Angoa-Pérez et al., 2013). In HD patients and also in mouse models, a commonly observed feature is compulsive, repetitive, stereotypic behaviour (Bolivar et al., 2004; Rodríguez-Urgellés, Casas-

Torremocha, Sancho-Balsells, Ballasch, García-García, Miquel-Rio, Manasanch, del Castillo, et al., 2023; Zadegan et al., 2024). Considering that the marble burying test is usually applied as a measure of obsessive-compulsive and anxiety behaviour, our hypothesis was that an increased number of buried marbles, and thus heightened compulsive behaviour, would be observed in HD. In contrast, R6/1 animals did not bury marbles and often merely touched them starting at 8 weeks, which we interpreted as indicative of anhedonia or apathy. Indeed, apathy is a feature observed in HD patients (J. Brandt, 2018; Mclauchlan et al., 2022). Crucially, in 2019 it was described that impairments in the white matter cortico-striatal tracts could predict apathy in HD (De Paepe et al., 2019). Emotional apathy has, in turn, been associated with the medial orbitofrontal circuit (Le Heron et al., 2018; Levy & Dubois, 2006). Consequently, our observations in a genetic mouse model indicate that this is a feature that may be a direct effect of mutated HTT and would confirm that arises due to orbitofrontal-cortex to striatal pathway impairments.

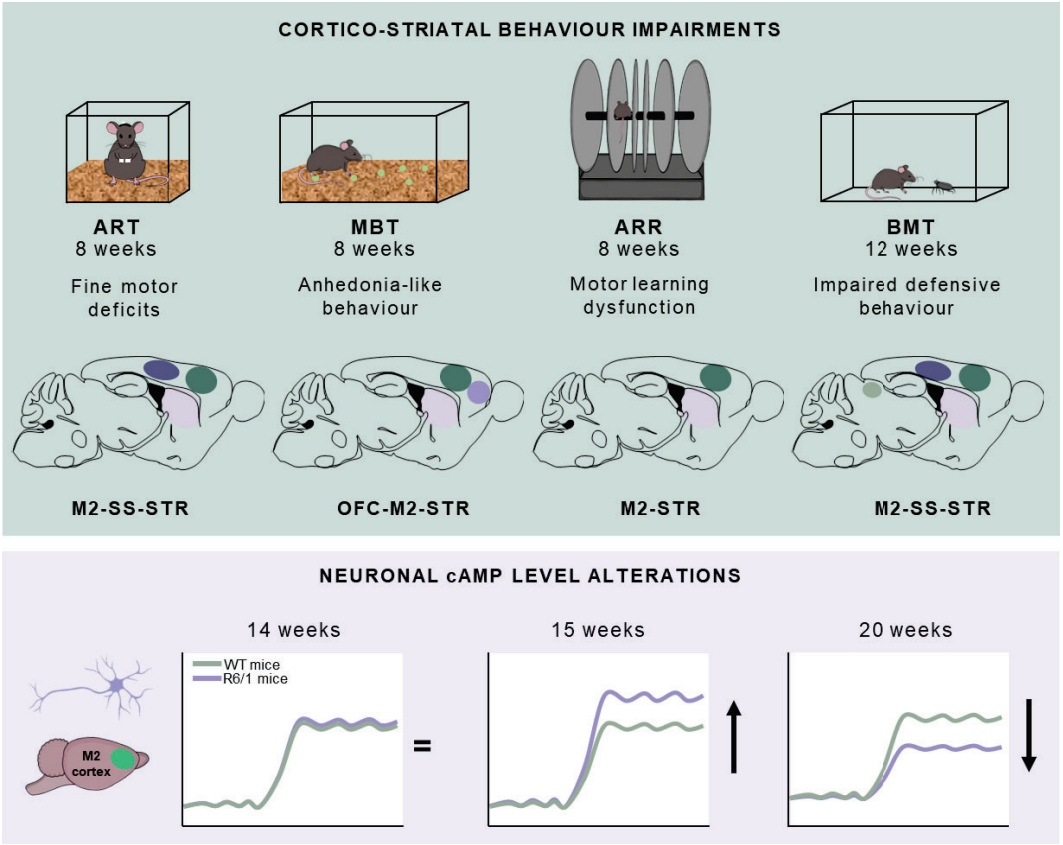

Figure 62. Cortical alterations in Huntington's Disease. Summary of the main cortical alterations observed in R6/1 mice. *Top:* cAMP signaling alterations observed at 15 and 20 weeks of age in R6/1 mice. *Bottom:* cortico-striatal behavioural deficits detected in R6/1 mice. Brain regions relevant to these findings are highlighted in the corresponding atlas sections. M2: secondary motor cortex; SS: somatosensory cortex; STR: striatum; OFC: orbitofrontal cortex.

In summary, these results confirm that cortical function has a highly relevant role in the physiopathology of HD. As a result, the cortico-striatal functions identified in this study offer new avenues for circuit-based treatments. Indeed, neuronal modulation of the M2-dorsolateral striatum through blue light stimulation of CHR2 has been shown to effectively restore behaviour in HD (Fernández-García et al., 2020), reinforcing the potential of the cortico-striatal pathway as target for novel therapies. Furthermore, these results strengthen the R6/1 mouse model of HD as a valuable tool for investigating early disease impairments, although studies with other more models should be performed in order to confirm these results. In summary, our findings provide a more refined understanding of HD pathology, offering potential for earlier diagnosis and the development of circuit-specific therapeutic interventions.

3. Non-invasive brain delivery of AAV constructs

A critical aspect in the development and establishment of potential non-invasive therapies is the efficient and targeted delivery of therapeutic agents to the brain. Given that the current standard in basic research involves direct brain injection, facilitating the clinical translation of optogenetics requires the development of minimally invasive strategies for delivering AAVs carrying the transgene of interest to the brain. Intravenous injections have emerged as minimally invasive alternatives for AAV delivery, requiring the engineering of AAV capsids to enable crossing of the BBB (Chan et al., 2017; Deverman et al., 2016b; Haery et al., 2019; Lykken et al., 2018). For instance, PHP.B and PHP.eB capsids have been used in recent years to target the brain via intravenous delivery due to their enhanced ability to cross the BBB (Chan et al., 2017; Deverman et al., 2016b). Nevertheless, they have shown certain limitations regarding the mouse strain and delivery route (Mathiesen et al., 2020). Therefore, establishing and AAV capsid and delivery route capable of effectively transducing specific brain cells of interest is of great importance.

In this thesis, we compared the widely used AAV9 capsid for neural infection with the enhanced PHP.eB capsid. Using a general CAG promoter to drive GFP expression, we confirmed that both AAV9 and PHP.eB can infect the brain following either local or retro-orbital injection. However, GFP fluorescence was limited to certain brain regions in both cases under CAG promoter, especially the CA2 region of the hippocampus, failing to spread throughout the whole brain. This CA2 phenomenon has recently been reported by other groups (Alexander et al., 2024; Okamoto et al., 2023), who observed an exaggerated tropism in these cells following intravenous injection of various AAV serotypes. Specifically, it has been suggested that this observation may result from increased expression of AAV receptors and the enrichment of cell-surface glycan receptors in these cells (Alexander et al., 2024), therefore potentially limiting its expression in other brain regions. When assessing the cell types expressing GFP following retro-orbital injection of the AVV9 capsid, we observed GFP expression in both neurons and astrocytes. AAV9 has shown increased tropism for neurons (Cearley & Wolfe, 2006; Haery et al., 2019) although it is also expressed in astrocytes (Hammond et al., 2017). Interestingly, when using the specific CamKIIa promoter, we

observed a broad expression throughout the brain with the PHP.eB capsid, but not with AAV9. The better performance of PHP.eB aligns with expectation, as PHP.B and its variants have been shown to enhance the efficiency of crossing the blood-brain barrier (Chan et al., 2017; Deverman et al., 2016b; Mathiesen et al., 2020). A recent study comparing transgene expression across different promoters reported a reduction with the hSyn1 promoter compared to CamKIIa. while no significant differences were observed with the CAG promoter (Finneran et al., 2021). Based on these results and considering that CAG retro-orbital injections were the first performed in our laboratory, we cannot rule out the possibility that the reduced GFP expression under the CAG promoter is due to technical factors. Therefore, our results demonstrate that retro-orbital injection is an effective method for driving transgene expression under specific promoters. However, this approach requires a substantially larger injection volume (100µl per animal) compared to local injections (0.5µl per animal). Additionally, the vg concentration needed for retro-orbital delivery is considerably higher, typically ranging from 10^{12} to 10^{14} vg (Finneran et al., 2021). These factors should be carefully considered when selecting an administration route, which still favour local injection for routine application.

Despite the advantages of PHP.eB for retro-orbital administration, this serotype exhibits limitations related to mouse strain or delivery route, as it has been shown to inefficiently transduce strains such as B6C3 or BALB/cJ mice (Hordeaux et al., 2018; Mathiesen et al., 2020). Our results demonstrated that PHP.eB, delivered via retro-orbital injection and expressing GFP under the CamKIIa promoter, efficiently infects the entire brain of WT B6CBA mice. Specifically, this mouse strain is an F1 cross between a C57Bl/6f and CBA mouse, the genetic background in which we maintain the R6/1 mouse model for HD. Notably, retro-orbital injection of PHP.eB successfully transduced the cortex, hippocampus, and striatum also in R6/1 mice. This data supports the feasibility of using this viral delivery route in our mouse model in future studies. Furthermore, retro-orbital injection of PHP.eB also targeted A2A-expressing cells in a region-specific manner in A2A-Cre mice. Consequently, our results highlight both strain and cell-type specificity of PHP.eB-mediated transduction, emphasising its potential for targeted gene delivery in specific neuronal populations.

Unfortunately, intranasal delivery of both AAV9 and PHP.eB was unsuccessful under all tested conditions. While intranasal drug delivery has been widely demonstrated in research studies, particularly for peptide administration (Alcalá-Barraza et al., 2010) its efficacy for AAV-mediated gene delivery to the brain remains controversial. Only a few studies have explored this approach (C. Chen et al., 2020; J. Wang et al., 2023), and among them, only one provides histological evidence of transgene expression. Notably, this study was conducted in BBB impaired rats, raising the possibility that species-specific physiological differences and disrupted BBB may influence viral delivery and expression. Therefore, further research is essential to engineer novel AAV variants capable of efficient, non-invasive

brain entry, a breakthrough that could significantly advance the development of future gene therapies.

4. DdPAC as a new tool to modulate synaptic plasticity through cAMP

A primary aim of this work was to optimise a tool capable of modulating synaptic plasticity in a specific and long-lasting manner. Currently, technological approaches such as DBS (Okun, 2012) and TMS (Barker et al., 1985) are employed to enhance neuronal plasticity in targeted brain areas. However, these techniques lack cellular specificity, and their effects often extend beyond the intended focus, impacting circuits outside the disease-relevant regions. In contrast, optogenetics, a technique that combines genetic and optical methods to control the activity of specific cells in living tissue (Boyden et al., 2005), offers a promising alternative to overcome these limitations. Despite its potential, the clinical application of optogenetics remains restricted, and its use is primarily confined to basic research. Since cAMP plays a crucial role in synaptic plasticity, the precise control of its signalling via optogenetic tools holds significant potential for modulating plasticity in a highly specific and temporally controlled manner. In this context, PACs are enzymes used in optogenetics to modulate cAMP levels in response to light stimulation. Particularly, DdPAC, an improved red-light-activated PAC employed in this thesis (Stüven et al., 2018), has proved its effectiveness in bacteria but was not yet been applied *in vivo*. Our data showed that expression and stimulation of DdPAC in cortical neurons and astrocytes potentiates neuronal activity, specifically inducing LTP. These findings align with previous studies that used non-cell-specific cAMP modulators, such as forskolin, an AC activator, to demonstrate the role of cAMP in synaptic potentiation (Otmakhov et al., 2004). Forskolin has been shown to enhance synaptic transmission in rat hippocampal cultures, indicating that cAMP elevation can directly facilitate synaptic strengthening (Sokolova et al., 2006). However, our study adds an important dimension to previous work by showing that the cellular context in which cAMP is modulated influences the outcome of synaptic plasticity. Our results related to proteomic analyses in DdPAC-mediated cAMP increase in the cortex and hippocampus from WT mice further support this idea. Proteomic analyses from DdPAC-activated hippocampal cells revealed that activation of DdPAC in neurons primarily modulated proteins associated with synaptic plasticity. In contrast, stimulation in astrocytes not only affected proteins related to plasticity but also those involved in immune activation, inflammation, and cytoskeletal remodelling. Cytoskeletal remodelling it also strongly associated with our proteomic analyses of cortical DdPAC stimulated samples, with key ontologies including axon guidance, supramolecular fibre organisation or neurofilament bundle assembly. Indeed, actin cytoskeleton is vital for both synaptic structure and function, regulating processes such as receptor anchoring, synaptic trafficking, and local protein translation (Hotulainen & Hoogenraad, 2010). Moreover, in both cortical and hippocampal experiments, proteins were predominantly found in the pre- and post-synaptic regions, further indicating synaptic modulation. This suggests that astrocytes play a more complex

role in synaptic modulation, potentially influencing both neuronal activity and its microenvironment.

Indeed, we observed a stronger effect when cAMP modulation occurred in astrocytes compared to neurons, both at proteomic and electrophysiological level. Recent studies have increasingly acknowledged the importance of astrocytes in synaptic plasticity, with evidence suggesting that astrocytic signalling can modulate synaptic strength, neuronal excitability, and synaptic function, all contributing to the maintenance of LTP (Henneberger et al., 2010; Perea et al., 2009). The enhanced effect of cAMP modulation in astrocytes could be attributed to their role in maintaining extracellular environment and their direct involvement with the tripartite synapse (Bonansco et al., 2011; Perea et al., 2009; Perea & Araque, 2007), by releasing gliotransmitters and responding to neurotransmitters, among other processes, which could be amplifying the effects of cAMP elevation on synaptic plasticity. Our results further support this hypothesis, as DdPAC-mediated cAMP increase in cortical astrocytes triggered release of glutamate, thereby activating neighbouring neurons.

While the mechanisms by which astrocytes are implicated in synaptic plasticity remains an active area of investigation, it is well established that Ca^{2+} elevations in astrocytes enhance the probability of transmitter release by liberating glutamate (Perea & Araque, 2007). In line with this, much of the research to date has mainly focused on Ca^{2+}-mediated signalling pathways, which have been well-documented for their role in regulating synaptic activity and modulating neuronal communication (Araque et al., 2014). Elevations in intracellular Ca^{2+} are known to trigger the release of gliotransmitters like glutamate, ATP, and D-serine, which in turn modulate synaptic strength and neuronal excitability (Butt, 2011; Mothet et al., 2005; Santello & Volterra, 2009). This focus on Ca^{2+} has overshadowed the exploration of other important intracellular pathways, such as those involving cAMP, which remains less understood, possibly due to the technical challenges associated with measuring cAMP dynamics in vivo. Notably, our data in cortical slices showed that cAMP induction specifically in astrocytes modulates synaptic potentiation through a PKA-dependent mechanism which does not require intracellular Ca^{2+} elevations. In our data, astrocytic cAMP signalling-dependent potentiation shares some of the mechanisms known to mediate synaptic plasticity by astrocytes, such glutamate release (Bonansco et al., 2011) and modulation of synaptic potentiation through NMDAR and D-serine (Perea & Araque, 2007). As previously mentioned, glutamate release from astrocytes has been classically associated to Ca^{2+} signalling. However, in our context, our results demonstrate that this glutamate release occurs independently of calcium, suggesting the involvement of alternative gliotransmission mechanisms. Ca^{2+}-dependent exocytosis has been suggested as the primary mechanism underlying the release of major gliotransmitters, including glutamate (Sahlender et al., 2014), however, our findings suggest that an alternative mechanism potentially regulating this process in our context could be non-vesicular release mediated by plasma membrane ion channels (Sahlender et al., 2014; Y. Wang et al., 2022). Crucially, the potentiation induced by astrocytic DdPAC stimulation was only observed in the presence of synaptic activity. This is

consistent with a situation where astrocyte cAMP-induced glutamate activates NMDAR and requires synaptically-induced neuronal depolarisation to enable NMDAR ionotropic signalling associated with classical LTP. Moreover, it also goes in line with the general knowledge that astrocytes are able to sense neuronal activity and respond accordingly (Y. Wang et al., 2022). Importantly, in addition to requiring activity in conjunction with DdPAC activation to induce DdPAC-LTP, the induction of LTP was frequency-independent, allowing even synaptic frequencies that normally induce LTD to instead induce LTP. It therefore appears that astrocyte cAMP elevation and downstream signalling pathways leads to a state where synapses are primed for potentiation. Interestingly, recent studies demonstrated that astrocytes increase cAMP signalling upon synaptic activity (Hasel et al., 2017; Theparambil et al., 2024), an effect attributed to extracellular adenosine, which is independent of intracellular calcium (Theparambil et al., 2024), suggesting that our DdPAC-mediated interventions are recruiting an existing physiological synaptically activated pathway.

The comprehensive analysis of molecular changes induced by cortical DdPAC stimulation shed further light on the involvement of cAMP signalling in astrocytes to synaptic plasticity. Particularly, DdPAC stimulation in astrocytes especially involved the phosphorylation of proteins linked to the modulation of synapses and the modulation of cell morphology. Indeed, it is well-known that cAMP contributes to morphological changes in astrocytes, as shown by forskolin-induced effects (Goldman & Abramson, 1990; Schweinhuber et al., 2015). Furthermore, Gene ontology enrichment analysis pointed to regulation of cytoskeletal proteins and mediators of the immune system by astrocytes (Sobolczyk & Boczek, 2022), similarly to what we observe in our data. These effects have been associates with the involvement of ARP2/3 activity (Murk et al., 2013), a major modulator of actin dynamics, which is also increased by DdPAC stimulation in our phosphoproteomic differential dataset. DdPAC activation also induced the phosphorylation of the PKA catalytic unit (PRKAR1A) and its effector proteins: adducin (Matsuoka et al., 2000), PXN (Turner, 2000), and VASP (Bachmann et al., 1999), highlighting the direct link between cAMP increase in astrocytes and the potential modulation of astrocyte morphology through actin and focal adhesion modulation. These effects are further supported by the induction of Rho GTPases signalling by DdPAC, which has been reported to modulate actin dynamics (Paskus et al., 2020). In this line, a concerted neuronal activity and astrocyte-dependent morphology changes appear necessary for synaptic plasticity, as previously shown in studies on dendrite dynamics and motor behaviour during critical periods (J. P. Brandt & Ackerman, 2025). Astrocyte processes and dendritic spines have been proved to physically interact via EphA4-ephrinA3 to the point that ephrin mutants dendritic spines overgrow and fail to mature, and consequently synaptic plasticity is inhibited (Filosa et al., 2009). In our samples, increased Ephrin receptor signalling in the SNC canonical pathway at the phospho-proteome level suggests enhanced neuronal-astrocyte interactions, which may contribute to the modulation of synaptic plasticity. Additionally, our phospho-proteome dataset has also reinforced the idea of cAMP modulation in astrocytes directly impacting on synaptic plasticity, as most of the synaptic proteins are found in the pre- and -post synaptic compartments.

Importantly, our results suggest that modulation of cAMP signalling in astrocytes has a broader impact beyond the astrocytic cell type itself. The phospho-proteomic and proteomic analyses revealed differential expression of proteins associated with astrocyte development, which suggest cell-autonomous effects. However, the impact of DdPAC stimulation was observed across multiple cell types, including neurons, microglia, and oligodendrocytes.

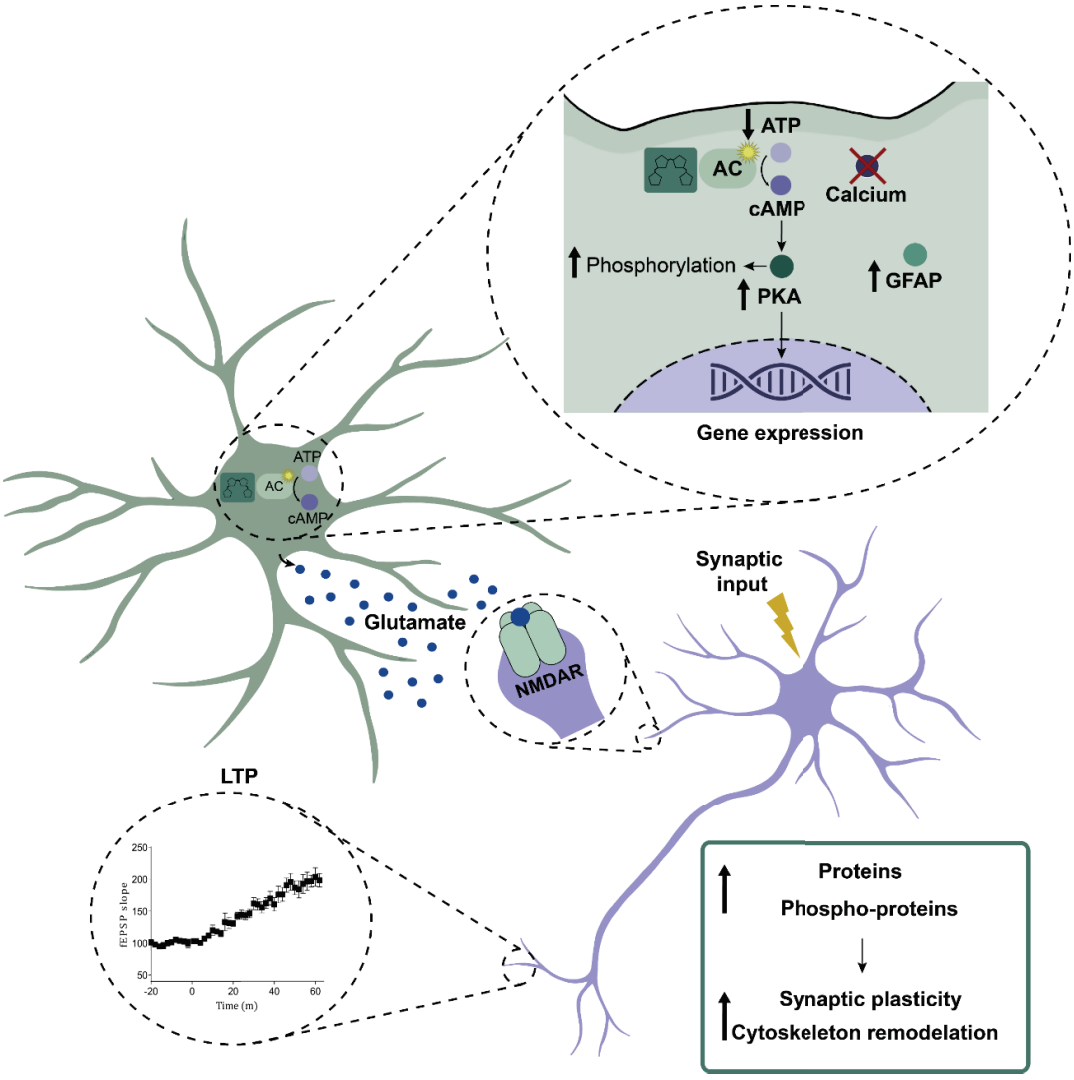

Figure 63. Mechanisms underlying enhanced plasticity in cortical DdPAC-activated astrocytes. Summary of key findings from electrophysiological, proteomic, metabolomic, and histological analyses following DdPAC activation in cortical astrocytes of WT mice.

These findings align with the growing understanding that astrocytes, traditionally thought of as support cells, play a more central role in regulating broader brain activity. As shown in previous work (Sobolczyk & Boczek, 2022), this broad response indicates that the activation of cAMP signalling in astrocytes can have a multifaceted effect, coordinating cellular activity across different brain cells types in a rapid and dynamic manner. Indeed, we also observed an increase in AQP4 expression and improved motor learning in WT mice after DdPAC

stimulation, which further supports this idea (expanded information can be found in the following section).

Moreover, the effects of DdPAC stimulation involve changes in many nucleotides' levels. While our metabolic analysis shows spared cAMP levels, the overall reduction of nucleotide levels highlights the complexity of cAMP regulation (Chandel, 2021). The decrease in ATP, the activation of antioxidant mechanisms, together with the large number of proteomic changes observed suggest the induction of high energy consumption by DdPAC stimulation. Notwithstanding, the decreased ATP and ADP levels along with constant cAMP suggest a tightly regulated system where cAMP synthesis is balanced with its degradation(Bielenberg et al., 2024; Conti & Beavo, 2007). Interestingly, ATP released from astrocytes has been shown to inhibit synaptic transmission through adenosine signalling. Therefore, it is possible that altered metabolites by DdPAC stimulation, such as reduced ATP levels, may also contribute to the facilitation of synaptic transmission. Nevertheless, these results highlight a limitation in our study. While we have robustly demonstrated that DdPAC activation signals through PKA activation, we lack a direct measurement of cAMP levels. This absence of direct quantification of cAMP elevation prevents us from conclusively linking the observed effects to cAMP signalling in a more precise manner. Future studies incorporating cAMP-specific sensors would be crucial for validating the precise role of cAMP in mediating the effects of DdPAC activation.

These findings underscore the therapeutic potential of targeting cAMP signalling to modulate synaptic plasticity in a controlled manner. Moreover, they contribute to a deeper understanding of the role of cAMP in astrocytes and its impact on synaptic plasticity, as well as its broader influence on brain activity, offering a promising opportunity for precision-based interventions.

5. cAMP modulation in astrocytes from Huntington's Disease

Currently, there is no cure of effective treatment available for Huntington's Disease that significantly improves patients' quality of life. Numerous clinical trials are ongoing in the search for therapeutic strategies, with several focusing on reducing or eliminating mutant huntingtin protein (Kwon, 2021). However, to date, these trials have not achieved success in delivering a clinically effective solution. In HD, as in many other neurodegenerative disorders, deficits in synaptic plasticity play a crucial role in the emergence of behavioural abnormalities (Cepeda & Levine, 2022). Therefore, identifying strategies that enhance synaptic plasticity may help ameliorate or delay the onset of disease symptoms. Our previous findings have demonstrated that the expression of DdPAC in astrocytes is able to enhance synaptic plasticity through DdPAC-mediated cAMP modulation. Building on this evidence, our study also aimed to explore this mechanism further and assess its potential implications for addressing synaptic dysfunction in HD. In fact, ongoing clinical trials are investigating the modulation of cAMP through the use of PDE inhibitors (Erro et al., 2021; Menniti et al., 2021). However, these efforts have not yet been successful, likely due to their lack of

region and cell specificity, a limitation that could potentially be addressed through the use of DdPAC in astrocytes.

To further understand the broader impact of astrocytic cAMP modulation, we investigated its influence beyond synaptic plasticity at cellular level. Since astrocytes play a crucial role in neurovascular coupling and metabolic support (Lia et al., 2023), we hypothesised that DdPAC-induced cAMP signalling could have functional consequences on whole-brain activity. Hemodynamic responses, which reflect neurovascular interactions and overall brain function, are a very useful readout of such effects. Thus, we examined hemodynamic responses before and after astrocytic DdPAC stimulation in both WT and R6/1 mice via DCS, to determine the extent to which astrocytic cAMP signalling contributes to global brain functions and its potential therapeutic implications. In this study, we were able to demonstrate the potential of DdPAC-induced cAMP signalling in modulating whole cortical function in R6/1 mice, as hemodynamic responses were induced *in vivo* by the stimulation of astrocytic DdPAC. This observation emphasises the importance of incorporating the astrocytic cAMP signalling pathway as an additional mechanism in the broader framework of neurovascular coupling (Petzold & Murthy, 2011). Interestingly, cAMP induced by PACs expressed in blood vessel cells have also shown to induce local hemodynamic increases (Abe et al., 2021). Furthermore, R6/1 mice showed a greater increase in blood flow than WT mice. This observation is consistent with our previous findings, which demonstrate that R6/1 mice exhibit neuronal cAMP hyperactivation in response to stimuli, suggesting that both neurons and astrocytes in HD might show altered cAMP responses, and which might require further investigation. In fact, no significant hemodynamic response was detected in WT, although a tendency was observed.

Moreover, we observed increased AQP4 levels in WT mice post-mortem tissue from the same cohort. AQP4 membrane trafficking modulate synaptic plasticity through astrocyte processes motility (Ciappelloni et al., 2019b). Interestingly, synaptic transmission involves the swelling of perisynaptic astrocyte processes as a consequence of extracellular K+ buffering and associated water movement through AQP4 (Walch & Fiacco, 2022). This aligns with the observed increase in GFAP expression in stimulated areas in the *in vivo* behavioural experiment, and increased modulation of cytoskeletal processes in the phospho-proteomic study. Besides, R6/1 mice were not able to show an increase in AQP4 levels. Indeed, the glymphatic system has been seen to be impaired in HD (H. Liu et al., 2024). Specifically, AQP4 levels are known to be disturbed in neurodegenerative diseases (H. Liu et al., 2024; Yang et al., 2011). Hence, cAMP modulation in astrocytes can influence brain function and the glymphatic system in WT mice; however, this response is disrupted in HD.

In 2021, Zhou and colleagues (Z. Zhou et al., 2021) increased cAMP in hippocampal astrocytes using blue activated PAC transgenic mouse lines and facilitated memory formation via NMDAR-dependent plasticity. In light of this and our previous results, we expressed DdPAC in M2 cortical astrocytes and evaluate motor behaviour after sustained stimulation. Yet, we first demonstrated that a 10-minute stimulation was sufficient to elicit detectable

changes in spontaneous behaviour in R6/1, but not in WT mice, specifically inducing stereotypic grooming. Grooming is an innate behaviour in mice and is known to be increased in HD, where the development of stereotypical behaviours likely indicates cortico-striatal dysfunction (Fernández-García et al., 2020). Notably, after repetitive DdPAC stimulation, motor learning was improved in WT mice. Indeed, alterations in astrocyte-neuron communication have been shown to impair motor learning while sparing locomotion and motor coordination (Lundquist et al., 2022). Accordingly, divergent responses were observed in DdPAC stimulated R6/1 mice, which did not improve motor learning and impaired their coordination. In Zhou's study (Z. Zhou et al., 2021), they reported that the effects of cAMP elevation vary depending on the timing of the stimulation in the context of memory, with increased cAMP levels disrupting memory retention. These findings highlight that the impact of astrocytic cAMP modulation is highly context-dependent, suggesting that its effects may be influenced by the synaptic molecular and disease-related environment. Additionally, alterations in astrocytic function and cAMP signalling are known in HD (Diaz-Castro et al., 2019; Gines et al., 2003; Kelly, 2018; Tyebji et al., 2015; Villanueva et al., 2023), which may be influencing DdPAC response.

The striatum, along with the cortex, is one of the regions most affected in HD. Consequently, we aimed to investigate the effects of DdPAC expression specifically in astrocytes within the striatum of R6/1 mice. In this context, we observed that an acute stimulation of DdPAC increased anxiety-like behaviour in R6/1, and impaired coordination in both WT and R6/1 mice. Furthermore, no improvement was observed in any of the tests performed. This data could be explained by another recently published study (X. Yu et al., 2020). In it, it was suggested that cAMP signalling in striatal astrocytes might include an inhibition of the GPCRi receptor in R6/2 mice, thereby increasing cAMP signalling. Still, more studies should be performed in order to known if astrocytes in the cortex of HD may also exhibit inhibited GPCRi signalling.

Furthermore, after both cortical and striatal DdPAC stimulation and behavioural experiments, we aimed to study the status of astrocytes in this samples. In both cases, we observed an increase in GFAP expression in DdPAC-activated astrocytes from WT mice. However, DdPAC stimulation in hippocampal astrocytes from WT mice in AD experiments, did not show differences in GFAP expression. Furthermore, only striatal astrocytes from R6/1 displayed also this increase. This astrocyte reactivity aligns with our previous results in which we observe modulation of the cytoskeleton after DdPAC-mediated cAMP increase. Other studies further support this idea, as it was observed that after increasing cAMP levels, RhoA phosphorylation, a key GTPase in cytoskeleton regulation, increased the hippocampus of R6/1 mice (Miguez et al., 2015). However, we observe regional heterogeneity, suggesting that astrocytes in the striatum, cortex, and hippocampus may respond differently to cAMP modulation, likely due to intrinsic molecular and functional differences. Notably, several studies highlight significant regional differences in astrocyte function. For instance, astrocytes exhibit diverse molecular profiles in different brain regions, with unique subtypes

contributing to synapse regulation and responses to stimuli (Bocci et al., 2016; Kruyer, 2022). Specifically, astrocytes can display distinct calcium flux patters and synaptic associations (Augusto-Oliveira et al., 2020; Kruyer, 2022; Martín et al., 2015), which may explain varying responses to cAMP modulation in different regions. The observed variability in response across brain regions further supports the idea that astrocytes are a heterogeneous population, whose functional diversity influences both disease mechanisms and the efficacy of therapeutic interventions.

In conclusion, our findings highlight the complex role of astrocytic cAMP modulation in HD. We demonstrated that cAMP modulation can influence whole brain function and behaviour, but with differential responses depending on the brain region and between WT and R6/1 mice. While astrocytic cAMP signalling shows potential as therapeutic strategy, our results underscore the importance of considering regional heterogeneity and the context-dependent nature of astrocytic responses. These findings emphasise the need for region-, cell-type specific therapeutic responses in HD.

Notably, we also demonstrated the ability of DCS to non-invasively detect differential CBF responses in vivo in HD. While these results support a role for astrocytic cAMP in regulating neurovascular coupling, they also underscore the potential of this technique for assessing brain-wide cortical responses. Blood flow can be visualised using DCS in an intact skull, by analysing the intensity fluctuations of laser light caused by the scattering of red blood cells (Sdobnov et al., 2024). A blue-light illumination of ChR2 in cortical neurons has proved that increased neuronal activity can be translated as increased hemodynamics and monitored through DCS. Neuronal activation has been related to the hemodynamic response *in vivo*, which has been studied using functional magnetic resonance imaging, based on the BOLD signal (Ogawa et al., 1993). Nevertheless, MRI is a costly and complex technique that demands significant expertise and specialized equipment. Thus, DCS could serve as a more affordable and accessible alternative for studying brain function.

6. cAMP modulation in neurons and astrocytes from Alzheimer's Disease

AD represents the most prevalent neurodegenerative disorder, with its incidence expected to rise due to global population aging (Schneider et al., 2009). Currently, no cure exists for AD, highlighting the need for novel therapeutic strategies. Synaptic plasticity impairments are central to AD pathology, leading to cognitive deficits and memory loss (Koss et al., 2016; Querfurth & LaFerla, 2010). The hippocampus, crucial for learning and memory, is particularly vulnerable, exhibiting significant neuronal degeneration and synaptic dysfunction in AD patients. cAMP is essential to synaptic plasticity and memory formation within hippocampal neurons. Increase in neuronal cAMP signalling have been associated with enhanced LTP and improved cognitive function (Glazewski et al., 1999; Kandel, 2012; Zamarbide et al., 2019). Astrocytes also use cAMP signalling to modulate neuronal activity, and disruptions in astrocytic cAMP pathways have been implicated in neurodegenerative processes (Sobolczyk & Boczek, 2022). Furthermore, modulation of hippocampal neurons

with bPAC has shown to modulate memory in mice (Z. Zhou et al., 2019). Building upon this information and our prior findings, which underscored the importance of the molecular context and brain region when modulating cAMP signalling, we investigated the effects of DdPAC-mediated cAMP increase in both neurons and astrocytes within the context of AD and in the hippocampus.

Aβ plaque accumulation and gliosis are main signatures of AD pathology (Braak & Braak, 1991; J. A. Hardy & Higgins, 1992; Stelzmann et al., 1995). Assessing these markers is crucial, as Aβ aggregation drives neurotoxicity, while reactive gliosis reflects neuroinflammation, both contributing to synaptic dysfunction and disease progression in AD. 24 hours after DdPAC stimulation, we observed that GFAP expression was elevated in both neuronal and astrocytic GFP histological analysis from 5xFAD compared to WT, consistent with the well-documented astrogliosis in AD (Fakhoury, 2017; Matsuoka et al., 2001). Interestingly, DdPAC-mediated cAMP increase in astrocytes did not alter GFAP levels in whole hippocampal slices from WT mice, but increased GFAP protein expression in our proteomic samples, confirming that cAMP is modulating GFAP expression in astrocytes, as observed in previous experiments. However, DdPAC activation in astrocytes from 5xFAD mice, significantly reduced GFAP expression in slices from 5xFAD astrocytes, and no differences were observed in GFAP protein expression. This suggests that astrocytic reactivity in AD may be partially modulated by cAMP signalling. Some studies reported GFAP modulation through cAMP signalling (Shafit-Zagardo et al., 1988), and cAMP in astrocytes is known to mediate inflammatory processes through NFKβ increase (Ageeva et al., 2024; Z. Zhou et al., 2019), though available data on this mechanism remains limited. Furthermore, it supports our hypothesis that the regional and molecular context influences the outcome of cAMP signalling modulation, as we previously observed no major changes in GFAP expression in the cortex but increase GFAP expression in the striatum of R6/1 mice. Conversely, neuronal DdPAC stimulation had no effect on GFAP expression, indicated by both our histological and proteomic analyses, suggesting that astrocytic reactivity was not indirectly affected by neuronal cAMP modulation. This further highlights the potential cell-specific response, where direct cAMP regulation in astrocytes is required to modulate astrogliosis. These findings support the idea that targeting astrocytic cAMP pathways could be a promising strategy to mitigate neuroinflammation in AD, potentially improving the glial environment and restoring synaptic function.

To further investigate the inflammatory state in the hippocampus, we next studied Iba1 expression, specifically in the dentate gyrus and CA1 regions, both known to be highly affected in AD (Nairuz et al., 2024). Iba1, a microglial marker, plays a critical role in the identification of microglial activation, which is an indicator of neuroinflammation. After DdPAC activation in astrocytes, we did not observe significant changes in Iba1 expression in the histological analysis from CA1 region, suggesting that cAMP modulation in astrocytes might not be impacting microglial activation in this specific hippocampal area. However, we did observe a modest effect in the DG, although differences were not striking. Still, genotype

differences were not observed in our histological data, limiting our ability to interpret these results. Importantly, these differences were confirmed with our proteomic analyses, in which Iba1 expression is increased in both WT and 5xFAD samples. Notably, DdPAC stimulation in neurons resulted in decreased Iba1 expression in histological analysis from the CA1 region of the hippocampus, indicating that neuronal cAMP elevation may have an inhibitory effect on microglial activation. Indeed, it is known that neurons communicate with microglia through the release of fractalkine, a known microglial chemoattractant, which could be modulated by cAMP signalling (Eyo et al., 2016; Harrison et al., 1998). Interestingly, fractalkine has been seen to be modulated by cAMP signalling in mesangial cells, which indicates that this mechanism could be shared with neurons (Y.-M. Chen et al., 2003). Indeed, our proteomic analyses indicate that fractalkine is differentially increase in our samples, further supporting our hypothesis. We did not observe differences in microglial activation in the DG following DdPAC activation of neurons, neither in our histological or proteomic analysis. However, similar to our previous findings, this interpretation should be considered with caution, as no genotype differences were observed in this group. While our analysis focused on GFAP and Iba1 expression levels, studying their morphological changes would provide a more detailed insights into glial activation. Astrocytes and microglia undergo characteristic morphological alterations in response to neuroinflammation, which correlate with functional changes, such as Aβ clearance, cytokine release, and neuroinflammation modulation.

We then assessed Aβ deposits in AD mice. We observed no changes in plaque depositions in the hippocampus where DdPAC was activated in neurons, suggesting that neuronal cAMP elevation does not directly impact Aβ plaque formation nor elimination. Furthermore, microglia are crucial for the clearance of Aβ plaques through several mechanisms, including phagocytosis (Y. Huang et al., 2021). When activated, microglia can migrate toward plaques and engulf Aβ, thereby reducing plaque load. In our study, DdPAC activation in neurons led to a decrease in microglial activation, aligning with our results on unaltered Aβ depositions. In contrast, DdPAC stimulation in astrocytes led to a significant reduction in both the number and percentage of Aβ plaques in the hippocampus. The reduction of Aβ plaques observed after DdPAC-mediated cAMP increase in astrocytes from 5xFAD mice could be linked to several mechanisms. Astrocytes play a key role in Aβ clearance through phagocytosis and secretion of Aβ-degrading enzymes (C.-C. Liu et al., 2017; Ries & Sastre, 2016). Elevated cAMP could be enhancing these clearance pathways, leading to a reduction in plaque deposition. Moreover, the observed decrease in GFAP expression in DdPAC-activated astrocytes may reduce astrogliosis, which could promote a more functional, less reactive astrocytic phenotype, thereby facilitating Aβ clearance. Previously, we hypothesised that the lack of altered plaque deposition in tissue where DdPAC was activated in neurons may be due to decreased microglial activation. Consequently, the third suggested mechanism through which we might be observing reduced Aβ deposition in tissue where DdPAC was activated in astrocytes could be the increase in Iba1 expression, as observed in our proteomic analysis. Therefore, cAMP-mediated astrocytic activation could be promoting Aβ clearance,

potentially through both release of Aβ-degrading enzymes and microglial engulfment of Aβ deposits, ultimately reducing plaque burden in 5xFAD mice.

To further investigate the mechanisms underlying the observed changes, we performed a more detailed analysis of the proteomic data. Proteomic analysis of DdPAC-activated astrocytes confirmed distinct profiles in WT and 5xFAD mice, with DdPAC inducing protein changes in both groups. Notably, WT DdPAC resembled 5xFAD GFP group, suggesting activation of pathways altered in 5xFAD pathology. However, proteomic analyses of tissue where DdPAC was activated in neurons revealed only genotype differences, with the proteomic shift induced by DdPAC being minimal. In line with this, DdPAC activation in astrocytes of WT mice induced a greater proteomic shift than in neurons, supporting our hypothesis that astrocytic cAMP modulation leads to broader brain-wide changes than neuronal modulation. Furthermore, the widespread effects of astrocytic cAMP modulation may be due to their extensive networks, allowing them to regulate multiple neuronal circuits and interactions with other glial cells. However, in 5xFAD mice, neuronal DdPAC activation resulted in a stronger proteomic shift than astrocytic activation, suggesting disease-specific alterations in cAMP signalling. These results may arise from astrocytic dysfunction in 5xFAD pathology (González-Reyes et al., 2017), known to have disrupted gliotransmission, neurotransmitter uptake, and altered calcium signalling due to Aβ deposits (Makitani et al., 2017; Matos et al., 2012; Mitew et al., 2013). Alternatively, neuronal cAMP signalling in 5xFAD mice might be more responsive due to compensatory mechanisms or altered cAMP regulation.

Since DdPAC modulates cAMP, we investigated the PKA interactome to better understand the direct consequences of DdPAC activation in both astrocytes and neurons. The differential impact of DdPAC activation on the PKA interactome in WT and 5xFAD mice highlights the complex role of astrocytes and neurons in regulating cAMP signalling pathways. In WT mice, the activation of DdPAC in astrocytes induced a larger PKA interactome shift than in neurons, suggesting that astrocytes may play a more central role in modulating the cAMP-PKA pathway at whole-tissue level. In contrast, in 5xFAD mice, DdPAC activation in neurons elicited a more significant effect on the PKA interactome than in astrocytes. Again, this could be reflecting compensatory mechanisms in neurons that are adapting to the pathological changes in AD, which may amplify the cAMP response in neurons. Additionally, the restricted and more focused PRKACA interactome in astrocytes in 5xFAD mice, compared to the broader interaction network in WT astrocytes, suggests that astrocytes may become less responsive to cAMP modulation in the context of neurodegeneration.

At a functional level, the proteins identified in the PKA interactome and gene ontology analysis of DdPAC-activated astrocytes, associated with the entire set of differential proteins, reveal similar functional trends both in WT and 5xFAD samples, particularly in cytoskeleton and immune function. However, in WT mice, changes in synaptic plasticity are also observed, while in 5xFAD mice, such changes appear less pronounced. In 5xFAD mice, the alterations

observed in immune response and gliosis might overshadow potential changes in synaptic plasticity, as these processes are already dysregulated in the context of AD pathology (Oakley et al., 2006; Westi et al., 2024). The neuroinflammatory environment could interfere with normal plasticity mechanisms that are usually present in healthy neurons. This increased immune response may impair normal signalling pathways required for plasticity, masking potential changes in neuronal function (Boulanger & Shatz, 2004). To confirm this hypothesis, further functional analysis, such as electrophysiological assessments of synaptic plasticity, would be necessary. In the case of DdPAC activation in neurons, synaptic plasticity remains the primary functional change observed in both WT and 5xFAD mice. In WT mice, this aligns with the expected role of cAMP signalling in the hippocampus, regulating synaptic strength and plasticity, which are crucial for learning and memory. However, in 5xFAD mice, while synaptic plasticity remains modulated, the primary change appears to be more pronounced cytoskeleton regulation. In 5xFAD, DdPAC-activated astrocytes also appear to prioritise immune response and glial activation over plasticity. The shift could be due to the pre-existing pathological state in the 5xFAD mice, where neuroinflammation and gliosis are already prominent. Thus, in both neurons and astrocytes, DdPAC activation in 5xFAD mice could be triggering compensatory mechanisms that focus more on maintaining cellular integrity and responding to stress, rather than promoting synaptic plasticity. This shift may suggest that the pathological environment in 5xFAD mice alters normal astrocytic and neuronal responses to cAMP signalling. Behavioural studies could help disentangle how these proteomic changes translate into a functional response.

In summary, these findings highlight the differential roles of cAMP-driven modulation in astrocytes and neurons and suggest that the cellular response to cAMP signalling interventions is influenced by the underlying health status, potentially varying in the context of neurodegenerative pathology. In astrocytes, DdPAC activation in 5xFAD mice reduced Aβ plaque depositions and reduced GFAP expression, suggesting that enhancing cAMP signalling in astrocytes could promote Aβ clearance and reduce astrogliosis, which is known to contribute to neuroinflammation and synaptic dysfunction in AD. These changes seem mainly driven by modulation of the cytoskeleton and immune response. In neurons, DdPAC activation modulated synaptic plasticity proteins in both WT and 5xFAD mice, but with a less pronounced effect in 5xFAD mice, which also show markers of cytoskeleton regulation and inflammation, likely due to pre-existing neuroinflammation. Moreover, the reduced microglial activation observed following neuronal DdPAC activation seems to limit its capacity to reduce Aβ deposition. These findings underline the complexity of cAMP signalling in AD and point to the need for a targeted, cell-specific approach in future therapeutic interventions.

7. Main findings and scientific relevance

In summary, this thesis provides new insights into the cAMP signalling pathway through the use of DdPAC, offering a deeper understanding of its specific role in synaptic plasticity and in the context of the neurodegenerative diseases HD and AD. First, our data demonstrates the involvement of neuronal cAMP in M2 cortical behaviours and reveal altered neuronal cAMP dynamics in HD mice. Additionally, we identify early motor and psychiatric M2-cortex related impairments, highlighting the potential for early therapeutic intervention. To facilitate in vivo application, we establish a minimally invasive method for AAV delivery that successfully achieves transgene expression in specific cell types and mouse strains. Notably, we demonstrate that DdPAC-mediated modulation of cAMP signalling can enhance synaptic plasticity in the cortex, particularly when activated in astrocytes, thereby positioning DdPAC as a powerful tool for plasticity modulation. In the context of neurodegeneration, DdPAC activation in HD and AD models produces differential effects: in HD cortical astrocyte activation improves motor learning in WT but impairs coordination in HD mice, while striatal astrocyte activation disrupts coordination in both. In AD, increasing cAMP in hippocampal astrocytes reduces astrogliosis and Aβ deposits, whereas neuronal activation decreases microglial reactivity. Proteomic analysis of hippocampal samples reveals distinct DdPAC-driven proteomic changes in neurons and astrocytes, as well as between WT and AD mice, linking cAMP-PKA pathway activation to synaptic plasticity and immune responses.

In conclusion, we present a novel tool to modulate cAMP signalling in vivo, uncovering its cell-specific roles and alterations under pathological conditions. Moreover, we propose cAMP signalling as a promising target for therapeutic modulation in neurodegenerative diseases through the use of DdPAC. Our findings demonstrate that DdPAC-mediated cAMP modulation in both neurons and astrocytes significantly influences neuronal plasticity, while also highlighting its cell-type-specific effects, as astrocytic cAMP-PKA modulation leads to broader effects than neuronal cAMP-PKA. Moreover, our results emphasise the critical role of brain region and molecular environment in determining the outcomes of cAMP modulation, as DdPAC activation elicits distinct effects in the cortex, striatum, and hippocampus, and depending on the disease state. Finally, we provide strong evidence supporting DdPAC as a versatile tool for modulating cAMP-PKA signalling, with potential application in both neuroscience research and therapeutic development.

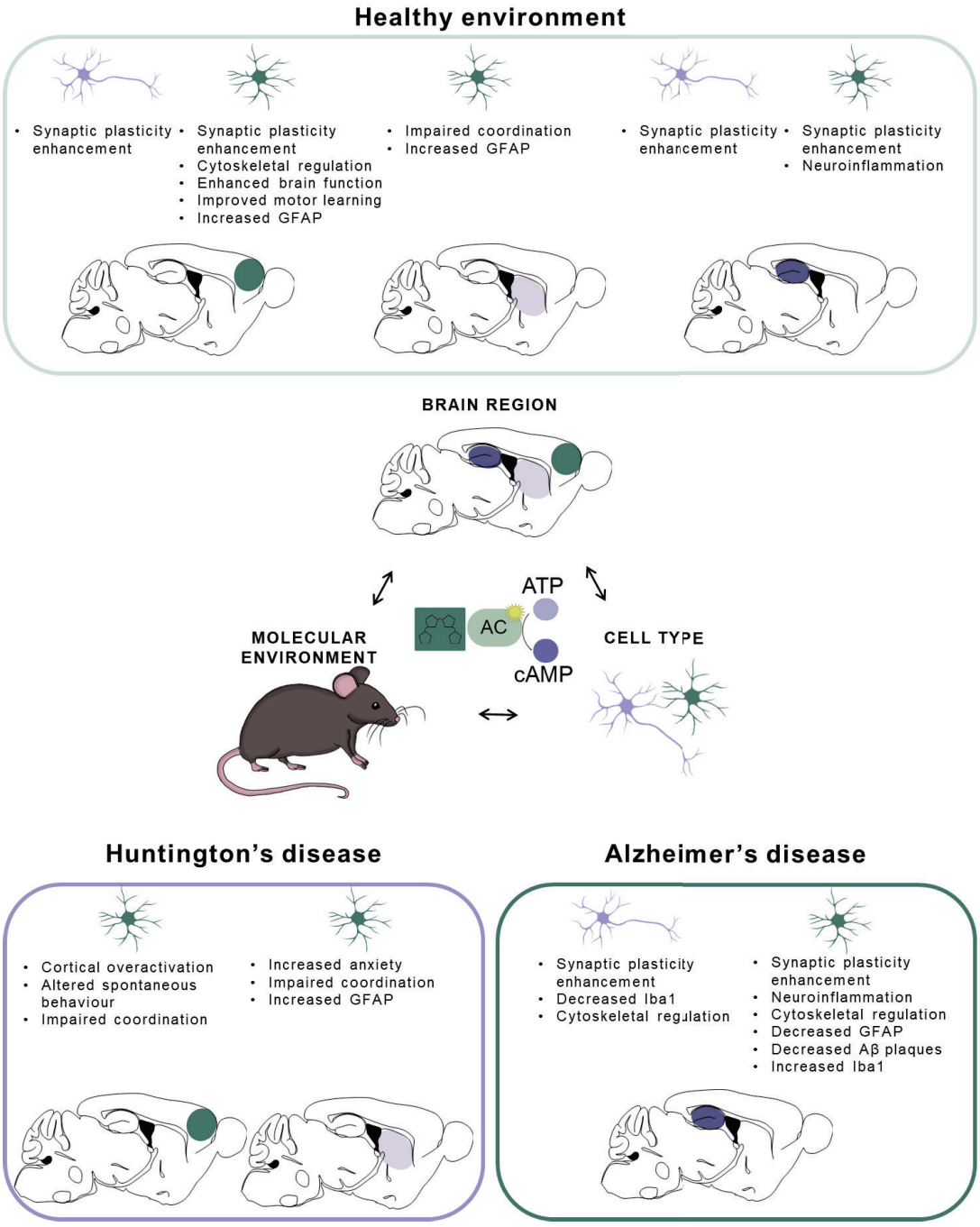

Figure 64. DdPAC-mediated cAMP effects are dependent on cell type, brain region and healthy or pathological context. Summary of key findings from behavioural, electrophysiological, proteomic, metabolomic, and histological analyses following DdPAC activation in neurons or astrocytes, from the cortex, striatum, or hippocampus, from WT, HD, or AD mice.

CONCLUSIONS

The main conclusions drawn from the results presented in this thesis are as follows:

1. Neuronal cAMP signalling plays a significant role in M2-cortex-associated behaviours, as evidenced by the increased cAMP levels during motor learning and beetle mania tasks in mice.
2. Alterations in neuronal cAMP dynamics during M2 cortex-dependent tasks are present in the R6/1 mouse model of Huntington's Disease, with the extend of these impairments being stage-dependent. However, these changes do not appear to correlate with behavioural alterations in the R6/1 mice.
3. Fine motor deficits and anhedonia-like behaviours, both linked to the M2 cortex, are evident at early stages of HD, preceding the onset of major motor symptoms and highlighting the potential for early therapeutic interventions.
4. The AAV serotype PHP.eB, but not AAV9, enable widespread construct expression in the brain via a minimally invasive retroorbital administration route, which can efficiently target specific cell types and different mouse strains.
5. Red-light stimulation of cortical DdPAC induces synaptic potentiation in both neurons and astrocytes, with a more pronounced effect after activation in astrocytes.
6. Astrocytic DdPAC-induced LTP is PKA- and NMDAR-dependent, calcium-independent, and requires a synaptic stimulus for induction.
7. DdPAC stimulation in M2 cortical astrocytes impacts on synaptic plasticity and cytoskeletal protein phosphorylation pathways in diverse brain cells within minutes.
8. DdPAC activation in astrocytes leads to an aberrant increase in cortical hemodynamics in R6/1 mice.
9. Repetitive DdPAC-mediated cAMP increase in cortical astrocytes is able to enhance motor learning in WT mice, but further impairs coordination in R6/1 mice.
10. Repetitive DdPAC-mediated cAMP increase in striatal astrocytes impairs coordination in WT mice and exacerbates its alterations in R6/1 mice.
11. Acute increase of DdPAC-mediated cAMP in hippocampal astrocytes reduces Alzheimer's Disease neuropathological hallmarks, such as astrogliosis and Aβ deposits, in 5xFAD mice, whereas no such effect is observed when cAMP levels are increased in neurons.
12. The outcomes of DdPAC-mediated cAMP elevation in the hippocampus differ between neurons and astrocytes. Neuronal DdPAC activation is confined to modulating synaptic plasticity, while astrocytic DdPAC activation induces broad responses, including synaptic plasticity together with glial and immune system activation.
13. The molecular and behavioural outcomes of cAMP modulation are influenced by brain region, underlying molecular impairments, and cell type. Thus, while DdPAC represents a versatile tool for modulating cAMP-PKA signalling at multiple levels, with potential applications in neuroscience research and therapeutic development, these factors must be carefully considered when designing novel therapeutic interventions for neurodegenerative diseases.

BIBLIOGRAPHY

Abe, Y., Kwon, S., Oishi, M., Unekawa, M., Takata, N., Seki, F., Koyama, R., Abe, M., Sakimura, K., Masamoto, K., Tomita, Y., Okano, H., Mushiake, H., & Tanaka, K. F. (2021). Optical manipulation of local cerebral blood flow in the deep brain of freely moving mice. *Cell Reports*, *36*(4). https://doi.org/10.1016/j.celrep.2021.109427

Adamsky, A., Kol, A., Kreisel, T., Doron, A., Ozeri-Engelhard, N., Melcer, T., Refaeli, R., Horn, H., Regev, L., Groysman, M., London, M., & Goshen, I. (2018). Astrocytic Activation Generates De Novo Neuronal Potentiation and Memory Enhancement. *Cell*, *174*(1), 59-71.e14. https://doi.org/10.1016/j.cell.2018.05.002

Agarwal, A., Wu, P.-H., Hughes, E. G., Fukaya, M., Tischfield, M. A., Langseth, A. J., Wirtz, D., & Bergles, D. E. (2017). Transient Opening of the Mitochondrial Permeability Transition Pore Induces Microdomain Calcium Transients in Astrocyte Processes. *Neuron*, *93*(3), 587-605.e7. https://doi.org/10.1016/j.neuron.2016.12.034

Agbandje-McKenna, M., & Kleinschmidt, J. (2011). AAV capsid structure and cell interactions. *Methods in Molecular Biology (Clifton, N.J.)*, *807*, 47–92. https://doi.org/10.1007/978-1-61779-370-7_3

Ageeva, T., Rizvanov, A., & Mukhamedshina, Y. (2024). NF-κB and JAK/STAT Signaling Pathways as Crucial Regulators of Neuroinflammation and Astrocyte Modulation in Spinal Cord Injury. *Cells*, *13*(7). https://doi.org/10.3390/cells13070581

Agulhon, C., Petravicz, J., McMullen, A. B., Sweger, E. J., Minton, S. K., Taves, S. R., Casper, K. B., Fiacco, T. A., & McCarthy, K. D. (2008). What Is the Role of Astrocyte Calcium in Neurophysiology? *Neuron*, *59*(6), 932–946. https://doi.org/10.1016/j.neuron.2008.09.004

Ahmad, R., Bourgeois, S., Postnov, A., Schmidt, M. E., Bormans, G., Van Laere, K., & Vandenberghe, W. (2014). PET imaging shows loss of striatal PDE10A in patients with Huntington disease. *Neurology*, *82*(3), 279–281. https://doi.org/10.1212/WNL.0000000000000037

Ahmadpour, N., Kantroo, M., Stobart, M. J., Meza-Resillas, J., Shabanipour, S., Parra-Nuñez, J., Salamovska, T., Muzaleva, A., O'Hara, F., Erickson, D., Di Gaetano, B., Carrion-Falgarona, S., Weber, B., Lamont, A., Lavine, N. E., Kauppinen, T. M., Jackson, M. F., & Stobart, J. L. (2024). Cortical astrocyte N-methyl-D-aspartate receptors influence whisker barrel activity and sensory discrimination in mice. *Nature Communications*, *15*(1). https://doi.org/10.1038/s41467-024-45989-3

Albin, R. L., Reiner, A., Anderson, K. D., Dure, L. S., Handelin, B., Balfour, R., Whetsell, W. O., Penney, J. B., & Young, A. B. (1992). Preferential loss of striato-external pallidal projection neurons in presymptomatic Huntington's Disease. *Annals of Neurology*, *31*(4), 425–430. https://doi.org/10.1002/ana.410310412

Alcalá-Barraza, S. R., Lee, M. S., Hanson, L. R., McDonald, A. A., Frey, W. H., & McLoon, L. K. (2010). Intranasal delivery of neurotrophic factors BDNF, CNTF, EPO, and NT-4 to the CNS. *Journal of Drug Targeting*, *18*(3), 179–190. https://doi.org/10.3109/10611860903318134

Alexander, G. M., He, B., Leikvoll, A., Jones, S., Wine, R., Kara, P., Martin, N., & Dudek, S. M. (2024). Hippocampal CA2 neurons disproportionately express AAV-delivered genetic cargo. *BioRxiv : The Preprint Server for Biology*. https://doi.org/10.1101/2024.11.27.625768

Almada, R. C., Genewsky, A. J., Heinz, D. E., Kaplick, P. M., Coimbra, N. C., & Wotjak, C. T. (2018). Stimulation of the Nigrotectal Pathway at the Level of the Superior Colliculus Reduces Threat Recognition and Causes a Shift From Avoidance to Approach Behavior. *Frontiers in Neural Circuits*, *12*, 36. https://doi.org/10.3389/fncir.2018.00036

Alvarez, J. I., Katayama, T., & Prat, A. (2013). Glial influence on the blood brain barrier. In *GLIA* (Vol. 61, Issue 12, pp. 1939–1958). https://doi.org/10.1002/glia.22575

Amiry-Moghaddam, M., & Ottersen, O. P. (2003). The molecular basis of water transport in the brain. *Nature Reviews. Neuroscience*, *4*(12), 991–1001. https://doi.org/10.1038/nrn1252

Andersson, M., Blomstrand, F., & Hanse, E. (2007). Astrocytes play a critical role in transient heterosynaptic depression in the rat hippocampal CA1 region. *Journal of Physiology*, *585*(3), 843–852. https://doi.org/10.1113/jphysiol.2007.142737

Angelopoulou, E., Pyrgelis, E. S., & Piperi, C. (2022). Emerging Potential of the Phosphodiesterase (PDE) Inhibitor Ibudilast for Neurodegenerative Diseases: An Update on Preclinical and Clinical Evidence. In *Molecules* (Vol. 27, Issue 23). MDPI. https://doi.org/10.3390/molecules27238448

Anglada-Huguet, M., Giralt, A., Rué, L., Alberch, J., & Xifró, X. (2016). Loss of striatal 90-kDa ribosomal S6 kinase (Rsk) is a key factor for motor, synaptic and transcription dysfunction in Huntington's Disease. *Biochimica et Biophysica Acta*, *1862*(7), 1255–1266. https://doi.org/10.1016/j.bbadis.2016.04.002

Angoa-Pérez, M., Kane, M. J., Briggs, D. I., Francescutti, D. M., & Kuhn, D. M. (2013). Marble burying and nestlet shredding as tests of repetitive, compulsive-like behaviors in mice. *Journal of Visualized Experiments : JoVE*, *82*, 50978. https://doi.org/10.3791/50978

Ankarcrona, M., Dypbukt, J. M., Bonfoco, E., Zhivotovsky, B., Orrenius, S., Lipton, S. A., & Nicotera, P. (1995). Glutamate-Induced Neuronal Death: A Succession of Necrosis or Apoptosis Depending on Mitochondrial Function. In *Neuron* (Vol. 15).

Araque, A., Carmignoto, G., Haydon, P. G., Oliet, S. H. R., Robitaille, R., & Volterra, A. (2014). Gliotransmitters travel in time and space. In *Neuron* (Vol. 81, Issue 4, pp. 728–739). https://doi.org/10.1016/j.neuron.2014.02.007

Araque, A., Martín, E. D., Perea, G., Arellano, J. I., & Buñ, W. (2002). *Synaptically Released Acetylcholine Evokes Ca 2 Elevations in Astrocytes in Hippocampal Slices*.

Araque, A., Parpura, V., Sanzgiri, R. P., & Haydon, P. G. (1999). Tripartite synapses: glia, the unacknowledged partner. *Trends in Neurosciences*, *22*(5), 208–215. https://doi.org/10.1016/s0166-2236(98)01349-6

Arnold, S. E., Hyman, B. T., Flory, J., Damasio, A. R., & Van Hoesen, G. W. (1991). The topographical and neuroanatomical distribution of neurofibrillary tangles and neuritic plaques in the cerebral cortex of patients with Alzheimer's Disease. *Cerebral Cortex (New York, N.Y. : 1991)*, *1*(1), 103–116. https://doi.org/10.1093/cercor/1.1.103

Arnsten, A. F. T., Datta, D., Del Tredici, K., & Braak, H. (2021). Hypothesis: Tau pathology is an initiating factor in sporadic Alzheimer's Disease. *Alzheimer's and Dementia*, *17*(1), 115–124. https://doi.org/10.1002/alz.12192

Artola, A., & Singer, W. (1993). Long-term depression of excitatory synaptic transmission and its relationship to long-term potentiation. *Trends in Neurosciences*, *16*(11), 480–487. https://doi.org/10.1016/0166-2236(93)90081-v

Aschauer, D. F., Kreuz, S., & Rumpel, S. (2013). Analysis of Transduction Efficiency, Tropism and Axonal Transport of AAV Serotypes 1, 2, 5, 6, 8 and 9 in the Mouse Brain. *PLoS ONE*, *8*(9). https://doi.org/10.1371/journal.pone.0076310

Augusto-Oliveira, M., Arrifano, G. P., Takeda, P. Y., Lopes-Araújo, A., Santos-Sacramento, L., Anthony, D. C., Verkhratsky, A., & Crespo-Lopez, M. E. (2020). Astroglia-specific contributions to the regulation of synapses, cognition and behaviour. *Neuroscience and Biobehavioral Reviews*, *118*, 331–357. https://doi.org/10.1016/j.neubiorev.2020.07.039

Aurnhammer, C., Haase, M., Muether, N., Hausl, M., Rauschhuber, C., Huber, I., Nitschko, H., Busch, U., Sing, A., Ehrhardt, A., & Baiker, A. (2012). Universal real-time PCR for the detection and quantification of adeno-associated virus serotype 2-derived inverted terminal repeat sequences. *Human Gene Therapy Methods*, *23*(1), 18–28. https://doi.org/10.1089/hgtb.2011.034

Azhar Chishti, M., Yang, D.-S., Janus, C., Phinney, A. L., Horne, P., Pearson, J., Strome, R., Zuker, N., Loukides, J., French, J., Turner, S., Lozza, G., Grilli, M., Kunicki, S., line Morissette, C., Paquette, J., Gervais, F., Bergeron, C., Fraser, P. E., … George-Hyslop, S. (2001). Early-onset Amyloid Deposition and Cognitive Deficits in Transgenic Mice Expressing a Double Mutant Form of Amyloid Precursor Protein 695* From the. *Journal of Biological Chemistry*, *276*, 21562–21570. https://doi.org/10.1074/jbc

Bachmann, C., Fischer, L., Walter, U., & Reinhard, M. (1999). The EVH2 domain of the vasodilator-stimulated phosphoprotein mediates tetramerization, F-actin binding, and actin bundle formation. *The Journal of Biological Chemistry*, *274*(33), 23549–23557. https://doi.org/10.1074/jbc.274.33.23549

Ball, M. J. (1977). Neuronal Loss, Neurofibrillary Tangles and Granulovaeuolar Degeneration in the Hippocampus with Ageing and Dementia A Quantitative Study. In *Acta neuropath. (Berl.)* (Vol. 37).

Bansal, A., Shikha, S., & Zhang, Y. (2023). Towards translational optogenetics. In *Nature Biomedical Engineering* (Vol. 7, Issue 4, pp. 349–369). Nature Research. https://doi.org/10.1038/s41551-021-00829-3

Barker, A. T., Jalinous, R., & Freeston, I. L. (1985). Non-invasive magnetic stimulation of human motor cortex. *Lancet (London, England)*, *1*(8437), 1106–1107. https://doi.org/10.1016/s0140-6736(85)92413-4

Barria, A., Muller, D., Derkach, V., Griffith, L. C., & Soderling, T. R. (1997). Regulatory phosphorylation of AMPA-type glutamate receptors by CaM-KII during long-term potentiation. *Science (New York, N.Y.)*, *276*(5321), 2042–2045. https://doi.org/10.1126/science.276.5321.2042

Basu, P., Custodio-Patsey, L., Prasoon, P., Smith, B. N., & Taylor, B. K. (2021). Sex Differences in Protein Kinase A Signaling of the Latent Postoperative Pain Sensitization That Is Masked by Kappa Opioid Receptors in the Spinal Cord. *The Journal of Neuroscience : The Official Journal of the Society for Neuroscience*, *41*(47), 9827–9843. https://doi.org/10.1523/JNEUROSCI.2622-20.2021

Bateman, R. J., Aisen, P. S., De Strooper, B., Fox, N. C., Lemere, C. A., Ringman, J. M., Salloway, S., Sperling, R. A., Windisch, M., & Xiong, C. (2011). Autosomal-dominant Alzheimer's Disease: a review and proposal for the prevention of Alzheimer's Disease. *Alzheimer's Research & Therapy*, *3*(1), 1. https://doi.org/10.1186/alzrt59

Beattie, E. C., Carroll, R. C., Yu, X., Morishita, W., Yasuda, H., von Zastrow, M., & Malenka, R. C. (2000). Regulation of AMPA receptor endocytosis by a signaling mechanism shared with LTD. *Nature Neuroscience*, *3*(12), 1291–1300. https://doi.org/10.1038/81823

Beaumont, V., Zhong, S., Lin, H., Xu, W. J., Bradaia, A., Steidl, E., Gleyzes, M., Wadel, K., Buisson, B., Padovan-Neto, F. E., Chakroborty, S., Ward, K. M., Harms, J. F., Beltran, J., Kwan, M., Ghavami, A., Häggkvist, J., Tóth, M., Halldin, C., … Munoz-Sanjuan, I. (2016). Phosphodiesterase 10A Inhibition Improves Cortico-Basal Ganglia Function in Huntington's Disease Models. *Neuron*, *92*(6), 1220–1237. https://doi.org/10.1016/j.neuron.2016.10.064

Beck, S. E., Jones, L. A., Chesnut, K., Walsh, S. M., Reynolds, T. C., Carter, B. J., Askin, F. B., Flotte, T. R., & Guggino, W. B. (1999). Repeated delivery of adeno-associated virus vectors to the rabbit airway. *Journal of Virology*, *73*(11), 9446–9455. https://doi.org/10.1128/JVI.73.11.9446-9455.1999

Bélanger, M., Allaman, I., & Magistretti, P. J. (2011). Brain energy metabolism: Focus on Astrocyte-neuron metabolic cooperation. In *Cell Metabolism* (Vol. 14, Issue 6, pp. 724–738). https://doi.org/10.1016/j.cmet.2011.08.016

Bell, C. L., Gurda, B. L., Van Vliet, K., Agbandje-McKenna, M., & Wilson, J. M. (2012). Identification of the Galactose Binding Domain of the Adeno-Associated Virus Serotype 9 Capsid. *Journal of Virology*, *86*(13), 7326–7333. https://doi.org/10.1128/jvi.00448-12

Bellenguez, C., Charbonnier, C., Grenier-Boley, B., Quenez, O., Le Guennec, K., Nicolas, G., Chauhan, G., Wallon, D., Rousseau, S., Richard, A. C., Boland, A., Bourque, G., Munter, H. M., Olaso, R., Meyer, V., Rollin-Sillaire, A., Pasquier, F., Letenneur, L., Redon, R., … Jurici, S. (2017). Contribution to Alzheimer's Disease risk of rare variants in TREM2, SORL1, and ABCA7 in 1779 cases and 1273 controls. *Neurobiology of Aging*, *59*, 220.e1-220.e9. https://doi.org/10.1016/j.neurobiolaging.2017.07.001

Benarroch, E. E. (2018). Glutamatergic synaptic plasticity and dysfunction in Alzheimer disease: Emerging mechanisms. *Neurology*, *91*(3), 125–132. https://doi.org/10.1212/WNL.0000000000005807

Benito, E., & Barco, A. (2010). CREB's control of intrinsic and synaptic plasticity: implications for CREB-dependent memory models. *Trends in Neurosciences*, *33*(5), 230–240. https://doi.org/10.1016/j.tins.2010.02.001

Bertram, L., Lill, C. M., & Tanzi, R. E. (2010). The genetics of alzheimer disease: Back to the future. In *Neuron* (Vol. 68, Issue 2, pp. 270–281). https://doi.org/10.1016/j.neuron.2010.10.013

Bezzi, P., Carmignoto, G., Pasti, L., Vesce, S., Rossi, D., Rizzini, B. L., Pozzan, T., & Volterra, A. (1998). Prostaglandins stimulate calcium-dependent glutamate release in astrocytes. *Nature*, *391*(6664), 281–285. https://doi.org/10.1038/34651

Bielenberg, M., Kurelic, R., Frantz, S., & Nikolaev, V. O. (2024). A mini-review: phosphodiesterases in charge to balance intracellular cAMP during T-cell activation. *Frontiers in Immunology*, *15*, 1365484. https://doi.org/10.3389/fimmu.2024.1365484

Bliss, T. V. P., Collingridge, G. L., Kaang, B. K., & Zhuo, M. (2016). Synaptic plasticity in the anterior cingulate cortex in acute and chronic pain. In *Nature Reviews Neuroscience* (Vol. 17, Issue 8, pp. 485–496). Nature Publishing Group. https://doi.org/10.1038/nrn.2016.68

Bliss, T. V. P., & L0mo, T. (1973). LONG-LASTING POTENTIATION OF SYNAPTIC TRANSMISSION IN THE DENTATE AREA OF THE ANAESTHETIZED RABBIT FOLLOWING STIMULATION OF THE PERFORANT PATH. In *J. Physiol* (Vol. 232).

Bliss, T. V, & Collingridge, G. L. (1993). A synaptic model of memory: long-term potentiation in the hippocampus. *Nature*, *361*(6407), 31–39. https://doi.org/10.1038/361031a0

Blumenstock, S., & Dudanova, I. (2020). Cortical and Striatal Circuits in Huntington's Disease. *Frontiers in Neuroscience*, *14*(February). https://doi.org/10.3389/fnins.2020.00082

Bocci, T., Hensghens, M. J. M., Di Rollo, A., Parenti, L., Barloscio, D., Rossi, S., & Sartucci, F. (2016). Impaired interhemispheric processing in early Huntington's Disease: A transcranial magnetic stimulation study. *Clinical Neurophysiology : Official Journal of the International Federation of Clinical Neurophysiology*, *127*(2), 1750–1752. https://doi.org/10.1016/j.clinph.2015.10.036

Boecker, H., Ceballos-Baumann, A., Bartenstein, P., Weindl, A., Siebner, H. R., Fassbender, T., Munz, F., Schwaiger, M., & Conrad, B. (1999). Investigations with 3D H 2 15 O-PET. In *Brain* (Vol. 122).

Bohlen, C. J., Friedman, B. A., Dejanovic, B., & Sheng, M. (2025). Annual Review of Genetics Microglia in Brain Development, Homeostasis, and Neurodegeneration. *Downloaded from Www.Annualreviews.Org. Guest*. https://doi.org/10.1146/annurev-genet-112618

Bohnsack, M. T., Czaplinski, K., & Gorlich, D. (2004). Exportin 5 is a RanGTP-dependent dsRNA-binding protein that mediates nuclear export of pre-miRNAs. *RNA (New York, N.Y.)*, *10*(2), 185–191. https://doi.org/10.1261/rna.5167604

Bolivar, V. J., Manley, K., & Messer, A. (2004). Early exploratory behavior abnormalities in R6/1 Huntington's Disease transgenic mice. *Brain Research*, *1005*(1–2), 29–35. https://doi.org/10.1016/j.brainres.2004.01.021

Bonansco, C., Couve, A., Perea, G., Ferradas, C. Á., Roncagliolo, M., & Fuenzalida, M. (2011). Glutamate released spontaneously from astrocytes sets the threshold for synaptic plasticity. *European Journal of Neuroscience*, *33*(8), 1483–1492. https://doi.org/10.1111/j.1460-9568.2011.07631.x

Bonkale, W. L., Fastbom, J., Wiehager ', B., Ravid, R., Winblad ', B., & Cowburn ' "* ' Karo~in, R. F. (1996). Impaired G-protein-stimulated adenylyl cyclase activity in Alzheimer's Disease brain is not accompanied by reduced cyclic-AMP-dependent protein kinase A activity. In *Brain Research* (Vol. 737). ELSEVIER.

Bonkale, W. L., Fastbom, J., Wiehager, B., Ravid, R., Winblad, B., & Cowburn, R. F. (1996). Impaired G-protein-stimulated adenylyl cyclase activity in Alzheimer's Disease brain is not accompanied by reduced cyclic-AMP-dependent protein kinase A activity. *Brain Research*, *737*(1–2), 155–161. https://doi.org/10.1016/0006-8993(96)00724-x

Bos, J. L. (2003). Epac: a new cAMP target and new avenues in cAMP research. *Nature Reviews. Molecular Cell Biology*, *4*(9), 733–738. https://doi.org/10.1038/nrm1197

Bouet, V., Boulouard, M., Toutain, J., Divoux, D., Bernaudin, M., Schumann-Bard, P., & Freret, T. (2009). The adhesive removal test: A sensitive method to assess sensorimotor deficits in mice. *Nature Protocols*, *4*(10), 1560–1564. https://doi.org/10.1038/nprot.2009.125

Boulanger, L. M., & Shatz, C. J. (2004). Immune signalling in neural development, synaptic plasticity and disease. *Nature Reviews. Neuroscience*, *5*(7), 521–531. https://doi.org/10.1038/nrn1428

Boury-Jamot, B., Carrard, A., Martin, J. L., Halfon, O., Magistretti, P. J., & Boutrel, B. (2016). Disrupting astrocyte-neuron lactate transfer persistently reduces conditioned responses to cocaine. *Molecular Psychiatry*, *21*(8), 1070–1076. https://doi.org/10.1038/mp.2015.157

Bowser, D. N., & Khakh, B. S. (2004). ATP excites interneurons and astrocytes to increase synaptic inhibition in neuronal networks. *Journal of Neuroscience*, *24*(39), 8606–8620. https://doi.org/10.1523/JNEUROSCI.2660-04.2004

Boyden, E. S., Zhang, F., Bamberg, E., Nagel, G., & Deisseroth, K. (2005). Millisecond-timescale, genetically targeted optical control of neural activity. *Nature Neuroscience*, *8*(9), 1263–1268. https://doi.org/10.1038/nn1525

Braak, H., & Braak, E. (1991). Acta H ' pathologica Neuropathological stageing of Alzheimer-related changes. In *Acta Neuropathol* (Vol. 82).

Brandt, J. (2018). Behavioral Changes in Huntington Disease. *Cognitive and Behavioral Neurology : Official Journal of the Society for Behavioral and Cognitive Neurology*, *31*(1), 26–35. https://doi.org/10.1097/WNN.0000000000000147

Brandt, J. P., & Ackerman, S. D. (2025). Astrocyte regulation of critical period plasticity across neural circuits. In *Current Opinion in Neurobiology* (Vol. 90). Elsevier Ltd. https://doi.org/10.1016/j.conb.2024.102948

Bredt, D. S., & Nicoll, R. A. (2003). Review AMPA Receptor Trafficking at Excitatory Synapses Characterization of Silent Synapses A resolution came with the discovery of "silent syn-apses" (Durand et al. In *Neuron* (Vol. 40).

Brodaty, H., Breteler, M. M. B., Dekosky, S. T., Dorenlot, P., Fratiglioni, L., Hock, C., Kenigsberg, P. A., Scheltens, P., & De Strooper, B. (2011). The world of dementia

beyond 2020. *Journal of the American Geriatrics Society*, *59*(5), 923–927. https://doi.org/10.1111/j.1532-5415.2011.03365.x

Brooks, S., Higgs, G., Janghra, N., Jones, L., & Dunnett, S. B. (2012). Longitudinal analysis of the behavioural phenotype in YAC128 (C57BL/6J) Huntington's Disease transgenic mice. *Brain Research Bulletin*, *88*(2–3), 113–120. https://doi.org/10.1016/j.brainresbull.2010.05.005

Buckley, R. F., Mormino, E. C., Rabin, J. S., Hohman, T. J., Landau, S., Hanseeuw, B. J., Jacobs, H. I. L., Papp, K. V., Amariglio, R. E., Properzi, M. J., Schultz, A. P., Kirn, D., Scott, M. R., Hedden, T., Farrell, M., Price, J., Chhatwal, J., Rentz, D. M., Villemagne, V. L., … Sperling, R. A. (2019). Sex Differences in the Association of Global Amyloid and Regional Tau Deposition Measured by Positron Emission Tomography in Clinically Normal Older Adults. *JAMA Neurology*, *76*(5), 542–551. https://doi.org/10.1001/jamaneurol.2018.4693

Bunner, K. D., & Rebec, G. V. (2016a). Corticostriatal Dysfunction in Huntington's Disease: The Basics. *Frontiers in Human Neuroscience*, *10*, 317. https://doi.org/10.3389/fnhum.2016.00317

Bunner, K. D., & Rebec, G. V. (2016b). Corticostriatal dysfunction in Huntington's Disease: The basics. In *Frontiers in Human Neuroscience* (Vol. 10). Frontiers Media S. A. https://doi.org/10.3389/fnhum.2016.00317

Butcher, J. B., Sims, R. E., Ngum, N. M., Bazzari, A. H., Jenkins, S. I., King, M., Hill, E. J., Nagel, D. A., Fox, K., Parri, H. R., & Glazewski, S. (2022a). A requirement for astrocyte IP3R2 signaling for whisker experience-dependent depression and homeostatic upregulation in the mouse barrel cortex. *Frontiers in Cellular Neuroscience*, *16*, 905285. https://doi.org/10.3389/fncel.2022.905285

Butcher, J. B., Sims, R. E., Ngum, N. M., Bazzari, A. H., Jenkins, S. I., King, M., Hill, E. J., Nagel, D. A., Fox, K., Parri, H. R., & Glazewski, S. (2022b). A requirement for astrocyte IP3R2 signaling for whisker experience-dependent depression and homeostatic upregulation in the mouse barrel cortex. *Frontiers in Cellular Neuroscience*, *16*. https://doi.org/10.3389/fncel.2022.905285

Butt, A. M. (2011). ATP: A ubiquitous gliotransmitter integrating neuron-glial networks. In *Seminars in Cell and Developmental Biology* (Vol. 22, Issue 2, pp. 205–213). Elsevier Ltd. https://doi.org/10.1016/j.semcdb.2011.02.023

Cadd, G., & McKnight, G. S. (1989). Distinct patterns of cAMP-dependent protein kinase gene expression in mouse brain. *Neuron*, *3*(1), 71–79. https://doi.org/10.1016/0896-6273(89)90116-5

Cao, A. hua, Yu, L., Wang, Y. wei, Wang, J. mei, Yang, L. jin, & Lei, G. fei. (2012). Effects of methylphenidate on attentional set-shifting in a genetic model of attention-

deficit/hyperactivity disorder. *Behavioral and Brain Functions*, *8*(1), 10. https://doi.org/10.1186/1744-9081-8-10

Cao, D., Su, Z., Wang, W., Wu, H., Liu, X., Akram, S., Qin, B., Zhou, J., Zhuang, X., Adams, G., Jin, C., Wang, X., Liu, L., Hill, D. L., Wang, D., Ding, X., & Yao, X. (2015). Signaling Scaffold Protein IQGAP1 Interacts with Microtubule Plus-end Tracking Protein SKAP and Links Dynamic Microtubule Plus-end to Steer Cell Migration. *The Journal of Biological Chemistry*, *290*(39), 23766–23780. https://doi.org/10.1074/jbc.M115.673517

Cao, V. Y., Ye, Y., Mastwal, S., Ren, M., Coon, M., Liu, Q., Costa, R. M., & Wang, K. H. (2015). Motor Learning Consolidates Arc-Expressing Neuronal Ensembles in Secondary Motor Cortex. *Neuron*, *86*(6), 1385–1392. https://doi.org/10.1016/j.neuron.2015.05.022

Carter, R. J., Lione, L. A., Humby, T., Mangiarini, L., Mahal, A., Bates, G. P., Dunnett, S. B., & Morton, A. J. (1999). Characterization of progressive motor deficits in mice transgenic for the human Huntington's Disease mutation. *The Journal of Neuroscience : The Official Journal of the Society for Neuroscience*, *19*(8), 3248–3257. https://doi.org/10.1523/JNEUROSCI.19-08-03248.1999

Cearley, C. N., & Wolfe, J. H. (2006). Transduction characteristics of adeno-associated virus vectors expressing cap serotypes 7, 8, 9, and Rh10 in the mouse brain. *Molecular Therapy*, *13*(3), 528–537. https://doi.org/10.1016/j.ymthe.2005.11.015

Cepeda, C., & Levine, M. S. (2022). Synaptic Dysfunction in Huntington's Disease: Lessons from Genetic Animal Models. In *Neuroscientist* (Vol. 28, Issue 1, pp. 20–40). SAGE Publications Inc. https://doi.org/10.1177/1073858420972662

Cepeda, C., Oikonomou, K. D., Cummings, D., Barry, J., Yazon, V. W., Chen, D. T., Asai, J., Williams, C. K., & Vinters, H. V. (2019). Developmental origins of cortical hyperexcitability in Huntington's Disease: Review and new observations. In *Journal of Neuroscience Research* (Vol. 97, Issue 12, pp. 1624–1635). John Wiley and Sons Inc. https://doi.org/10.1002/jnr.24503

Cepeda, C., & Tong, X. P. (2018). Huntington's Disease: From basic science to therapeutics. *CNS Neuroscience and Therapeutics*, *24*(4), 247–249. https://doi.org/10.1111/cns.12841

Cepeda, C., Wu, N., André, V. M., Cummings, D. M., & Levine, M. S. (2007). The corticostriatal pathway in Huntington's Disease. *Progress in Neurobiology*, *81*(5–6), 253–271. https://doi.org/10.1016/j.pneurobio.2006.11.001

Challis, R. C., Ravindra Kumar, S., Chan, K. Y., Challis, C., Beadle, K., Jang, M. J., Kim, H. M., Rajendran, P. S., Tompkins, J. D., Shivkumar, K., Deverman, B. E., & Gradinaru, V. (2019). Systemic AAV vectors for widespread and targeted gene delivery in rodents. *Nature Protocols*, *14*(2), 379–414. https://doi.org/10.1038/s41596-018-0097-3

Chan, K. Y., Jang, M. J., Yoo, B. B., Greenbaum, A., Ravi, N., Wu, W. L., Sánchez-Guardado, L., Lois, C., Mazmanian, S. K., Deverman, B. E., & Gradinaru, V. (2017). Engineered AAVs for efficient noninvasive gene delivery to the central and peripheral nervous systems. *Nature Neuroscience*, *20*(8), 1172–1179. https://doi.org/10.1038/nn.4593

Chandel, N. S. (2021). Nucleotide Metabolism. *Cold Spring Harbor Perspectives in Biology*, *13*(7). https://doi.org/10.1101/cshperspect.a040592

Charles, A. C., Merrill, J. E., Dirksen, E. R., & Sanderson, M. J. (1991). Intercellular signaling in glial cells: calcium waves and oscillations in response to mechanical stimulation and glutamate. *Neuron*, *6*(6), 983–992. https://doi.org/10.1016/0896-6273(91)90238-u

Chen, C., Dong, Y., Liu, F., Gao, C., Ji, C., Dang, Y., Ma, X., & Liu, Y. (2020). A study of antidepressant effect and mechanism on intranasal delivery of BDNF-HA2TAT/AAV to rats with post-stroke depression. *Neuropsychiatric Disease and Treatment*, *16*, 637–649. https://doi.org/10.2147/NDT.S227598

Chen, K.-Z., Liu, S.-X., Li, Y.-W., He, T., Zhao, J., Wang, T., Qiu, X.-X., & Wu, H.-F. (2023). Vimentin as a potential target for diverse nervous system diseases. *Neural Regeneration Research*, *18*(5), 969–975. https://doi.org/10.4103/1673-5374.355744

Chen, N., Sugihara, H., Sharma, J., Perea, G., Petravicz, J., Le, C., & Sur, M. (2012). Nucleus basalis-enabled stimulus-specific plasticity in the visual cortex is mediated by astrocytes. *Proceedings of the National Academy of Sciences of the United States of America*, *109*(41). https://doi.org/10.1073/pnas.1206557109

Chen, Y., Huang, X., Zhang, Y., Rockenstein, E., Bu, G., Golde, T. E., Masliah, E., & Xu, H. (2012a). Alzheimer's β-secretase (BACE1) regulates the cAMP/PKA/CREB pathway independently of β-amyloid. *The Journal of Neuroscience : The Official Journal of the Society for Neuroscience*, *32*(33), 11390–11395. https://doi.org/10.1523/JNEUROSCI.0757-12.2012

Chen, Y., Huang, X., Zhang, Y. wu, Rockenstein, E., Bu, G., Golde, T. E., Masliah, E., & Xu, H. (2012b). Alzheimer's β-secretase (BACE1) regulates the cAMP/PKA/CREB pathway independently of β-amyloid. *Journal of Neuroscience*, *32*(33), 11390–11395. https://doi.org/10.1523/JNEUROSCI.0757-12.2012

Chen, Y.-M., Lin, S.-L., Chen, C.-W., Chiang, W.-C., Tsai, T.-J., & Hsieh, B.-S. (2003). Tumor necrosis factor-alpha stimulates fractalkine production by mesangial cells and regulates monocyte transmigration: down-regulation by cAMP. *Kidney International*, *63*(2), 474–486. https://doi.org/10.1046/j.1523-1755.2003.00766.x

Choi, D. W. (1988). Glutamate neurotoxicity and diseases of the nervous system. *Neuron*, *1*(8), 623–634. https://doi.org/10.1016/0896-6273(88)90162-6

Choi, H. B., Gordon, G. R. J., Zhou, N., Tai, C., Rungta, R. L., Martinez, J., Milner, T. A., Ryu, J. K., McLarnon, J. G., Tresguerres, M., Levin, L. R., Buck, J., & MacVicar, B. A. (2012). Metabolic Communication between Astrocytes and Neurons via Bicarbonate-Responsive Soluble Adenylyl Cyclase. *Neuron*, *75*(6), 1094–1104. https://doi.org/10.1016/j.neuron.2012.08.032

Choi, V. W., Asokan, A., Haberman, R. A., & Samulski, R. J. (2007). Production of recombinant adeno-associated viral vectors for in vitro and in vivo use. *Current Protocols in Molecular Biology*, *Chapter 16*, Unit 16.25. https://doi.org/10.1002/0471142727.mb1625s78

Ciappelloni, S., Bouchet, D., Dubourdieu, N., Boué-Grabot, E., Kellermayer, B., Manso, C., Marignier, R., Oliet, S. H. R., Tourdias, T., & Groc, L. (2019a). Aquaporin-4 Surface Trafficking Regulates Astrocytic Process Motility and Synaptic Activity in Health and Autoimmune Disease. *Cell Reports*, *27*(13), 3860-3872.e4. https://doi.org/10.1016/j.celrep.2019.05.097

Ciappelloni, S., Bouchet, D., Dubourdieu, N., Boué-Grabot, E., Kellermayer, B., Manso, C., Marignier, R., Oliet, S. H. R., Tourdias, T., & Groc, L. (2019b). Aquaporin-4 Surface Trafficking Regulates Astrocytic Process Motility and Synaptic Activity in Health and Autoimmune Disease. *Cell Reports*, *27*(13), 3860-3872.e4. https://doi.org/10.1016/j.celrep.2019.05.097

Citri, A., & Malenka, R. C. (2008). Synaptic plasticity: Multiple forms, functions, and mechanisms. In *Neuropsychopharmacology* (Vol. 33, Issue 1, pp. 18–41). https://doi.org/10.1038/sj.npp.1301559

Cohen-Pfeffer, J. L., Gururangan, S., Lester, T., Lim, D. A., Shaywitz, A. J., Westphal, M., & Slavc, I. (2017). Intracerebroventricular Delivery as a Safe, Long-Term Route of Drug Administration. *Pediatric Neurology*, *67*, 23–35. https://doi.org/10.1016/j.pediatrneurol.2016.10.022

Collingridge, G. L., Peineau, S., Howland, J. G., & Wang, Y. T. (2010). Long-term depression in the CNS. In *Nature Reviews Neuroscience* (Vol. 11, Issue 7, pp. 459–473). https://doi.org/10.1038/nrn2867

Conde-Berriozabal, S., García-Gilabert, L., García-García, E., Sitjà-Roqueta, L., López-Gil, X., Muñoz-Moreno, E., Boudjadja, M. B., Soria, G., Rodríguez, M. J., Alberch, J., & Masana, M. (2023). M2 Cortex Circuitry and Sensory-Induced Behavioral Alterations in Huntington's Disease: Role of Superior Colliculus. *Journal of Neuroscience*, *43*(18), 3379–3390. https://doi.org/10.1523/JNEUROSCI.1172-22.2023

Conde-Berriozabal, S., Sitjà-Roqueta, L., García-García, E., García-Gilabert, L., Sancho-Balsells, A., Fernández-García, S., Rodriguez-Urgellés, E., Giralt, A., Castañé, A., Rodríguez, M. J., Alberch, J., & Masana, M. (2025). Differential impact of optogenetic

stimulation of direct and indirect pathways from dorsolateral and dorsomedial striatum on motor symptoms in Huntington's Disease mice. *Experimental Neurology*, *383*, 114991. https://doi.org/10.1016/j.expneurol.2024.114991

Conti, M., & Beavo, J. (2007). Biochemistry and physiology of cyclic nucleotide phosphodiesterases: essential components in cyclic nucleotide signaling. *Annual Review of Biochemistry*, *76*, 481–511. https://doi.org/10.1146/annurev.biochem.76.060305.150444

Cooper, D. M., Mons, N., & Karpen, J. W. (1995). Adenylyl cyclases and the interaction between calcium and cAMP signalling. *Nature*, *374*(6521), 421–424. https://doi.org/10.1038/374421a0

Corbetta, S., Gualdoni, S., Ciceri, G., Monari, M., Zuccaro, E., Tybulewicz, V. L. J., & De Curtis, I. (2009). Essential role of Rac1 and Rac3 GTPases in neuronal development. *The FASEB Journal*, *23*(5), 1347–1357. https://doi.org/10.1096/fj.08-121574

Cornell, J., Salinas, S., Huang, H. Y., & Zhou, M. (2022). Microglia regulation of synaptic plasticity and learning and memory. In *Neural Regeneration Research* (Vol. 17, Issue 4, pp. 705–716). Wolters Kluwer Medknow Publications. https://doi.org/10.4103/1673-5374.322423

Cornell-Bell, A. H., Finkbeiner, S. M., Cooper, M. S., & Smith, S. J. (1990). Glutamate induces calcium waves in cultured astrocytes: long-range glial signaling. *Science (New York, N.Y.)*, *247*(4941), 470–473. https://doi.org/10.1126/science.1967852

Cotter, M. J., & Muruve, D. A. (2005). THE INDUCTION OF INFLAMMATION BY ADENOVIRUS VECTORS USED FOR GENE THERAPY. In *Frontiers in Bioscience* (Vol. 10).

Cowburn, R. F., O'Neill, C., Ravid, R., Alafuzoff, I., Winblad, B., & Fowler, C. J. (1992). Adenylyl cyclase activity in postmortem human brain: evidence of altered G protein mediation in Alzheimer's Disease. *Journal of Neurochemistry*, *58*(4), 1409–1419. https://doi.org/10.1111/j.1471-4159.1992.tb11357.x

Cowburn, R. F., O'Neill, C., Ravid, R., Winblad, B., & Fowler, C. J. (1992). Preservation of Gi-protein inhibited adenylyl cyclase activity in the brains of patients with Alzheimer's Disease. *Neuroscience Letters*, *141*(1), 16–20. https://doi.org/10.1016/0304-3940(92)90324-z

Creus-Muncunill, J., Badillos-Rodríguez, R., Garcia-Forn, M., Masana, M., Garcia-Díaz Barriga, G., Guisado-Corcoll, A., Alberch, J., Malagelada, C., Delgado-García, J. M., Gruart, A., & Pérez-Navarro, E. (2019). Increased translation as a novel pathogenic mechanism in Huntington's Disease. *Brain : A Journal of Neurology*, *142*(10), 3158–3175. https://doi.org/10.1093/brain/awz230

Cummings, B. J., & Cotman, C. W. (1995). Image analysis of beta-amyloid load in Alzheimer's Disease and relation to dementia severity. *Lancet (London, England)*, *346*(8989), 1524–1528. https://doi.org/10.1016/s0140-6736(95)92053-6

Daida, A., Kurotani, T., Yamaguchi, K., Takahashi, Y., & Ichinohe, N. (2024). Different Numbers of Conjunctive Stimuli Induce LTP or LTD in Mouse Cerebellar Purkinje Cell. *Cerebellum*. https://doi.org/10.1007/s12311-024-01726-6

Dallérac, G. M., Levasseur, G., Vatsavayai, S. C., Milnerwood, A. J., Cummings, D. M., Kraev, I., Huetz, C., Evans, K. A., Walters, S. W., Rezaie, P., Cho, Y., Hirst, M. C., & Murphy, K. P. S. J. (2015). Dysfunctional dopaminergic neurones in mouse models of Huntington's Disease: A role for SK3 channels. *Neurodegenerative Diseases*, *15*(2), 93–108. https://doi.org/10.1159/000375126

de Lecea, L., Criado, J. R., Rivera, S., Wen, W., Soriano, E., Henriksen, S. J., Taylor, S. S., Gall, C. M., & Sutcliffe, J. G. (1998). Endogenous protein kinase A inhibitor (PKIalpha) modulates synaptic activity. *Journal of Neuroscience Research*, *53*(3), 269–278. https://doi.org/10.1002/(SICI)1097-4547(19980801)53:3<269::AID-JNR1>3.0.CO;2-8

De Luca, C., Colangelo, A. M., Virtuoso, A., Alberghina, L., & Papa, M. (2020). Neurons, glia, extracellular matrix and neurovascular unit: A systems biology approach to the complexity of synaptic plasticity in health and disease. In *International Journal of Molecular Sciences* (Vol. 21, Issue 4). MDPI AG. https://doi.org/10.3390/ijms21041539

De Marchi, N., Morris, M., Mennella, R., La Pia, S., & Nestadt, G. (1998). Association of obsessive-compulsive disorder and pathological gambling with Huntington's Disease in an Italian pedigree: Possible association with Huntington's Disease mutation. *Acta Psychiatrica Scandinavica*, *97*(1), 62–65. https://doi.org/10.1111/j.1600-0447.1998.tb09964.x

De Paepe, A. E., Sierpowska, J., Garcia-Gorro, C., Martinez-Horta, S., Perez-Perez, J., Kulisevsky, J., Rodriguez-Dechicha, N., Vaquer, I., Subira, S., Calopa, M., Muñoz, E., Santacruz, P., Ruiz-Idiago, J., Mareca, C., de Diego-Balaguer, R., & Camara, E. (2019). White matter cortico-striatal tracts predict apathy subtypes in Huntington's Disease. *NeuroImage: Clinical*, *24*. https://doi.org/10.1016/j.nicl.2019.101965

DeFelipe, J. (2006). Brain plasticity and mental processes: Cajal again. *Nature Reviews. Neuroscience*, *7*(10), 811–817. https://doi.org/10.1038/nrn2005

Deisseroth, K. (2011). Optogenetics. In *Nature Methods* (Vol. 8, Issue 1, pp. 26–29). https://doi.org/10.1038/nmeth.f.324

Dejanovic, B., Sheng, M., & Hanson, J. E. (2024). Targeting synapse function and loss for treatment of neurodegenerative diseases. In *Nature Reviews Drug Discovery* (Vol. 23, Issue 1, pp. 23–42). Nature Research. https://doi.org/10.1038/s41573-023-00823-1

Dementia. (n.d.). Retrieved April 6, 2025, from https://www.who.int/news-room/fact-sheets/detail/dementia?utm_source

Devasani, K., & Yao, Y. (2022). Expression and functions of adenylyl cyclases in the CNS. In *Fluids and Barriers of the CNS* (Vol. 19, Issue 1). BioMed Central Ltd. https://doi.org/10.1186/s12987-022-00322-2

Deverman, B. E., Pravdo, P. L., Simpson, B. P., Kumar, S. R., Chan, K. Y., Banerjee, A., Wu, W. L., Yang, B., Huber, N., Pasca, S. P., & Gradinaru, V. (2016a). Cre-dependent selection yields AAV variants for widespread gene transfer to the adult brain. *Nature Biotechnology*, *34*(2), 204–209. https://doi.org/10.1038/nbt.3440

Deverman, B. E., Pravdo, P. L., Simpson, B. P., Kumar, S. R., Chan, K. Y., Banerjee, A., Wu, W.-L., Yang, B., Huber, N., Pasca, S. P., & Gradinaru, V. (2016b). Cre-dependent selection yields AAV variants for widespread gene transfer to the adult brain. *Nature Biotechnology*, *34*(2), 204–209. https://doi.org/10.1038/nbt.3440

Diaz-Castro, B., Gangwani, M. R., Yu, X., Coppola, G., & Khakh, B. S. (2019). Astrocyte molecular signatures in Huntington's Disease. *Science Translational Medicine*, *11*(514). https://doi.org/10.1126/scitranslmed.aaw8546

Dickerson, B. C., Bakkour, A., Salat, D. H., Feczko, E., Pacheco, J., Greve, D. N., Grodstein, F., Wright, C. I., Blacker, D., Rosas, H. D., Sperling, R. A., Atri, A., Growdon, J. H., Hyman, B. T., Morris, J. C., Fischl, B., & Buckner, R. L. (2009). The cortical signature of Alzheimer's Disease: regionally specific cortical thinning relates to symptom severity in very mild to mild AD dementia and is detectable in asymptomatic amyloid-positive individuals. *Cerebral Cortex (New York, N.Y.: 1991)*, *19*(3), 497–510. https://doi.org/10.1093/cercor/bhn113

Didier, S., Sauvé, F., Domise, M., Buée, L., Marinangeli, C., & Vingtdeux, V. (2018). AMP-activated protein kinase controls immediate early genes expression following synaptic activation through the PKA/CREB pathway. *International Journal of Molecular Sciences*, *19*(12). https://doi.org/10.3390/ijms19123716

Dietler, J., Gelfert, R., Kaiser, J., Borin, V., Renzl, C., Pilsl, S., Ranzani, A. T., García de Fuentes, A., Gleichmann, T., Diensthuber, R. P., Weyand, M., Mayer, G., Schapiro, I., & Möglich, A. (2022). Signal transduction in light-oxygen-voltage receptors lacking the active-site glutamine. *Nature Communications*, *13*(1), 2618. https://doi.org/10.1038/s41467-022-30252-4

Dinamarca, M. C., Colombo, L., Tousiaki, N. E., Müller, M., & Pecho-Vrieseling, E. (2022). Synaptic and functional alterations in the development of mutant huntingtin expressing hiPSC-derived neurons. *Frontiers in Molecular Biosciences*, *9*. https://doi.org/10.3389/fmolb.2022.916019

DiProspero, N. A., Chen, E.-Y., Charles, V., Plomann, M., Kordower, J. H., & Tagle, D. A. (2004). Early changes in Huntington's Disease patient brains involve alterations in cytoskeletal and synaptic elements. *Journal of Neurocytology*, *33*(5), 517–533. https://doi.org/10.1007/s11068-004-0514-8

Dixon, R. A., Kobilka, B. K., Strader, D. J., Benovic, J. L., Dohlman, H. G., Frielle, T., Bolanowski, M. A., Bennett, C. D., Rands, E., Diehl, R. E., Mumford, R. A., Slater, E. E., Sigal, I. S., Caron, M. G., Lefkowitz, R. J., & Strader, C. D. (1986). Cloning of the gene and cDNA for mammalian beta-adrenergic receptor and homology with rhodopsin. *Nature*, *321*(6065), 75–79. https://doi.org/10.1038/321075a0

Do-Ha, D., Buskila, Y., & Ooi, L. (2018). Impairments in Motor Neurons, Interneurons and Astrocytes Contribute to Hyperexcitability in ALS: Underlying Mechanisms and Paths to Therapy. In *Molecular Neurobiology* (Vol. 55, Issue 2, pp. 1410–1418). Humana Press Inc. https://doi.org/10.1007/s12035-017-0392-y

Dong, X. X., Wang, Y., & Qin, Z. H. (2009). Molecular mechanisms of excitotoxicity and their relevance to pathogenesis of neurodegenerative diseases. In *Acta Pharmacologica Sinica* (Vol. 30, Issue 4, pp. 379–387). https://doi.org/10.1038/aps.2009.24

Dong, Y., Green, T., Saal, D., Marie, H., Neve, R., Nestler, E. J., & Malenka, R. C. (2006). CREB modulates excitability of nucleus accumbens neurons. *Nature Neuroscience*, *9*(4), 475–477. https://doi.org/10.1038/nn1661

Du, H., Guo, L., Wu, X., Sosunov, A. A., McKhann, G. M., Chen, J. X., & Yan, S. S. (2014). Cyclophilin D deficiency rescues Aβ-impaired PKA/CREB signaling and alleviates synaptic degeneration. *Biochimica et Biophysica Acta*, *1842*(12 Pt A), 2517–2527. https://doi.org/10.1016/j.bbadis.2013.03.004

Duan, S., Anderson, C. M., Stein, B. A., & Swanson, R. A. (1999). Glutamate induces rapid upregulation of astrocyte glutamate transport and cell-surface expression of GLAST. *The Journal of Neuroscience : The Official Journal of the Society for Neuroscience*, *19*(23), 10193–10200. https://doi.org/10.1523/JNEUROSCI.19-23-10193.1999

Dudek, S. M., & Bear, M. F. (1992). Homosynaptic long-term depression in area CA1 of hippocampus and effects of N-methyl-D-aspartate receptor blockade. *Proceedings of the National Academy of Sciences of the United States of America*, *89*(10), 4363–4367. https://doi.org/10.1073/pnas.89.10.4363

Dugger, B. N., & Dickson, D. W. (2017). Pathology of neurodegenerative diseases. In *Cold Spring Harbor Perspectives in Biology* (Vol. 9, Issue 7). Cold Spring Harbor Laboratory Press. https://doi.org/10.1101/cshperspect.a028035

Dunn, A. R., O'Connell, K. M. S., & Kaczorowski, C. C. (2019). Gene-by-environment interactions in Alzheimer's Disease and Parkinson's disease. *Neuroscience and Biobehavioral Reviews*, *103*, 73–80. https://doi.org/10.1016/j.neubiorev.2019.06.018

Dupraz, S., Hilton, B. J., Husch, A., Santos, T. E., Coles, C. H., Stern, S., Brakebusch, C., & Bradke, F. (2019). RhoA Controls Axon Extension Independent of Specification in the Developing Brain. *Current Biology*, *29*(22), 3874-3886.e9. https://doi.org/10.1016/j.cub.2019.09.040

Durkee, C. A., & Araque, A. (2019). Diversity and Specificity of Astrocyte–neuron Communication. In *Neuroscience* (Vol. 396, pp. 73–78). Elsevier Ltd. https://doi.org/10.1016/j.neuroscience.2018.11.010

Erro, R., Mencacci, N. E., & Bhatia, K. P. (2021). The Emerging Role of Phosphodiesterases in Movement Disorders. *Movement Disorders*, *36*(10), 2225–2243. https://doi.org/10.1002/mds.28686

Estrada-Sánchez, A. M., & Rebec, G. V. (2012). Corticostriatal dysfunction and glutamate transporter 1 (GLT1) in Huntington's Disease: Interactions between neurons and astrocytes. In *Basal Ganglia* (Vol. 2, Issue 2, pp. 57–66). https://doi.org/10.1016/j.baga.2012.04.029

Etzl, S., Lindner, R., Nelson, M. D., & Winkler, A. (2018). Structure-guided design and functional characterization of an artificial red light–regulated guanylate/adenylate cyclase for optogenetic applications. *Journal of Biological Chemistry*, *293*(23), 9078–9089. https://doi.org/10.1074/jbc.RA118.003069

Eyo, U. B., Peng, J., Murugan, M., Mo, M., Lalani, A., Xie, P., Xu, P., Margolis, D. J., & Wu, L.-J. (2016). Regulation of Physical Microglia-Neuron Interactions by Fractalkine Signaling after Status Epilepticus. *ENeuro*, *3*(6). https://doi.org/10.1523/ENEURO.0209-16.2016

Faideau, M., Kim, J., Cormier, K., Gilmore, R., Welch, M., Auregan, G., Dufour, N., Guillermier, M., Brouillet, E., Hantraye, P., DéGlon, N., Ferrante, R. J., & Bonvento, G. (2010). In vivo expression of polyglutamine-expanded huntingtin by mouse striatal astrocytes impairs glutamate transport: A correlation with Huntington's Disease subjects. *Human Molecular Genetics*, *19*(15), 3053–3067. https://doi.org/10.1093/hmg/ddq212

Fakhoury, M. (2017). Microglia and astrocytes in Alzheimer's Disease: implications for therapy. *Current Neuropharmacology*, *15*. https://doi.org/10.2174/1570159x15666170720095240

Federici, T., Taub, J. S., Baum, G. R., Gray, S. J., Grieger, J. C., Matthews, K. A., Handy, C. R., Passini, M. A., Samulski, R. J., & Boulis, N. M. (2012). Robust spinal motor neuron transduction following intrathecal delivery of AAV9 in pigs. *Gene Therapy*, *19*(8), 852–859. https://doi.org/10.1038/gt.2011.130

Feher, J. (2012). Cells, Synapses, and Neurotransmitters. *Quantitative Human Physiology*, 307–320. https://doi.org/10.1016/B978-0-12-382163-8.00034-7

Fernández-García, S., Conde-Berriozabal, S., García-García, E., Gort-Paniello, C., Bernal-Casas, D., García-Díaz Barriga, G., López-Gil, J., Muñoz-Moreno, E., Soria, G., Campa, L., Artigas, F., Rodríguez, M. J., Alberch, J., & Masana, M. (2020). M2 cortex-dorsolateral striatum stimulation reverses motor symptoms and synaptic deficits in Huntington's Disease. *ELife*, *9*. https://doi.org/10.7554/eLife.57017

Ferrante, R. J., Kowall, N. W., Beal, M. F., Martin, J. B., Bird, E. D., & Richardson, E. P. (1987). Morphologic and histochemical characteristics of a spared subset of striatal neurons in Huntington's Disease. *Journal of Neuropathology and Experimental Neurology*, *46*(1), 12–27. https://doi.org/10.1097/00005072-198701000-00002

Filosa, A., Paixão, S., Honsek, S. D., Carmona, M. A., Becker, L., Feddersen, B., Gaitanos, L., Rudhard, Y., Schoepfer, R., Klopstock, T., Kullander, K., Rose, C. R., Pasquale, E. B., & Klein, R. (2009). Neuron-glia communication via EphA4/ephrin-A3 modulates LTP through glial glutamate transport. *Nature Neuroscience*, *12*(10), 1285–1292. https://doi.org/10.1038/nn.2394

Finneran, D. J., Njoku, I. P., Flores-Pazarin, D., Ranabothu, M. R., Nash, K. R., Morgan, D., & Gordon, M. N. (2021). Toward Development of Neuron Specific Transduction After Systemic Delivery of Viral Vectors. *Frontiers in Neurology*, *12*. https://doi.org/10.3389/fneur.2021.685802

Foust, K. D., Nurre, E., Montgomery, C. L., Hernandez, A., Chan, C. M., & Kaspar, B. K. (2009). Intravascular AAV9 preferentially targets neonatal neurons and adult astrocytes. *Nature Biotechnology*, *27*(1), 59–65. https://doi.org/10.1038/nbt.1515

Fricker, M., Tolkovsky, A. M., Borutaite, V., Coleman, M., & Brown, G. C. (2018). NEURONAL CELL DEATH. *Neuronal Cell Death. Physiol Rev*, *98*, 813–880. https://doi.org/10.1152/physrev.00011.2017.-Neuronal

Fu, Q., Wang, Y., Yan, C., & Xiang, Y. K. (2024). Phosphodiesterase in heart and vessels-From Physiology to Diseases. *Physiological Reviews*, *104*(2), 765–834. https://doi.org/10.1152/physrev.00015.2023

Furutani, Y., Kawasaki, M., Matsuno, H., Mitsui, S., Mori, K., & Yoshihara, Y. (2012). Vitronectin induces phosphorylation of ezrin/radixin/moesin actin-binding proteins through binding to its novel neuronal receptor telencephalin. *The Journal of Biological Chemistry*, *287*(46), 39041–39049. https://doi.org/10.1074/jbc.M112.383851

Gadenstaetter, A. J., SCHMUTZLER, L., GRIMM, D. I. R. K., & LANDEGGER, L. D. (2022). Intranasal application of adeno-associated viruses: a systematic review. In *Translational Research* (Vol. 248, pp. 87–110). Elsevier Inc. https://doi.org/10.1016/j.trsl.2022.05.002

Games, D., Adams, D., Alessandrini, R., Barbour, R., Berthelette, P., Blackwell, C., Carr, T., Clemens, J., Donaldson, T., & Gillespie, F. (1995). Alzheimer-type neuropathology in

transgenic mice overexpressing V717F beta-amyloid precursor protein. *Nature*, *373*(6514), 523–527. https://doi.org/10.1038/373523a0

Garcia-Alloza, M., Robbins, E. M., Zhang-Nunes, S. X., Purcell, S. M., Betensky, R. A., Raju, S., Prada, C., Greenberg, S. M., Bacskai, B. J., & Frosch, M. P. (2006). Characterization of amyloid deposition in the APPswe/PS1dE9 mouse model of Alzheimer disease. *Neurobiology of Disease*, *24*(3), 516–524. https://doi.org/10.1016/j.nbd.2006.08.017

Gatz, M., Reynolds, C. A., Fratiglioni, L., Mortimer, J. A., Berg, S., Fiske, A., & Pedersen, N. L. (2006). Role of Genes and Environments for Explaining Alzheimer Disease. In *Arch Gen Psychiatry* (Vol. 63).

Ghiglieri, V., Campanelli, F., Marino, G., Natale, G., Picconi, B., & Calabresi, P. (2019). Corticostriatal synaptic plasticity alterations in the R6/1 transgenic mouse model of Huntington's Disease. *Journal of Neuroscience Research*, *97*(12), 1655–1664. https://doi.org/10.1002/jnr.24521

Giannakopoulos, P., Herrmann, F. R., Bussière, T., Bouras, C., Kövari, E., Perl, D. P., Morrison, J. H., Gold, G., & Hof, P. R. (2003). Tangle and neuron numbers, but not amyloid load, predict cognitive status in Alzheimer's Disease. *Neurology*, *60*(9), 1495–1500. https://doi.org/10.1212/01.wnl.0000063311.58879.01

Gines, S., Seong, I. S., Fossale, E., Ivanova, E., Trettel, F., Gusella, J. F., Wheeler, V. C., Persichetti, F., & MacDonald, M. E. (2003). Specific progressive cAMP reduction implicates energy deficit in presymptomatic Huntington's Disease knock-in mice. *Human Molecular Genetics*, *12*(5), 497–508. https://doi.org/10.1093/hmg/ddg046

Giralt, A., Carretán, O., Lao-Peregrin, C., Martín, E. D., & Alberch, J. (2011). Conditional BDNF release under pathological conditions improves Huntington's Disease pathology by delaying neuronal dysfunction. *Molecular Neurodegeneration*, *6*(1). https://doi.org/10.1186/1750-1326-6-71

Giralt, A., Saavedra, A., Alberch, J., & Pérez-Navarro, E. (2012). Cognitive dysfunction in Huntington's Disease: Humans, mouse models and molecular mechanisms. In *Journal of Huntington's Disease* (Vol. 1, Issue 2, pp. 155–173). IOS Press. https://doi.org/10.3233/JHD-120023

Giralt, A., Saavedra, A., Carretón, O., Arumí, H., Tyebji, S., Alberch, J., & Pérez-Navarro, E. (2013). PDE10 inhibition increases GluA1 and CREB phosphorylation and improves spatial and recognition memories in a Huntington's Disease mouse model. *Hippocampus*, *23*(8), 684–695. https://doi.org/10.1002/hipo.22128

Glazewski, S., Barth, A. L., Wallace, H., McKenna, M., Silva, A., & Fox, K. (1999). Impaired experience-dependent plasticity in barrel cortex of mice lacking the alpha and delta isoforms of CREB. *Cerebral Cortex (New York, N.Y. : 1991)*, *9*(3), 249–256. https://doi.org/10.1093/cercor/9.3.249

Glenner, G. G., & Wong, C. W. (1984). *BIOCHEMICAL AND BIOPHYSICAL RESEARCH COMMUNICATIONS Pages 885-890 AND CHARACTERIZATION OF A NOVEL CEREBROVASCULAR AMYLOID PROTEIN* (Vol. 120, Issue 3).

Goldman, J. E., & Abramson, B. (1990). Cyclic AMP-induced shape changes of astrocytes are accompanied by rapid depolymerization of actin. *Brain Research*, *528*(2), 189–196. https://doi.org/10.1016/0006-8993(90)91657-3

González-Reyes, R. E., Nava-Mesa, M. O., Vargas-Sánchez, K., Ariza-Salamanca, D., & Mora-Muñoz, L. (2017). Involvement of Astrocytes in Alzheimer's Disease from a Neuroinflammatory and Oxidative Stress Perspective. *Frontiers in Molecular Neuroscience*, *10*, 427. https://doi.org/10.3389/fnmol.2017.00427

Goraya, T. A., Masada, N., Ciruela, A., & Cooper, D. M. F. (2004). Sustained entry of Ca2+ is required to activate Ca 2+-calmodulin-dependent phosphodiesterase 1A. *Journal of Biological Chemistry*, *279*(39), 40494–40504. https://doi.org/10.1074/jbc.M313441200

Gottesman, R. F., Albert, M. S., Alonso, A., Coker, L. H., Coresh, J., Davis, S. M., Deal, J. A., McKhann, G. M., Mosley, T. H., Sharrett, A. R., Schneider, A. L. C., Windham, B. G., Wruck, L. M., & Knopman, D. S. (2017). Associations between midlife vascular risk factors and 25-year incident dementia in the Atherosclerosis Risk in Communities (ARIC) cohort. *JAMA Neurology*, *74*(10), 1246–1254. https://doi.org/10.1001/jamaneurol.2017.1658

Gourinchas, G., Etzl, S., Göbl, C., Vide, U., Madl, T., & Winkler, A. (n.d.). *Long-range allosteric signaling in red light-regulated diguanylyl cyclases*. https://www.science.org

Gray, M., Shirasaki, D. I., Cepeda, C., André, V. M., Wilburn, B., Lu, X. H., Tao, J., Yamazaki, I., Li, S. H., Sun, Y. E., Li, X. J., Levine, M. S., & Yang, X. W. (2008). Full-length human mutant huntingtin with a stable polyglutamine repeat can elicit progressive and selective neuropathogenesis in BACHD mice. *Journal of Neuroscience*, *28*(24), 6182–6195. https://doi.org/10.1523/JNEUROSCI.0857-08.2008

Griffiths, J., & Grant, S. G. N. (2023). Synapse pathology in Alzheimer's Disease. In *Seminars in Cell and Developmental Biology* (Vol. 139, pp. 13–23). Elsevier Ltd. https://doi.org/10.1016/j.semcdb.2022.05.028

Guntas, G., Hallett, R. A., Zimmerman, S. P., Williams, T., Yumerefendi, H., Bear, J. E., & Kuhlman, B. (2015). Engineering an improved light-induced dimer (iLID) for controlling the localization and activity of signaling proteins. *Proceedings of the National Academy of Sciences of the United States of America*, *112*(1), 112–117. https://doi.org/10.1073/pnas.1417910112

Gurevich, V. V. (2022). β-Adrenergic receptors. In *Primer on the Autonomic Nervous System, Fourth Edition* (pp. 53–55). Elsevier. https://doi.org/10.1016/B978-0-323-85492-4.00035-1

Gusella, J. F., Wexler, N. S., Conneally, P. M., Naylor, S. L., Anderson, M. A., Tanzi, R. E., Watkins, P. C., Ottina, K., Wallace, M. R., & Sakaguchi, A. Y. (1983). A polymorphic DNA marker genetically linked to Huntington's Disease. *Nature*, *306*(5940), 234–238. https://doi.org/10.1038/306234a0

Haass, C., & Selkoe, D. J. (2007). Soluble protein oligomers in neurodegeneration: Lessons from the Alzheimer's amyloid β-peptide. In *Nature Reviews Molecular Cell Biology* (Vol. 8, Issue 2, pp. 101–112). https://doi.org/10.1038/nrm2101

Haery, L., Deverman, B. E., Matho, K. S., Cetin, A., Woodard, K., Cepko, C., Guerin, K. I., Rego, M. A., Ersing, I., Bachle, S. M., Kamens, J., & Fan, M. (2019). Adeno-Associated Virus Technologies and Methods for Targeted Neuronal Manipulation. *Frontiers in Neuroanatomy*, *13*(November), 1–16. https://doi.org/10.3389/fnana.2019.00093

Halassa, M. M., Fellin, T., & Haydon, P. G. (2007). The tripartite synapse: roles for gliotransmission in health and disease. *Trends in Molecular Medicine*, *13*(2), 54–63. https://doi.org/10.1016/j.molmed.2006.12.005

Hammond, S. L., Leek, A. N., Richman, E. H., & Tjalkens, R. B. (2017). Cellular selectivity of AAV serotypes for gene delivery in neurons and astrocytes by neonatal intracerebroventricular injection. *PLoS ONE*, *12*(12). https://doi.org/10.1371/journal.pone.0188830

Hansen, D. V., Hanson, J. E., & Sheng, M. (2018). Microglia in Alzheimer's Disease. In *Journal of Cell Biology* (Vol. 217, Issue 2, pp. 459–472). Rockefeller University Press. https://doi.org/10.1083/jcb.201709069

Hanson, L. R., Fine, J. M., Svitak, A. L., & Faltesek, K. A. (2013). Intranasal administration of CNS therapeutics to awake mice. *Journal of Visualized Experiments : JoVE*, *74*. https://doi.org/10.3791/4440

Hansson, O., Guatteo, E., Mercuri, N. B., Bernardi, G., Li, X. J., Castilho, R. F., & Brundin, P. (2001). Resistance to NMDA toxicity correlates with appearance of nuclear inclusions, behavioural deficits and changes in calcium homeostasis in mice transgenic for exon 1 of the huntington gene. *European Journal of Neuroscience*, *14*(9), 1492–1504. https://doi.org/10.1046/j.0953-816X.2001.01767.x

Harada, K., Ito, M., Wang, X., Tanaka, M., Wongso, D., Konno, A., Hirai, H., Hirase, H., Tsuboi, T., & Kitaguchi, T. (2017). Red fluorescent protein-based cAMP indicator applicable to optogenetics and in vivo imaging. *Scientific Reports*, *7*(1), 1–9. https://doi.org/10.1038/s41598-017-07820-6

Hardy, J. A., & Higgins, G. A. (1992). Alzheimer's Disease: the amyloid cascade hypothesis. *Science (New York, N.Y.)*, *256*(5054), 184–185. https://doi.org/10.1126/science.1566067

Hardy, J., & Selkoe, D. J. (2002). The amyloid hypothesis of Alzheimer's Disease: progress and problems on the road to therapeutics. *Science (New York, N.Y.)*, *297*(5580), 353–356. https://doi.org/10.1126/science.1072994

Harper, S. M., Neil, L. C., & Gardner, K. H. (2003). Structural basis of a phototropin light switch. *Science (New York, N.Y.)*, *301*(5639), 1541–1544. https://doi.org/10.1126/science.1086810

Harrison, J. K., Jiang, Y., Chen, S., Xia, Y., Maciejewski, D., McNamara, R. K., Streit, W. J., Salafranca, M. N., Adhikari, S., Thompson, D. A., Botti, P., Bacon, K. B., & Feng, L. (1998). Role for neuronally derived fractalkine in mediating interactions between neurons and CX3CR1-expressing microglia. *Proceedings of the National Academy of Sciences of the United States of America*, *95*(18), 10896–10901. https://doi.org/10.1073/pnas.95.18.10896

Hasel, P., Dando, O., Jiwaji, Z., Baxter, P., Todd, A. C., Heron, S., Márkus, N. M., McQueen, J., Hampton, D. W., Torvell, M., Tiwari, S. S., McKay, S., Eraso-Pichot, A., Zorzano, A., Masgrau, R., Galea, E., Chandran, S., Wyllie, D. J. A., Simpson, T. I., & Hardingham, G. E. (2017). Neurons and neuronal activity control gene expression in astrocytes to regulate their development and metabolism. *Nature Communications*, *8*. https://doi.org/10.1038/ncomms15132

Hebb, A. L. O., Robertson, H. A., & Denovan-Wright, E. M. (2004). Striatal phosphodiesterase mRNA and protein levels are reduced in Huntington's Disease transgenic mice prior to the onset of motor symptoms. *Neuroscience*, *123*(4), 967–981. https://doi.org/10.1016/j.neuroscience.2003.11.009

Heckman, P. R. A., Blokland, A., Bollen, E. P. P., & Prickaerts, J. (2018). Phosphodiesterase inhibition and modulation of corticostriatal and hippocampal circuits: Clinical overview and translational considerations. In *Neuroscience and Biobehavioral Reviews* (Vol. 87, pp. 233–254). Elsevier Ltd. https://doi.org/10.1016/j.neubiorev.2018.02.007

Heinz, D. E., Genewsky, A., & Wotjak, C. T. (2017). Enhanced anandamide signaling reduces flight behavior elicited by an approaching robo-beetle. *Neuropharmacology*, *126*, 233–241. https://doi.org/10.1016/j.neuropharm.2017.09.010

Hell, J. W., & Ehlers, M. D. (2008). Structural and functional organization of the synapse. In *Structural And Functional Organization Of The Synapse*. Springer US. https://doi.org/10.1007/978-0-387-77232-5/COVER

Henneberger, C., Papouin, T., Oliet, S. H. R., & Rusakov, D. A. (2010). Long-term potentiation depends on release of D-serine from astrocytes. *Nature*, *463*(7278), 232–236. https://doi.org/10.1038/nature08673

Hertz, L., Xu, J., Song, D., Du, T., Li, B., Yan, E., & Peng, L. (2015). Astrocytic glycogenolysis: mechanisms and functions. *Metabolic Brain Disease*, *30*(1), 317–333. https://doi.org/10.1007/s11011-014-9536-1

Hiess, F., Yao, J., Song, Z., Sun, B., Zhang, Z., Huang, J., Chen, L., Institoris, A., Estillore, J. P., Wang, R., Ter Keurs, H. E. D. J., Stys, P. K., Gordon, G. R., Zamponi, G. W., Ganguly, A., & Chen, S. R. W. (2022). Subcellular localization of hippocampal ryanodine receptor 2 and its role in neuronal excitability and memory. *Communications Biology*, *5*(1), 183. https://doi.org/10.1038/s42003-022-03124-2

Hintiryan, H., Foster, N. N., Bowman, I., Bay, M., Song, M. Y., Gou, L., Yamashita, S., Bienkowski, M. S., Zingg, B., Zhu, M., Yang, X. W., Shih, J. C., Toga, A. W., & Dong, H. W. (2016). The mouse cortico-striatal projectome. *Nature Neuroscience*, *19*(8), 1100–1114. https://doi.org/10.1038/nn.4332

Hirose, T., Tamaru, T., Okumura, N., Nagai, K., & Okada, M. (1997). PCTAIRE 2, a Cdc2-related serine/threonine kinase, is predominantly expressed in terminally differentiated neurons. *European Journal of Biochemistry*, *249*(2), 481–488. https://doi.org/10.1111/j.1432-1033.1997.t01-1-00481.x

Hoey, S. E., Williams, R. J., & Perkinton, M. S. (2009). Synaptic NMDA receptor activation stimulates α-secretase amyloid precursor protein processing and inhibits amyloid-β Production. *Journal of Neuroscience*, *29*(14), 4442–4460. https://doi.org/10.1523/JNEUROSCI.6017-08.2009

Holtzclaw, L. A., Pandhit, S., Bare, D. J., Mignery, G. A., & Russell, J. T. (2002). Astrocytes in adult rat brain express type 2 inositol 1,4,5-trisphosphate receptors. *Glia*, *39*(1), 69–84. https://doi.org/10.1002/glia.10085

Hong, S., Beja-Glasser, V. F., Nfonoyim, B. M., Frouin, A., Li, S., Ramakrishnan, S., Merry, K. M., Shi, Q., Rosenthal, A., Barres, B. A., Lemere, C. A., Selkoe, D. J., & Stevens, B. (2016). Complement and microglia mediate early synapse loss in Alzheimer mouse models. *Science (New York, N.Y.)*, *352*(6286), 712–716. https://doi.org/10.1126/science.aad8373

Hordeaux, J., Wang, Q., Katz, N., Buza, E. L., Bell, P., & Wilson, J. M. (2018). The Neurotropic Properties of AAV-PHP.B Are Limited to C57BL/6J Mice. *Molecular Therapy*, *26*(3), 664–668. https://doi.org/10.1016/j.ymthe.2018.01.018

Horvat, A., Zorec, R., & Vardjan, N. (2016). Adrenergic stimulation of single rat astrocytes results in distinct temporal changes in intracellular Ca2+ and cAMP-dependent PKA responses. *Cell Calcium*, *59*(4), 156–163. https://doi.org/10.1016/j.ceca.2016.01.002

Hösli, E., & Hösli, L. (1984). Autoradiographic localization of binding sites for [3H]histamine and H1- and H2-antagonists on cultured neurones and glial cells. *Neuroscience*, *13*(3), 863–870. https://doi.org/10.1016/0306-4522(84)90101-5

Hotulainen, P., & Hoogenraad, C. C. (2010). Actin in dendritic spines: Connecting dynamics to function. In *Journal of Cell Biology* (Vol. 189, Issue 4, pp. 619–629). https://doi.org/10.1083/jcb.201003008

Hotz, A., König, N., Taniguchi, H., Chrivia, J. C., & Kinzel, V. (1989). Catalytic subunit of cAMP-dependent protein kinase from bovine heart: several isoforms demonstrated by high resolution focusing in immobilized pH gradient. *Biochemical and Biophysical Research Communications*, *160*(2), 596–601. https://doi.org/10.1016/0006-291x(89)92474-1

Hsiao, K., Chapman, P., Nilsen, S., Eckman, C., Harigaya, Y., Younkin, S., Yang, F., & Cole, G. (1996). Correlative memory deficits, Abeta elevation, and amyloid plaques in transgenic mice. *Science (New York, N.Y.)*, *274*(5284), 99–102. https://doi.org/10.1126/science.274.5284.99

Huang, C. C., & Hsu, K. Sen. (2006). Presynaptic mechanism underlying cAMP-induced synaptic potentiation in medial prefrontal cortex pyramidal neurons. *Molecular Pharmacology*, *69*(3), 846–856. https://doi.org/10.1124/mol.105.018093

Huang, Y., Happonen, K. E., Burrola, P. G., O'Connor, C., Hah, N., Huang, L., Nimmerjahn, A., & Lemke, G. (2021). Microglia use TAM receptors to detect and engulf amyloid β plaques. *Nature Immunology*, *22*(5), 586–594. https://doi.org/10.1038/s41590-021-00913-5

Huffels, C. F. M., Middeldorp, J., & Hol, E. M. (2023). Aß Pathology and Neuron–Glia Interactions: A Synaptocentric View. In *Neurochemical Research* (Vol. 48, Issue 4, pp. 1026–1046). Springer. https://doi.org/10.1007/s11064-022-03699-6

Huntington, G. (2003). On chorea. George Huntington, M.D. *The Journal of Neuropsychiatry and Clinical Neurosciences*, *15*(1), 109–112. https://doi.org/10.1176/jnp.15.1.109

Huynh, T. P. V., Davis, A. A., Ulrich, J. D., & Holtzman, D. M. (2017). Apolipoprotein E and Alzheimer's Disease: The influence of apolipoprotein E on amyloid-β and other amyloidogenic proteins. In *Journal of Lipid Research* (Vol. 58, Issue 5, pp. 824–836). American Society for Biochemistry and Molecular Biology Inc. https://doi.org/10.1194/jlr.R075481

Hyman, B. T., Phelps, C. H., Beach, T. G., Bigio, E. H., Cairns, N. J., Carrillo, M. C., Dickson, D. W., Duyckaerts, C., Frosch, M. P., Masliah, E., Mirra, S. S., Nelson, P. T., Schneider, J. A., Thal, D. R., Thies, B., Trojanowski, J. Q., Vinters, H. V, & Montine, T. J. (2012). National Institute on Aging-Alzheimer's Association guidelines for the neuropathologic assessment of Alzheimer's Disease. *Alzheimer's & Dementia : The Journal of the Alzheimer's Association*, *8*(1), 1–13. https://doi.org/10.1016/j.jalz.2011.10.007

Iliff, J. J., Wang, M., Liao, Y., Plogg, B. A., Peng, W., Gundersen, G. A., Benveniste, H., Vates, G. E., Deane, R., Goldman, S. A., Nagelhus, E. A., & Nedergaard, M. (2012). A Paravascular Pathway Facilitates CSF Flow Through the Brain Parenchyma and the

Clearance of Interstitial Solutes, Including Amyloid β. *Science Translational Medicine*, *4*(147). https://doi.org/10.1126/scitranslmed.3003748

Impey, S., Obrietan, K., Wong, S. T., Poser, S., Yano, S., Wayman, G., Deloulme, J. C., Chan, G., & Storm, D. R. (1998). Cross talk between ERK and PKA is required for Ca2+ stimulation of CREB-dependent transcription and ERK nuclear translocation. *Neuron*, *21*(4), 869–883. https://doi.org/10.1016/s0896-6273(00)80602-9

Ingelsson, M., Fukumoto, H., Newell, K. L., Growdon, J. H., Hedley-Whyte, E. T., Frosch, M. P., Albert, M. S., Hyman, B. T., & Irizarry, M. C. (2004). Early Abeta accumulation and progressive synaptic loss, gliosis, and tangle formation in AD brain. *Neurology*, *62*(6), 925–931. https://doi.org/10.1212/01.wnl.0000115115.98960.37

Inoue, R., & Nishimune, H. (2023). Neuronal Plasticity and Age-Related Functional Decline in the Motor Cortex. In *Cells* (Vol. 12, Issue 17). Multidisciplinary Digital Publishing Institute (MDPI). https://doi.org/10.3390/cells12172142

Iseki, M., & Park, S.-Y. (2021). Photoactivated Adenylyl Cyclases: Fundamental Properties and Applications. *Advances in Experimental Medicine and Biology*, *1293*, 129–139. https://doi.org/10.1007/978-981-15-8763-4_7

Jain, A., Huang, G. Z., & Woolley, C. S. (2019). Latent Sex Differences in Molecular Signaling That Underlies Excitatory Synaptic Potentiation in the Hippocampus. *The Journal of Neuroscience : The Official Journal of the Society for Neuroscience*, *39*(9), 1552–1565. https://doi.org/10.1523/JNEUROSCI.1897-18.2018

Jankowsky, J. L., Slunt, H. H., Ratovitski, T., Jenkins, N. A., Copeland, N. G., & Borchelt, D. R. (2001). Co-expression of multiple transgenes in mouse CNS: a comparison of strategies. In *Biomolecular Engineering* (Vol. 17). www.elsevier.com/locate/geneanabioeng

Jansen, A. H. P., van Hal, M., Op den Kelder, I. C., Meier, R. T., de Ruiter, A.-A., Schut, M. H., Smith, D. L., Grit, C., Brouwer, N., Kamphuis, W., Boddeke, H. W. G. M., den Dunnen, W. F. A., van Roon, W. M. C., Bates, G. P., Hol, E. M., & Reits, E. A. (2017). Frequency of nuclear mutant huntingtin inclusion formation in neurons and glia is cell-type-specific. *Glia*, *65*(1), 50–61. https://doi.org/10.1002/glia.23050

Jauhar, S., & Ritchie, S. (2010). Psychiatric and behavioural manifestations of Huntington's Disease. *Advances in Psychiatric Treatment*, *16*(3), 168–175. https://doi.org/10.1192/apt.bp.107.005371

Jawhar, S., Trawicka, A., Jenneckens, C., Bayer, T. A., & Wirths, O. (2012). Motor deficits, neuron loss, and reduced anxiety coinciding with axonal degeneration and intraneuronal Aβ aggregation in the 5XFAD mouse model of Alzheimer's Disease. *Neurobiology of Aging*, *33*(1), 196.e29-196.e40. https://doi.org/10.1016/j.neurobiolaging.2010.05.027

Jiang, R., Diaz-Castro, B., Looger, L. L., & Khakh, B. S. (2016a). Dysfunctional Calcium and Glutamate Signaling in Striatal Astrocytes from Huntington's Disease Model Mice. *The Journal of Neuroscience : The Official Journal of the Society for Neuroscience*, *36*(12), 3453–3470. https://doi.org/10.1523/JNEUROSCI.3693-15.2016

Jiang, R., Diaz-Castro, B., Looger, L. L., & Khakh, B. S. (2016b). Dysfunctional Calcium and Glutamate Signaling in Striatal Astrocytes from Huntington's Disease Model Mice. *The Journal of Neuroscience : The Official Journal of the Society for Neuroscience*, *36*(12), 3453–3470. https://doi.org/10.1523/JNEUROSCI.3693-15.2016

Jones-Tabah, J., Mohammad, H., Paulus, E. G., Clarke, P. B. S., & Hébert, T. E. (2022). The Signaling and Pharmacology of the Dopamine D1 Receptor. In *Frontiers in Cellular Neuroscience* (Vol. 15). Frontiers Media S.A. https://doi.org/10.3389/fncel.2021.806618

Joo, K. M., Chung, Y. H., Kim, M. K., Nam, R. H., Lee, B. L., Lee, K. H., & Cha, C. I. (2004). Distribution of vasoactive intestinal peptide and pituitary adenylate cyclase-activating polypeptide receptors (VPAC1, VPAC2, and PAC1 receptor) in the rat brain. *The Journal of Comparative Neurology*, *476*(4), 388–413. https://doi.org/10.1002/cne.20231

Jost, B. C., & Grossberg, G. T. (1995). The Natural History of Alzheimer's Disease: A Brain Bank Study. *Journal of the American Geriatrics Society*, *43*(11), 1248–1255. https://doi.org/10.1111/j.1532-5415.1995.tb07401.x

Jourdain, P., Bergersen, L. H., Bhaukaurally, K., Bezzi, P., Santello, M., Domercq, M., Matute, C., Tonello, F., Gundersen, V., & Volterra, A. (2007). Glutamate exocytosis from astrocytes controls synaptic strength. *Nature Neuroscience*, *10*(3), 331–339. https://doi.org/10.1038/nn1849

Kalueff, A. V, Stewart, A. M., Song, C., Berridge, K. C., Graybiel, A. M., & Fentress, J. C. (2016). Neurobiology of rodent self-grooming and its value for translational neuroscience. *Nature Reviews. Neuroscience*, *17*(1), 45–59. https://doi.org/10.1038/nrn.2015.8

Kandel, E. R. (2012). The molecular biology of memory: cAMP, PKA, CRE, CREB-1, CREB-2, and CPEB. *Molecular Brain*, *5*, 14. https://doi.org/10.1186/1756-6606-5-14

Keller, L. A., Merkel, O., & Popp, A. (2022). Intranasal drug delivery: opportunities and toxicologic challenges during drug development. *Drug Delivery and Translational Research*, *12*(4), 735–757. https://doi.org/10.1007/s13346-020-00891-5

Kelly, M. P. (2018). Cyclic nucleotide signaling changes associated with normal aging and age-related diseases of the brain. *Cellular Signalling*, *42*, 281–291. https://doi.org/10.1016/j.cellsig.2017.11.004

Kennedy, M. J., Hughes, R. M., Peteya, L. A., Schwartz, J. W., Ehlers, M. D., & Tucker, C. L. (2010). Rapid blue-light-mediated induction of protein interactions in living cells. *Nature Methods*, *7*(12), 973–975. https://doi.org/10.1038/nmeth.1524

Khakh, B. S., & Goldman, S. A. (2023). Astrocytic contributions to Huntington's Disease pathophysiology. In *Annals of the New York Academy of Sciences* (Vol. 1522, Issue 1, pp. 42–59). John Wiley and Sons Inc. https://doi.org/10.1111/nyas.14977

Kieburtz, K. (1996). Unified Huntington's Disease rating scale: Reliability and consistency. *Movement Disorders*, *11*(2), 136–142. https://doi.org/10.1002/mds.870110204

Kilanowska, A., & Ziółkowska, A. (2020). Role of phosphodiesterase in the biology and pathology of diabetes. In *International Journal of Molecular Sciences* (Vol. 21, Issue 21, pp. 1–26). MDPI AG. https://doi.org/10.3390/ijms21218244

Kim, A., Lalonde, K., Truesdell, A., Welter, P. G., Brocardo, P. S., Rosenstock, T. R., & Gil-mohapel, J. (2021). New avenues for the treatment of Huntington's Disease. In *International Journal of Molecular Sciences* (Vol. 22, Issue 16). MDPI AG. https://doi.org/10.3390/ijms22168363

Kim, C. K., Lee, Y. R., Ong, L., Gold, M., Kalali, A., & Sarkar, J. (2022). Alzheimer's Disease: Key Insights from Two Decades of Clinical Trial Failures. In *Journal of Alzheimer's Disease* (Vol. 87, Issue 1, pp. 83–100). IOS Press BV. https://doi.org/10.3233/JAD-215699

Kim, J., Basak, J. M., & Holtzman, D. M. (2009). The Role of Apolipoprotein E in Alzheimer's Disease. In *Neuron* (Vol. 63, Issue 3, pp. 287–303). https://doi.org/10.1016/j.neuron.2009.06.026

Kim, S. H., Nairn, A. C., Cairns, N., & Lubec, G. (2001). Decreased levels of ARPP-19 and PKA in brains of Down syndrome and Alzheimer's Disease. *Journal of Neural Transmission. Supplementum*, *61*, 263–272. https://doi.org/10.1007/978-3-7091-6262-0_21

Kim, U. H., Kim, J. W., & Rhee, S. G. (1989). Phosphorylation of phospholipase C-gamma by cAMP-dependent protein kinase. *The Journal of Biological Chemistry*, *264*(34), 20167–20170.

Knopman, D. S., Amieva, H., Petersen, R. C., Chételat, G., Holtzman, D. M., Hyman, B. T., Nixon, R. A., & Jones, D. T. (2021). Alzheimer disease. *Nature Reviews Disease Primers*, *7*(1). https://doi.org/10.1038/s41572-021-00269-y

Kofuji, P., & Araque, A. (2021). G-Protein-Coupled Receptors in Astrocyte–Neuron Communication. In *Neuroscience* (Vol. 456, pp. 71–84). Elsevier Ltd. https://doi.org/10.1016/j.neuroscience.2020.03.025

Koopmans, F., van Nierop, P., Andres-Alonso, M., Byrnes, A., Cijsouw, T., Coba, M. P., Cornelisse, L. N., Farrell, R. J., Goldschmidt, H. L., Howrigan, D. P., Hussain, N. K.,

Imig, C., de Jong, A. P. H., Jung, H., Kohansalnodehi, M., Kramarz, B., Lipstein, N., Lovering, R. C., MacGillavry, H., … Verhage, M. (2019). SynGO: An Evidence-Based, Expert-Curated Knowledge Base for the Synapse. *Neuron*, *103*(2), 217-234.e4. https://doi.org/10.1016/j.neuron.2019.05.002

Kopach, O., Zheng, K., & Rusakov, D. A. (2020). Optical monitoring of glutamate release at multiple synapses in situ detects changes following LTP induction. *Molecular Brain*, *13*(1), 39. https://doi.org/10.1186/s13041-020-00572-x

Korrell, K. V., Disser, J., Parley, K., Vadisiute, A., Requena-Komuro, M. C., Fodder, H., Pollart, C., Knott, G., Molnár, Z., & Hoerder-Suabedissen, A. (2019). Differential effect on myelination through abolition of activity-dependent synaptic vesicle release or reduction of overall electrical activity of selected cortical projections in the mouse. *Journal of Anatomy*, *235*(3), 452–467. https://doi.org/10.1111/joa.12974

Koss, D. J., Jones, G., Cranston, A., Gardner, H., Kanaan, N. M., & Platt, B. (2016). Soluble pre-fibrillar tau and β-amyloid species emerge in early human Alzheimer's Disease and track disease progression and cognitive decline. *Acta Neuropathologica*, *132*(6), 875–895. https://doi.org/10.1007/s00401-016-1632-3

Koubek, E. J., & Santy, L. C. (2022). Actin Up: An Overview of the Rac GEF Dock1/Dock180 and Its Role in Cytoskeleton Rearrangement. *Cells*, *11*(22). https://doi.org/10.3390/cells11223565

Kowiański, P., Lietzau, G., Czuba, E., Waśkow, M., Steliga, A., & Moryś, J. (2018). BDNF: A Key Factor with Multipotent Impact on Brain Signaling and Synaptic Plasticity. In *Cellular and Molecular Neurobiology* (Vol. 38, Issue 3, pp. 579–593). Springer New York LLC. https://doi.org/10.1007/s10571-017-0510-4

Krämer, A., Green, J., Pollard, J., & Tugendreich, S. (2014). Causal analysis approaches in Ingenuity Pathway Analysis. *Bioinformatics*, *30*(4), 523. https://doi.org/10.1093/BIOINFORMATICS/BTT703

Krauss, J. K., Lipsman, N., Aziz, T., Boutet, A., Brown, P., Chang, J. W., Davidson, B., Grill, W. M., Hariz, M. I., Horn, A., Schulder, M., Mammis, A., Tass, P. A., Volkmann, J., & Lozano, A. M. (2021). Technology of deep brain stimulation: current status and future directions. In *Nature Reviews Neurology* (Vol. 17, Issue 2, pp. 75–87). Nature Research. https://doi.org/10.1038/s41582-020-00426-z

Kreitzer, A. C., & Malenka, R. C. (2008). Striatal Plasticity and Basal Ganglia Circuit Function. In *Neuron* (Vol. 60, Issue 4, pp. 543–554). https://doi.org/10.1016/j.neuron.2008.11.005

Kremer, B., Almqvist, E., Theilmann, J., Spence, ' N, Telenius, H., Goldberg, Y. P., & Hayden', M. R. (1995). Sex-Dependent Mechanisms For Expansions and Contractions

of the CAG Repeat on Affected Huntington Disease Chromosomes. In *Am. J. Hum. Genet* (Vol. 57).

Kruyer, A. (2022). Astrocyte Heterogeneity in Regulation of Synaptic Activity. In *Cells* (Vol. 11, Issue 19). MDPI. https://doi.org/10.3390/cells11193135

Kupferschmidt, D. A., Juczewski, K., Cui, G., Johnson, K. A., & Lovinger, D. M. (2017). Parallel, but Dissociable, Processing in Discrete Corticostriatal Inputs Encodes Skill Learning. *Neuron*, *96*(2), 476-489.e5. https://doi.org/10.1016/j.neuron.2017.09.040

Kwon, D. (2021). Failure of genetic therapies for Huntington's devastates community. *Nature*, *593*(7858), 180. https://doi.org/10.1038/d41586-021-01177-7

Lane, C. A., Hardy, J., & Schott, J. M. (2018). Alzheimer's Disease. In *European Journal of Neurology* (Vol. 25, Issue 1, pp. 59–70). Blackwell Publishing Ltd. https://doi.org/10.1111/ene.13439

Le Heron, C., Apps., M. A. J., & Husain, M. (2018). The anatomy of apathy: A neurocognitive framework for amotivated behaviour. *Neuropsychologia*, *118*, 54–67. https://doi.org/10.1016/j.neuropsychologia.2017.07.003

Leahy, M. J., de Mul, F. F., Nilsson, G. E., & Maniewski, R. (1999). Principles and practice of the laser-Doppler perfusion technique. *Technology and Health Care : Official Journal of the European Society for Engineering and Medicine*, *7*(2–3), 143–162.

Lee, J. H., Tecedor, L., Chen, Y. H., Monteys, A. M., Sowada, M. J., Thompson, L. M., & Davidson, B. L. (2015). Reinstating aberrant mTORC1 activity in Huntington's Disease mice improves disease phenotypes. *Neuron*, *85*(2), 303–315. https://doi.org/10.1016/j.neuron.2014.12.019

Lefkimmiatis, K., & Zaccolo, M. (2014). cAMP signaling in subcellular compartments. *Pharmacology & Therapeutics*, *143*(3), 295–304. https://doi.org/10.1016/j.pharmthera.2014.03.008

Lehmann, M., Ghosh, P. M., Madison, C., Laforce, R., Corbetta-Rastelli, C., Weiner, M. W., Greicius, M. D., Seeley, W. W., Gorno-Tempini, M. L., Rosen, H. J., Miller, B. L., Jagust, W. J., & Rabinovici, G. D. (2013). Diverging patterns of amyloid deposition and hypometabolism in clinical variants of probable Alzheimer's Disease. *Brain*, *136*(3), 844–858. https://doi.org/10.1093/brain/aws327

Lehtinen, K., Nokia, M. S., & Takala, H. (2022). Red Light Optogenetics in Neuroscience. In *Frontiers in Cellular Neuroscience* (Vol. 15). Frontiers Media S.A. https://doi.org/10.3389/fncel.2021.778900

Lemere, C. A., Munger, J. S., Shi, G. P., Natkin, L., Haass, C., Chapman, H. A., & Selkoe, D. J. (1995). The lysosomal cysteine protease, cathepsin S, is increased in Alzheimer's

Disease and Down syndrome brain. An immunocytochemical study. *The American Journal of Pathology*, *146*(4), 848–860.

Lemiere, J., Decruyenaere, M., Evers-Kiebooms, G., Vandenbussche, E., & Dom, R. (2004). Cognitive changes in patients with Huntington?s disease (HD) and asymptomatic carriers of the HD mutation. *Journal of Neurology*, *251*(8). https://doi.org/10.1007/s00415-004-0461-9

Leopold, A. V., Chernov, K. G., Shemetov, A. A., & Verkhusha, V. V. (2019). Neurotrophin receptor tyrosine kinases regulated with near-infrared light. *Nature Communications*, *10*(1). https://doi.org/10.1038/s41467-019-08988-3

Levine, M. S., Cepeda, C., Hickey, M. A., Fleming, S. M., & Chesselet, M.-F. (2004). Genetic mouse models of Huntington's and Parkinson's diseases: illuminating but imperfect. *Trends in Neurosciences*, *27*(11), 691–697. https://doi.org/10.1016/j.tins.2004.08.008

Levy, R., & Dubois, B. (2006). Apathy and the functional anatomy of the prefrontal cortex-basal ganglia circuits. In *Cerebral Cortex* (Vol. 16, Issue 7, pp. 916–928). https://doi.org/10.1093/cercor/bhj043

Li, J. Y., Plomann, M., & Brundin, P. (2003). Huntington's Disease: A synaptopathy? *Trends in Molecular Medicine*, *9*(10), 414–420. https://doi.org/10.1016/j.molmed.2003.08.006

Li, Y., Bor, Y.-C., Fitzgerald, M. P., Lee, K. S., Rekosh, D., & Hammarskjold, M.-L. (2016). An NXF1 mRNA with a retained intron is expressed in hippocampal and neocortical neurons and is translated into a protein that functions as an Nxf1 cofactor. *Molecular Biology of the Cell*, *27*(24), 3903–3912. https://doi.org/10.1091/mbc.E16-07-0515

Lia, A., Di Spiezio, A., Speggiorin, M., & Zonta, M. (2023). Two decades of astrocytes in neurovascular coupling. In *Frontiers in Network Physiology* (Vol. 3). Frontiers Media SA. https://doi.org/10.3389/fnetp.2023.1162757

Liang, Z., Liu, F., Grundke-Iqbal, I., Iqbal, K., & Gong, C.-X. (2007). Down-regulation of cAMP-dependent protein kinase by over-activated calpain in Alzheimer disease brain. *Journal of Neurochemistry*, *103*(6), 2462–2470. https://doi.org/10.1111/j.1471-4159.2007.04942.x

Liddelow, S. A., & Barres, B. A. (2017). Reactive Astrocytes: Production, Function, and Therapeutic Potential. In *Immunity* (Vol. 46, Issue 6, pp. 957–967). Cell Press. https://doi.org/10.1016/j.immuni.2017.06.006

Liévens, J. C., Woodman, B., Mahal, A., Spasic-Boscovic, O., Samuel, D., Kerkerian-Le Goff, L., & Bates, G. P. (2001). Impaired glutamate uptake in the R6 Huntington's Disease transgenic mice. *Neurobiology of Disease*, *8*(5), 807–821. https://doi.org/10.1006/nbdi.2001.0430

Lin, C.-H., Tallaksen-Greene, S., Chien, W.-M., Cearley, J. A., Jackson, W. S., Crouse, A. B., Ren, S., Li, X.-J., Albin, R. L., & Detloff, P. J. (2001). Neurological abnormalities in a knock-in mouse model of Huntington's Disease. In *Human Molecular Genetics* (Vol. 10, Issue 2).

Lin, J.-T., Chang, W.-C., Chen, H.-M., Lai, H.-L., Chen, C.-Y., Tao, M.-H., & Chern, Y. (2013). Regulation of Feedback between Protein Kinase A and the Proteasome System Worsens Huntington's Disease. *Molecular and Cellular Biology*, *33*(5), 1073–1084. https://doi.org/10.1128/mcb.01434-12

Lisman, J. E., & Harris, K. M. (1993). Quantal analysis and synaptic anatomy--integrating two views of hippocampal plasticity. *Trends in Neurosciences*, *16*(4), 141–147. https://doi.org/10.1016/0166-2236(93)90122-3

Lisman, J., Schulman, H., & Cline, H. (2002). The molecular basis of CaMKII function in synaptic and behavioural memory. *Nature Reviews. Neuroscience*, *3*(3), 175–190. https://doi.org/10.1038/nrn753

Liu, C.-C., Hu, J., Zhao, N., Wang, J., Wang, N., Cirrito, J. R., Kanekiyo, T., Holtzman, D. M., & Bu, G. (2017). Astrocytic LRP1 Mediates Brain Aβ Clearance and Impacts Amyloid Deposition. *The Journal of Neuroscience : The Official Journal of the Society for Neuroscience*, *37*(15), 4023–4031. https://doi.org/10.1523/JNEUROSCI.3442-16.2017

Liu, G., Martins, I. H., Chiorini, J. A., & Davidson, B. L. (2005). Adeno-associated virus type 4 (AAV4) targets ependyma and astrocytes in the subventricular zone and RMS. *Gene Therapy*, *12*(20), 1503–1508. https://doi.org/10.1038/sj.gt.3302554

Liu, H., Chen, L., Zhang, C., Liu, C., Li, Y., Cheng, L., Ouyang, Y., Rutledge, C., Anderson, J., Wei, Z., Zhang, Z., Lu, H., Van Zijl, P. C. M., Iliff, J. J., Xu, J., & Duan, W. (2024). Glymphatic influx and clearance are perturbed in Huntington's Disease. *JCI Insight*. https://doi.org/10.1172/jci.insight.172286

Liu, P. P., Xie, Y., Meng, X. Y., & Kang, J. S. (2019). History and progress of hypotheses and clinical trials for Alzheimer's Disease. In *Signal Transduction and Targeted Therapy* (Vol. 4, Issue 1). Springer Nature. https://doi.org/10.1038/s41392-019-0063-8

Liu, S., Anderson, P. J., Rajagopal, S., Lefkowitz, R. J., & Rockman, H. A. (2024). G Protein-Coupled Receptors: A Century of Research and Discovery. In *Circulation Research* (Vol. 135, Issue 1, pp. 174–197). Lippincott Williams and Wilkins. https://doi.org/10.1161/CIRCRESAHA.124.323067

Livingston, G., Huntley, J., Sommerlad, A., Ames, D., Ballard, C., Banerjee, S., Brayne, C., Burns, A., Cohen-Mansfield, J., Cooper, C., Costafreda, S. G., Dias, A., Fox, N., Gitlin, L. N., Howard, R., Kales, H. C., Kivimäki, M., Larson, E. B., Ogunniyi, A., … Mukadam, N. (2020). Dementia prevention, intervention, and care: 2020 report of the

Lancet Commission. In *The Lancet* (Vol. 396, Issue 10248, pp. 413–446). Lancet Publishing Group. https://doi.org/10.1016/S0140-6736(20)30367-6

London, E., Noguchi, A., Springer, D., Faidas, M., Gavrilova, O., Eisenhofer, G., & Stratakis, C. A. (2019). The Catalytic Subunit β of PKA Affects Energy Balance and Catecholaminergic Activity. *Journal of the Endocrine Society*, *3*(5), 1062–1078. https://doi.org/10.1210/js.2019-00029

Long, J. D., Gantman, E. C., Mills, J. A., Vaidya, J. G., Mansbach, A., Tabrizi, S. J., & Sampaio, C. (2023). Applying the Huntington's Disease Integrated Staging System (HD-ISS) to Observational Studies. *Journal of Huntington's Disease*, *12*(1), 57–69. https://doi.org/10.3233/JHD-220555

Losi, A., Gardner, K. H., & Möglich, A. (2018). Blue-Light Receptors for Optogenetics. *Chemical Reviews*, *118*(21), 10659–10709. https://doi.org/10.1021/acs.chemrev.8b00163

Lundquist, A. J., Llewellyn, G. N., Kishi, S. H., Jakowec, N. A., Cannon, P. M., Petzinger, G. M., & Jakowec, M. W. (2022). Knockdown of Astrocytic Monocarboxylate Transporter 4 in the Motor Cortex Leads to Loss of Dendritic Spines and a Deficit in Motor Learning. *Molecular Neurobiology*, *59*(2), 1002–1017. https://doi.org/10.1007/s12035-021-02651-z

Luo, C., Kuner, T., & Kuner, R. (2014). Synaptic plasticity in pathological pain. In *Trends in Neurosciences* (Vol. 37, Issue 6, pp. 343–355). Elsevier Ltd. https://doi.org/10.1016/j.tins.2014.04.002

Luyben, T. T., Rai, J., Li, H., Georgiou, J., Avila, A., Zhen, M., Collingridge, G. L., Tominaga, T., & Okamoto, K. (2020). Optogenetic Manipulation of Postsynaptic cAMP Using a Novel Transgenic Mouse Line Enables Synaptic Plasticity and Enhances Depolarization Following Tetanic Stimulation in the Hippocampal Dentate Gyrus. *Frontiers in Neural Circuits*, *14*. https://doi.org/10.3389/fncir.2020.00024

Lykken, E. A., Shyng, C., Edwards, R. J., Rozenberg, A., & Gray, S. J. (2018). Recent progress and considerations for AAV gene therapies targeting the central nervous system. *Journal of Neurodevelopmental Disorders*, *10*(1), 1–10. https://doi.org/10.1186/s11689-018-9234-0

Ma, X. C., Chu, Z., Zhang, X. L., Jiang, W. H., Jia, M., Dang, Y. H., & Gao, C. G. (2016). Intranasal Delivery of Recombinant NT4-NAP/AAV Exerts Potential Antidepressant Effect. *Neurochemical Research*, *41*(6), 1375–1380. https://doi.org/10.1007/s11064-016-1841-0

Mahmoudi, P., Veladi, H., & Pakdel, F. G. (2017). Optogenetics, Tools and Applications in Neurobiology. *Journal of Medical Signals and Sensors*, *7*(2), 71–79.

Maki, T., Okamoto, Y., Carare, R. O., Hase, Y., Hattori, Y., Hawkes, C. A., Saito, S., Yamamoto, Y., Terasaki, Y., Ishibashi-Ueda, H., Taguchi, A., Takahashi, R., Miyakawa, T., Kalaria, R. N., Lo, E. H., Arai, K., & Ihara, M. (2014). Phosphodiesterase III inhibitor promotes drainage of cerebrovascular β-amyloid. *Annals of Clinical and Translational Neurology*, *1*(8), 519–533. https://doi.org/10.1002/acn3.79

Makitani, K., Nakagawa, S., Izumi, Y., Akaike, A., & Kume, T. (2017). Inhibitory effect of donepezil on bradykinin-induced increase in the intracellular calcium concentration in cultured cortical astrocytes. *Journal of Pharmacological Sciences*, *134*(1), 37–44. https://doi.org/10.1016/j.jphs.2017.03.008

Malarkey, E. B., Ni, Y., & Parpura, V. (2008). Ca2+ entry through TRPC1 channels contributes to intracellular Ca2+ dynamics and consequent glutamate release from rat astrocytes. *GLIA*, *56*(8), 821–835. https://doi.org/10.1002/glia.20656

Malenka, R. C. (1991). Postsynaptic factors control the duration of synaptic enhancement in area CA1 of the hippocampus. *Neuron*, *6*(1), 53–60. https://doi.org/10.1016/0896-6273(91)90121-f

Malenka, R. C., & Bear, M. F. (2004). Review LTP and LTD: An Embarrassment of Riches useful to conceptualize LTP and LTD as a general class of cellular/synaptic phenomena. Just as different neu-rons express different complements of ion channels to. In *Neuron* (Vol. 44).

Man, H. Y., Lin, J. W., Ju, W. H., Ahmadian, G., Liu, L., Becker, L. E., Sheng, M., & Wang, Y. T. (2000). Regulation of AMPA receptor-mediated synaptic transmission by clathrin-dependent receptor internalization. *Neuron*, *25*(3), 649–662. https://doi.org/10.1016/s0896-6273(00)81067-3

Mangiarini, L., Sathasivam, K., Seller, M., Cozens, B., Harper, A., Hetherington, C., Davies, S. W., & Bates, G. P. (1996). Exon 1 of the HD Gene with an Expanded CAG Repeat Is Sufficient to Cause a Progressive Neurological Phenotype in Transgenic Mice The onset of symptoms is generally in midlife although. In *Cell* (Vol. 87).

Mariotti, L., Losi, G., Lia, A., Melone, M., Chiavegato, A., Gómez-Gonzalo, M., Sessolo, M., Bovetti, S., Forli, A., Zonta, M., Requie, L. M., Marcon, I., Pugliese, A., Viollet, C., Bettler, B., Fellin, T., Conti, F., & Carmignoto, G. (2018). Interneuron-specific signaling evokes distinctive somatostatin-mediated responses in adult cortical astrocytes. *Nature Communications*, *9*(1). https://doi.org/10.1038/s41467-017-02642-6

Martín, R., Bajo-Grañeras, R., Moratalla, R., Perea, G., & Araque, A. (2015). Circuit-specific signaling in astrocyte-neuron networks in basal ganglia pathways. *Science (New York, N.Y.)*, *349*(6249), 730–734. https://doi.org/10.1126/science.aaa7945

Martin, S. J., Grimwood, P. D., & Morris, R. G. (2000). Synaptic plasticity and memory: an evaluation of the hypothesis. *Annual Review of Neuroscience*, *23*, 649–711. https://doi.org/10.1146/annurev.neuro.23.1.649

Martinez-Val, A., Bekker-Jensen, D. B., Hogrebe, A., & Olsen, J. V. (2021). Data Processing and Analysis for DIA-Based Phosphoproteomics Using Spectronaut. *Methods in Molecular Biology*, *2361*, 95–107. https://doi.org/10.1007/978-1-0716-1641-3_6

Massengill, C. I., Day-Cooney, J., Mao, T., & Zhong, H. (2021). Genetically encoded sensors towards imaging cAMP and PKA activity in vivo. *Journal of Neuroscience Methods*, *362*(July), 109298. https://doi.org/10.1016/j.jneumeth.2021.109298

Masters, C. L., Simms, G., Weinman, N. A., Multhaup, G., McDonald, B. L., & Beyreuther, K. (1985). Amyloid plaque core protein in Alzheimer disease and Down syndrome. *Proceedings of the National Academy of Sciences of the United States of America*, *82*(12), 4245–4249. https://doi.org/10.1073/pnas.82.12.4245

Mathiesen, S. N., Lock, J. L., Schoderboeck, L., Abraham, W. C., & Hughes, S. M. (2020). CNS Transduction Benefits of AAV-PHP.eB over AAV9 Are Dependent on Administration Route and Mouse Strain. *Molecular Therapy Methods and Clinical Development*, *19*, 447–458. https://doi.org/10.1016/j.omtm.2020.10.011

Matos, M., Augusto, E., Machado, N. J., dos Santos-Rodrigues, A., Cunha, R. A., & Agostinho, P. (2012). Astrocytic adenosine A2A receptors control the amyloid-β peptide-induced decrease of glutamate uptake. *Journal of Alzheimer's Disease : JAD*, *31*(3), 555–567. https://doi.org/10.3233/JAD-2012-120469

Matsuoka*, Y., Li, X., & Bennett, V. (2000). Adducin: structure, function and regulation. *Cellular and Molecular Life Sciences*, *57*(6), 884–895. https://doi.org/10.1007/PL00000731

Matsuoka, Y., Picciano, M., Maleste, B., LaFrancois, J., Zehr, C., Daeschner, J. A. M., Olschowka, J. A., Fonseca, M. I., O'Banion, M. K., Tenner, A. J., Lemere, C. A., & Duff, K. (2001). Inflammatory responses to amyloidosis in a transgenic mouse model of Alzheimer's Disease. *American Journal of Pathology*, *158*(4), 1345–1354. https://doi.org/10.1016/S0002-9440(10)64085-0

Mayer, M. L., Westbrook, G. L., & Guthrie, P. B. (1984). Voltage-dependent block by Mg2+ of NMDA responses in spinal cord neurones. *Nature*, *309*(5965), 261–263. https://doi.org/10.1038/309261a0

McColgan, P., & Tabrizi, S. J. (2018). Huntington's Disease: a clinical review. *European Journal of Neurology*, *25*(1), 24–34. https://doi.org/10.1111/ene.13413

McKnight, G. S. (1991). Cyclic AMP second messenger systems. *Current Opinion in Cell Biology*, *3*(2), 213–217. https://doi.org/10.1016/0955-0674(91)90141-k

McLachlan, C. S., Chen, M. L., Lynex, C. N., Goh, D. L. M., Brenner, S., & Tay, S. K. H. (2007). Changes in PDE4D isoforms in the hippocampus of a patient with advanced Alzheimer disease. *Archives of Neurology*, *64*(3), 456–457. https://doi.org/10.1001/archneur.64.3.456

Mclauchlan, D. J., Lancaster, T., Craufurd, D., Linden, D. E. J., & Rosser, A. E. (2022). Different depression: motivational anhedonia governs antidepressant efficacy in Huntington's Disease. *Brain Communications*, *4*(6). https://doi.org/10.1093/braincomms/fcac278

Medina, A., Mahjoub, Y., Shaver, L., & Pringsheim, T. (2022). Prevalence and Incidence of Huntington's Disease: An Updated Systematic Review and Meta-Analysis. In *Movement Disorders* (Vol. 37, Issue 12, pp. 2327–2335). John Wiley and Sons Inc. https://doi.org/10.1002/mds.29228

Mehta, R. I., & Mehta, R. I. (2023). The Vascular-Immune Hypothesis of Alzheimer's Disease. In *Biomedicines* (Vol. 11, Issue 2). MDPI. https://doi.org/10.3390/biomedicines11020408

Menalled, L. B. (2005). Knock-in mouse models of Huntington's Disease. *NeuroRx : The Journal of the American Society for Experimental NeuroTherapeutics*, *2*(3), 465–470. https://doi.org/10.1602/neurorx.2.3.465

Menalled, L. B., Kudwa, A. E., Miller, S., Fitzpatrick, J., Watson-Johnson, J., Keating, N., Ruiz, M., Mushlin, R., Alosio, W., McConnell, K., Connor, D., Murphy, C., Oakeshott, S., Kwan, M., Beltran, J., Ghavami, A., Brunner, D., Park, L. C., Ramboz, S., & Howland, D. (2012). Comprehensive Behavioral and Molecular Characterization of a New Knock-In Mouse Model of Huntington's Disease: ZQ175. *PLoS ONE*, *7*(12). https://doi.org/10.1371/journal.pone.0049838

Menniti, F. S., Chappie, T. A., & Schmidt, C. J. (2021). PDE10A Inhibitors—Clinical Failure or Window Into Antipsychotic Drug Action? In *Frontiers in Neuroscience* (Vol. 14). Frontiers Media S.A. https://doi.org/10.3389/fnins.2020.600178

Miguez, A., Barriga, G. G. D., Brito, V., Straccia, M., Giralt, A., Ginés, S., Canals, J. M., & Alberch, J. (2015). Fingolimod (FTY720) enhances hippocampal synaptic plasticity and memory in Huntington's Disease by preventing p75NTR up-regulation and astrocyte-mediated inflammation. *Human Molecular Genetics*, *24*(17), 4958–4970. https://doi.org/10.1093/hmg/ddv218

Miller, B. R., Walker, A. G., Barton, S. J., & Rebec, G. V. (2011). Dysregulated neuronal activity patterns implicate corticostriatal circuit dysfunction in multiple rodent models of Huntington's Disease. *Frontiers in Systems Neuroscience*, *MAY 2011*. https://doi.org/10.3389/fnsys.2011.00026

Milnerwood, A. J., & Raymond, L. A. (2010). Early synaptic pathophysiology in neurodegeneration: insights from Huntington's Disease. *Trends in Neurosciences*, *33*(11), 513–523. https://doi.org/10.1016/j.tins.2010.08.002

Min, R., & Nevian, T. (2012). Astrocyte signaling controls spike timing-dependent depression at neocortical synapses. *Nature Neuroscience*, *15*(5), 746–753. https://doi.org/10.1038/nn.3075

Mirallave, A., Morales, M., Cabib, C., Muñoz, E. J., Santacruz, P., Gasull, X., & Valls-Sole, J. (2017). Sensory processing in Huntington's Disease. *Clinical Neurophysiology*, *128*(5), 689–696. https://doi.org/10.1016/j.clinph.2017.01.009

Mitew, S., Kirkcaldie, M. T. K., Dickson, T. C., & Vickers, J. C. (2013). Altered synapses and gliotransmission in Alzheimer's Disease and AD model mice. *Neurobiology of Aging*, *34*(10), 2341–2351. https://doi.org/10.1016/j.neurobiolaging.2013.04.010

Miyake, K., Miyake, N., & Shimada, T. (2015). Gene Delivery into the Central Nervous System (CNS) Using AAV Vectors. In *Gene Therapy - Principles and Challenges*. InTech. https://doi.org/10.5772/61638

Miyazaki, I., Asanuma, M., Diaz-Corrales, F. J., Miyoshi, K., & Ogawa, N. (2004). Direct evidence for expression of dopamine receptors in astrocytes from basal ganglia. *Brain Research*, *1029*(1), 120–123. https://doi.org/10.1016/j.brainres.2004.09.014

Möglich, A., Yi, C., Golonka, D., Meier, S., Tang, K., Ihalainen, J., & Zurbriggen, M. (2025). *Commutability of Bilin Chromophores in Plant Phytochromes*. https://doi.org/10.21203/rs.3.rs-6196749/v1

Moiani, A., Paleari, Y., Sartori, D., Mezzadra, R., Miccio, A., Cattoglio, C., Cocchiarella, F., Lidonnici, M. R., Ferrari, G., & Mavilio, F. (2012). Lentiviral vector integration in the human genome induces alternative splicing and generates aberrant transcripts. *Journal of Clinical Investigation*, *122*(5), 1653–1666. https://doi.org/10.1172/JCI61852

Mojca Jurič, D., Miklič, Š., & Čarman-Kržan, M. (2006). Monoaminergic neuronal activity up-regulates BDNF synthesis in cultured neonatal rat astrocytes. *Brain Research*, *1108*(1), 54–62. https://doi.org/10.1016/j.brainres.2006.06.008

Montine, T. J., Phelps, C. H., Beach, T. G., Bigio, E. H., Cairns, N. J., Dickson, D. W., Duyckaerts, C., Frosch, M. P., Masliah, E., Mirra, S. S., Nelson, P. T., Schneider, J. A., Thal, D. R., Trojanowski, J. Q., Vinters, H. V., & Hyman, B. T. (2012). National institute on aging-Alzheimer's association guidelines for the neuropathologic assessment of Alzheimer's Disease: A practical approach. *Acta Neuropathologica*, *123*(1), 1–11. https://doi.org/10.1007/s00401-011-0910-3

Morris, R. G. (1999). D.O. Hebb: The Organization of Behavior, Wiley: New York; 1949. *Brain Research Bulletin*, *50*(5–6), 437. https://doi.org/10.1016/s0361-9230(99)00182-3

Mothet, J.-P., Pollegioni, L., Ouanounou, G., Martineau, M., Fossier, P., & Rard Baux, G. (2005). Glutamate receptor activation triggers a calcium-dependent and SNARE protein-dependent release of the gliotransmitter D-serine. In *PNAS April* (Vol. 12, Issue 15). www.pnas.orgcgidoi10.1073pnas.0408483102

Moujalled, D., Strasser, A., & Liddell, J. R. (2021). Molecular mechanisms of cell death in neurological diseases. In *Cell Death and Differentiation* (Vol. 28, Issue 7, pp. 2029–2044). Springer Nature. https://doi.org/10.1038/s41418-021-00814-y

Mucke, L., Masliah, E., Yu, G. Q., Mallory, M., Rockenstein, E. M., Tatsuno, G., Hu, K., Kholodenko, D., Johnson-Wood, K., & McConlogue, L. (2000). High-level neuronal expression of abeta 1-42 in wild-type human amyloid protein precursor transgenic mice: synaptotoxicity without plaque formation. *The Journal of Neuroscience : The Official Journal of the Society for Neuroscience*, *20*(11), 4050–4058. https://doi.org/10.1523/JNEUROSCI.20-11-04050.2000

Mukherjee, K., Ishii, K., Pillalamarri, V., Kammin, T., Atkin, J. F., Hickey, S. E., Xi, Q. J., Zepeda, C. J., Gusella, J. F., Talkowski, M. E., Morton, C. C., Maas, R. L., & Liao, E. C. (2016). Actin capping protein CAPZB regulates cell morphology, differentiation, and neural crest migration in craniofacial morphogenesis†. *Human Molecular Genetics*, *25*(7), 1255–1270. https://doi.org/10.1093/hmg/ddw006

Mulkey, R. M., Herron, C. E., & Malenka, R. C. (1993). An essential role for protein phosphatases in hippocampal long-term depression. *Science (New York, N.Y.)*, *261*(5124), 1051–1055. https://doi.org/10.1126/science.8394601

Munday, M. R., & Hemingway, C. J. (1999). The regulation of acetyl-CoA carboxylase--a potential target for the action of hypolipidemic agents. *Advances in Enzyme Regulation*, *39*, 205–234. https://doi.org/10.1016/s0065-2571(98)00016-8

Murk, K., Blanco Suarez, E. M., Cockbill, L. M. R., Banks, P., & Hanley, J. G. (2013). The antagonistic modulation of Arp2/3 activity by N-WASP, WAVE2 and PICK1 defines dynamic changes in astrocyte morphology. *Journal of Cell Science*, *126*(Pt 17), 3873–3883. https://doi.org/10.1242/jcs.125146

Nagel, G., Ollig, D., Fuhrmann, M., Kateriya, S., Musti, A. M., Bamberg, E., & Hegemann, P. (2002). Channelrhodopsin-1: a light-gated proton channel in green algae. *Science (New York, N.Y.)*, *296*(5577), 2395–2398. https://doi.org/10.1126/science.1072068

Nagel, G., Szellas, T., Huhn, W., Kateriya, S., Adeishvili, N., Berthold, P., Ollig, D., Hegemann, P., & Bamberg, E. (2003). Channelrhodopsin-2, a directly light-gated cation-selective membrane channel. *Proceedings of the National Academy of Sciences of the United States of America*, *100*(24), 13940–13945. https://doi.org/10.1073/pnas.1936192100

Nagele, R. G., D'Andrea, M. R., Lee, H., Venkataraman, V., & Wang, H. Y. (2003). Astrocytes accumulate Aβ42 and give rise to astrocytic amyloid plaques in Alzheimer disease brains. *Brain Research*, *971*(2), 197–209. https://doi.org/10.1016/S0006-8993(03)02361-8

Nairuz, T., Heo, J. C., & Lee, J. H. (2024). Differential Glial Response and Neurodegenerative Patterns in CA1, CA3, and DG Hippocampal Regions of 5XFAD Mice. *International Journal of Molecular Sciences*, *25*(22). https://doi.org/10.3390/ijms252212156

Naso, M. F., Tomkowicz, B., Perry, W. L., & Strohl, W. R. (2017). Adeno-Associated Virus (AAV) as a Vector for Gene Therapy. *BioDrugs*, *31*(4), 317–334. https://doi.org/10.1007/s40259-017-0234-5

Navarrete, M., & Araque, A. (2010). Endocannabinoids potentiate synaptic transmission through stimulation of astrocytes. *Neuron*, *68*(1), 113–126. https://doi.org/10.1016/j.neuron.2010.08.043

Naver, B., Stub, C., Møller, M., Fenger, K., Hansen, A. K., Hasholt, L., & Sørensen, S. A. (2003). Molecular and behavioral analysis of the R6/1 Huntington's Disease transgenic mouse. *Neuroscience*, *122*(4), 1049–1057. https://doi.org/10.1016/j.neuroscience.2003.08.053

Nazarian, A., Sun, W.-L., Zhou, L., Kemen, L. M., Jenab, S., & Quinones-Jenab, V. (2009). Sex differences in basal and cocaine-induced alterations in PKA and CREB proteins in the nucleus accumbens. *Psychopharmacology*, *203*(3), 641–650. https://doi.org/10.1007/s00213-008-1411-5

Nectow, A. R., & Nestler, E. J. (2020). Viral tools for neuroscience. *Nature Reviews Neuroscience*, *21*(12), 669–681. https://doi.org/10.1038/s41583-020-00382-z

Nedergaard, M. (1994). Direct signaling from astrocytes to neurons in cultures of mammalian brain cells. *Science (New York, N.Y.)*, *263*(5154), 1768–1771. https://doi.org/10.1126/science.8134839

Nguyen, P. V., & Kandel, E. R. (1997). Brief Θ-burst stimulation induces a transcription-dependent late phase of LTP requiring cAMP in area CA1 of the mouse hippocampus. In *Learning and Memory* (Vol. 4, Issue 2, pp. 230–243). Cold Spring Harbor Laboratory Press. https://doi.org/10.1101/lm.4.2.230

Nicoll, R. A., & Malenka, R. C. (1999). Expression mechanisms underlying NMDA receptor-dependent long-term potentiation. *Annals of the New York Academy of Sciences*, *868*, 515–525. https://doi.org/10.1111/j.1749-6632.1999.tb11320.x

Niu, H., Álvarez-Álvarez, I., Guillén-Grima, F., & Aguinaga-Ontoso, I. (2017). Prevalence and incidence of Alzheimer's Disease in Europe: A meta-analysis. *Neurologia (Barcelona, Spain)*, *32*(8), 523–532. https://doi.org/10.1016/j.nrl.2016.02.016

Oakley, H., Cole, S. L., Logan, S., Maus, E., Shao, P., Craft, J., Guillozet-Bongaarts, A., Ohno, M., Disterhoft, J., Van Eldik, L., Berry, R., & Vassar, R. (2006). Intraneuronal β-amyloid aggregates, neurodegeneration, and neuron loss in transgenic mice with five familial Alzheimer's Disease mutations: Potential factors in amyloid plaque formation. *Journal of Neuroscience*, *26*(40), 10129–10140. https://doi.org/10.1523/JNEUROSCI.1202-06.2006

Odaka, H., Arai, S., Inoue, T., & Kitaguchi, T. (2014). Genetically-encoded yellow fluorescent cAMP indicator with an expanded dynamic range for dual-color imaging. *PLoS ONE*, *9*(6). https://doi.org/10.1371/journal.pone.0100252

Oddo, S., Caccamo, A., Shepherd, J. D., Murphy, M. P., Golde, T. E., Kayed, R., Metherate, R., Mattson, M. P., Akbari, Y., & Laferla, F. M. (2003). Triple-Transgenic Model of Alzheimer's Disease with Plaques and Tangles: Intracellular A and Synaptic Dysfunction. In *Neuron* (Vol. 39).

O'Donnell, J., Zeppenfeld, D., McConnell, E., Pena, S., & Nedergaard, M. (2012). Norepinephrine: A neuromodulator that boosts the function of multiple cell types to optimize CNS performance. In *Neurochemical Research* (Vol. 37, Issue 11, pp. 2496–2512). https://doi.org/10.1007/s11064-012-0818-x

Oesterhelt, D., & Stoeckenius, W. (1971). Rhodopsin-like protein from the purple membrane of Halobacterium halobium. *Nature: New Biology*, *233*(39), 149–152. https://doi.org/10.1038/newbio233149a0

Ogawa, S., Menon, R. S., Tank, D. W., Kim, S. G., Merkle, H., Ellermann, J. M., & Ugurbil, K. (1993). Functional brain mapping by blood oxygenation level-dependent contrast magnetic resonance imaging. A comparison of signal characteristics with a biophysical model. *Biophysical Journal*, *64*(3), 803–812. https://doi.org/10.1016/S0006-3495(93)81441-3

Ohta, Y., Furuta, T., Nagai, T., & Horikawa, K. (2018). Red fluorescent cAMP indicator with increased affinity and expanded dynamic range. *Scientific Reports*, *8*(1), 1–9. https://doi.org/10.1038/s41598-018-20251-1

Oishi, Y., Hashimoto, K., Abe, A., Kuroda, M., Fujii, A., & Miyamoto, Y. (2021). Vitronectin regulates the axon specification of mouse cerebellar granule cell precursors via αvβ5 integrin in the differentiation stage. *Neuroscience Letters*, *746*, 135648. https://doi.org/10.1016/j.neulet.2021.135648

Okamoto, K., Kamikubo, Y., Yamauchi, K., Okamoto, S., Takahashi, M., Ishida, Y., Koike, M., Ikegaya, Y., Sakurai, T., & Hioki, H. (2023). Specific AAV2/PHP.eB-mediated gene

transduction of CA2 pyramidal cells via injection into the lateral ventricle. *Scientific Reports*, *13*(1). https://doi.org/10.1038/s41598-022-27372-8

O'Keeffe, M., Booker, S. A., Walsh, D., Li, M., Henley, C., Simões de Oliveira, L., Liu, M., Wang, X., Banqueri, M., Ridley, K., Dissanayake, K. N., Martinez-Gonzalez, C., Craigie, K. J., Vasoya, D., Leah, T., He, X., Hume, D. A., Duguid, I., Nolan, M. F., … Hardingham, G. E. (2025). Typical development of synaptic and neuronal properties can proceed without microglia in the cortex and thalamus. *Nature Neuroscience*, *28*(2), 268–279. https://doi.org/10.1038/s41593-024-01833-x

Okun, M. S. (2012). Deep-Brain Stimulation for Parkinson's Disease. *New England Journal of Medicine*, *367*(16), 1529–1538. https://doi.org/10.1056/NEJMct1208070

O'Neill, C., Wiehager, B., Fowler, C. J., Ravid, R., Winblad, B., & Cowburn, R. F. (1994a). Regionally selective alterations in G protein subunit levels in the Alzheimer's Disease brain. *Brain Research*, *636*(2), 193–201. https://doi.org/10.1016/0006-8993(94)91017-0

O'Neill, C., Wiehager, B., Fowler, C. J., Ravid, R., Winblad, B., & Cowburn, R. F. (1994b). Regionally selective alterations in G protein subunit levels in the Alzheimer's Disease brain. *Brain Research*, *636*(2), 193–201. https://doi.org/10.1016/0006-8993(94)91017-0

Ostrom, K. F., Lavigne, J. E., Brust, T. F., Seifert, R., Dessauer, C. W., Watts, V. J., & Ostrom, R. S. (2022). PHYSIOLOGICAL ROLES OF MAMMALIAN TRANSMEMBRANE ADENYLYL CYCLASE ISOFORMS. In *Physiological Reviews* (Vol. 102, Issue 2, pp. 815–857). American Physiological Society. https://doi.org/10.1152/physrev.00013.2021

Otmakhov, N., Khibnik, L., Otmakhova, N., Carpenter, S., Riahi, S., Asrican, B., & Lisman, J. (2004). Forskolin-Induced LTP in the CA1 Hippocampal Region Is NMDA Receptor Dependent. *Journal of Neurophysiology*, *91*(5), 1955–1962. https://doi.org/10.1152/jn.00941.2003

Ozawa, K., Nagao, M., Konno, A., Iwai, Y., Vittani, M., Kusk, P., Mishima, T., Hirai, H., Nedergaard, M., & Hirase, H. (2023). Astrocytic GPCR-Induced Ca2+ Signaling Is Not Causally Related to Local Cerebral Blood Flow Changes. *International Journal of Molecular Sciences*, *24*(17). https://doi.org/10.3390/ijms241713590

Pádua, M. S., Guil-Guerrero, J. L., & Lopes, P. A. (2024). Behaviour Hallmarks in Alzheimer's Disease 5xFAD Mouse Model. In *International Journal of Molecular Sciences* (Vol. 25, Issue 12). Multidisciplinary Digital Publishing Institute (MDPI). https://doi.org/10.3390/ijms25126766

Paes, D., Lardenoije, R., Carollo, R. M., Roubroeks, J. A. Y., Schepers, M., Coleman, P., Mastroeni, D., Delvaux, E., Pishva, E., Lunnon, K., Vanmierlo, T., van den Hove, D., & Prickaerts, J. (2021). Increased isoform-specific phosphodiesterase 4D expression is

associated with pathology and cognitive impairment in Alzheimer's Disease. *Neurobiology of Aging*, *97*, 56–64. https://doi.org/10.1016/j.neurobiolaging.2020.10.004

Palop, J. J., Chin, J., & Mucke, L. (2006). A network dysfunction perspective on neurodegenerative diseases. *Nature*, *443*(7113), 768–773. https://doi.org/10.1038/nature05289

Palop, J. J., & Mucke, L. (2010). Amyloid-B-induced neuronal dysfunction in Alzheimer's Disease: From synapses toward neural networks. In *Nature Neuroscience* (Vol. 13, Issue 7, pp. 812–818). https://doi.org/10.1038/nn.2583

Palop, J. J., & Mucke, L. (2016). Network abnormalities and interneuron dysfunction in Alzheimer disease. In *Nature Reviews Neuroscience* (Vol. 17, Issue 12, pp. 777–792). Nature Publishing Group. https://doi.org/10.1038/nrn.2016.141

Pang, Z., Lu, Y., Zhou, G., Hui, F., Xu, L., Viau, C., Spigelman, A. F., MacDonald, P. E., Wishart, D. S., Li, S., & Xia, J. (2024). MetaboAnalyst 6.0: towards a unified platform for metabolomics data processing, analysis and interpretation. *Nucleic Acids Research*, *52*(W1), W398–W406. https://doi.org/10.1093/nar/gkae253

Paradisi, I., Hernández, A., & Arias, S. (2008). Huntington disease mutation in Venezuela: Age of onset, haplotype analyses and geographic aggregation. *Journal of Human Genetics*, *53*(2), 127–135. https://doi.org/10.1007/s10038-007-0227-1

Park, H., Kim, N. Y., Lee, S., Kim, N., Kim, J., & Heo, W. Do. (2017). Optogenetic protein clustering through fluorescent protein tagging and extension of CRY2. *Nature Communications*, *8*(1), 30. https://doi.org/10.1038/s41467-017-00060-2

Park, H., & Poo, M. M. (2012). Neurotrophin regulation of neural circuit development and function. In *Nature Reviews Neuroscience* (Vol. 14, Issue 1, pp. 7–23). Nature Publishing Group. https://doi.org/10.1038/nrn3379

Park, M., Penick, E. C., Edwards, J. G., Kauer, J. A., & Ehlers, M. D. (2004). Recycling endosomes supply AMPA receptors for LTP. *Science (New York, N.Y.)*, *305*(5692), 1972–1975. https://doi.org/10.1126/science.1102026

Paroni, G., Bisceglia, P., & Seripa, D. (2019). Understanding the Amyloid Hypothesis in Alzheimer's Disease. *Journal of Alzheimer's Disease : JAD*, *68*(2), 493–510. https://doi.org/10.3233/JAD-180802

Parri, H. R., Gould, T. M., & Crunelli, V. (2001). Spontaneous astrocytic Ca2+ oscillations in situ drive NMDAR-mediated neuronal excitation. *Nature Neuroscience*, *4*(8), 803–812. https://doi.org/10.1038/90507

Paskus, J. D., Herring, B. E., & Roche, K. W. (2020). Kalirin and Trio: RhoGEFs in Synaptic Transmission, Plasticity, and Complex Brain Disorders. *Trends in Neurosciences*, *43*(7), 505–518. https://doi.org/10.1016/j.tins.2020.05.002

Peng, Q., Wu, B., Jiang, M., Jin, J., Hou, Z., Zheng, J., Zhang, J., & Duan, W. (2016). Characterization of behavioral, neuropathological, brain metabolic and key molecular changes in zQ175 knock-in mouse model of Huntington's Disease. *PLoS ONE*, *11*(2). https://doi.org/10.1371/journal.pone.0148839

Perea, G., & Araque, A. (2005). Properties of synaptically evoked astrocyte calcium signal reveal synaptic information processing by astrocytes. *Journal of Neuroscience*, *25*(9), 2192–2203. https://doi.org/10.1523/JNEUROSCI.3965-04.2005

Perea, G., & Araque, A. (2007). Astrocytes potentiate transmitter release at single hippocampal synapses. *Science (New York, N.Y.)*, *317*(5841), 1083–1086. https://doi.org/10.1126/science.1144640

Perea, G., Navarrete, M., & Araque, A. (2009). Tripartite synapses: astrocytes process and control synaptic information. In *Trends in Neurosciences* (Vol. 32, Issue 8, pp. 421–431). https://doi.org/10.1016/j.tins.2009.05.001

Pérez-Torres, S., Cortés, R., Tolnay, M., Probst, A., Palacios, J. M., & Mengod, G. (2003). Alterations on phosphodiesterase type 7 and 8 isozyme mRNA expression in Alzheimer's Disease brains examined by in situ hybridization. *Experimental Neurology*, *182*(2), 322–334. https://doi.org/10.1016/S0014-4886(03)00042-6

Petzold, G. C., & Murthy, V. N. (2011). Role of Astrocytes in Neurovascular Coupling. *Neuron*, *71*(5), 782–797. https://doi.org/10.1016/J.NEURON.2011.08.009

Peyrl, A., Chocholous, M., Azizi, A. A., Czech, T., Dorfer, C., Mitteregger, D., Gojo, J., Minichmayr, E., & Slavc, I. (2014). Safety of Ommaya reservoirs in children with brain tumors: a 20-year experience with 5472 intraventricular drug administrations in 98 patients. *Journal of Neuro-Oncology*, *120*(1), 139–145. https://doi.org/10.1007/s11060-014-1531-1

Phosphodiesterase Inhibitors | DrugBank Online. (n.d.). Retrieved April 6, 2025, from https://go.drugbank.com/categories/DBCAT000509

Pirttimaki, T. M., Sims, R. E., Saunders, G., Antonio, S. A., Codadu, N. K., & Parri, H. R. (2017). Astrocyte-Mediated Neuronal Synchronization Properties Revealed by False Gliotransmitter Release. *The Journal of Neuroscience : The Official Journal of the Society for Neuroscience*, *37*(41), 9859–9870. https://doi.org/10.1523/JNEUROSCI.2761-16.2017

Pišlar, A., Bolčina, L., & Kos, J. (2021). New Insights into the Role of Cysteine Cathepsins in Neuroinflammation. *Biomolecules*, *11*(12). https://doi.org/10.3390/biom11121796

Porter, J. T., & McCarthy, K. D. (1997). Astrocytic neurotransmitter receptors in situ and in vivo. *Progress in Neurobiology*, *51*(4), 439–455. https://doi.org/10.1016/s0301-0082(96)00068-8

Pringsheim, T., Wiltshire, K., Day, L., Dykeman, J., Steeves, T., & Jette, N. (2012). The incidence and prevalence of Huntington's Disease: a systematic review and meta-analysis. *Movement Disorders : Official Journal of the Movement Disorder Society*, *27*(9), 1083–1091. https://doi.org/10.1002/mds.25075

Pugazhenthi, S., Wang, M., Pham, S., Sze, C. I., & Eckman, C. B. (2011). Downregulation of CREB expression in Alzheimer's brain and in Aβ-treated rat hippocampal neurons. *Molecular Neurodegeneration*, *6*(1). https://doi.org/10.1186/1750-1326-6-60

Puigdellívol, M., Cherubini, M., Brito, V., Giralt, A., Suelves, N., Ballesteros, J., Zamora-Moratalla, A., Martín, E. D., Eipper, B. A., Alberch, J., & Ginés, S. (2015). A role for Kalirin-7 in corticostriatal synaptic dysfunction in Huntington's Disease. *Human Molecular Genetics*, *24*(25), 7265–7285. https://doi.org/10.1093/hmg/ddv426

Puzzo, D., Gulisano, W., Palmeri, A., & Arancio, O. (2015). Rodent models for Alzheimer's Disease drug discovery. In *Expert Opinion on Drug Discovery* (Vol. 10, Issue 7, pp. 703–711). Informa Healthcare. https://doi.org/10.1517/17460441.2015.1041913

Querfurth, H. W., & LaFerla, F. M. (2010). Alzheimer's Disease. *New England Journal of Medicine*, *362*(4), 329–344. https://doi.org/10.1056/NEJMra0909142

Rabinowitz, J. E., Rolling, F., Li, C., Conrath, H., Xiao, W., Xiao, X., & Samulski, R. J. (2002). Cross-Packaging of a Single Adeno-Associated Virus (AAV) Type 2 Vector Genome into Multiple AAV Serotypes Enables Transduction with Broad Specificity. *Journal of Virology*, *76*(2), 791–801. https://doi.org/10.1128/jvi.76.2.791-801.2002

Ramaswamy, S., McBride, J. L., & Kordower, J. H. (2007). Animal models of Huntington's Disease. *ILAR Journal*, *48*(4), 356–373. https://doi.org/10.1093/ilar.48.4.356

Ranen, N. G., Stine, C., Abbott, M. H., Sherr, M., Codori, A.-M., Louise Franz, M., Chung, A. S., Pleasant, N., Callahan, C., Kasch, L. M., Ghaffari, M., Chase, G. A., Kazazian, H. H., Brandt, J., Folstein, S. E., & Ross, C. A. (1995). Anticipation and Instability of IT-IS (CAG)N Repeats in Parent-Offspring Pairs with Huntington Disease. In *Am. J. Hum. Genet* (Vol. 57).

Raymond, C. R. (2007). LTP forms 1, 2 and 3: different mechanisms for the "long" in long-term potentiation. In *Trends in Neurosciences* (Vol. 30, Issue 4, pp. 167–175). https://doi.org/10.1016/j.tins.2007.01.007

Rebec, G. V. (2018). Corticostriatal network dysfunction in Huntington's Disease: Deficits in neural processing, glutamate transport, and ascorbate release. *CNS Neuroscience & Therapeutics*, *24*(4), 281–291. https://doi.org/10.1111/cns.12828

Reiner, A., Dragatsis, I., Zeitlin, S., & Goldowitz, D. (2003). Wild-Type Huntingtin Plays a Role in Brain Development and Neuronal Survival. In *Molecular Neurobiology* (Vol. 259). http://us.expasy.org/sprot

Remoli, G., Tariciotti, L., Remore, L. G., Palmisciano, P., Sciancalepore, F., Canevelli, M., Lacorte, E., Da Re, F., Bruno, G., Ferrarese, C., Appollonio, I., Locatelli, M., & Vanacore, N. (2023). An updated overview of recent and ongoing deep brain stimulation (DBS) trials in patients with dementia: a systematic review. In *Neurological Sciences* (Vol. 44, Issue 10, pp. 3395–3427). Springer-Verlag Italia s.r.l. https://doi.org/10.1007/s10072-023-06821-w

Ries, M., & Sastre, M. (2016). Mechanisms of Aβ Clearance and Degradation by Glial Cells. *Frontiers in Aging Neuroscience*, *8*, 160. https://doi.org/10.3389/fnagi.2016.00160

Rockwell, N., & Lagarias, C. (2010). A brief history of phytochromes. *Chemphyschem.*, *11*(6), 1172–1180. https://doi.org/10.1002/cphc.200900894.A

Rodríguez-Urgellés, E., Casas-Torremocha, D., Sancho-Balsells, A., Ballasch, I., García-García, E., Miquel-Rio, L., Manasanch, A., Del Castillo, I., Chen, W., Pupak, A., Brito, V., Tornero, D., Rodríguez, M. J., Bortolozzi, A., Sanchez-Vives, M. V, Giralt, A., & Alberch, J. (2023). Thalamic Foxp2 regulates output connectivity and sensory-motor impairments in a model of Huntington's Disease. *Cellular and Molecular Life Sciences : CMLS*, *80*(12), 367. https://doi.org/10.1007/s00018-023-05015-z

Rodríguez-Urgellés, E., Casas-Torremocha, D., Sancho-Balsells, A., Ballasch, I., García-García, E., Miquel-Rio, L., Manasanch, A., del Castillo, I., Chen, W., Pupak, A., Brito, V., Tornero, D., Rodríguez, M. J., Bortolozzi, A., Sanchez-Vives, M. V., Giralt, A., & Alberch, J. (2023). Thalamic Foxp2 regulates output connectivity and sensory-motor impairments in a model of Huntington's Disease. *Cellular and Molecular Life Sciences*, *80*(12). https://doi.org/10.1007/s00018-023-05015-z

Ronzano, R., Thetiot, M., Lubetzki, C., & Desmazieres, A. (2020). Myelin Plasticity and Repair: Neuro-Glial Choir Sets the Tuning. In *Frontiers in Cellular Neuroscience* (Vol. 14). Frontiers Media S.A. https://doi.org/10.3389/fncel.2020.00042

Ross, C. A., Aylward, E. H., Wild, E. J., Langbehn, D. R., Long, J. D., Warner, J. H., Scahill, R. I., Leavitt, B. R., Stout, J. C., Paulsen, J. S., Reilmann, R., Unschuld, P. G., Wexler, A., Margolis, R. L., & Tabrizi, S. J. (2014). Huntington disease: Natural history, biomarkers and prospects for therapeutics. *Nature Reviews Neurology*, *10*(4), 204–216. https://doi.org/10.1038/nrneurol.2014.24

Rost, B. R., Schneider-Warme, F., Schmitz, D., & Hegemann, P. (2017). Optogenetic Tools for Subcellular Applications in Neuroscience. In *Neuron* (Vol. 96, Issue 3, pp. 572–603). Cell Press. https://doi.org/10.1016/j.neuron.2017.09.047

Ruzha, Y., Ni, J., Quan, Z., Li, H., & Qing, H. (2022). Role of Vitronectin and Its Receptors in Neuronal Function and Neurodegenerative Diseases. *International Journal of Molecular Sciences*, *23*(20). https://doi.org/10.3390/ijms232012387

Ryu, M. H., & Gomelsky, M. (2014). Near-infrared light responsive synthetic c-di-GMP module for optogenetic applications. *ACS Synthetic Biology*, *3*(11), 802–810. https://doi.org/10.1021/sb400182x

Sahel, J. A., Boulanger-Scemama, E., Pagot, C., Arleo, A., Galluppi, F., Martel, J. N., Esposti, S. D., Delaux, A., de Saint Aubert, J. B., de Montleau, C., Gutman, E., Audo, I., Duebel, J., Picaud, S., Dalkara, D., Blouin, L., Taiel, M., & Roska, B. (2021). Partial recovery of visual function in a blind patient after optogenetic therapy. *Nature Medicine*, *27*(7), 1223–1229. https://doi.org/10.1038/s41591-021-01351-4

Sahlender, D. A., Savtchouk, I., & Volterra, A. (2014). What do we know about gliotransmitter release from astrocytes? In *Philosophical Transactions of the Royal Society B: Biological Sciences* (Vol. 369, Issue 1654). Royal Society of London. https://doi.org/10.1098/rstb.2013.0592

Saito, T., Matsuba, Y., Mihira, N., Takano, J., Nilsson, P., Itohara, S., Iwata, N., & Saido, T. C. (2014). Single App knock-in mouse models of Alzheimer's Disease. *Nature Neuroscience*, *17*(5), 661–663. https://doi.org/10.1038/nn.3697

Saito, Y. D., Jensen, A. R., Salgia, R., & Posadas, E. M. (2010). Fyn: a novel molecular target in cancer. *Cancer*, *116*(7), 1629–1637. https://doi.org/10.1002/cncr.24879

Sancho, L., Contreras, M., & Allen, N. J. (2021). Glia as sculptors of synaptic plasticity. In *Neuroscience Research* (Vol. 167, pp. 17–29). Elsevier Ireland Ltd. https://doi.org/10.1016/j.neures.2020.11.005

Sanders, O., & Rajagopal, L. (2020). Phosphodiesterase Inhibitors for Alzheimer's Disease: A Systematic Review of Clinical Trials and Epidemiology with a Mechanistic Rationale. In *Journal of Alzheimer's Disease Reports* (Vol. 4, Issue 1, pp. 185–215). IOS Press BV. https://doi.org/10.3233/ADR-200191

Santello, M., Toni, N., & Volterra, A. (2019). Astrocyte function from information processing to cognition and cognitive impairment. In *Nature Neuroscience* (Vol. 22, Issue 2, pp. 154–166). Nature Publishing Group. https://doi.org/10.1038/s41593-018-0325-8

Santello, M., & Volterra, A. (2009). Synaptic modulation by astrocytes via Ca2+-dependent glutamate release. In *Neuroscience* (Vol. 158, Issue 1, pp. 253–259). https://doi.org/10.1016/j.neuroscience.2008.03.039

Sapp, E., Ge, P., Aizawa, H., Bird, E., Penney, J., Young, A. B., Vonsattel, J. P., & DiFiglia, M. (1995). Evidence for a preferential loss of enkephalin immunoreactivity in the external globus pallidus in low grade Huntington's Disease using high resolution image analysis. *Neuroscience*, *64*(2), 397–404. https://doi.org/10.1016/0306-4522(94)00427-7

Sassone-Corsi, P. (2012). The Cyclic AMP pathway. *Cold Spring Harbor Perspectives in Biology*, *4*(12), 3–5. https://doi.org/10.1101/cshperspect.a011148

Saudou, F., & Humbert, S. (2016). The Biology of Huntingtin. In *Neuron* (Vol. 89, Issue 5, pp. 910–926). Cell Press. https://doi.org/10.1016/j.neuron.2016.02.003

Schaeffer, E. L., Figueiró, M., & Gattaz, W. F. (2011). Insights into Alzheimer disease pathogenesis from studies in transgenic animal models. In *Clinics* (Vol. 66, Issue SUPPL.1, pp. 45–54). https://doi.org/10.1590/S1807-59322011001300006

Scheltens, P., De Strooper, B., Kivipelto, M., Holstege, H., Chételat, G., Teunissen, C. E., Cummings, J., & van der Flier, W. M. (2021). Alzheimer's Disease. In *The Lancet* (Vol. 397, Issue 10284, pp. 1577–1590). Elsevier B.V. https://doi.org/10.1016/S0140-6736(20)32205-4

Schindelin, J., Arganda-Carreras, I., Frise, E., Kaynig, V., Longair, M., Pietzsch, T., Preibisch, S., Rueden, C., Saalfeld, S., Schmid, B., Tinevez, J.-Y., White, D. J., Hartenstein, V., Eliceiri, K., Tomancak, P., & Cardona, A. (2012). Fiji: an open-source platform for biological-image analysis. *Nature Methods*, *9*(7), 676–682. https://doi.org/10.1038/nmeth.2019

Schmid, A., Meili, D., & Salathe, M. (2014). Soluble adenylyl cyclase in health and disease. *Biochimica et Biophysica Acta - Molecular Basis of Disease*, *1842*(12), 2584–2592. https://doi.org/10.1016/j.bbadis.2014.07.010

Schnecko, A., Witte, K., Bohl, J., Ohm, T., & Lemmer, B. (1994). Adenylyl cyclase activity in Alzheimer's Disease brain: stimulatory and inhibitory signal transduction pathways are differently affected. *Brain Research*, *644*(2), 291–296. https://doi.org/10.1016/0006-8993(94)91692-6

Schneider, J. A., Arvanitakis, Z., Leurgans, S. E., & Bennett, D. A. (2009). The neuropathology of probable Alzheimer disease and mild cognitive impairment. *Annals of Neurology*, *66*(2), 200–208. https://doi.org/10.1002/ana.21706

Schröder-Lang, S., Schwärzel, M., Seifert, R., Strünker, T., Kateriya, S., Looser, J., Watanabe, M., Kaupp, U. B., Hegemann, P., & Nagel, G. (2007). Fast manipulation of cellular cAMP level by light in vivo. *Nature Methods*, *4*(1), 39–42. https://doi.org/10.1038/nmeth975

Schweinhuber, S. K., Meßerschmidt, T., Hänsch, R., Korte, M., & Rothkegel, M. (2015). Profilin isoforms modulate astrocytic morphology and the motility of astrocytic processes. *PloS One*, *10*(1), e0117244. https://doi.org/10.1371/journal.pone.0117244

Sdobnov, A., Piavchenko, G., Bykov, A., & Meglinski, I. (2024). Advances in Dynamic Light Scattering Imaging of Blood Flow. In *Laser and Photonics Reviews* (Vol. 18, Issue 2). John Wiley and Sons Inc. https://doi.org/10.1002/lpor.202300494

Selkoe, D. J. (2002). Alzheimer's Disease Is a Synaptic Failure. In *Proc. Natl. Acad. Sci. U.S.A* (Vol. 20). https://doi.org/10.1126/science.1074069

Seung, H. S. (2000). Half a century of Hebb. *Nature Neuroscience*, *3 Suppl*, 1166. https://doi.org/10.1038/81430

Sgambato, V. (2024). The Serotonin 4 Receptor Subtype: A Target of Particular Interest, Especially for Brain Disorders. In *International Journal of Molecular Sciences* (Vol. 25, Issue 10). Multidisciplinary Digital Publishing Institute (MDPI). https://doi.org/10.3390/ijms25105245

Shafit-Zagardo, B., Kume-Iwaki, A., & Goldman, J. E. (1988). Astrocytes regulate GFAP mRNA levels by cyclic AMP and protein kinase C-dependent mechanisms. *Glia*, *1*(5), 346–354. https://doi.org/10.1002/glia.440010507

Shanmughapriya, S., Rajan, S., Hoffman, N. E., Zhang, X., Guo, S., Kolesar, J. E., Hines, K. J., Ragheb, J., Jog, N. R., Caricchio, R., Baba, Y., Zhou, Y., Kaufman, B. A., Cheung, J. Y., Kurosaki, T., Gill, D. L., & Madesh, M. (2015). Ca2+ signals regulate mitochondrial metabolism by stimulating CREB-mediated expression of the mitochondrial Ca2+ uniporter gene MCU. *Science Signaling*, *8*(366), ra23. https://doi.org/10.1126/scisignal.2005673

Shao, Y., & Sutin, J. (1992). Expression of Adrenergic Receptors in Individual Astrocytes and Motor Neurons Isolated From the Adult Rat Brain. In *GLIA* (Vol. 6).

Sharma, K., Schmitt, S., Bergner, C. G., Tyanova, S., Kannaiyan, N., Manrique-Hoyos, N., Kongi, K., Cantuti, L., Hanisch, U.-K., Philips, M.-A., Rossner, M. J., Mann, M., & Simons, M. (2015). Cell type- and brain region-resolved mouse brain proteome. *Nature Neuroscience*, *18*(12), 1819–1831. https://doi.org/10.1038/nn.4160

Shcherbakova, D. M., Baloban, M., Pletnev, S., Malashkevich, V. N., Xiao, H., Dauter, Z., & Verkhusha, V. V. (2015). Molecular Basis of Spectral Diversity in Near-Infrared Phytochrome-Based Fluorescent Proteins. *Chemistry & Biology*, *22*(11), 1540–1551. https://doi.org/10.1016/j.chembiol.2015.10.007

Shcherbakova, D. M., Shemetov, A. A., Kaberniuk, A. A., & Verkhusha, V. V. (2015). Natural photoreceptors as a source of fluorescent proteins, biosensors, and optogenetic tools. In *Annual Review of Biochemistry* (Vol. 84). https://doi.org/10.1146/annurev-biochem-060614-034411

Shepherd, G. M., & Erulkar, S. D. (1997). Centenary of the synapse: from Sherrington to the molecular biology of the synapse and beyond. *Trends in Neurosciences*, *20*(9), 385–392. https://doi.org/10.1016/s0166-2236(97)01059-x

Sherwood, M. W., Arizono, M., Hisatsune, C., Bannai, H., Ebisui, E., Sherwood, J. L., Panatier, A., Oliet, S. H. R., & Mikoshiba, K. (2017). Astrocytic IP3 Rs: Contribution

to Ca2+ signalling and hippocampal LTP. *Glia*, *65*(3), 502–513. https://doi.org/10.1002/glia.23107

Shi, J., Qian, W., Yin, X., Iqbal, K., Grundke-Iqbal, I., Gu, X., Ding, F., Gong, C. X., & Liu, F. (2011). Cyclic AMP-dependent protein kinase regulates the alternative splicing of tau exon 10: A mechanism involved in tau pathology of Alzheimer disease. *Journal of Biological Chemistry*, *286*(16), 14639–14648. https://doi.org/10.1074/jbc.M110.204453

Shigetomi, E., Bowser, D. N., Sofroniew, M. V, & Khakh, B. S. (2008). Two forms of astrocyte calcium excitability have distinct effects on NMDA receptor-mediated slow inward currents in pyramidal neurons. *The Journal of Neuroscience : The Official Journal of the Society for Neuroscience*, *28*(26), 6659–6663. https://doi.org/10.1523/JNEUROSCI.1717-08.2008

Shin, J. Y., Fang, Z. H., Yu, Z. X., Wang, C. E., Li, S. H., & Li, X. J. (2005). Expression of mutant huntingtin in glial cells contributes to neuronal excitotoxicity. *Journal of Cell Biology*, *171*(6), 1001–1012. https://doi.org/10.1083/jcb.200508072

Slow, E. J., van Raamsdonk, J., Rogers, D., Coleman, S. H., Graham, R. K., Deng, Y., Oh, R., Bissada, N., Hossain, S. M., Yang, Y. Z., Li, X. J., Simpson, E. M., Gutekunst, C. A., Leavitt, B. R., & Hayden, M. R. (2003). Selective striatal neuronal loss in a YAC128 mouse model of Huntington disease. In *Human Molecular Genetics* (Vol. 12, Issue 13, pp. 1555–1567). https://doi.org/10.1093/hmg/ddg169

Smalley, E. (2017). First AAV gene therapy poised for landmark approval. *Nature Biotechnology*, *35*(11), 998–999. https://doi.org/10.1038/nbt1117-998

Snell', R. G., Macmillan1, J. C., Cheadle', J. P., Fenton', I., Lazarou, L. P., Davies', P., Macdonald2, M. E., Gusella, J. F., Harper', P. S., & Shaw, D. J. (1993). *Relationship between trinucleotide repeat expansion and phenotypic variation in Huntington's Disease*. http://www.nature.com/naturegenetics

Sobolczyk, M., & Boczek, T. (2022). Astrocytic Calcium and cAMP in Neurodegenerative Diseases. In *Frontiers in Cellular Neuroscience* (Vol. 16). Frontiers Media S.A. https://doi.org/10.3389/fncel.2022.889939

Sokolova, I. V., Lester, H. A., & Davidson, N. (2006). Postsynaptic mechanisms are essential for forskolin-induced potentiation of synaptic transmission. *Journal of Neurophysiology*, *95*(4), 2570–2579. https://doi.org/10.1152/jn.00617.2005

Somjen, G. G. (1988). Nervenkitt: Notes on the History of the Concept of Neuroglia. In *GLIA* (Vol. 1).

Song, W., Chen, J., Petrilli, A., Liot, G., Klinglmayr, E., Zhou, Y., Poquiz, P., Tjong, J., Pouladi, M. A., Hayden, M. R., Masliah, E., Ellisman, M., Rouiller, I., Schwarzenbacher, R., Bossy, B., Perkins, G., & Bossy-Wetzel, E. (2011). Mutant huntingtin binds the

mitochondrial fission GTPase dynamin-related protein-1 and increases its enzymatic activity. *Nature Medicine*, *17*(3), 377–383. https://doi.org/10.1038/nm.2313

Song, Y., & Gunnarson, E. (2012). Potassium dependent regulation of astrocyte water permeability is mediated by cAMP signaling. *PloS One*, *7*(4), e34936. https://doi.org/10.1371/journal.pone.0034936

Spampanato, J., Gu, X., Yang, X. W., & Mody, I. (2008). Progressive synaptic pathology of motor cortical neurons in a BAC transgenic mouse model of Huntington's Disease. *Neuroscience*, *157*(3), 606–620. https://doi.org/10.1016/j.neuroscience.2008.09.020

Spires-Jones, T. L., & Hyman, B. T. (2014). The Intersection of Amyloid Beta and Tau at Synapses in Alzheimer's Disease. In *Neuron* (Vol. 82, Issue 4, pp. 756–771). Cell Press. https://doi.org/10.1016/j.neuron.2014.05.004

Stanton, P. K., Winterer, J., Bailey, C. P., Kyrozis, A., Raginov, I., Laube, G., Veh, R. W., Nguyen, C. Q., & Müller, W. (2003). *Long-Term Depression of Presynaptic Release from the Readily Releasable Vesicle Pool Induced by NMDA Receptor-Dependent Retrograde Nitric Oxide*.

Stefan, K., Kunesch, E., Cohen, L. G., Benecke, R., & Classen, J. (2000). Induction of plasticity in the human motor cortex by paired associative stimulation. *Brain : A Journal of Neurology*, *123 Pt 3*, 572–584. https://doi.org/10.1093/brain/123.3.572

Stelzmann, R. A., Norman Schnitzlein, H., & Reed Murtagh, F. (1995). An english translation of alzheimer's 1907 paper, "über eine eigenartige erkankung der hirnrinde." *Clinical Anatomy*, *8*(6), 429–431. https://doi.org/10.1002/ca.980080612

Stern, Y. (2012). Cognitive reserve in ageing and Alzheimer's Disease. In *The Lancet Neurology* (Vol. 11, Issue 11, pp. 1006–1012). https://doi.org/10.1016/S1474-4422(12)70191-6

Stierl, M., Stumpf, P., Udwari, D., Gueta, R., Hagedorn, R., Losi, A., Gärtner, W., Petereit, L., Efetova, M., Schwarzel, M., Oertner, T. G., Nagel, G., & Hegemann, P. (2011). Light modulation of cellular cAMP by a small bacterial photoactivated adenylyl cyclase, bPAC, of the soil bacterium Beggiatoa. *Journal of Biological Chemistry*, *286*(2), 1181–1188. https://doi.org/10.1074/jbc.M110.185496

Stoker, T. B., Mason, S. L., Greenland, J. C., Holden, S. T., Santini, H., & Barker, R. A. (2022). Huntington's Disease: diagnosis and management. *Practical Neurology*, *22*(1), 32–41. https://doi.org/10.1136/practneurol-2021-003074

Sturchler-Pierrat, C., Abramowski, D., Duke, M., Wiederhold, K. H., Mistl, C., Rothacher, S., Ledermann, B., Bürki, K., Frey, P., Paganetti, P. A., Waridel, C., Calhoun, M. E., Jucker, M., Probst, A., Staufenbiel, M., & Sommer, B. (1997). Two amyloid precursor protein transgenic mouse models with Alzheimer disease-like pathology. *Proceedings of the National Academy of Sciences of the United States of America*, *94*(24), 13287–13292. https://doi.org/10.1073/pnas.94.24.13287

Stüven, B., Stabel, R., Ohlendorf, R., Beck, J., Schubert, R., & Möglich, A. (2018). Characterization and engineering of photoactivated adenylyl cyclases. *Biological Chemistry*. https://doi.org/10.1515/hsz-2018-0375

Sun, Q., Sun, L., Liu, H.-H., Chen, X., Seth, R. B., Forman, J., & Chen, Z. J. (2006). The specific and essential role of MAVS in antiviral innate immune responses. *Immunity*, *24*(5), 633–642. https://doi.org/10.1016/j.immuni.2006.04.004

SUTHERLAND, E. W., & RALL, T. W. (1958). Fractionation and characterization of a cyclic adenine ribonucleotide formed by tissue particles. *The Journal of Biological Chemistry*, *232*(2), 1077–1091. https://doi.org/10.1016/s0021-9258(19)77423-7

Suzuki, A., Stern, S. A., Bozdagi, O., Huntley, G. W., Walker, R. H., Magistretti, P. J., & Alberini, C. M. (2011). Astrocyte-neuron lactate transport is required for long-term memory formation. *Cell*, *144*(5), 810–823. https://doi.org/10.1016/j.cell.2011.02.018

Tabrizi, S. J., Langbehn, D. R., Leavitt, B. R., Roos, R. A., Durr, A., Craufurd, D., Kennard, C., Hicks, S. L., Fox, N. C., Scahill, R. I., Borowsky, B., Tobin, A. J., Rosas, H. D., Johnson, H., Reilmann, R., Landwehrmeyer, B., Stout, J. C., & TRACK-HD investigators. (2009). Biological and clinical manifestations of Huntington's Disease in the longitudinal TRACK-HD study: cross-sectional analysis of baseline data. *The Lancet. Neurology*, *8*(9), 791–801. https://doi.org/10.1016/S1474-4422(09)70170-X

Tabrizi, S. J., Schobel, S., Gantman, E. C., Mansbach, A., Borowsky, B., Konstantinova, P., Mestre, T. A., Panagoulias, J., Ross, C. A., Zauderer, M., Mullin, A. P., Romero, K., Sivakumaran, S., Turner, E. C., Long, J. D., Sampaio, C., & Huntington's Disease Regulatory Science Consortium (HD-RSC). (2022). A biological classification of Huntington's Disease: the Integrated Staging System. *The Lancet. Neurology*, *21*(7), 632–644. https://doi.org/10.1016/S1474-4422(22)00120-X

Tanaka, M., Ishizuka, K., Nekooki-Machida, Y., Endo, R., Takashima, N., Sasaki, H., Komi, Y., Gathercole, A., Huston, E., Ishii, K., Hui, K. K. W., Kurosawa, M., Kim, S. H., Nukina, N., Takimoto, E., Houslay, M. D., & Sawa, A. (2017). Aggregation of scaffolding protein DiSC1 dysregulates phosphodiesterase 4 in Huntington's Disease. *Journal of Clinical Investigation*, *127*(4), 1438–1450. https://doi.org/10.1172/JCI85594

Taylor, J. P., Hardy, J., & Fischbeck, K. H. (2002). Toxic proteins in neurodegenerative disease. *Science (New York, N.Y.)*, *296*(5575), 1991–1995. https://doi.org/10.1126/science.1067122

Taylor, S. S., Knighton, D. R., Zheng, J., Ten Eyck, L. F., & Sowadski, J. M. (1992). Structural framework for the protein kinase family. *Annual Review of Cell Biology*, *8*, 429–462. https://doi.org/10.1146/annurev.cb.08.110192.002241

Taymans, J. M., Vandenberghe, L. H., Van Den Haute, C., Thiry, I., Deroose, C. M., Mortelmans, L., Wilson, J. M., Debyser, Z., & Baekelandt, V. (2007). Comparative

analysis of adeno-associated viral vector serotypes 1, 2, 5, 7, and 8 in mouse brain. *Human Gene Therapy*, *18*(3), 195–206. https://doi.org/10.1089/hum.2006.178

The Huntington's Disease Collaborative Research Group. (1993a). A novel gene containing a trinucleotide repeat that is expanded and unstable on Huntington's Disease chromosomes. The Huntington's Disease Collaborative Research Group. *Cell*, *72*(6), 971–983. https://doi.org/10.1016/0092-8674(93)90585-e

The Huntington's Disease Collaborative Research Group. (1993b). *A Novel Gene Containing a Trinucleotide Repeat That Is Expanded and Unstable on Huntington's Disease Chromosomes*.

Theparambil, S. M., Kopach, O., Braga, A., Nizari, S., Hosford, P. S., Sagi-Kiss, V., Hadjihambi, A., Konstantinou, C., Esteras, N., Gutierrez Del Arroyo, A., Ackland, G. L., Teschemacher, A. G., Dale, N., Eckle, T., Andrikopoulos, P., Rusakov, D. A., Kasparov, S., & Gourine, A. V. (2024). Adenosine signalling to astrocytes coordinates brain metabolism and function. *Nature*, *632*(8023), 139–146. https://doi.org/10.1038/s41586-024-07611-w

Thiruvady, D. R., Georgiou-Karistianis, N., Egan, G. F., Ray, S., Sritharan, A., Farrow, M., Churchyard, A., Chua, P., Bradshaw, J. L., Brawn, T. L., & Cunnington, R. (2007). Functional connectivity of the prefrontal cortex in Huntington's Disease. *Journal of Neurology, Neurosurgery and Psychiatry*, *78*(2), 127–133. https://doi.org/10.1136/jnnp.2006.098368

Todd, K. J., Darabid, H., & Robitaille, R. (2010). Perisynaptic glia discriminate patterns of motor nerve activity and influence plasticity at the neuromuscular junction. *Journal of Neuroscience*, *30*(35), 11870–11882. https://doi.org/10.1523/JNEUROSCI.3165-10.2010

Tokumitsu, H., & Sakagami, H. (2022). Molecular Mechanisms Underlying Ca2+/Calmodulin-Dependent Protein Kinase Kinase Signal Transduction. *International Journal of Molecular Sciences*, *23*(19). https://doi.org/10.3390/ijms231911025

Tolias, K. F., Duman, J. G., & Um, K. (2011). Control of synapse development and plasticity by Rho GTPase regulatory proteins. *Progress in Neurobiology*, *94*(2), 133–148. https://doi.org/10.1016/j.pneurobio.2011.04.011

Tong, X., Ao, Y., Faas, G. C., Nwaobi, S. E., Xu, J., Haustein, M. D., Anderson, M. A., Mody, I., Olsen, M. L., Sofroniew, M. V., & Khakh, B. S. (2014). Astrocyte Kir4.1 ion channel deficits contribute to neuronal dysfunction in Huntington's Disease model mice. *Nature Neuroscience*, *17*(5), 694–703. https://doi.org/10.1038/nn.3691

Travessa, A. M., Rodrigues, F. B., Mestre, T. A., & Ferreira, J. J. (2017). Fifteen Years of Clinical Trials in Huntington's Disease: A Very Low Clinical Drug Development Success Rate. *Journal of Huntington's Disease*, *6*(2), 157–163. https://doi.org/10.3233/JHD-170245

Trinchese, F., Liu, S., Battaglia, F., Walter, S., Mathews, P. M., & Arancio, O. (2004). Progressive age-related development of Alzheimer-like pathology in APP/PS1 mice. *Annals of Neurology*, *55*(6), 801–814. https://doi.org/10.1002/ana.20101

Turmaine, M., Raza, A., Mahal, A., Mangiarini, L., Bates, G. P., & Davies, S. W. (2000). Nonapoptotic neurodegeneration in a transgenic mouse model of Huntington's Disease. *Proceedings of the National Academy of Sciences of the United States of America*, *97*(14), 8093–8097. https://doi.org/10.1073/pnas.110078997

Turner, C. E. (2000). Paxillin and focal adhesion signalling. *Nature Cell Biology*, *2*(12), E231–E236. https://doi.org/10.1038/35046659

Tyanova, S., Temu, T., Sinitcyn, P., Carlson, A., Hein, M. Y., Geiger, T., Mann, M., & Cox, J. (2016). The Perseus computational platform for comprehensive analysis of (prote)omics data. *Nature Methods 2016 13:9*, *13*(9), 731–740. https://doi.org/10.1038/nmeth.3901

Tyebji, S., Saavedra, A., Canas, P. M., Pliassova, A., Delgado-García, J. M., Alberch, J., Cunha, R. A., Gruart, A., & Pérez-Navarro, E. (2015). Hyperactivation of D1 and A2A receptors contributes to cognitive dysfunction in Huntington's Disease. *Neurobiology of Disease*, *74*, 41–57. https://doi.org/10.1016/j.nbd.2014.11.004

Ujita, S., Sasaki, T., Asada, A., Funayama, K., Gao, M., Mikoshiba, K., Matsuki, N., & Ikegaya, Y. (2017). cAMP-Dependent Calcium Oscillations of Astrocytes: An Implication for Pathology. *Cerebral Cortex (New York, N.Y. : 1991)*, *27*(2), 1602–1614. https://doi.org/10.1093/cercor/bhv310

van der Lee, S. J., Wolters, F. J., Ikram, M. K., Hofman, A., Ikram, M. A., Amin, N., & van Duijn, C. M. (2018). The effect of APOE and other common genetic variants on the onset of Alzheimer's Disease and dementia: a community-based cohort study. *The Lancet Neurology*, *17*(5), 434–444. https://doi.org/10.1016/S1474-4422(18)30053-X

Van Raamsdonk, J. M., Murphy, Z., Slow, E. J., Leavitt, B. R., & Hayden, M. R. (2005). Selective degeneration and nuclear localization of mutant huntingtin in the YAC128 mouse model of Huntington disease. *Human Molecular Genetics*, *14*(24), 3823–3835. https://doi.org/10.1093/hmg/ddi407

Vasilkovska, T., Salajeghe, S., Vanreusel, V., Van Audekerke, J., Verschuuren, M., Hirschler, L., Warnking, J., Pintelon, I., Pustina, D., Cachope, R., Mrzljak, L., Muñoz-Sanjuan, I., Barbier, E. L., De Vos, W. H., Van der Linden, A., & Verhoye, M. (2024). Longitudinal alterations in brain perfusion and vascular reactivity in the zQ175DN mouse model of Huntington's Disease. *Journal of Biomedical Science*, *31*(1). https://doi.org/10.1186/s12929-024-01028-3

Venkatesan, A., Satin, L. S., & Raghavan, M. (2021). Roles of Calreticulin in Protein Folding, Immunity, Calcium Signaling and Cell Transformation. *Progress in Molecular and Subcellular Biology*, *59*, 145–162. https://doi.org/10.1007/978-3-030-67696-4_7

Ventura, R., & Harris, K. M. (1999). *Three-Dimensional Relationships between Hippocampal Synapses and Astrocytes*. http://synapses.tch.harvard.edu

Verkhratsky, A., & Kettenmann, H. (1996). Calcium signalling in glial cells. *Trends in Neurosciences*, *19*(8), 346–352. https://doi.org/10.1016/0166-2236(96)10048-5

Verma, M., Lizama, B. N., & Chu, C. T. (2022). Excitotoxicity, calcium and mitochondria: a triad in synaptic neurodegeneration. In *Translational Neurodegeneration* (Vol. 11, Issue 1). BioMed Central Ltd. https://doi.org/10.1186/s40035-021-00278-7

Verret, L., Mann, E. O., Hang, G. B., Barth, A. M. I., Cobos, I., Ho, K., Devidze, N., Masliah, E., Kreitzer, A. C., Mody, I., Mucke, L., & Palop, J. J. (2012). Inhibitory interneuron deficit links altered network activity and cognitive dysfunction in alzheimer model. *Cell*, *149*(3), 708–721. https://doi.org/10.1016/j.cell.2012.02.046

Villanueva, C. B., Stephensen, H. J. T., Mokso, R., Benraiss, A., Sporring, J., & Goldman, S. A. (2023). Astrocytic engagement of the corticostriatal synaptic cleft is disrupted in a mouse model of Huntington's Disease. *Proceedings of the National Academy of Sciences of the United States of America*, *120*(24), e2210719120. https://doi.org/10.1073/pnas.2210719120

Vincent, P., Castro, L. R. V., & Bompierre, S. (2021). Cellular context shapes cyclic nucleotide signaling in neurons through multiple levels of integration. In *Journal of Neuroscience Methods* (Vol. 362). Elsevier B.V. https://doi.org/10.1016/j.jneumeth.2021.109305

Vitolo, O. V, Sant'Angelo, A., Costanzo, V., Battaglia, F., Arancio, O., & Shelanski, M. (2002). Amyloid beta -peptide inhibition of the PKA/CREB pathway and long-term potentiation: reversibility by drugs that enhance cAMP signaling. *Proceedings of the National Academy of Sciences of the United States of America*, *99*(20), 13217–13221. https://doi.org/10.1073/pnas.172504199

Volterra, A., Liaudet, N., & Savtchouk, I. (2014). Astrocyte Ca2+ signalling: An unexpected complexity. In *Nature Reviews Neuroscience* (Vol. 15, Issue 5, pp. 327–335). Nature Publishing Group. https://doi.org/10.1038/nrn3725

Volterra, A., & Meldolesi, J. (2005). Astrocytes, from brain glue to communication elements: The revolution continues. In *Nature Reviews Neuroscience* (Vol. 6, Issue 8, pp. 626–640). https://doi.org/10.1038/nrn1722

Vonsattel, J. P., & DiFiglia, M. (1998). Huntington disease. *Journal of Neuropathology and Experimental Neurology*, *57*(5), 369–384. https://doi.org/10.1097/00005072-199805000-00001

Vonsattel, J. P., Myers, R. H., Stevens, T. J., Ferrante, R. J., Bird, E. D., & Richardson, E. P. (1985). Neuropathological classification of Huntington's Disease. *Journal of Neuropathology and Experimental Neurology*, *44*(6), 559–577. https://doi.org/10.1097/00005072-198511000-00003

Walch, E., & Fiacco, T. A. (2022). Honey, I shrunk the extracellular space: Measurements and mechanisms of astrocyte swelling. *Glia*, *70*(11), 2013–2031. https://doi.org/10.1002/GLIA.24224

Walker, F. O. (2007). Huntington's Disease. *Lancet*, *369*(9557), 218–228. https://doi.org/10.1016/S0140-6736(07)60111-1

Walsh, D. A., Ashby, C. D., Gonzalez, C., Calkins, D., & Fischer, E. H. (1971). Krebs EG: Purification and characterization of a protein inhibitor of adenosine 3',5'-monophosphate-dependent protein kinases. *Journal of Biological Chemistry*, *246*(7), 1977–1985. https://doi.org/10.1016/s0021-9258(19)77177-4

Waltereit, R., & Weller, M. (2003). Signaling from cAMP/PKA to MAPK and synaptic plasticity. *Molecular Neurobiology*, *27*(1), 99–106. https://doi.org/10.1385/MN:27:1:99

Wang, J., Cai, Y., Sun, J., Feng, H., Zhu, X., Chen, Q., Gao, F., Ni, Q., Mao, L., Yang, M., & Sun, B. (2023). Administration of intramuscular AAV-BDNF and intranasal AAV-TrkB promotes neurological recovery via enhancing corticospinal synaptic connections in stroke rats. *Experimental Neurology*, *359*. https://doi.org/10.1016/j.expneurol.2022.114236

Wang, J., Lee, J. E., Riemondy, K., Yu, Y., Marquez, S. M., Lai, E. C., & Yi, R. (2020). XPO5 promotes primary miRNA processing independently of RanGTP. *Nature Communications*, *11*(1), 1845. https://doi.org/10.1038/s41467-020-15598-x

Wang, L., Wu, C., Peng, W., Zhou, Z., Zeng, J., Li, X., Yang, Y., Yu, S., Zou, Y., Huang, M., Liu, C., Chen, Y., Li, Y., Ti, P., Liu, W., Gao, Y., Zheng, W., Zhong, H., Gao, S., … Chu, J. (2022a). A high-performance genetically encoded fluorescent indicator for in vivo cAMP imaging. *Nature Communications*, *13*(1), 5363. https://doi.org/10.1038/s41467-022-32994-7

Wang, L., Wu, C., Peng, W., Zhou, Z., Zeng, J., Li, X., Yang, Y., Yu, S., Zou, Y., Huang, M., Liu, C., Chen, Y., Li, Y., Ti, P., Liu, W., Gao, Y., Zheng, W., Zhong, H., Gao, S., … Chu, J. (2022b). A high-performance genetically encoded fluorescent indicator for in vivo cAMP imaging. *Nature Communications*, *13*(1). https://doi.org/10.1038/s41467-022-32994-7

Wang, Q. wen, Rowan, M. J., & Anwyl, R. (2009). Inhibition of LTP by beta-amyloid is prevented by activation of β2 adrenoceptors and stimulation of the cAMP/PKA signalling pathway. *Neurobiology of Aging*, *30*(10), 1608–1613. https://doi.org/10.1016/j.neurobiolaging.2007.12.004

Wang, X., Lou, N., Xu, Q., Tian, G. F., Peng, W. G., Han, X., Kang, J., Takano, T., & Nedergaard, M. (2006). Astrocytic Ca2+ signaling evoked by sensory stimulation in vivo. *Nature Neuroscience*, *9*(6), 816–823. https://doi.org/10.1038/nn1703

Wang, Y., Fu, A. K. Y., & Ip, N. Y. (2022). Instructive roles of astrocytes in hippocampal synaptic plasticity: neuronal activity-dependent regulatory mechanisms. *FEBS Journal*, *289*(8), 2202–2218. https://doi.org/10.1111/febs.15878

Wanker, E. E., Ast, A., Schindler, F., Trepte, P., & Schnoegl, S. (2019). The pathobiology of perturbed mutant huntingtin protein–protein interactions in Huntington's Disease. In *Journal of Neurochemistry* (Vol. 151, Issue 4, pp. 507–519). Blackwell Publishing Ltd. https://doi.org/10.1111/jnc.14853

Watakabe, A., Ohtsuka, M., Kinoshita, M., Takaji, M., Isa, K., Mizukami, H., Ozawa, K., Isa, T., & Yamamori, T. (2015). Comparative analyses of adeno-associated viral vector serotypes 1, 2, 5, 8 and 9 in marmoset, mouse and macaque cerebral cortex. *Neuroscience Research*, *93*, 144–157. https://doi.org/10.1016/j.neures.2014.09.002

Watamura, N., Sato, K., & Saido, T. C. (2022). Mouse models of Alzheimer's Disease for preclinical research. *Neurochemistry International*, *158*. https://doi.org/10.1016/j.neuint.2022.105361

Wątroba, M., Maślińska, D., & Maśliński, S. (2012). Current overview of functions of FoxO proteins, with special regards to cellular homeostasis, cell response to stress, as well as inflammation and aging. *Advances in Medical Sciences*, *57*(2), 183–195. https://doi.org/10.2478/v10039-012-0039-1

Weissleder, R. (2001). A clearer vision for in vivo imaging. *Nature Biotechnology*, *19*(4), 316–317. https://doi.org/10.1038/86684

Wendlandt, M., Kürten, A. J., Beiersdorfer, A., Schubert, C., Samad-Yazdtchi, K., Sauer, J., Pinto, M. C., Schulz, K., Friese, M. A., Gee, C. E., Hirnet, D., & Lohr, C. (2023). A2A adenosine receptor-driven cAMP signaling in olfactory bulb astrocytes is unaffected in experimental autoimmune encephalomyelitis. *Frontiers in Immunology*, *14*. https://doi.org/10.3389/fimmu.2023.1273837

Westi, E. W., Molhemi, S., Hansen, C. T., Skoven, C. S., Knopper, R. W., Ahmad, D. A., Rindshøj, M. B., Ameen, A. O., Hansen, B., Kohlmeier, K. A., & Aldana, B. I. (2024). Comprehensive Analysis of the 5xFAD Mouse Model of Alzheimer's Disease Using dMRI, Immunohistochemistry, and Neuronal and Glial Functional Metabolic Mapping. *Biomolecules*, *14*(10). https://doi.org/10.3390/biom14101294

Whitlock, J. R., Heynen, A. J., Shuler, M. G., & Bear, M. F. (2006). Learning induces long-term potentiation in the hippocampus. *Science (New York, N.Y.)*, *313*(5790), 1093–1097. https://doi.org/10.1126/science.1128134

Wild, A. R., & Dell'Acqua, M. L. (2018). Potential for therapeutic targeting of AKAP signaling complexes in nervous system disorders. *Pharmacology & Therapeutics*, *185*, 99–121. https://doi.org/10.1016/j.pharmthera.2017.12.004

Willoughby, D., Halls, M. L., Everett, K. L., Ciruela, A., Skroblin, P., Klussmann, E., & Cooper, D. M. F. (2012). A key phosphorylation site in AC8 mediates regulation of Ca2+-dependent camp dynamics by an AC8- AKAP79-PKA signalling complex. *Journal of Cell Science*, *125*(23), 5850–5859. https://doi.org/10.1242/jcs.111427

Wilson, D. M., Cookson, M. R., Van Den Bosch, L., Zetterberg, H., Holtzman, D. M., & Dewachter, I. (2023). Hallmarks of neurodegenerative diseases. In *Cell* (Vol. 186, Issue 4, pp. 693–714). Elsevier B.V. https://doi.org/10.1016/j.cell.2022.12.032

Wilson, H., Niccolini, F., Haider, S., Marques, T. R., Pagano, G., Coello, C., Natesan, S., Kapur, S., Rabiner, E. A., Gunn, R. N., Tabrizi, S. J., & Politis, M. (2016). Loss of extra-striatal phosphodiesterase 10A expression in early premanifest Huntington's Disease gene carriers. *Journal of the Neurological Sciences*, *368*, 243–248. https://doi.org/10.1016/j.jns.2016.07.033

Wilton, D. K., Mastro, K., Heller, M. D., Gergits, F. W., Willing, C. R., Fahey, J. B., Frouin, A., Daggett, A., Gu, X., Kim, Y. A., Faull, R. L. M., Jayadev, S., Yednock, T., Yang, X. W., & Stevens, B. (2023). Microglia and complement mediate early corticostriatal synapse loss and cognitive dysfunction in Huntington's Disease. *Nature Medicine*, *29*(11), 2866–2884. https://doi.org/10.1038/s41591-023-02566-3

Wolf, D. A., Hanson, L. R., Aronovich, E. L., Nan, Z., Low, W. C., Frey, W. H., & McIvor, R. S. (2012). Lysosomal enzyme can bypass the blood-brain barrier and reach the CNS following intranasal administration. *Molecular Genetics and Metabolism*, *106*(1), 131–134. https://doi.org/10.1016/j.ymgme.2012.02.006

Wolf, R. C., Vasic, N., Schönfeldt-Lecuona, C., Landwehrmeyer, G. B., & Ecker, D. (2007). Dorsolateral prefrontal cortex dysfunction in presymptomatic Huntington's Disease: Evidence from event-related fMRI. *Brain*, *130*(11), 2845–2857. https://doi.org/10.1093/brain/awm210

Wong, T.-H., Mcgeer, P. L., Rossor, M., & Mcgeer, E. G. (1982). Ornithine aminotransferase in Huntington's Disease. In *Brain Research* (Vol. 231).

Wong, W., & Scott, J. D. (2004). AKAP signalling complexes: Focal points in space and time. In *Nature Reviews Molecular Cell Biology* (Vol. 5, Issue 12, pp. 959–970). https://doi.org/10.1038/nrm1527

Wong, Y. C., & Holzbaur, E. L. F. (2014). The regulation of autophagosome dynamics by huntingtin and HAP1 is disrupted by expression of mutant huntingtin, leading to defective cargo degradation. *Journal of Neuroscience*, *34*(4), 1293–1305. https://doi.org/10.1523/JNEUROSCI.1870-13.2014

Wu, D., Chen, Q., Chen, X., Han, F., Chen, Z., & Wang, Y. (2023). The blood–brain barrier: structure, regulation, and drug delivery. In *Signal Transduction and Targeted Therapy* (Vol. 8, Issue 1). Springer Nature. https://doi.org/10.1038/s41392-023-01481-w

Wu, Y. T., Beiser, A. S., Breteler, M. M. B., Fratiglioni, L., Helmer, C., Hendrie, H. C., Honda, H., Ikram, M. A., Langa, K. M., Lobo, A., Matthews, F. E., Ohara, T., Pérès, K., Qiu, C., Seshadri, S., Sjölund, B. M., Skoog, I., & Brayne, C. (2017). The changing prevalence and incidence of dementia over time-current evidence. In *Nature Reviews Neurology* (Vol. 13, Issue 6, pp. 327–339). Nature Publishing Group. https://doi.org/10.1038/nrneurol.2017.63

Xiang, Y., Naik, S., Zhao, L., Shi, J., & Ke, H. (2024). Emerging phosphodiesterase inhibitors for treatment of neurodegenerative diseases. In *Medicinal Research Reviews* (Vol. 44, Issue 4, pp. 1404–1445). John Wiley and Sons Inc. https://doi.org/10.1002/med.22017

Xu, Q., Vogt, A., Frechen, F., Yi, C., Küçükerden, M., Ngum, N., Sitjà-Roqueta, L., Greiner, A., Parri, R., Masana, M., Wenger, N., Wachten, D., & Möglich, A. (2024). Engineering Bacteriophytochrome-coupled Photoactivated Adenylyl Cyclases for Enhanced Optogenetic cAMP Modulation. *Journal of Molecular Biology*, *436*(5), 168257. https://doi.org/10.1016/j.jmb.2023.168257

Yang, J., Lunde, L. K., Nuntagij, P., Oguchi, T., Camassa, L. M. A., Nilsson, L. N. G., Lannfelt, L., Xu, Y., Amiry-Moghaddam, M., Ottersen, O. P., & Torp, R. (2011). Loss of astrocyte polarization in the tg-ArcSwe mouse model of Alzheimer's Disease. *Journal of Alzheimer's Disease : JAD*, *27*(4), 711–722. https://doi.org/10.3233/JAD-2011-110725

Yang, J., Ruchti, E., Petit, J. M., Jourdain, P., Grenningloh, G., Allaman, I., & Magistretti, P. J. (2014). Lactate promotes plasticity gene expression by potentiating NMDA signaling in neurons. *Proceedings of the National Academy of Sciences of the United States of America*, *111*(33), 12228–12233. https://doi.org/10.1073/pnas.1322912111

Yardeni, T., Eckhaus, M., Morris, H. D., Huizing, M., & Hoogstraten-Miller, S. (2011). Retro-orbital injections in mice. *Lab Animal*, *40*(5), 155–160. https://doi.org/10.1038/laban0511-155

Yasuda, H., Huang, Y., & Tsumoto, T. (2008). Regulation of excitability and plasticity by endocannabinoids and PKA in developing hippocampus. *Proceedings of the National Academy of Sciences of the United States of America*, *105*(8), 3106–3111. https://doi.org/10.1073/pnas.0708349105

Yoshida, K., Tsunoda, S. P., Brown, L. S., & Kandori, H. (2017). A unique choanoflagellate enzyme rhodopsin exhibits lightdependent cyclic nucleotide phosphodiesterase activity. *Journal of Biological Chemistry*, *292*(18), 7531–7541. https://doi.org/10.1074/jbc.M117.775569

Yoshimasa, T., Sibley, D. R., Bouvier, M., Lefkowitz, R. J., & Caron, M. G. (1987). Cross-talk between cellular signalling pathways suggested by phorbol-ester-induced adenylate cyclase phosphorylation. *Nature*, *327*(6117), 67–70. https://doi.org/10.1038/327067a0

Yu, C. J., Wang, M., Li, R. Y., Wei, T., Yang, H. C., Yin, Y. S., Mi, Y. X., Qin, Q., & Tang, Y. (2023). TREM2 and Microglia Contribute to the Synaptic Plasticity: from Physiology to Pathology. In *Molecular Neurobiology* (Vol. 60, Issue 2, pp. 512–523). Springer. https://doi.org/10.1007/s12035-022-03100-1

Yu, X., Moye, S. L., & Khakh, B. S. (2021). Local and CNS-Wide Astrocyte Intracellular Calcium Signaling Attenuation In Vivo with CalExflox Mice. *The Journal of Neuroscience : The Official Journal of the Society for Neuroscience*, *41*(21), 4556–4574. https://doi.org/10.1523/JNEUROSCI.0085-21.2021

Yu, X., Nagai, J., Marti-Solano, M., Soto, J. S., Coppola, G., Babu, M. M., & Khakh, B. S. (2020). Context-Specific Striatal Astrocyte Molecular Responses Are Phenotypically Exploitable. *Neuron*, *108*(6), 1146-1162.e10. https://doi.org/10.1016/j.neuron.2020.09.021

Yuan, T. F., Li, W. G., Zhang, C., Wei, H., Sun, S., Xu, N. J., Liu, J., & Xu, T. Le. (2020). Targeting neuroplasticity in patients with neurodegenerative diseases using brain stimulation techniques. In *Translational Neurodegeneration* (Vol. 9, Issue 1). BioMed Central Ltd. https://doi.org/10.1186/s40035-020-00224-z

Zaccolo, M., & Pozzan, T. (2003). CAMP and Ca2+ interplay: a matter of oscillation patterns. *Trends in Neurosciences*, *26*(2), 53–55. https://doi.org/10.1016/s0166-2236(02)00017-6

Zaccolo, M., Zerio, A., & Lobo, M. J. (2021). Subcellular Organization of the cAMP Signaling Pathway. *Pharmacological Reviews*, *73*(1), 278–309. https://doi.org/10.1124/pharmrev.120.000086

Zadegan, S. A., Kupcha, L., Patino, J., Rocha, N. P., Teixeira, A. L., & Furr Stimming, E. (2024). Obsessive-compulsive and perseverative behaviors in Huntington's Disease. In *Behavioural Brain Research* (Vol. 458). Elsevier B.V. https://doi.org/10.1016/j.bbr.2023.114767

Zamarbide, M., Mossa, A., Muñoz-Llancao, P., Wilkinson, M. K., Pond, H. L., Oaks, A. W., & Manzini, M. C. (2019). Male-Specific cAMP Signaling in the Hippocampus Controls Spatial Memory Deficits in a Mouse Model of Autism and Intellectual Disability. *Biological Psychiatry*, *85*(9), 760–768. https://doi.org/10.1016/j.biopsych.2018.12.013

Zeinstra, E. M., Wilczak, N., Wilschut, J. C., Glazenburg, L., Chesik, D., Kroese, F. G. M., & De Keyser, J. (2006). 5HT4 agonists inhibit interferon-γ-induced MHC class II and B7 costimulatory molecules expression on cultured astrocytes. *Journal of Neuroimmunology*, *179*(1–2), 191–195. https://doi.org/10.1016/j.jneuroim.2006.06.012

Zemelman, B. V, Lee, G. A., Ng, M., & Miesenböck, G. (2002). Selective photostimulation of genetically chARGed neurons. *Neuron*, *33*(1), 15–22. https://doi.org/10.1016/s0896-6273(01)00574-8

Zhang, J., Guo, J., Zhao, X., Chen, Z., Wang, G., Liu, A., Wang, Q., Zhou, W., Xu, Y., & Wang, C. (2013). Phosphodiesterase-5 inhibitor sildenafil prevents neuroinflammation, lowers beta-amyloid levels and improves cognitive performance in APP/PS1 transgenic mice. *Behavioural Brain Research*, *250*, 230–237. https://doi.org/10.1016/j.bbr.2013.05.017

Zhang, J.-M., Wang, H.-K., Ye, C.-Q., Ge, W., Chen, Y., Jiang, Z.-L., Wu, C.-P., Poo, M.-M., & Duan, S. (2003). ATP Released by Astrocytes Mediates Glutamatergic Activity-Dependent Heterosynaptic Suppression and glia (for review, see Fields and Stevens, 2000). Al-though astrocytes, the most abundant glial cells in the. In *Neuron* (Vol. 40).

Zhang, Y. M., Qi, Y. B., Gao, Y. N., Chen, W. G., Zhou, T., Zang, Y., & Li, J. (2023). Astrocyte metabolism and signaling pathways in the CNS. In *Frontiers in Neuroscience* (Vol. 17). Frontiers Media SA. https://doi.org/10.3389/fnins.2023.1217451

Zhou, K., Han, J., Wang, Y., Zhang, Y., & Zhu, C. (2022). Routes of administration for adeno-associated viruses carrying gene therapies for brain diseases. In *Frontiers in Molecular Neuroscience* (Vol. 15). Frontiers Media S.A. https://doi.org/10.3389/fnmol.2022.988914

Zhou, Y., Zhou, B., Pache, L., Chang, M., Khodabakhshi, A. H., Tanaseichuk, O., Benner, C., & Chanda, S. K. (2019). Metascape provides a biologist-oriented resource for the analysis of systems-level datasets. *Nature Communications*, *10*(1). https://doi.org/10.1038/S41467-019-09234-6

Zhou, Z., Chen, Q. Y., Zhuo, M., & Xu, P. Y. (2024). Inhibition of calcium-stimulated adenylyl cyclase subtype 1 (AC1) for the treatment of pain and anxiety symptoms in Parkinson's disease mice model. *Molecular Pain*, *20*. https://doi.org/10.1177/17448069241266683

Zhou, Z., Ikegaya, Y., & Koyama, R. (2019). The astrocytic cAMP pathway in health and disease. In *International Journal of Molecular Sciences* (Vol. 20, Issue 3). MDPI AG. https://doi.org/10.3390/ijms20030779

Zhou, Z., Okamoto, K., Onodera, J., Hiragi, T., Andoh, M., Ikawa, M., Tanaka, K. F., Ikegaya, Y., & Koyama, R. (2021). Astrocytic cAMP modulates memory via synaptic plasticity. *Proceedings of the National Academy of Sciences of the United States of America*, *118*(3), 1–10. https://doi.org/10.1073/PNAS.2016584118

Zhuang, Z., Yang, B., Theus, M. H., Sick, J. T., Bethea, J. R., Sick, T. J., & Liebl, D. J. (2010). EphrinBs regulate D-serine synthesis and release in astrocytes. *Journal of Neuroscience*, *30*(47), 16015–16024. https://doi.org/10.1523/JNEUROSCI.0481-10.2010

Zucker, R. S., & Regehr, W. G. (2002). Short-term synaptic plasticity. In *Annual Review of Physiology* (Vol. 64, pp. 355–405). https://doi.org/10.1146/annurev.physiol.64.092501.114547